# A spatial kinetic structure applied to an active acoustic ceiling for a multipurpose theatre

Delft University of Technology

MSc thesis report

Faculty of Civil Engineering and Geosciences
Track Structural Engineering
Matteo Soru - June 2014

# A spatial kinetic structure applied to an active acoustic ceiling for a multipurpose theatre

Matteo Soru, June 2014
Delft University of Technology
Faculty of Civil Engineering and Geosciences
Department of Design & Construction
Section Structural and Building Engineering

**Graduation committee:**


**Prof.ir. R. Nijsse**
Delft University of Technology
Faculty of Civil Engineering and Geosciences
Section Structural and Building Engineering
Room 1.36, Stevinweg 1, 2628 CN Delft
r.nijsse@tudelft.nl

**Ir. H.R. Schipper (Daily Supervisor)**
Delft University of Technology
Faculty of Civil Engineering and Geosciences
Section Structural and Building Engineering
Room 1.55, Stevinweg 1, 2628 CN Delft
h.r.schipper@tudelft.nl

**Dr.Ir. P.C.J. Hoogenboom**
Delft University of Technology
Faculty of Civil Engineering and Geosciences
Structural Mechanics Section
Room 6.48, Stevinweg 1, 2628 CN Delft
p.c.j.hoogenboom@tudelft.nl

**Abstract**

Conventional buildings and structures are not designed usually for adapting to contextual aspects and needs: an instant adaptation of building systems by different configurations can result in an instant adaptation to these needs. The research is here applied for the design of an adaptive acoustic ceiling for a multi-purpose theatre.

High real estate, construction, and maintenance costs frequently preclude the creation of single purpose facilities:  moreover, the design and construction of a new theater represents the investment of a large amount of money. The main motivation of the research is to propose an adaptive acoustic ceiling that, by motion, is able to adjust its properties in response to changing sonic conditions, altering the sound of space according to performance needs.
By relying on research of kinetic systems and their possible implementation with an optional function based on paneling, a case study is carried out for a multipurpose theatre in the Netherlands.
The study on kinetic typology revealed that an innovative motion structure based on the biomechanical behavior of backbone-like assemblies can be applied to such design tasks: a procedure regarding design procedure and motion triggering system for the case study, at a conceptual stage is presented.

**Aknowledgements**

Hereby I would like to express my deepest appreciation to all those who helped me in completing this thesis and my engineering studies.

First of all, I would like to thank to Ir. Roel Schipper, for his guidance during the entire thesis process and for have been a friend during this time. His useful advises and practical approach helped me a lot in conducting this research. I also want to express my appreciation to Prof. Rob Nijsse for proposing and trusting me with this challenging but very stimulating topic. I want also to express my gratitude to Dr. Pierre Hoogenboom for his support and constructive critics that inspired me throughout this process.

Special thanks go to the Grasshopper web community: without its priceless help I couldn't completed this research: in particular I would like to mention Daniel Piker, for have developed and shared Kangaroo and David Rutten for being always ready to contribute with its invaluable knowledge to Grasshopper forums.

I am very grateful to my family and especially my father and my sisters who always believed in me and for their moral support throughout all my studies at TU Delft.

Last but not least, I am thankful to all my friends in Delft, Klodi, Vasi, Mirela, Ravi, Peter and Agustin who gave me many unforgettable memories during my studies.

Matteo Soru

Delft, June 2014

**Table of Contents**

# Part 1

# Theoretical Prerequisites

Chapter 1 // Introduction

### 1.1 Theoretical background

Adaptability is the capacity of a system to change, or to be changed, its intrinsic characteristics, behaviors and performance to fit altered circumstances (Thün 2012). This concept concerns transversally numerous fields of science and humanistic disciplines. Research on general adaptive systems have been set up at the beginning of modern science and nowadays, even more, this topic stimulates philosophers, scientists, engineers, economists to get more acquainted with the behavior of emergence systems.

In life sciences the term adaptability is used variously. In ecology, adaptability has been described as the capacity to cope with unexpected disturbances in the environment. In biology, adaptation is the evolutionary process whereby an organism becomes better able to live in its habitat. These concepts have been translated to economic theories and models to achieve survival, efficiency and success.

What does make a system able to mature adaptive traits? The answer can be found in the interaction among the system and the environments where the system itself stays: in this case, adaptation is the response of a system to the condition imposed by the surrounding environment in order to establish or reestablish an adequate performance.
The study of relationship among systems and environments is the basis of the so called complexity science (Wikipedia): this is not a single theory, it includes more than one theoretical framework and is highly interdisciplinary, seeking the answers to some fundamental questions about living, adaptable, changeable systems.

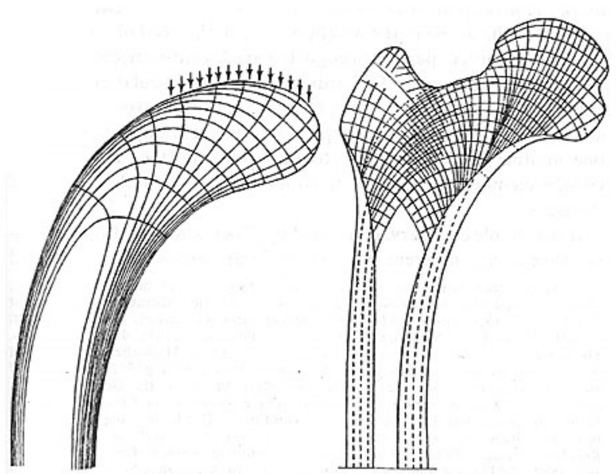

Image 1.1. Femur shape is a configuration that adapted to external forces. Form is the result of an emergencing evolution process. Material distribution follows isostatics lines (image courtesy of D'Arcy Thompson).

With the same viewpoint the built environment can be perceived as the incubator that provides the setting for human activity, ranging in scale from buildings, cities and infrastructures supporting the settlements. This surrounding has been shaped according to human necessities and natural available resources and its emergence has been dictated by environmental conditions. To note that the interaction between system and environment is not just univocal, but the system itself, or its relative adaptation, contribute to outline the original surrounding.

The thesis is founded on the observation that the functionality of an engineering system can pursue an adaptive behavior that, first is the result of an adaptation of the system to the variable surrounding circumstances and, secondly has as result an enhancement of the properties of the environment itself.



Chapter 1 // Introduction

Aim of the designers has been always to shape the built environment with solutions able to meet the requirements of society in its whole. The last decades experienced a shifting of the design approaches towards new envisioned methodologies orientated to optimize performances and to meet the mutable requirements that a building experiences during its life cycle.

Already during the Modernist movement, architects had seen in the technology a mean to transpose in the design practice ideals of functionality, efficiency and productivity originated by the new industrial paradigms that rapidly were influencing the culture of industrialized society (Zevi 2006).
In opposition to the Vitruvian idea of *firmitas* (statics, solidity, firmness), signature of classic architecture, modernists started to be fascinated by those concepts of dynamism, motion, ephemeral instant solutions that could, with more effectiveness, advance and serve human life. In 1923 Le Corbusier (1977) imagined the house not more like a static immutable living space, but like an assembly of hyper-technologic elements: his famous remarks 'a house is a machine for living in' sums up his approach to design.

Image 1.2. Centre George Pompidou in Paris, Renzo Piano and Richard Rogers design. The building is envisioned as an hyper-technologic machine (image courtesy of RPBW).

The latter half of the twentieth century witnessed a fast technological development in many fields. This growth of knowledge and technology is constituting a fertile field within architects and engineers are embracing new design paradigms. In this innovative cultural background the concept of adaptive architecture is arising

(Lelieveld 2013).
This concept is here envisioned through the ‘ecological paradigm’, where living environment are shaped through the complex interplay of matter, geometry forces, information and activities (Thün 2012).

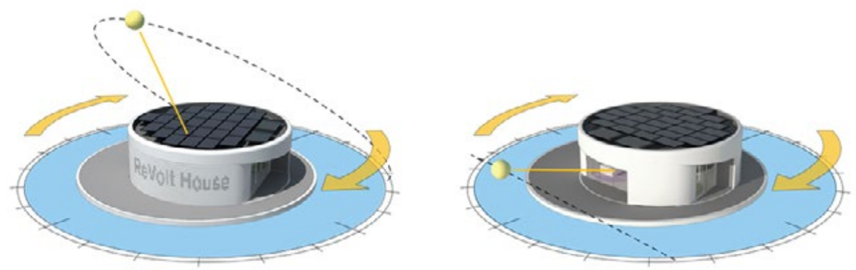


Image 1.3. Form and system follow environmetal functions (image courtesy of TU Delft RevoltHouse team).

Designers are now more informed and concerned about the various project aspects that influences the building performance like architectural criteria, multiple environmental impacts and user behavior.
Specific examples are sun, wind, temperatures, function, occupancy, socio-cultural aspects and other contextual aspects and needs. Even though these aspects are acknowledged to be variable, conventional buildings are conceived to provide one design solution, represented in a static configuration (Teuffel 2011). Due to the changes in needs and context, a static building cannot guarantee the same level of performances over time.





**1.2 Problem statement and Motivation for Research**

The thesis explores the potentiality of adopting an ecological design approach to shape a dynamic system able to create flexible sound environments for multiple acoustic performance situations.
Conventional buildings and structures are not designed for adaptation to contextual aspects and needs. An instant adaptation of building systems by different configuration can result in an instant adaptation to context and needs (Teuffel 2011). This last idea is here applied for the design of an adaptive acoustic ceiling for a multi-purpose theatre.

High real estate, construction, and maintenance costs frequently preclude the creation of single purpose facilities for musical performance (Ballou 1987). The design and construction of a new concert hall, or even a major remodeling of an existing hall, is a great event in a community. It represents the investment of a large amount of money and is, probably, the culmination of years of effort by a large group of civic leaders (Pezzi 2003).

Acoustic performances for multi-purpose facilities are designed typically to suite nominal acoustic performance to the most common use or to provide acoustic qualities that averagely can suite to several performance requirements (Thün et al 2012). This last intent is based on the analysis of several scenarios toward the synthesis of an acceptable solution for the several situations. The main motivation of the research is to overcome this synthesis on the way to optimize the soundscape for various artistic performances.

Image 1.4. Greek theatre: the form is an optimal but fixed solution for acoustic performance.

Although there are precedents for the control of room acoustics through the use of kinetic systems designed to manipulate height and orientation of sound ceiling (Peutz 1978), the attempt to improve these structures that are now based on elementary motions is worth to be enhanced: development of adaptive systems to control wavefront curvature, level, time of arrival of early reflections constitutes an unexplored territory in acoustic control. The research is driven by the intent to improve the state-of-the-art of adaptive ceiling, especially in Dutch theatres, that are programmatically characterized by the hosting of a broad spectrum of performance types. They have to meet the requirements of theatre, dance, opera and classical music as well as pop music, congresses and cinema.

Image 1.5. Form and system follow acoustic functions: ceiling shape is an optimal but non adaptive system (Ravello Auditorium, Oscar Niemeyer desing)



Chapter 1 // Introduction

**1.3 Objective and Research Questions**

The main goal of the thesis is to design a flexible and reactive structure for a theatre ceiling systems, able to adjust its properties in response to changing sonic conditions, altering the sound of space according to performance needs and improve acoustic perception to music played. In order to achieve this goal, the following objectives were formed:

-First, the thesis aims to understand the kinematic behavior of motion structures, and consequently to control and synthetize these systems in a digital environment in order to set-up an auxiliary tool for the design of an adaptive assembly. Mechanism are possible because of the existence of particular geometric conditions among element assemblies (You et al 2012): objective of the research is to understand the relations among these geometric configurations that allow structures to undergo the desired movements.

-The thesis analysis the precedents of kinetic structures, their applications and the potentialities of these in the field of adaptive acoustic ceiling. Moreover the research aims to augment the range of kinetic structures drawing from mechanical and biomechanical engineering fields that might be applied to civil engineering applications.

-Even though some acousticians has been already carried out designs on the performance of flexible acoustic ceiling for theaters, there is a lack of system automation as well as the lack of optimal configuration finding in relation to the required acoustic performance.
Generally, layouts of acoustic panels are tweaked manually: while this can work well, it requires a fair amount of time to adjust a large room and does not allow for a performance scene that can be quickly turned from one type of event to another (Ballou 1987). The system should be designed with an acceptable level of automation.

-The thesis aims to set-up a basic and rough parametric acoustic computational strategy that can be used to assess ‘on live’ the performance of the ceiling: this intention is quite useful on the very first stages of the design process where several scenarios need to be explored and evaluated.

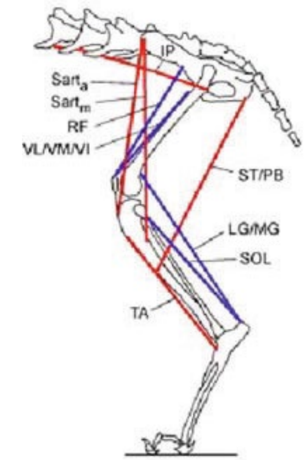


Image 1.6. A bio-mechanical system. The flexor tendons (red) and the extensor tendons (blue) of a cat's hind legs (image courtesy of Oliveira 2009)

-Apart from studying the kinetic and structural behavior of adaptive system, the thesis also aims to analyze the possibilities of integration in a theater from the aesthetic point of view. The system should be combined with the appearance of the theatre hall and contribute to the creation and identification of the inner space.

-Finally, the thesis aims to synthetize a system for an existing multipurpose theatre in the Netherlands and test its performances in relation to acoustic demands.

Research questions has been composed by the above introduced objectives about the development and demands in the field of kinetic structures and in particular from the request for a design of a new and advanced type of acoustic ceiling applied to an existing building. In conclusion the research question are formed as follows:

01- What are the geometric parameters of a structure that by motion can influence the performance (kinetically and structurally) of the overall ceiling? What are design criteria and their relative adjustments that can enhance the performance of the acoustic ceiling?

02- What is the motion structural typology that has the most suitable characteristic to execute a function based on paneling?

03- What is the motion structure typology assembly that has the most suitable characteristic to modify its global geometric qualities (concavity, planarity, convexity) that influence wave propagation? What is the simplest system that can modify the inner volume of the hall which influences the soundscape?

04- What are the available and functional automated systems and motion actuators coming from the mechanical engineering field that might be applied to the adaptive ceiling?





### 1.4 Research Methodology

In order to gain knowledge on the subject of structures that adapt their configuration by motion, a wide range of the precedents of this field will be study. Within this step, special emphasis is given to the study of the kinematic conditions that allow structures to move. Special importance is laid on understanding the relations between kinematics metrics and geometric settings; for the particular case of tension structures other structural mechanical aspects will be considered (stresses, strains, axial forces, prestressing) in order to have a deeper understanding on the motion of this typology.
To carry on this part, an associative and parametric approach will be used. Parametric design is based on non-Euclidean geometry, where multi-dimensional solutions provide an infinite number of geometrical models (Kolarevic 2003). The output geometric model is the result of an associative network and in-a-hierarchy-connected elements, further connected to changing parameters. Within this step the visual programming language (VPL) Grasshopper 3D™ (integrated with the 3D modeling software Rhinoceros 3D™) is used. In computer science, a VPL is a programming language that lets users create algorithms by manipulating programming elements graphically rather than by specifying them textually (Wikipedia).

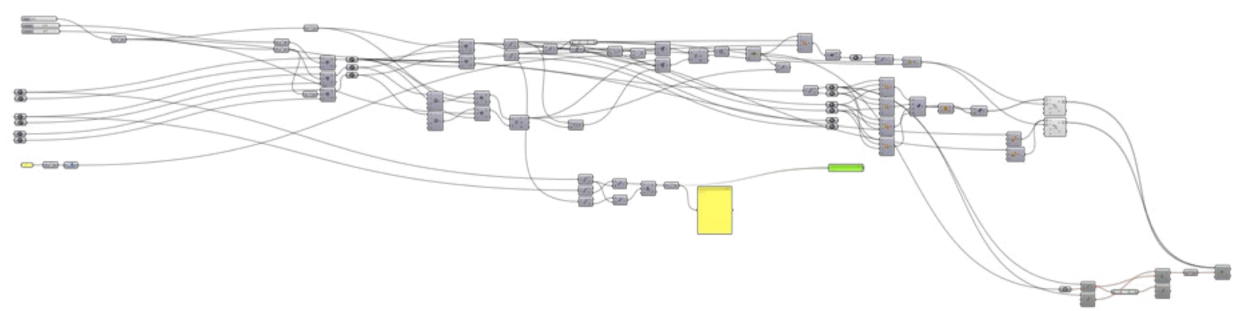

Image 1.7. A complex geometric associative and parametric network for the syntesis of Bricard linkage.

Grasshopper 3D™ allows to build generative algorithms where the elements are associate by univocal relations (Payne et al 2009). One consequence is that parametric design permits to create complex models based on geometric associations and to explore several solutions by a proper set-up of mutable parameters.

Parameterization increases complexity of both designer task and interface as designers must model not only the artifact being designed, but a conceptual structure that guides variation (Aish et al 2005). Parameterization can enhance the search for designs better adapted to context, can facilitate discovery of new forms and kinds of form-making, can reduce the time an effort required for change and reuse and can give better understandings of the conceptual structure of the artifact being designed.

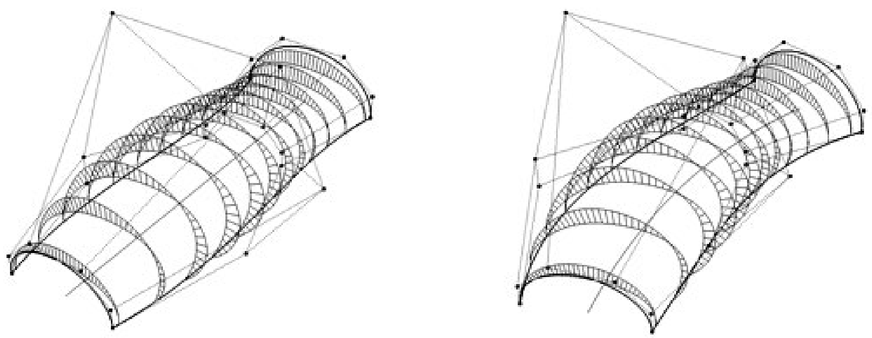

Image 1.8. Parametric model of a roof with efficiently shaped trusses (image courtesy of Lorenz Lachauer, ETHZ).

At a conceptual stage associative design will be used not only to generate geometrically motion structures but also to create performative visual algorithms and scripts to assess acoustic performance of the ceiling. At this step generative design tools will be developed by translating parametric model entries into tangible adaptive systems. Elements and element assemblies will be here enhance with acoustic metrics.

The main function of this methodology is to evaluate rapidly and ‘in live’ both kinetics and building acoustic performance. This procedure is particularly





powerful during the conceptual stage, where designer is tasked to consider several scenarios and to choose for the most performative. Generally parameterization may require additional effort to the set-up of assessing algorithms: at a conceptual stage this algorithm are characterizes by low precisions and rough calculations.

At a more advanced design stage, mechanics and acoustic performance will be assessed by the use of standard, but more advanced and precise tools.

Mechanics will be evaluated with the Finite Element Analysis (FEA) Oasys GSA.

In this environment, the static solutions will be here transfered and evaluated their mechanical behaviour.

### 1.5 Report Outline

Based on the discussed research methodology the thesis report can be divided into six main parts:

Chapter 1 // Introduction
This part summarizes the background and the main motivation of this master's thesis together with the followed research methodology.

Chapter 2 // Motion Structures
It gives a picture of the state of art of kinetic structure together with a foundation research of biomechanical systems.

Chapter 3 // Considerations on Acoustics
Illustrates the basis of room acoustic, techniques to tune soundscape and an explanation of the development of two parametric acoustic tools.

Chapter 4 // Design Concept
This part shows the conceptual design results of a case study, then applied to an existing multipurpose theatre in the Netherlands.

Chapter 5 // Further Design Considerations
This chapter explore further design considerations with an eye oriented to possible implementation of the design concept presented in the preceding chapter.

Chapter 6 // Conclusions and Recommendations
Based on the acquired knowledge from the theoretical and applied case study, the most important conclusions are drawn and summarized in this part together with the recommendations for further research on the subject.

# Part 1

# Theoretical Prerequisites

## 2.1 An Introduction to Adaptive Structures

An adaptive structure is a mechanical structure with the ability to alter its configuration, form or properties in response to changes in the environment. Adaptive structures can be transformed from a configuration to another, in which they are stable and carry loads. Due to this inherent transformability they are characterized by their ability to adapt their shape, mechanical and physical properties and then their overall behavior to the external excitations and the requirements emanating from their use at any given time (Gantes 2000).
Various terms, such as dynamic, responsive, interactive, intelligent and active are used for structures which have adaptive characteristics in some way.

Image 2.1. An example of dynamic structure (Lelieveld 2013): Cyclebowl, Atelier Brückner design. Pneumatic control of roof and façade transparency. Sensor controlled louver system.

Image 2.2. An example of responsive system (Lelieveld 2013): Enteractive, Electroland design. Adaptive lighting and sound system.

In literature, the term dynamic structure is used to define an environment which is able to adapt to the varying needs of the users, to changing environmental circumstances or to the designers desires and imaginations. Here, the adaptation is set in a framework determined by parameters (Lelieveld 2013).

Another term, responsive, is found as a definition of an intelligent environment, which has purpose and intentions characteristics, and can be indicated as a self-reproducing autogenic environment (Negroponte 1975). The definition of dynamic indicates a predefined performance, where responsive appears to dispose over self-initiative characteristics (Lelieveld 2013).

The term interactive relates to a physical change of the architectural space as a result of embedded computation (Fox et al. 2009).

Intelligent architecture refers to build forms whose integrated systems are capable of anticipating and responsive phenomena, that affect the performance of the building and its occupants, whether internal or external (Kroner 1997). The integrated systems can be indicated as the initiator and controller of the alteration based on user performances and requirements, where in some cases the environment is added as a stimulator (Lelieveld 2013).

On the contrary an active building component is fully controlled by the user, whereby a pre-set reaction is given to a specific command. The user is the initiator of a pre-set performance. The command can be, for example, given by the push





of a button or via a touch screen. System technology, such as actuating systems, plays an important role in the translation of the command into a certain action. Additionally, an energy source is required to execute the command (Lelieveld 2013).

Image 2.3. An example of active structure. Kuwait Pavilion '92 World Exposition, Santiago Calatrava design. The pavilion was designed as a sculpture with flexible wooden arms that open and close to resemble a palm leaf (images and model courtesy of Siti Rafe'ah Omer).

Thesis research is limited to the study of active structures also here defined as motion structures.

***Mechanisms versus Deformable Structures.***

Another further categorization can be done for motion structures: in accordance to the deployment process (You et al 2012) and strain magnitude (Beatini 2006), we can distinguish two types of active or motion structures.

The last category is the deformable structure characterized by the fact that the overall strain energy varies prominently during motion: typical examples include inflatable structures, membrane structures or tensegrity systems. This typologies can also be termed as tension structures (Wang 2004).

The other category is essentially a mechanism. The motion is executed by activation of one or a number of carefully designed internal mechanisms (Motro 2003).
In this case the structure is composed by rigid bodies. In a rigid body the distance between any two given points remains constant regardless of external forces exerted on it (Meriam 2003).
The rigid body is only an approximate reality in practice. This assumption reduces

the study of the motion of a movable structure to geometric considerations. This is true if the bearing clearance and elastic deformation of members are sufficiently small. With this assumption the motion of a structure based on geometric consideration is equal to the real structure without noticeable error.

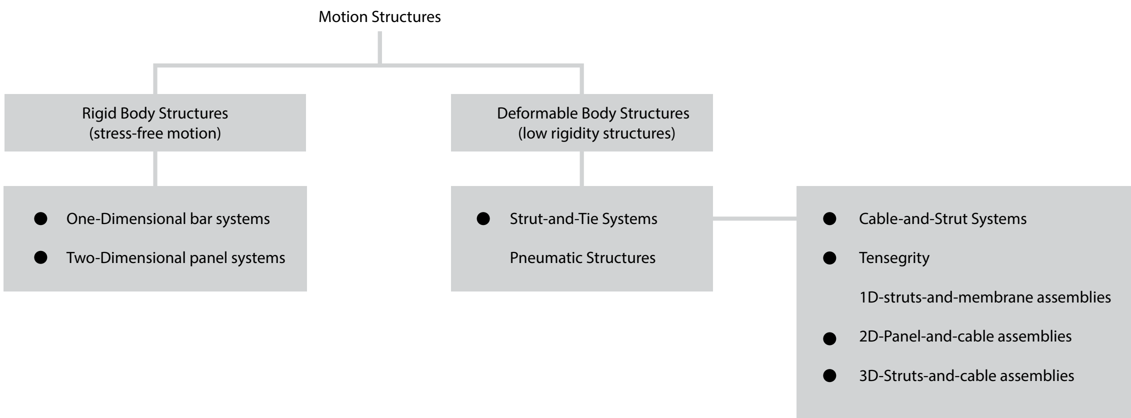


Table 2.1. Cathegorization of motion structure, in turn augmented from Beatini (2006). Signed with bullet points, the typopologies that will be studied along the research.

This categorization (Table 2.1) can be augmented according to the degree of spatial dimension for the elements that compose the structure: elements can be prominently linear, planar or tridimensional.

Image 2.4. Left: an example of 1D-strut-and-membrane structure, MOON tensegritic membrane structure, Tokyo University of Science design (image courtesy of Tensegrity Wiki). Right: an example of configurative pneumatic structure for Casa da Musica, OMA desing (image courtesy of insideoutside.nl).
These two structural typologies won't be study along the research.





### 2.1.1 A Glimpse on History of Motion Structures

The history of transformable structures goes back to centuries before. In ancient time tribes used to move from place to place in search for better living conditions (Friedman 2012).
Everybody is familiar for instance with the light deployable Indian tepees that could be transported by animals.
An interesting Babylonian bas relief shows a hunter sit in a deployable chair: this is formed by three bars connected by means of a hinge whose mechanism is blocked with a leather rag.

Image 2.5. Hunter's chair, Babilionian bas relief.

In the first century Romans engineers used to design mobile textile roofs for amphitheaters (*velaria*) composed by sails and struts, movable by means of ropes: this was meant to guarantee to audience an adequate protection in case of rain or strong sun.

Image 2.6. Roman velaria.

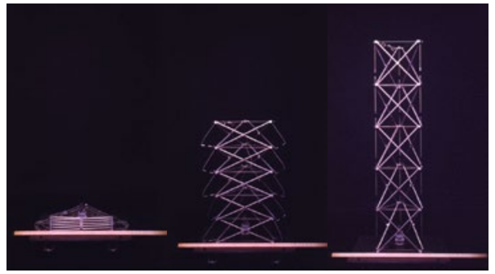

Image 2.7. Pantographic deployable mast (image courtesy of Z. You and S. Pellegrino).

With the industrial age, machine and technology broke into civil engineering practice with a wide range of technical innovations and inspiring solutions for designers (Zevi 2004). The comparison of architecture with a machine is typical for this period. To understand the history of adaptive architecture a parallel revision with other discipline should be considered (Beatini 2006): first the mechanical engineering and then aerospace industry have been seen as font of inspiration for architects that designed motion structures for civil applications.

In the second half of the 20th century deployable and inflatable structures development were first achieved in spatial engineering (Gantes 2000) with the construction of super compact and light solar panels, antennas, reflectors, as the volume and the weight of these structures to be transported is crucial.

Very important is the outstanding research work of Frei Otto at the Institute for Lightweight Design and Construction (ILEK) in Stuttgart: Otto was mainly interested in understand how and why natural structures emerge, and how and why they adapt. Among all the precious researches produces, he was also interesting in mobile and adaptive systems, but more importantly he translated the concept of adaptation (even if only in a theoretical level) into a design approach. This notion is still influencing designers and even more, with the introduction in architecture of mechanical and electronic devices that simulates surrounding environmental perceptions (sensors) and reactions (motion actuators), these envisioned theories are being applied nowadays in architectural practice.

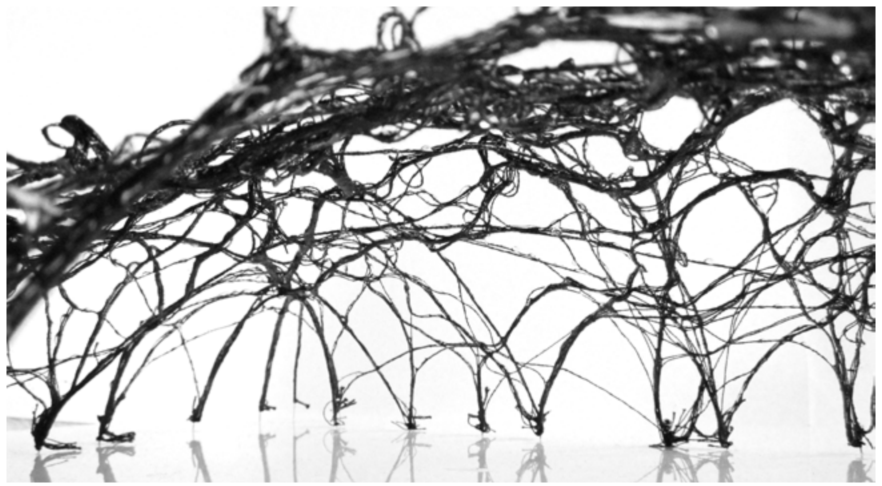

Image 2.8. Form-finding physical model based on Frei Otto's studies about form emergence and optimal minimum path (image courtesy of WeWantToLearn.net).





The building is now perceived as a working machine, whose all parts (not just the load bearing ones) contribute to adapt environmental conditions: the use of adaptive shadings devices or Heating, Ventilation and Air Conditioning (HVAC) systems is an example of the first adaptive solutions applied to buildings (Image 1.2).

Not as extensive collections of adaptive systems designed, I would like to mention the most representative works.

The façade for the *Institut du Monde Arabe* designed by Jean Nouvel in the '90 is composed by a repeated system that works as a photographic diaphragm: sensors can perceive the light level inside the building and according to it, the system automatically regulates the mechanical 'iris' openings.

Image 2.9. Institut du Monde Arabe, Jean Nouvel design.

The shading system for the Al Bahr towers in Abu Dhabi is formed by developing a series of translucent umbrella-like components which open and close in response to the movement of the sun. The dynamic screen avoids the need for heavily tinted glass thereby reducing the need for significant artificial lighting while providing better views for occupants of the building. This is the first time such a moveable façade has been used at this scale. The façade will be controlled via an electronic building management system, creating an intelligent façade.

Image 2.10. Al Bahr Towers adaptive façade. Aedas design.

A prototype of a responsive acoustic ceiling was design and installed in 2012 at the University of Michigan’s Taubman College of Architecture and Urban Planning (Thün et al 2012). The prototype is comprised of a thick, rigid origami surface consisting of reflective, absorptive and electro-acoustically enhanced panels equipped with actuators and communication technologies that make it capable of kinetic adjustment, actively transforming the acoustic performance of a host space relative to different types of auditory demand.

Image 2.11. Resonant Chamber, prototypes for an adaptive acoustic ceiling (image courtesy of eVolo.us).





### 2.1.2 Fundamentals of Kinematics

Kinematics is the study of classical mechanics which describes the motion of points, bodies and systems of bodies without consideration of the causes of motion. The term is the English version of Andre-Marie Ampere’s *cinématique*, which he constructed from the Greek *kinema* (movement, motion). The study of kinematics is often referred also as the geometry of motion. To describe motion, kinematics studies the trajectories of points, lines and other geometric objects and their differential properties such as velocity and acceleration (Meriam 2003 and Wikipedia).

Aim of this section is not to be about the wide topic of kinematics, but only to shortly give an insight to the subject. An extensive, but accessible knowledge of kinematics can be found at Meriam (2003) and Zhang et al (2012). Knowledge of kinematics is essential to study the behavior and to design adaptive motion structures.

Changing a system shape requires the introduction of an instability or, more precisely, the introduction of finite mechanisms that will make it possible to transform the system’s shape.
For rigid body assemblies the creation of mechanisms is usually obtained by suppressing some connections. For this assemblies and also for tension structures one can also introduce mechanisms by changing the length of some connections (cables or struts). Mechanisms are activated then by applying actions in the required direction of motion (Motro 2003).

Following, some kinematics concept are introduced in order to give to the reader an overall insight of motion phenomenon and its relative mechanical concepts.

#### ***Mobility Formula***

As first step it must be verified if the system is a stable structure or a mechanism, so to prove if the assembly as enough degree of freedom to move.
In three dimensional space, the number of degrees of freedom of a rigid body is

six: three directional displacements and three directional rotations. Thus n free rigid bodies will have 6·n degrees of freedom (DoFs). By fixing one rigid body, the remaining DoFs are 6·(n-1). A joint with f DoFs connecting two bodies reduces the total DoFs by 6-f. For a mechanism composed of n rigid bodies that are connected with a total of j joints, each of which has $f_i$ (i=1,2,…, j) DoFs, the mobility of the mechanism m is:

$$m = 6(\mathrm{n} - 1 - \mathrm{j}) + \sum_{i=1}^{j} f_i$$

This is called the Grübler-Kutzbach mobility criterion or Kutzbach criterion, or more easily, mobility formula (You at al 2012).
If m is zero or smaller than zero the structure assembly is not a mechanism and motion is locked.

### *Planar versus Spatial Mechanisms*

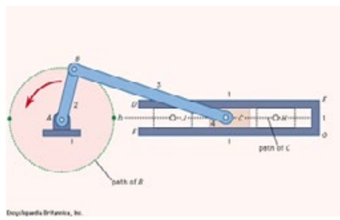

Image 2.12. A planar mechanism.

A planar mechanism (Meriam 2003 and You et al 2012) is a mechanism such that the trajectories of all points constituting a movable rigid body are parallel to a plane. The plane is known as plane of motion. The axis of rotation of all revolute joints must be normal to the plane of motion and the directions of all prismatic bars must be parallel to the plane of motion.
In a plane, each free rigid body has three degrees of freedom. The mobility criterion therefore becomes:

$$m = 3(\mathrm{n} - 1 - \mathrm{j}) + \sum_{i=1}^{j} f_i$$

Image 2.13. A spherical mechanism.

A spatial or spherical mechanism (Meriam 2003 and You et al 2012) is a mechanism where the rigid bodied are constrained to rotate about the same fixed point in space. Therefore, the trajectories of points belonging to the rigid body lie on concentric spheres. The revolute joint axes are parallel in a planar mechanism, while for a spatial one they intersect at a point known as the concurrency point: a planar mechanism can also be thought as a spherical mechanism for which the concurrency point is at infinity.





### *Center of Rotation for Kinematic chains*

Image 2.14. This lamp can be regarded as a three-rigid-bodies kinematic chain.

A kinematic chain is a collection of rigid bodies connected through internal links and constrained in plane or space with external links. A two rigid body system connected with a link takes the name of kinematic pair (Meriam 2003).
Once is proved that a system is a mechanism the center of rotations for all the bodies must be found. The center of rotation, in case of planar mechanism, is the point in a plane around which all other points are rotating at a specific instant of time (Ferro et 2013).
According to the characteristics of the center of rotation one can distinguish an absolute center of rotation $C_i$ for a body I and a relative center of rotation $C_{ij}$ for a kinematic pair formed by a body I and J.
These centers can be found by means of the theorems for kinematic chain.
The first theorem of kinematic chains states that a kinematic pair (composed by two bodies I and J) is a mechanism if the two absolute centers of rotation $C_{i\text{-}j}$ and the relative center of rotation $C_{ij}$ lay on the same line.
The second theorem of kinematic chains states that if three body I, J and K mutually connected by means of hinges are a mechanism if the relative center of rotations $C_{ij}$,$C_{ik}$ and $C_{jk}$ lay on the same line (Ferro et al 2013).

The theorems for kinematic chains are necessary and sufficient condition to individuate a mechanism: on the contrary the mobility formula is a necessary but not sufficient condition. As example, let us consider in the plane two bars aligned, connected by means of a hinge and constrained at their uncommon ends by a pin. According to the mobility formula the system is stable and statically determinate, (m=0), but being the center of rotation aligned the system is a mechanism.

### 2.1.3 Method to Synthetize Kinematics of Rigid Body Assemblies

The classical analytical approach is based on rigorous use of fundamental theorem of kinematics: with this, the study of mechanism is simply abstracted into purely mathematical functions.
For instance, position of a particle in the plane can be expressed by means of a three row vector. If we want to rotate this onto a plane, the vector must be multiplied to a matrix operator, the rotation operator, a three dimensional matrix, easily derivable from planar trigonometry (Zhang et al 2012).
The same can be done if the point must be translated or roto-translated: linear algebra provides with the proper matrix transformation operators to study kinetics of a particle. The identical procedure can be done for rigid body transformations, both in plane and in space.
Before using the matrix transformation, the system must be analyzed to verify whether is a stable structure or a mechanism. Hereafter the centers of rotations of the rigid body must be identified and together with the knowledge concerning internal and external constrains the kinematic can be described.
Graphic can be used to visualize the motion by translating transformation outputs into motion diagrams.
This method is quite straightforward for simple planar mechanism, but it turns to be complicated when a spatial system must be studied. All the geometric entities are here described with mathematics entries, and mathematical operators are needed to investigate the mechanism: for this reason an extra relatively time-expensive procedure is needed to interface mathematical outputs with visualization.

Another approach can be used and implemented: this is here named ‘associative geometric method’. The geometric approach has been used by Deng et al (2011) for the synthesis of foldable single loop over-constrained mechanism (§2.2.2), but in this work it was used also for the study of complex 2D-rigid panel systems: the further term ‘associative’ refers to the use of an associative and parametric software (Grasshopper™) to synthetize the mechanism and visualize the motion.
Also this method is based on rigorous use of fundamental theorem of kinematics, but the main difference is that this is an intuitive approach. Items and relations that form the mechanism are purely geometric. Bars, revolute joint axis, rotation centers (together with more abstract elements like planes or vectors) are here pure geometric entities intertwined among them according to kinematics characteristics of mechanisms.
By having a good knowledge of fundamentals of kinematics is possible to synthetize easily very complex mechanisms: moreover the visualization of the motion is immediate. This is a great advantage for the designer because by constructing the associative network of geometry he/she already acquires a good understanding of the motion behavior of the mechanisms.

#### *Slider Crank*

In order to illustrate the difference between the two methods above presented, let us analyze with both approaches a planar elementary mechanism.

Object of analysis is a slider crank (Image 2.15.A): this system is composed by two rigid bodies connected through a hinge and constrained at their ends not in common with a pin and a roll on a plane.

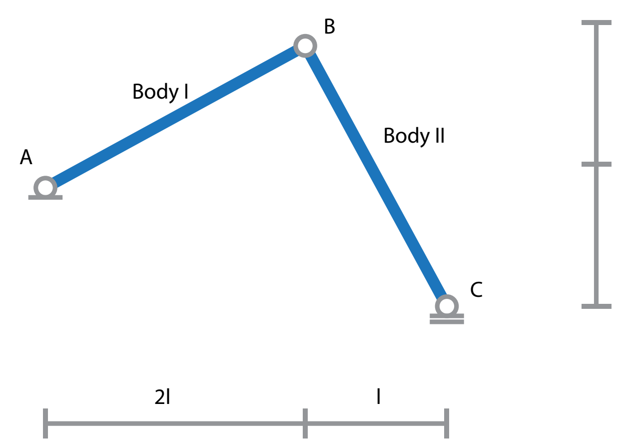


Image 2.15.A. Geometric set-up of the slider crank.

By means of the analytical graphic approach the motion behavior of the mechanism is illustrate as follows. As first step the structure typology must be identified to comprehend whether this is a stable system or a mechanism. Motion criterion for the system yields:

$$m = 3(2-1-3)+5 = 1$$

That shows the assembly is a mechanism with 1 DoF.
After this stage the centers of rotation of rigid bodies I and II must be sought (Image 2.15.B). Because the point in A is constrained with a pin the absolute center of rotation of the rigid body I $C_1$ is here; being point B an hinge at the same location the Relative Center of Rotation $C_{12}$ of rigid body I and II is found. On the contrary, roll at point C gives incomplete information about the Absolute Center of Rotation for rigid body II: this lays on the line n perpendicular to roll sliding line, but at this stage isn't known where.
According to first theorem of kinematic chains, in order to have a mechanism the Absolute Centers of Rotation must be aligned with the Relative Center of Rotation: with this knowledge the Center of Rotation $C_2$ is found as intersection between the line n and the direction passing by $C_1$ and $C_{12}$.

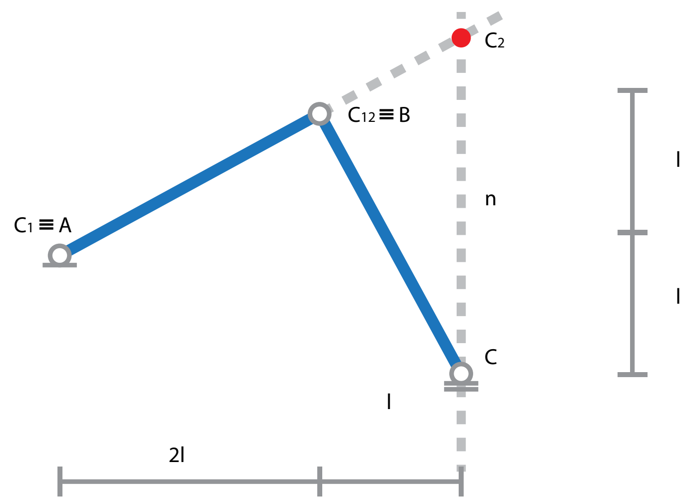


Image 2.15.B. Center of rotations.

In order to yield now the displacement vectors of rigid bodies we have to compose these by considering the projection of displacement onto the horizontal and vertical axis: furthermore, being 1 DoF system, the full motion can be expressed as one single parameter, in this case selected as the angle of rotation $\theta$ of rigid body I. Let





us denote as $\phi$ the angle of rotation of rigid body II, which might be expressed as function of $\theta$.
Let us consider vertex vertical displacement (Image 2.15.B): being rigid body I and II connected at B they undergo the same displacement equal to $l \cdot \tan(\phi) = 2\, l \cdot \tan(\theta)$, from which can be yielded $\theta = 0.5 \cdot \mathrm{atan} \cdot (\tan(\phi)) = 0.5 \cdot \phi$.
With the same procedure the horizontal displacement are calculated, so that the finally displacement vectors can be composed: with this data mode of the mechanism can be yielded.

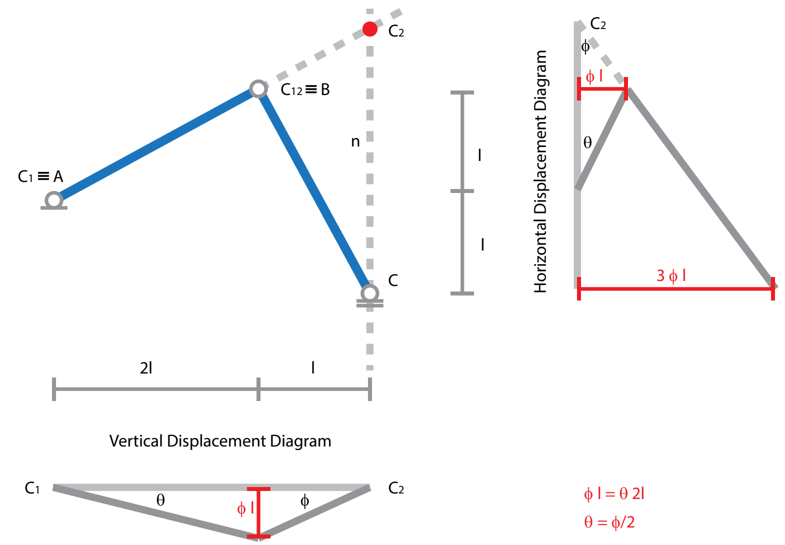


Image 2.15.C. Projections of displacement vectors.

Infinitesimal displacement vectors are respectively:

$$V_b = \begin{pmatrix} 2l\theta \\ 2l\theta \end{pmatrix} \qquad V_c = \begin{pmatrix} 6l\theta \\ 0 \end{pmatrix}$$

Let us synthetize now the same mechanism by means of the associative geometric method.
As first step, input elements are defined (Image 2.16.A): these are respectively the center lines of the rigid bodies I and II, a point associated with the pin at A, and the roll sliding direction as line at C.

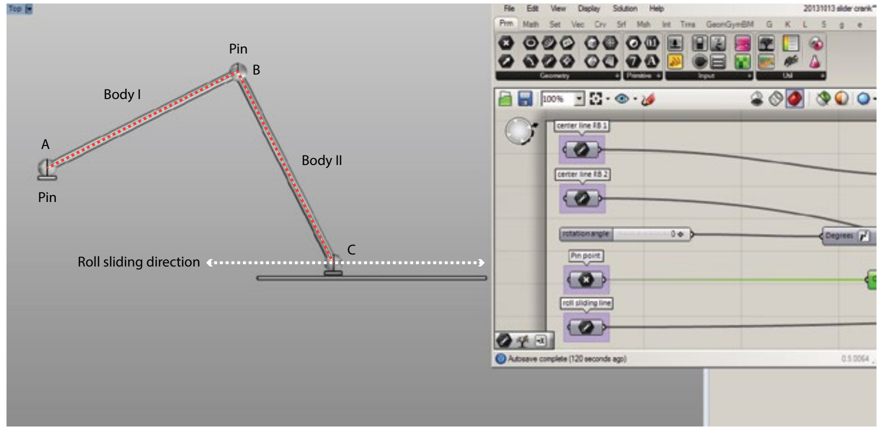


Image 2.16.A. Associative set-up for the geometric elements.

The unique kinematic variable chosen, through which is possible to describe the motion, is the rigid body I rotation angle θ around A.
The motion of rigid body I is now triggered by the ‘rotate an object in a plane’ component. As output the component give the rotated rigid body I, from which the node B’ can be extracted (Image 2.16.B).

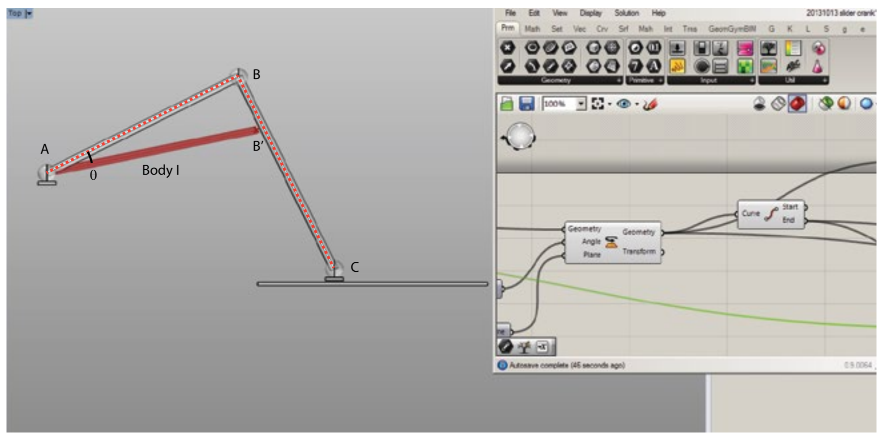


Image 2.16.B. Rotation of rigid body I.

Now the position of C’(θ) is found by considering that rigid body II has length defined and its end point C’ always lying on the roll sliding direction line: with this





observation point C’ is found by intersecting a circle with origin at B’ and radius equal to rigid body II center line length with the roll sliding direction line. Once point C’ is found the synthesis of the mechanism is complete (Image 2.16.C).

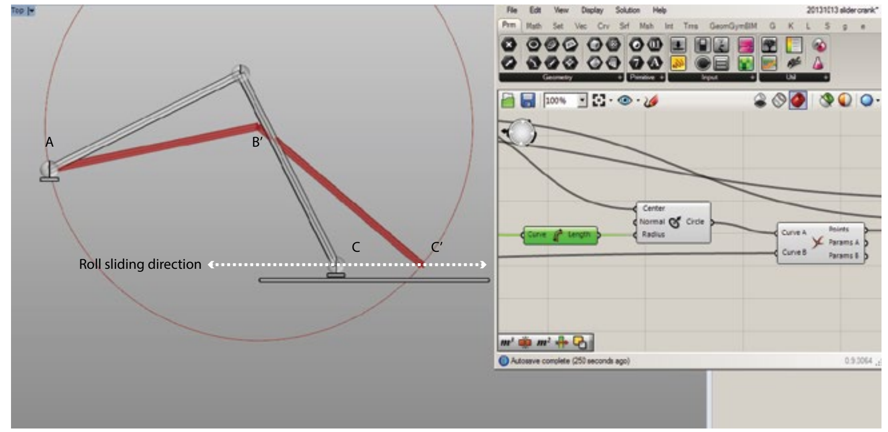


Image 2.16.C. Complete sinthesys of the mechanism.

Architect Santiago Calatrava made use of this simple mechanism to design a very elegant kinetic structure for the bay doors at Ernstings Warehouse (Image 2.17).

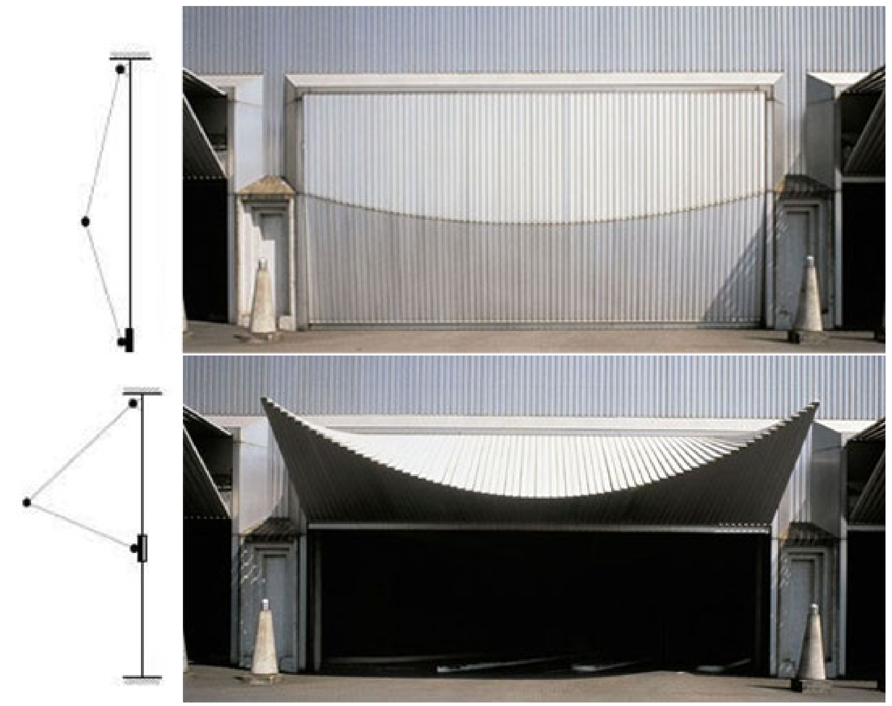

Image 2.17. Bay doors at Ernstings Warehouse, Santiago Calatrava design.

An animation of motion for the slider crank is presented in the frame below.

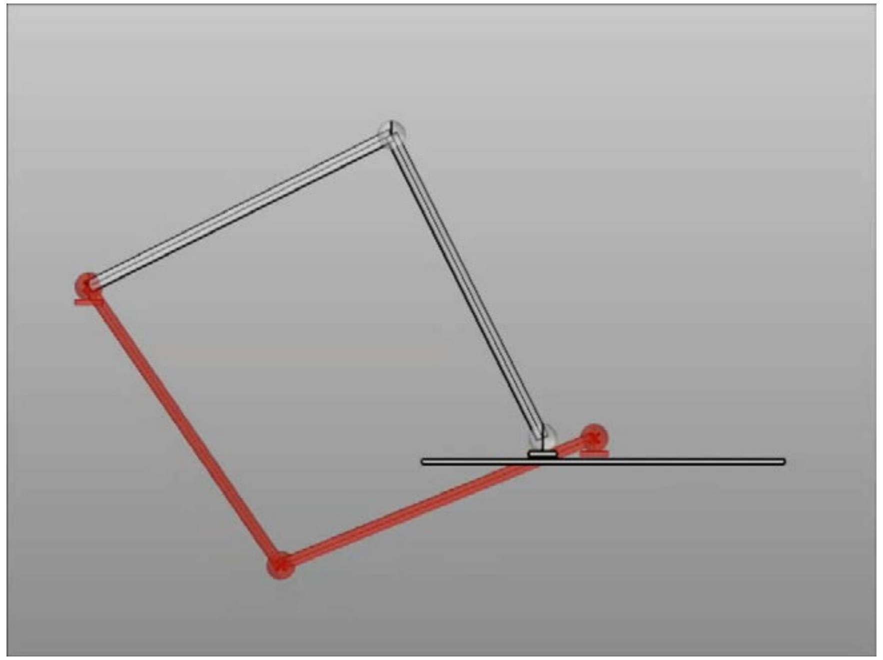

Animation 2.1
Slider crank.





### 2.2 Kinetics of 1D-rigid-bar Structures

Motion structures based on interconnected one-dimensional bars are the simplest and the most versatile systems. Due to their simplicity these structures have been the first motion system that have been designed and constructed by men.
Their strength stays in the fact that they can be, if properly designed, fully folded in a compact bundle of bars, and together with their lightness these can also be easily transported (De Temmerman 2007 and Gantes 2000).
For these reasons 1D-rigid-body structures are extensively designed for mobile shelters, retractable roofs, deployable space antennas and temporary emergency bridges.

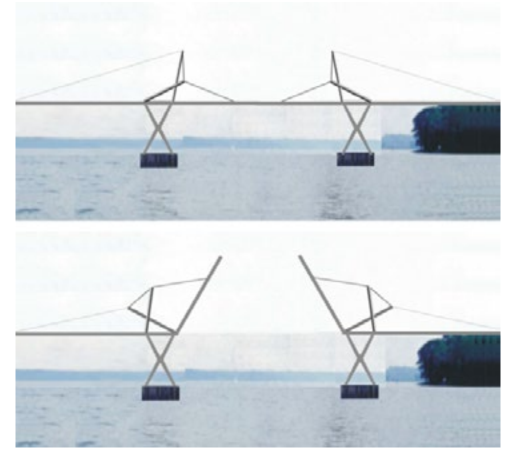

Image 2.18. Concept for a Movable bridge, based on 1D linkages (image courtesy of formfindinglab.princeton.edu).

From the architectonic point of view these system can only accomplish structural duties while further envelope or paneling functions must be integrated with these

From the design point of view the challenge consists of finding a kinematic configuration that allows structure to move, where all the elements displace in synchrony, and to avoid locking patterns that can block the motion

In the following section motion structures based on planar and spatial mechanisms will be synthetized by means of the associative geometric approach.

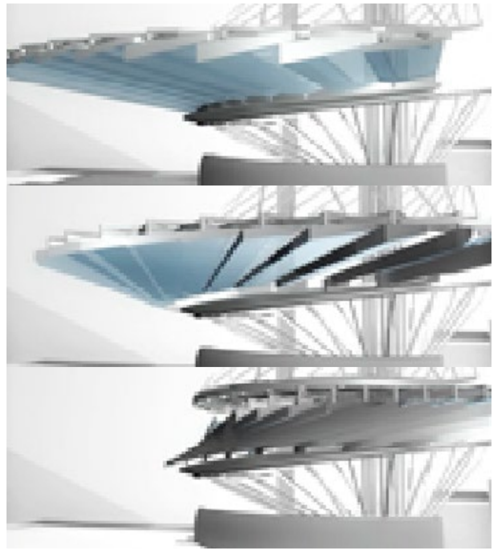

Image 2.19. Transformable Canopy SHoP and Hoberman design. The canopy is developed from a unique spiral geometry, constructed of structural panels and supported by a series of tension rods.

### 2.2.1 Kinetics of 1D-rigid-bar Structures based on Planar Mechanisms

Planar mechanisms based on 1D-rigid-bar are the simplest that can be designed. Mechanical engineering practice make an extensive use of these. Cam and gears are some examples of these simple planar mechanisms.
In architecture and civil engineering the 1D-rigid-bar motion structures are mostly based on scissor like element (SLE) and its derived assemblies. The SLE is also commonly known as pantograph or pantographic mechanism (Gantes 2000).

The prime component of a SLE consists of a pair of beams joined together by a pivot (a revolute joint) so that free rotation of one beam relative to another about the axis of the pivot is allowed and any other relative motion of the rod is prevented (De Temmerman 2007).

The conventional SLE is quite versatile. A number of element can be placed in a sequence to form a deployable assembly, also known as double chain (Image 2.20), because it appears like two interwoven individual chains. Carefully designed double chain can even expand to a curved profile (Gantes 2000).

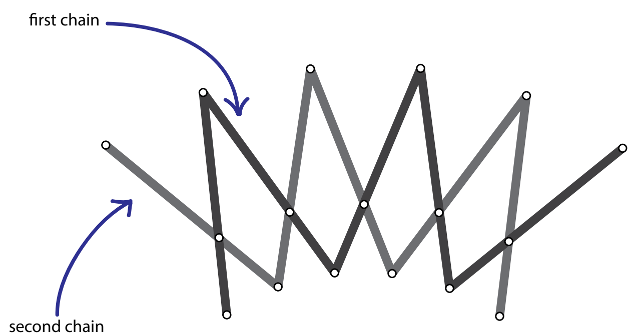


Image 2.20. Two interwoven kinematic chains form a curved linear SLE deployable element.

This model has achieved resounding success in the research field of deployable structures in fact, despite the Scissor Like Element (SLE) is based on an elementary planar mechanisms, this can be assembled in order to form spatial structures of several shapes.

By joining six struts together in three pairs of SLEs a ‘trissor’ (tri-scissor) is





obtained. Eight struts mounted together in four pairs of SLE’s forms a tetrascissor element (Gantes 2000).

Even if assemblies are now tridimensional, the mechanism that describes the motion still remain planar.
These two basic modules can be used as bays for flat slabs, shells and geodesic domes with different assembly patterns (Friedman 2012).

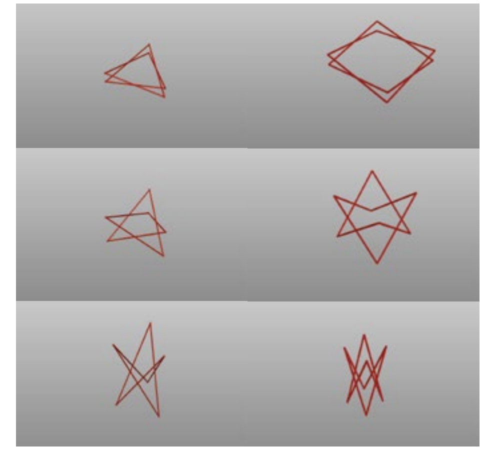

Image 2.21. Deployment process of a trissor and a tetrascissor element.

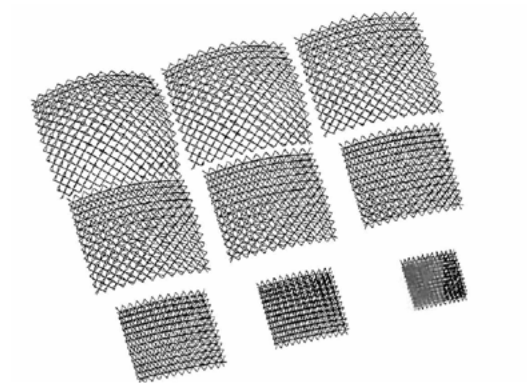

Image 2.22. A dome build with SLE elements during deployment (image courtesy of Emilio M. Gutierrez).

#### ***Kinetics of a Scissor Element and its Assemblies***

The conventional SLE kinematics is quite simple (Image 2.23 Left): being O the center of the motion plane and pivot of the elements with link length L, the displacement vector function of the angle $\alpha$, for instance of the upper-left node, is:

$$v_{node} = \begin{pmatrix} 0.5L(\cos\alpha - 1) \\ 0.5L\sin\alpha \end{pmatrix}$$

For spatial assemblies, in order to maintain rod length compatibility, a further motion vector for the plane on the SLE lays must be added (Image 2.23 Right). For instance, let us consider a tetrascissor element, whose parameters are the same as the SLE above introduced, moving about its barycenter. The plane motion vector of the first element is:

$$v_{plane} = \begin{pmatrix} 0.5L(1-\cos\alpha) \\ 0 \\ 0 \end{pmatrix}$$

By considering that the tetra-scissor element has four plane of symmetry the kinetic of the whole simplex can be easily generated.

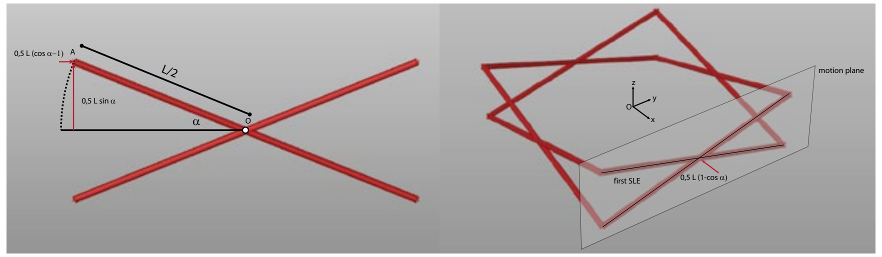


Image 2.23. Left: kinematics of SLE element. Right: motion place for SLE composing a tretrascissor element.

With the same approach kinematics of trissor and hexagonal SLE assemblies have been yielded (Image 2.21 and Animation 2.2).

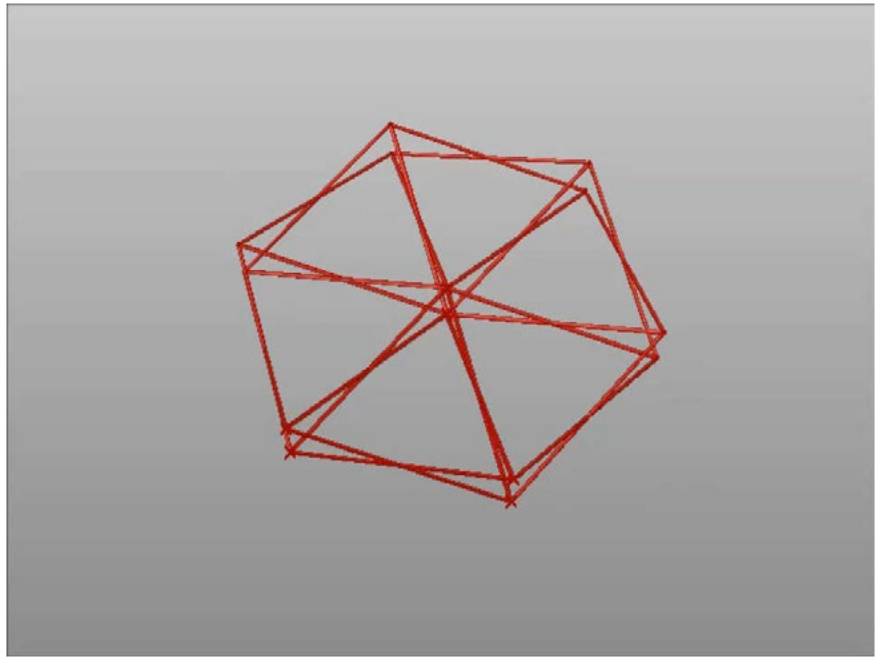

Animation 2.2
Hexagonal SLE structural modul.





### 2.2.2 Kinetics of 1D-rigid-bar structures based on spatial mechanisms

In architecture and civil engineering the use of spatial deployable mechanisms is very infrequent while all the knowledge regarding these systems has been developed within the field of mechanical engineering. The most interesting of these mechanisms stays in the category of over-constrained revolute joint mechanisms: these are closed chains of revolute joints (Image 2.25). According to the mobility criterion, to obtain a mobility of one, a single closed loop linkage with revolute joints needs seven links: however, the minimum number of links to construct a mobile closed loop with revolute joints has been found to be four with four links (You et al 2012).

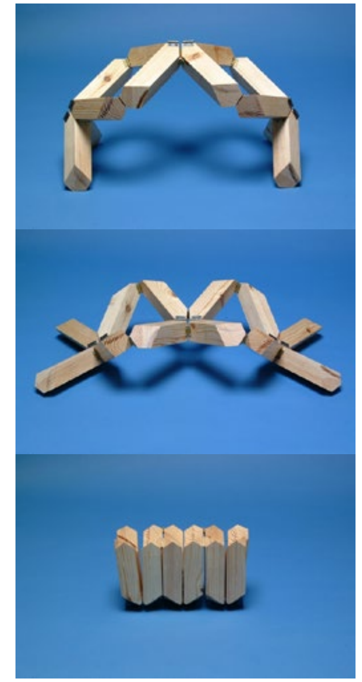

Image 2.24. Network of Bennett linkages (image courtesy of You et al 2012).

Their mobility is due to the existence of special geometry conditions between the links and joint axes that are often referred to over-constrained conditions. The invention of the linkages is driven by the kinematic challenges rather than the practical functions, which makes this linkage family known only academically: in fact, basically, mechanical engineers still prefer to design by means of well-known and tested simpler mechanisms (Deng et al 2008, You et al 2012). Although, over-constrained mechanisms shown in this research have a lot of potentiality in the field of civil engineering.

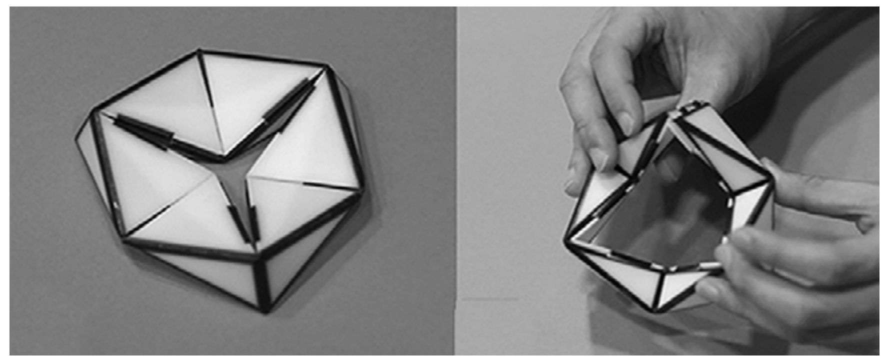

Image 2.25. An ovecontsrained mechanism as a closed chain of revolute joints

From the kinematic point of view an over-constrained mechanism is defined as a linkage that has more degrees of freedom than is predicted by the mobility criterion: if a system of links and joints has mobility $m=0$ or less, yet still moves, then it is called an over-constrained mechanism. Closed chain linkages have a good potential within the field of kinetic structures by way of they can provide very

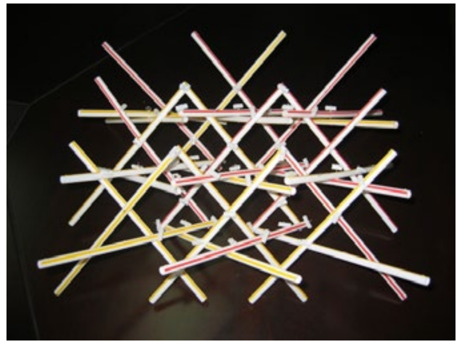

Image 2.26. Expandable arch based on a grid of Bennett linkages (image courtesy of Zhong You).

good stiffness and high expansion to packaging ratio and easily can be extended to large scale deployable networks (Wikipedia, Chen et al 2008, Liu et al 2009, You et al 2005 and 2012).
Additionally, because of being over-constrained, their full mobility can be actuated by a unique revolute joint activation, limiting at the least the number of motion actuators.

So far, a total of sixteen types of spatial over-constrained linkages with revolute joints have been discovered. Only two of these linkages (namely the Bennett and Bricard linkages) can be regarded as completely independent, whereas the rest are combinations or derivatives of the two linkages (You et al 2012).

Following these two mechanisms will be synthetized together with another well-known mechanism derived from the Bennett linkage, known as Myard Linkage.





***The Bennett linkage***

A typical Bennett linkage consists of a closed chain of 4 bars and 4 revolute joints (4R-Linkage) which span the shortest distance between two axes of adjacent joints, with these laying on the lines described by the vectors $s_1$, $s_2$, $s_3$ and $s_4$. Two opposite revolute axis intersect at point P and Q respectively: these mustn't be parallel neither concurrent. Each of the bars has lengths and twists identical to those of the bars which is not directly connected to it (You et al 2005 and 2012, Deng et al 2008).
A diagram is presented with the relative geometric and kinematic parameter associate to the model (Image 2.27).

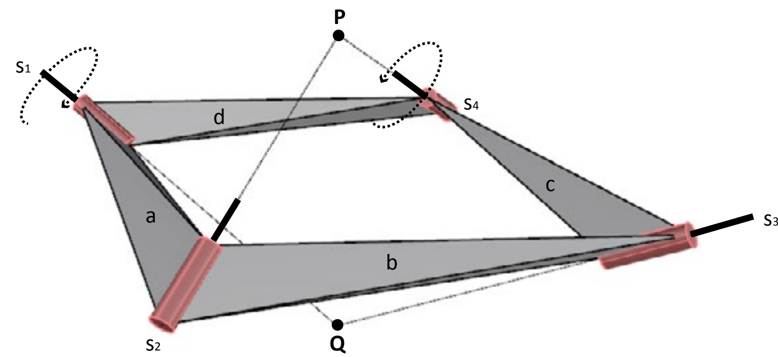


Image 2.27. Geometric set-up.

This system is known also as single-fold rotational symmetry linkage: its name comes from Dr. Geoffrey Thomas Bennett which discovered it in 1903 and identified mathematically the conditions for the linkage to have a single degree of freedom. At that time, the only multi-hinged mechanism with one independent variable discovered was a 7-rods-chain. Bennett used the fewest rods possible to build a useful mechanism
For Bennett linkage mobility formula is:

$$m = 6(4-1-4)+4 = -2$$

which shows this mechanism is highly constrained (You et al 2005 and 2012).

Due to symmetry, kinematics is described by two variables, the revolute angles $\theta_1$ and $\theta_2$; in addition, being the linkage overconstrained, the full motion can be triggered by only one of the variables.

Starting from the fully deployed configuration the mechanisms is in this way synthetized (Image 2.28): the variation of $\theta_1$ activate mobility of rods a and d together with the revolute axis $s_2$, and $s_4$ (intersecting at P): the only left unknown, the motion of revolute joint $s_3$ is yielded considering the symmetry plane $\Xi$ built on the vector $s_2$ and $s_4$, whose movement is activated by the instant variation of $\theta_2$ and intersecting at Q (or equivalently, on 3 points out of 4 that define vector $s_2$ and $s_4$). Hence $s_3$ is the symmetric geometry of $s_1$.

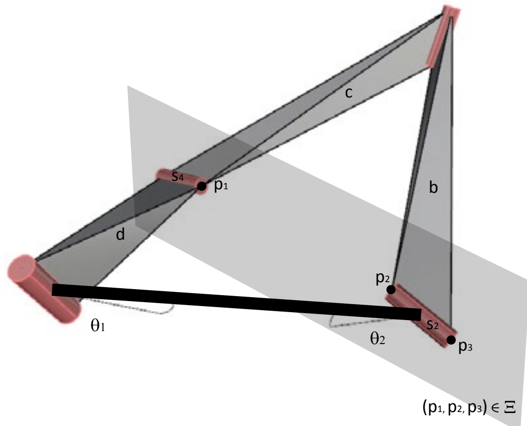


Image 2.28. Sinthesys for Bennett linkage.

The behavior of this mechanism, is strictly related to some basic geometric parameters (You et al 2012). A parametric model has been set-up in order to investigate linkage operability in relation to two design parameters: the rod corner angle $\omega$ and the axis tilting angle $\lambda$ (Image 2.29).

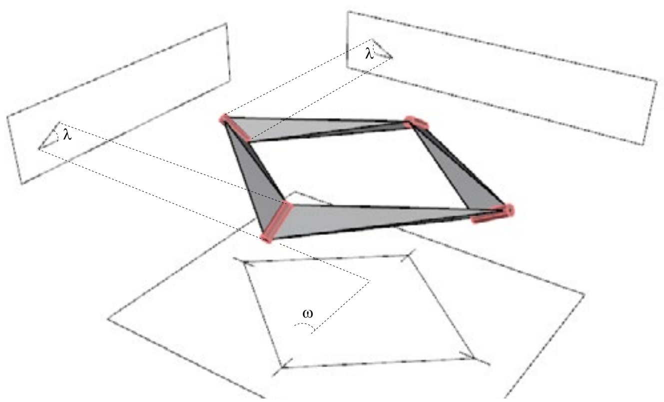


Image 2.29. Parameters for revolute joints and links.





Not all the sets of these angles allow the system to shift from a deployed rhombus to a fully compact bundle: heuristically two of these sets have been found (Image 2.30).

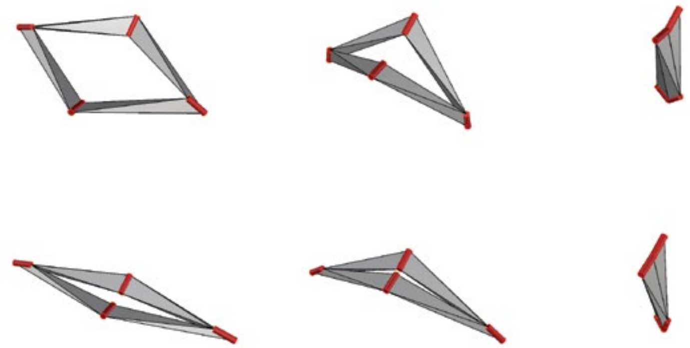

Image 2.30.
Top: a fully foldable Bennett linkage with $\lambda = 32°$ and $\omega = 30°$.
Bottom: a fully foldable Bennett linkage with $\lambda = 15°$ and $\omega = 10°$.

Additionally the relationship between $\theta_1$ and $\theta_2$ has been investigated: the reason for this study is to understand how fast a single module rotate or folds in accordance to the single variation of just one angle.

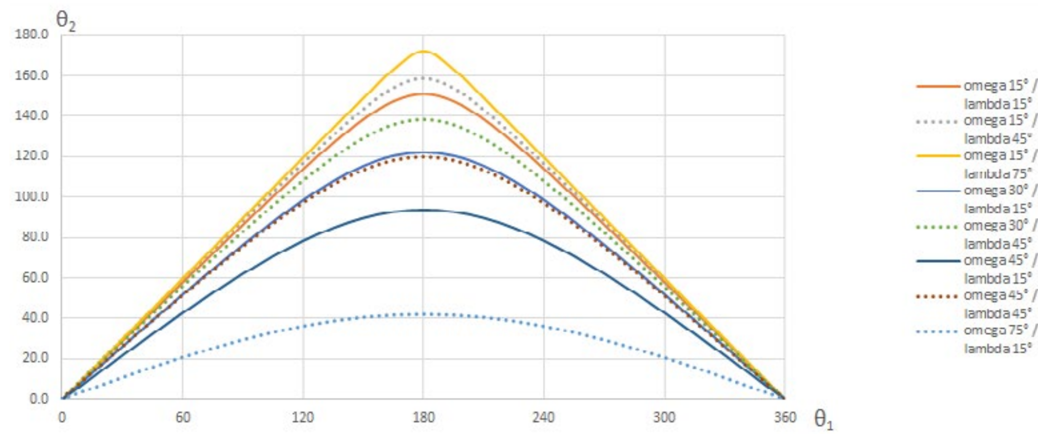


Graphic 2.1. Relationship between $\theta_1$ and $\theta_2$ for different parameters.

It is worth to mention that for the particularly boundary case of $\lambda$ equal to $\pi/2$ all the four revolute joint axis intersect at infinity, hence the mechanism in now planar, and nodes displacement vectors are parallel to the plane normal to the revolute axis.

An animation for the Bennett linkage, is presented in the frame below (animation 2.3).

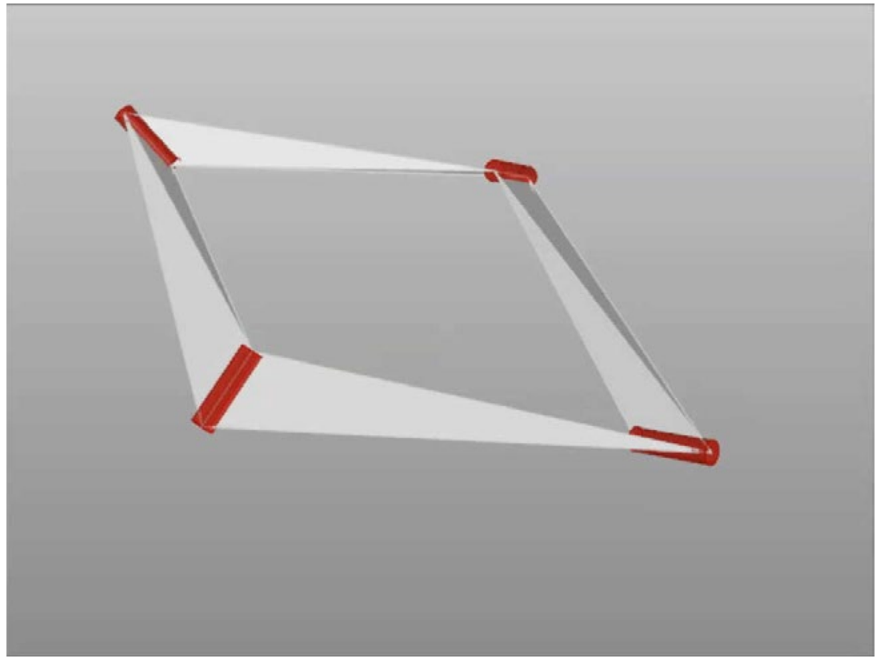

Animation 2.3
Bennett linkage.





***The Bricard linkage***

A Bricard linkage is a six-bar over-constrained mechanisms with equal number of revolute joints (You et al 2012). For Bricard linkage mobility formula is:

$$m = 6(6-1-6)+6 = 0$$

which shows this mechanism is over constrained (Chen et al 2004).

Consider a chain of six equal isosceles tetrahedrons (a, b, c, d, e and f), where each tetrahedron is linked to an adjoining one along an edge, which is the base of a triangle. If the height of the triangles is not smaller than their base, and the number of tetrahedrons is six, the ends of the chain can be brought together to form a closed loop (Image 2.31). This ring of tetrahedrons can turn round with continuous motion like a smoke ring (Chen et al 2004).

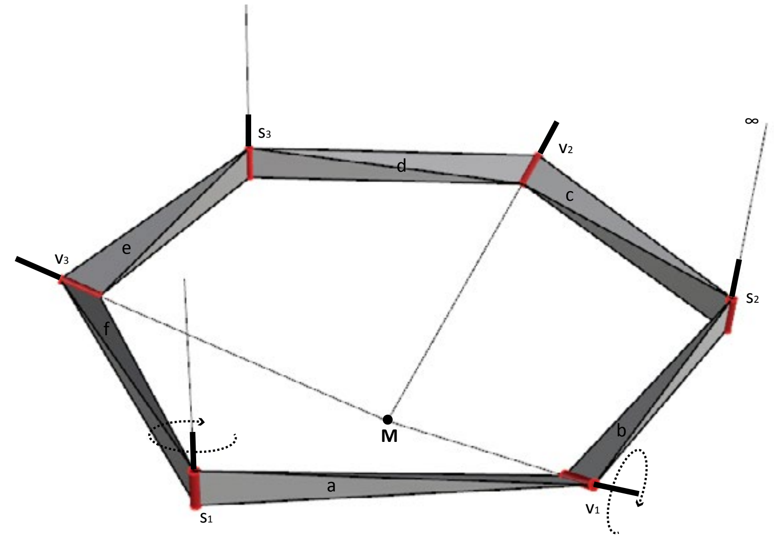


Image 2.31. Geometric set-up.

Peculiarities of this system is that on the common joining edges are laying the revolute joints, one different to each other's if are opposite, but with the odd ($s_i$) and even ones ($v_i$) with equal geometric parameters. The revolute axis $s_1$, $s_2$ and $s_3$ meet at point Q while $v_1$, $v_2$ and $v_3$ meet at point M: finally, a set of two tetrahedrons composing an elementary chain joint along $s_i$ rotate around this by $|\theta_1|$, while those having in common an edge collinear to $v_i$ revolve by $|\theta_2|$ (Deng et al 2008).

This angles are also the two kinematic dependent variable of the system. Hence, being the linkage overconstrained, the full motion can be triggered by activating only one of these angles.

The synthesis of the mechanism is fairly complicated, but facilitated by the fact that the Bricard linkage has three planes of symmetry in any configuration: for this reason the mechanisms is also well known as three-fold rotational symmetry linkage. By intuition it can be seen that these planes are the symmetric ones of the tetrahedron drawn through some elements that compose the system: this tetrahedron has as base the equilateral triangle passing by the revolting edge control points $p_1$, $p_2$ and $p_3$ and, as side triangles, three isosceles triangles with apex M or Q and as singular side the edge in common with the base. The full geometry can be reconstruct by looking at the consequences that the instant rotation of the independent variable $\theta_1$ causes: as soon as the variation of this angle triggers, for instance, rotation of bar a and b, the point M or Q moves in space. To reestablish tetrahedron symmetry conditions, the point $p_3$ is now sought as intersection of two circles: the first one has radius length constrained to the distance between point M or Q to the known position of point $p_1$ or $p_2$, $R_1$ equal to $||(M,p_1)||$, and the second one having as radius length the height of the tetrahedron base isosceles triangle, $R_2$ equal to $0{,}5||(p_1,p_2)||\tan(\pi/3)$. The tetrahedron depending on motion constrained geometries is now found as well as, finally, the three symmetric planes $\Xi_1$, $\Xi_2$ and $\Xi_3$ (Image 2.32).

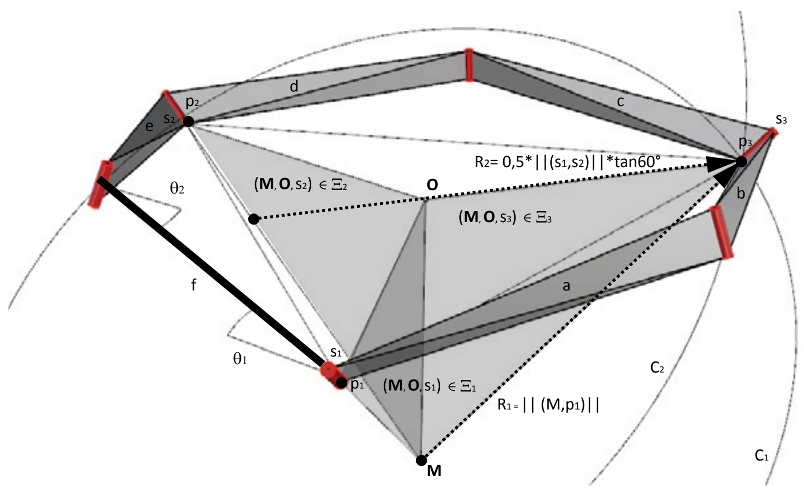


Image 2.32. Synthesis of Bricard linkage.



Chapter 2 // Motion Structures

A number of distinctive features of the threefold-symmetric Bricard Linkage can be recognized by studying the relationship among revolving axis geometric parameters and deploying behavior. The tilting angle parameter $\lambda_1$ and $\lambda_2$ is respectively introduced for the revolving axis $s_i$ and $v_i$ (Image 2.33).

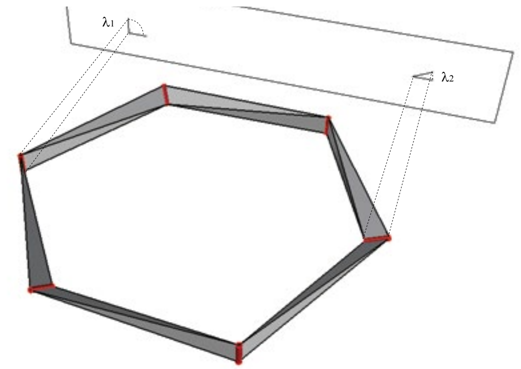


Image 2.33. Parameters for revolute joint typologies.

Considering the value of $\lambda_1$ locked at $\pi/2$, it has found experimentally (You et al 2012) and proved here with the associated geometry model, that for $0 \leq \lambda_2 \leq \pi/3$, or $2\pi/3 \leq \lambda_2 \leq \pi$ the movement of the linkage is not continuous. Thus, the linkage is physically blocked in the position where all links cross, at center, forming a 3-rays-star-like partially fold configuration (Image 2.34 Top).
In the particular case where $\lambda_2 = \pi/3$ or $2\pi/3$ angles $\theta_1$ and $\theta_2$ reach contemporary the value of $2\pi/3$, which correspond to a fully bundled outline: with this set of parameters, $\theta_1$ and $\theta_2$ change with the same speed, moreover it is easy to see that for $\theta_1 = \theta_2 = \pi/3$ the system undertakes a planar equilateral configuration (Image 2.34 Bottom).

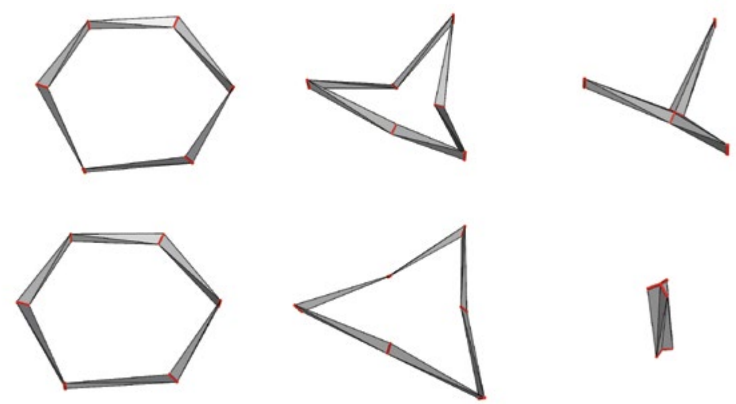

Image 2.34.
Top: a partially foldable Bricard linkage with $\lambda_1 = 90°$ and $\lambda_2 = 30°$.
Bottom: a fully foldable Bricard linkage with $\lambda_1 = 90°$ and $\lambda_2 = 60°$.

Finally the particular case of $\lambda_1$ and $\lambda_2$ equals to $|\pi/2|$ is not of interest for the spatial mechanisms because all the revolute axis meets at infinity in a plane that describe the planar motion of the linkage.

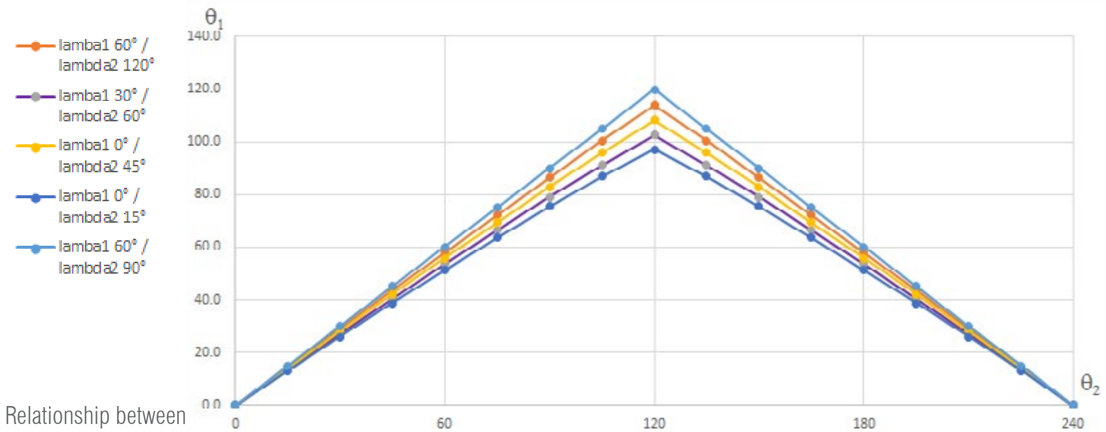


Graphic 2.2. Relationship between $\theta_1$ and $\theta_2$ for different parameters.

An animation for the Bricard linkage, is presented in the frame below (Animation 2.4).

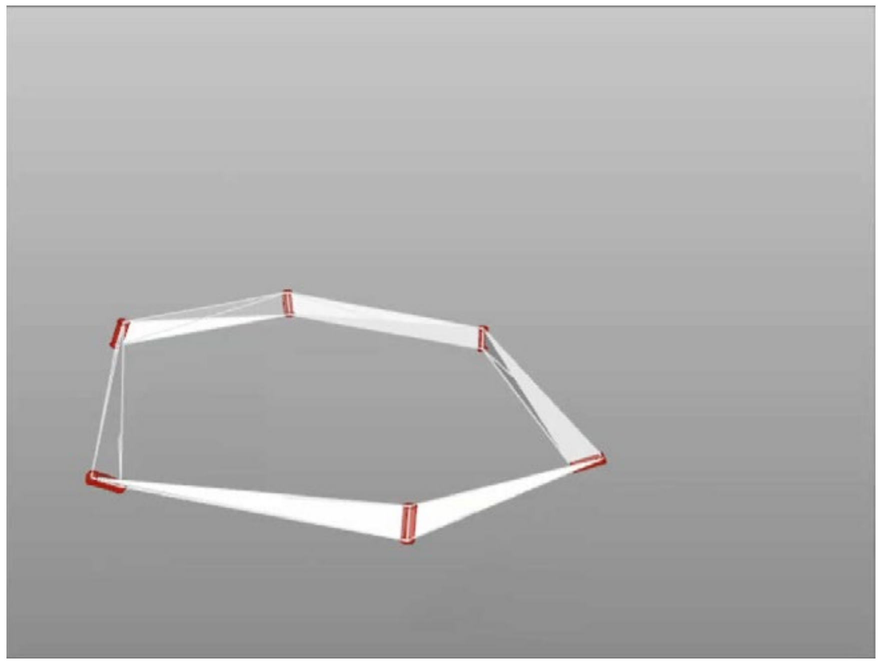

Animation 2.4
Bricard linkage.



Chapter 2 // Motion Structures

***The 5-R linkage and the Myard linkage***

A closed chain of five bars and five revolute joints is knows as 5-R linkage. Bars are assembled to form an irregular pentagon with a single plane of symmetry: for this last reason the behavior of this mechanism is firmly dependent to the Bennett's one (Chen et al 2008).

The five bars (a,b,c,d and e) are connected through three different revolve axis $s_i$, $v_i$ and $u_1$ (Image 2.35). To note that while orientation of axis $s_i$ and $v_i$ is arbitrary, the direction of the singular $u_1$ is dependent to these (Deng et al 2008).

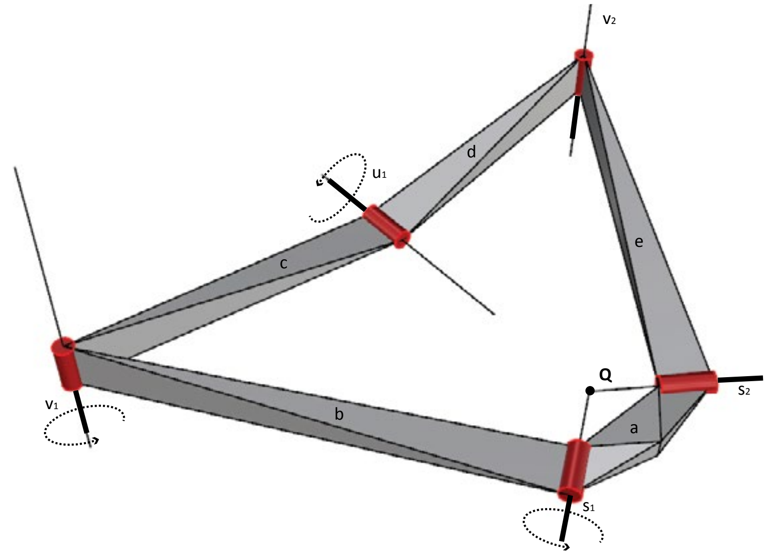


Image 2.35. Geometric set-up.

The rotation of the bars is described with 3 dependent angle variables $\theta_1$, $\theta_2$ and $\theta_3$. Being the mechanism over constrained the activation of one rotation is enough to initiate the full system motion. In the case the a bar length is zero the configuration takes the name of Myard linkage (Image 2.37).
For 5-R linkage mobility formula is:

$$m = 6(5-1-5)+5 = -1$$

which shows this mechanism is over constrained.

The kinematic hierarchy of the 5-R linkage is synthetized as follows (Image 2.36):

instant rotations of bars b and e around $s_1$ and $s_2$ by $\theta_1$ make the whole system active. Being unknown the relation between $\theta_1$ and $\theta_2$ the position of point P and revolve axis $u_1$ are sought by setting up some geometric relationships: for length compatibility, the point P is found by intersecting two circles $C_1$ and $C_2$ having radius length equal to bar c and d and always lying in the plane normal to the rotation axis $v_1$ and $v_2$. The last unknown is a second point M that together with P describe the revolute axis $u_1$. Point M continuous lies on the line $L = \Xi_2 \cap \Xi_3$, where $\Xi_2 = \{s_1, s_2\}$ and $\Xi_3 = \{v_1, v_2\}$. For symmetry, point $M = L \cap \Xi_1$, where the plane $\Xi_1$ is the unique linkage symmetry plane easily definable.

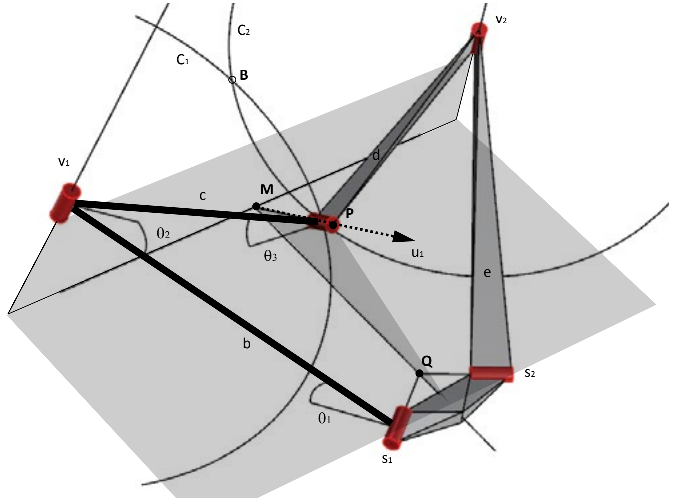


Image 2.36. Synthesis for a 5-R linkage.

To note that circle intersections has two solutions for $\theta_1 \neq 0$, the points P and B; this means that for $\theta_1 = 0$ the mechanism can undertake two different configurations.
This phenomena takes the name of kinematics bifurcation (You et al 2012).

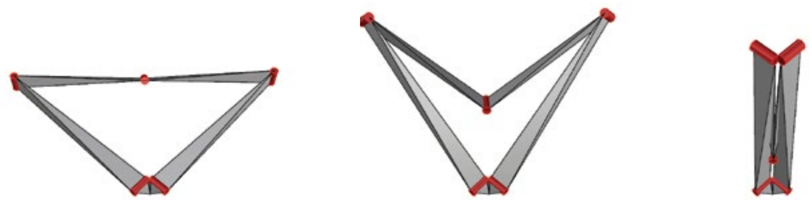

Image 2.37. Myard linkage during the folding process.





An animation for the Myard linkage, is presented in the frame below (Animation 2.5).

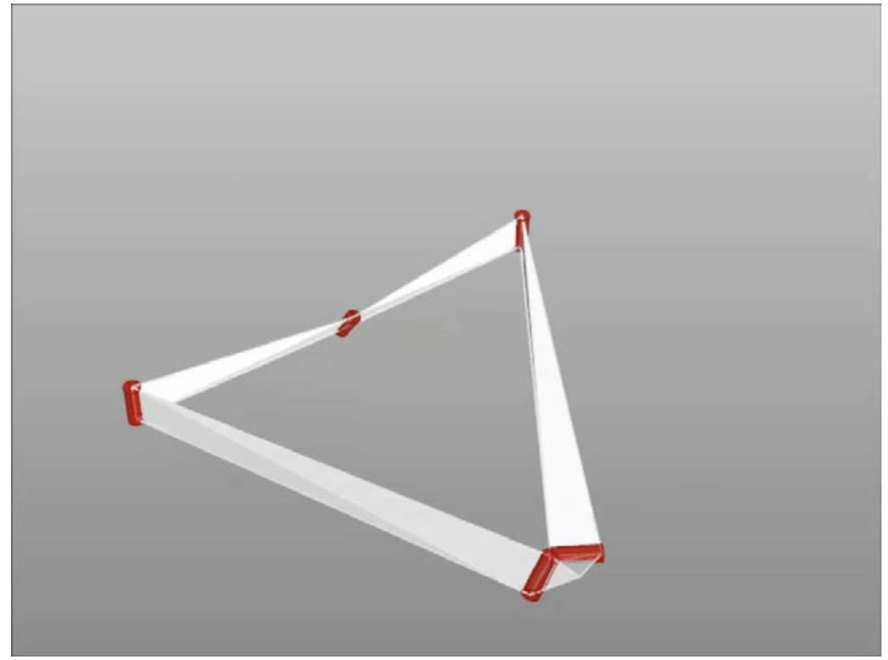

Animation 2.5
Mayard linkage.

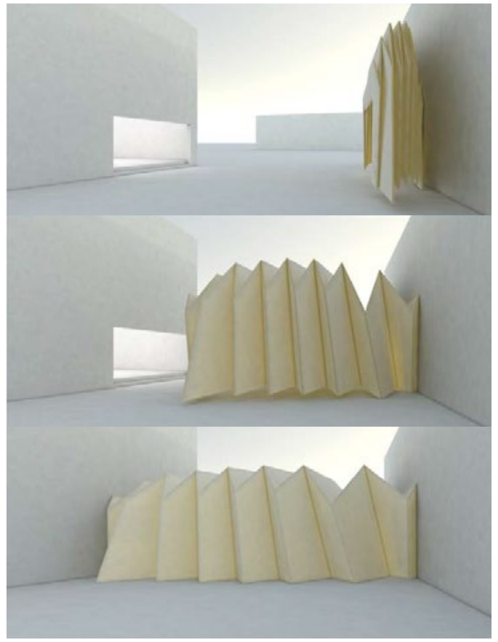

Image 2.39. Design concept for a foldable cover passage connecting two buildings (image courtesy of Tachi 2010)

### 2.3 Kinetics of 2D-rigid-panel Structures

Structures consisting on Two-Dimensional rigid panels are discrete developable surface that can realize a deployment mechanics if their facets and fold lines are substituted with rigid panels and hinges respectively (Tachi 2010).

Such systems can be classified in structures with planar mechanism and spatial mechanism.
In the first case two adjacent panels have a common seamed edge (a revolute joint) around which rotation of panels occurs: this allows panels to have one single rotational degree of freedom.
Generally assembly of panels that described a planar mechanism have only one seamed edge, while the remaining are free and unconstrained. The mechanism of these systems can be associate to linear one-dimensional kinematic chains, where the number of DoF's is equal, in the planar mechanism, to the number of panels connected among each other by revolute joints.
These systems take the name of planar mechanism because the hinges are normal to the planes onto which planar mechanism is described .

In opposition, in order to have a spatial mechanism panels in the assembly must have more than one seamed edge.

Image 2.40. Shenzen Airport, Massimiliano and Doriana Fuksas design. An example of functional integration of structure and environmental control executed by 2D-rigid panels.





Designing such a deployment mechanism has a significant meaning in an engineering context, particularly in architecture for the following reasons (Tachi 2010):

- The structure based on a watertight surface is suitable for constructing an envelope of a space, a roof, or a facade. Here there is a matching of structure and accessory function that panel can execute.

- Purely geometric mechanism that does not rely on the elasticity of materials can realize robust kinetic structure in a larger scale under gravity.

- The transformation of the configuration is controlled, in case on spatial mechanism, by a small number of degrees of freedom. This enables a semi-automatic deployment of the structure.

Image 2.41. EN-FOLD, Woods&Bagot design: a foldable 2D-rigid structure working as envelope (image courtesy of Woods&Bagot).

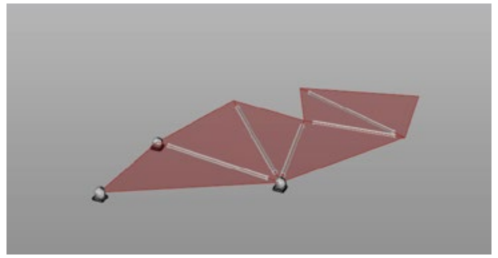

Image 2.42. An irregular bi-pyramid unfolded in a continous strip.

### 2.3.1 Kinetics of 2D-rigid-panel Structures based on Planar Mechanisms

A basic planar mechanism composed by assembly of two-dimensional rigid panels is here researched. This is a bi-pyramid composed by 2 irregular tetrahedrons with six facets. Seamed edges have been chosen in order to obtain in the full deployed state a flat stripe of facets (Image 2.42). Unfolding a polyhedron into a flat pattern is a particular and well-known problem that have been extensively researched by mathematician: with these method is possible to unfold any kind of facet discrete surface (Demaine 2007).

From kinematics point of view such a structure is a kinematic chain composed by six rigid bodies: if one facet is fully constrained, and considering that the possible motion of a panel with respect to the adjacent one is an unique rotation around the common seamed edge, the systems has now five independent DoFs, so that five independent actuators are needed to fully control the motion of the system that can move in $\infty^5$ possible configurations.

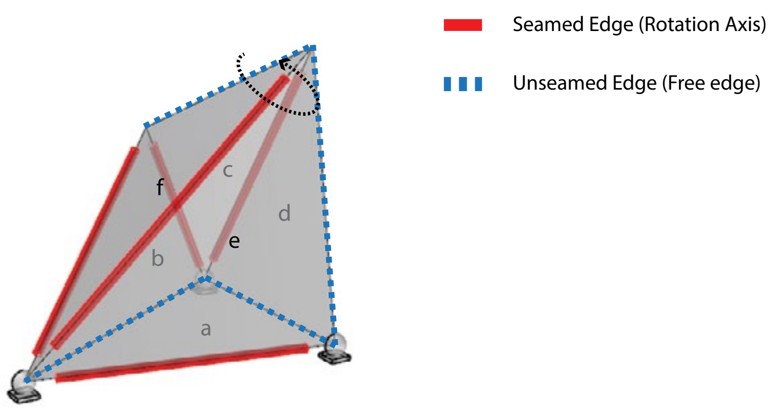


Image 2.43. Revolute joint set-up.

The synthesis of the mechanism for such a structure is simple: after revolute joints (matching with the seamed edges) are defined, also the planes normal to these can be associated (Image 2.43). These are the motion planes through which the movement of each facet can be described: in other words, the minimum distance between any point of the panel and the plane itself remaines the same. The parametric model has been implemented so that during folding the facets





are synchronized in order to arrive contemporary to a final closed polyhedron configuration once fully folded and to a flat strip after deployment (Animation 2.6).

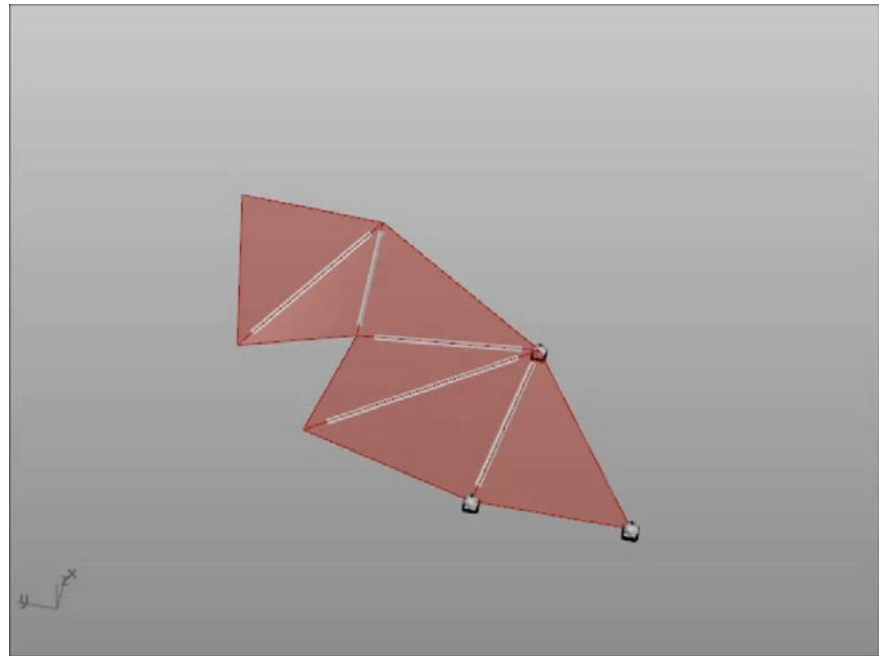

Animation 2.6
By-pyramid unfolding.

This easy example of mechanism of a 2D-rigid panel assembly is only one of the wide range of possible configurations that can be designed based on planar mechanisms. Another system is presented (Image 2.45).

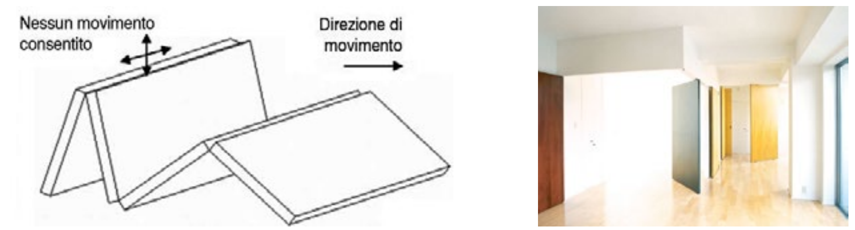


Image 2.44. Void/Space Hinged Space, Steven Holl design (image courtesy of Beatini 2006)

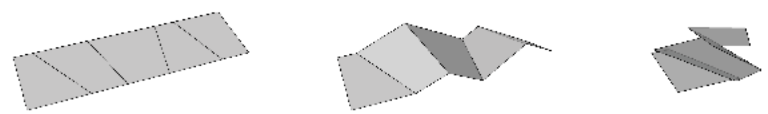

Image 2.45. A continous strip of facets folding like an accordeon.

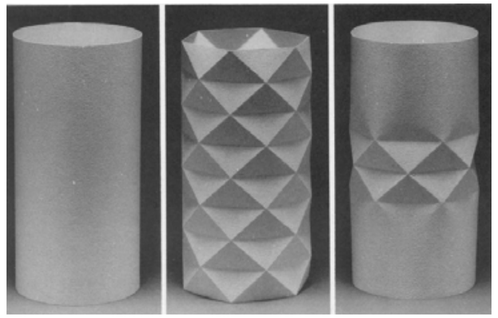

Image 2.46. Yoshimura pattern, another well-known rigid origami system.

### 2.3.2 Kinetics of 2D-rigid Panel Structures based on Spatial Mechanisms

In this section spatial mechanisms based on assembly of two-dimensional rigid panel systems are investigated. These systems are basically transformable polyhedral surfaces with rigid facets that can be also demarcated as rigid origami (Tachi 2013).

In general, there is no guarantee that a developable folding pattern applied on a mesh can be folded: the reason for this is that facet rigid roto-translation might be locked in the case the geometric constrain characteristic of the whole facet collection doesn't provide a mechanism.
The first step to design such a system is to find a pattern that allows facets to undergo rigid roto-translation: this is a particular challenging tasks that only mathematicians have been able to solve by developing that particular branch of mathematics known as mathematics of paper folding or mathematics of rigid origami (Demaine 2007).

Aim of this section is not to find new folding pattern, but to synthetize those already discovered by the precursors of this disciplines. In particular the motion of three well-known foldable origami patterns will be synthetized.

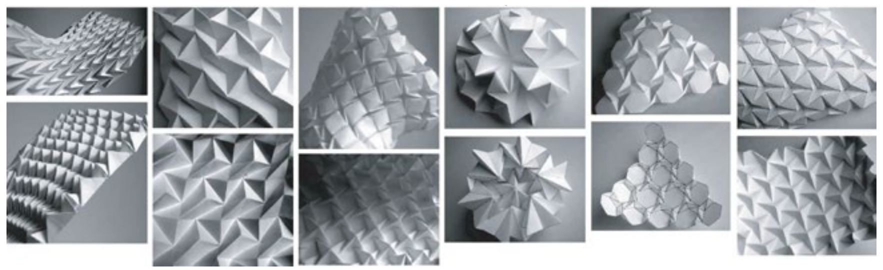

Image 2.47. Ron Resch's patterns

These three patterns have been invented by the American mathematician Ron Resch (Resch 1972and Tachi 2013). Resch proposed a rigorous analytical method to study the kinematics of these systems: this approach is based on the use of rigid transformation operators that guarantee that facets undergo a rigid body motion.
Resch's patterns are 1 DoF systems: this means that the single motion of one facet will trigger folding or deployment of the whole mesh composed by n facets.
The pattern invented by Resch are also well-known as waterbomb patterns (Tachi 2010) for the visual effect given by the mesh during deploying.
In opposition to Resch's mathematical method, a geometric synthesis approach will be used.

First the geometric relations of a single module will be sought by means of the associative geometric approach. Coming up the motion of assembly of several modules will be reproduced by means of a physical simulation engine Kangaroo (§2.4), that is integrated with Grasshopper™.

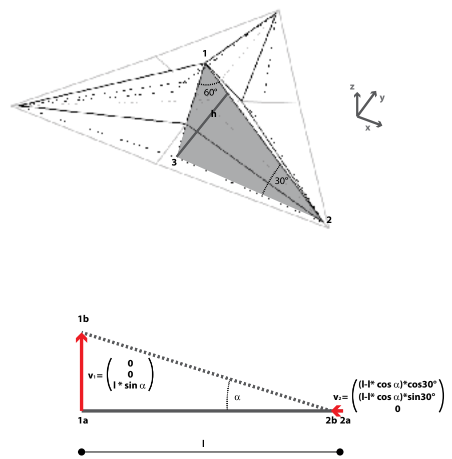

Image 2.48. Geometric set-up.

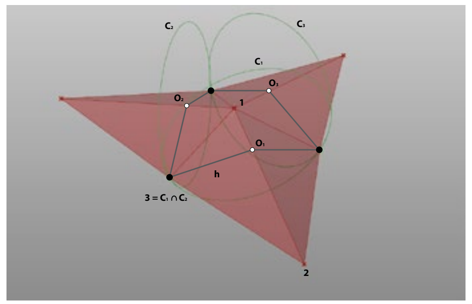

Image 2.49. Geometric relationships to yield position of the 3rd point of the facet.

### *Star-like triangular pattern*

An equilateral triangle is the simplex of this pattern. This triangle is discrete with 6 sub-rectangular triangles whose hypotenuses with length l are the bisectors of the angles of the main equilateral triangle.

Being 1 and 2 the respectively the inner and outer vertex of the hypotenuse above considered, the displacement vectors of these nodes, function of the unique DoF angle $\alpha$, are respectively:

$$v_1 = \begin{pmatrix} 0 \\ 0 \\ l\sin\alpha \end{pmatrix}$$

$$v_2 = \begin{pmatrix} -l(l-\cos\alpha)\cos 30° \\ l(l-\cos\alpha)\sin 30° \\ 0 \end{pmatrix}$$

At this point the challenge consists on finding the position of the third point in order to maintain facet rigidity under motion. As hypothesis, if the facet doesn't deform also the height h of the rectangular triangle facet with hypotenuse as base doesn't change in length.

Moreover it can be seen that the point 3 sought is in common with adjacent triangles. The problem is solved by looking at the intersection of two circles ($C_1$ and $C_2$) having radius equal to h and being laying in a plane normal to the hypotenuse at $O_1$ passing by the height h inner vertex. To note that contiguous circles intersect twice, but only one is compatible with the sought solution.

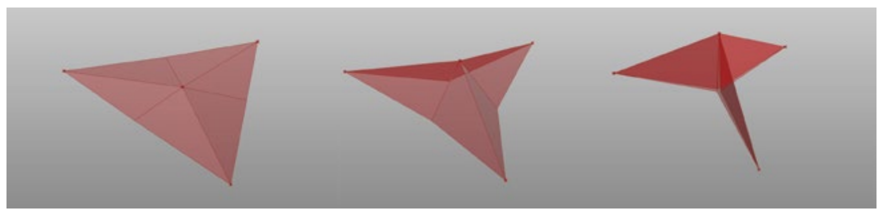

Image 2.50. Simplex deployment

Finally, the motion of the simplex is fully solved considering that this is characterized by having three plane of symmetry intersecting in its barycenter. Once the simplex is folded this takes the shape of a three-ray star (Image 2.50).





This module has been used to design the reactive façade of the Al Bahr towers (§2.1.1).

The simplex can be also repeated following Resch's layout (Animation 2.7): in order to have a continuous mesh in-between triangles are seamed to outer edge simplexes. These last, during motion, undertake a planar rotation in synchrony with simplex folding.
This system was used to build the prototype for an adaptive acoustic ceiling at the University of Michigan (§2.1.1). Authors (Thün 2012) used based the design procedure by means of the same physical simulation engine adopted for this research.

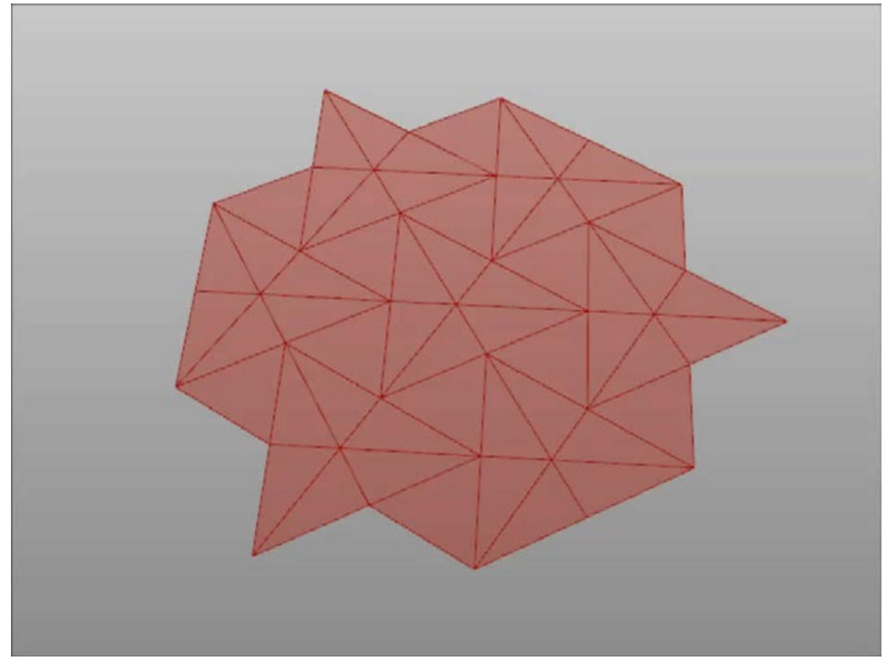

Animation 2.7
Star-like triangular pattern.

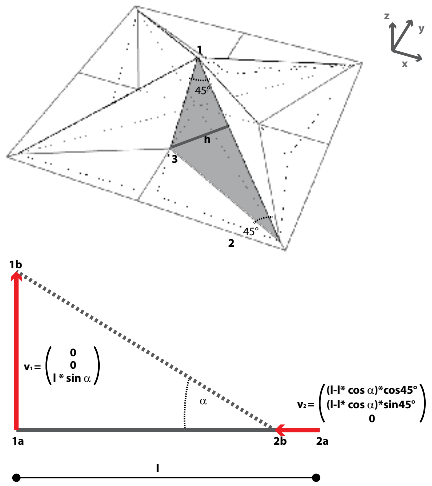


Image 2.51. Geometric set-up.

### *Star-like square pattern*

A square is the simplex that composes this pattern. The square is subdivided with 8 rectangular isosceles triangles with hypotenuse of length l defined by the bisector of the square, and basis of length b defined as half edge length of the square

The point 1 and 2 are respectively the inner and outer vertex of the hypotenuse of one of the rectangular isosceles triangle that describe one facet of the simplex. The displacement vector of these nodes, function of the unique DoF angle $\alpha$, are respectively for the highlighted panel:

$$v_1 = \begin{pmatrix} 0 \\ 0 \\ l\sin\alpha \end{pmatrix}$$

$$v_2 = \begin{pmatrix} -l(l - l\cos\alpha)\cos 45° \\ -l(l - l\cos\alpha)\sin 45° \\ 0 \end{pmatrix}$$

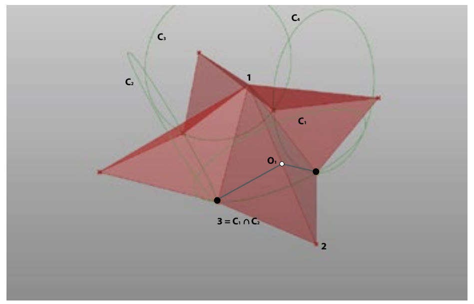

Image 2.52. Geometric relationships to yield position of the 3rd point of the facet.

The relation between the angle $\alpha$ and the angle that describe the rotation of the edge 1-3 is not linear. In order to yield the position of the third point of the triangle during folding and to maintain facet rigidity, its position has been sought as intersection of two circles having as radius the height h of the rectangular triangle with hypotenuse as base.
For the highlighted facet, the two circles $C_1$ and $C_2$ with origin in $O_1$ and laying in a plane normal to the hypotenuse intersect at point 3. To note that contiguous circles intersect twice, but only one is compatible with the sought solution.

Finally, the motion of the simplex is fully solved considering that is characterized by having four plane of symmetry intersecting in its barycenter. Once the simplex is folded takes the shape of a four-ray star (Image 2.53).

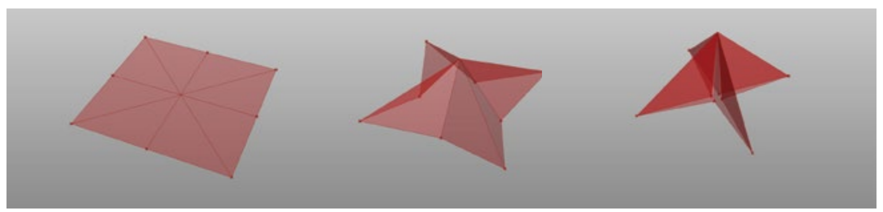

Image 2.53. Symplex deployment.





Folding of an assembly of 4 seven star-like simplexes is then reproduced: in order to have a continuous mesh in-between squares are seamed to outer edge simplexes. These last, during motion, undertake a planar rotation in synchrony with simplex folding (Animation 2.8).

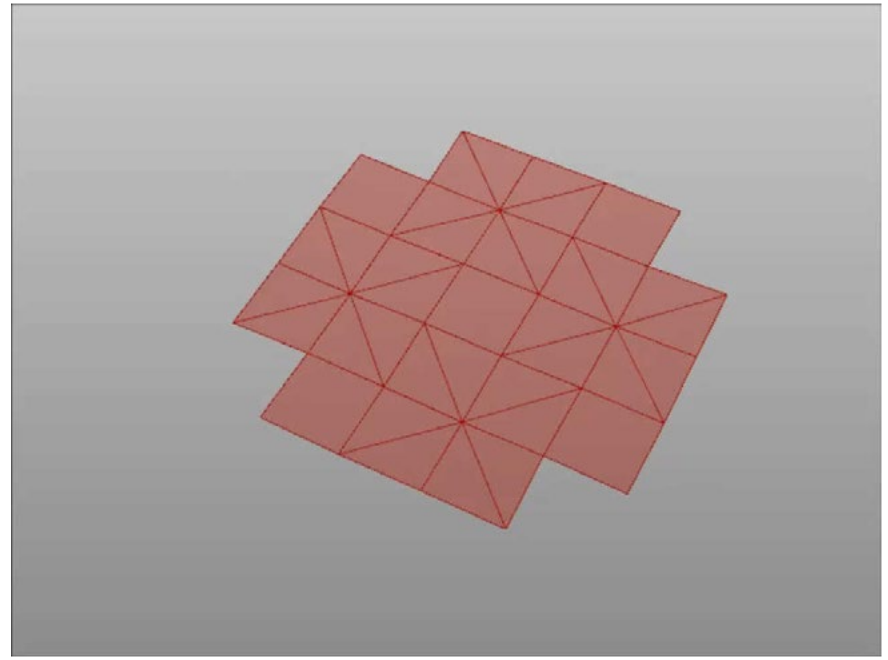

Animation 2.8
Star-like square pattern.

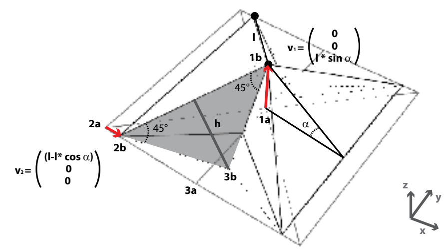

Image 2.54. Geometric set-up.

### *Pocket-like square pattern*

A square is the simplex that composes this pattern. The square is subdivided with 2 big rectangular isosceles triangles and four small rectangular isosceles triangles: these last are basically equal to the two big rectangular isosceles triangles divide by two by one of the symmetry axis of the main square. Being all the facets rectangular isosceles triangles they have same proportions.

The motion of the simplex is described by the rotation angle $\alpha$ of the height of one of the big facet. Being the point 1 and 2 respectively the inner and outer vertex of the hypotenuse of one small facet, the displacement vector of these nodes, function of the unique DoF angle $\alpha$, are respectively, for the highlighted panel:

$$v_1 = \begin{pmatrix} 0 \\ 0 \\ l\sin\alpha \end{pmatrix}$$

$$v_2 = \begin{pmatrix} l - l\cos\alpha \\ l - l\cos\alpha \\ 0 \end{pmatrix}$$

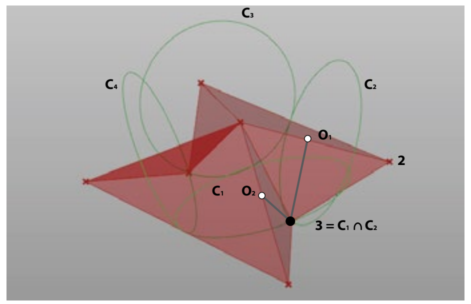

Image 2.55. Geometric relationships to yield position of the 3rd point of the facet.

The motion vector above introduce is enough to described the rigid body motion of the big facets but doesn’t solve completely the kinetic of the small ones.

The position of the third point that is in common with adjacent small facet is found at the intersection of two circles ($C_1$ and $C_2$) having radius equal to h and being laying in a plane normal to the hypotenuse at $O_1$ passing by the height h inner vertex. To note that contiguous circles intersect twice, but only one is compatible with the sought solution.

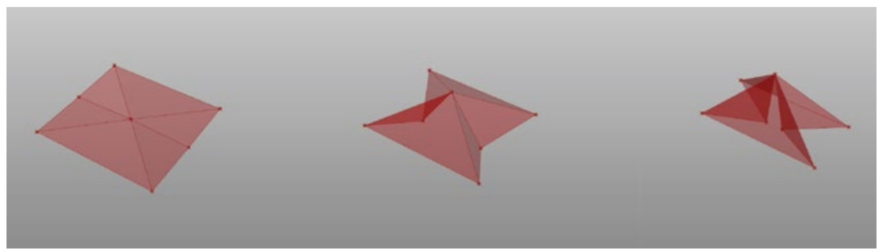

Image 2.56. Simplex deployment.





By mirroring the remaining vertices about the planes of symmetry easily recognizable from the simplex, the rigid body motion of the full simplex can be finally described. Once the simplex is folded takes the shape of a porte monnaie (Image 2.56).

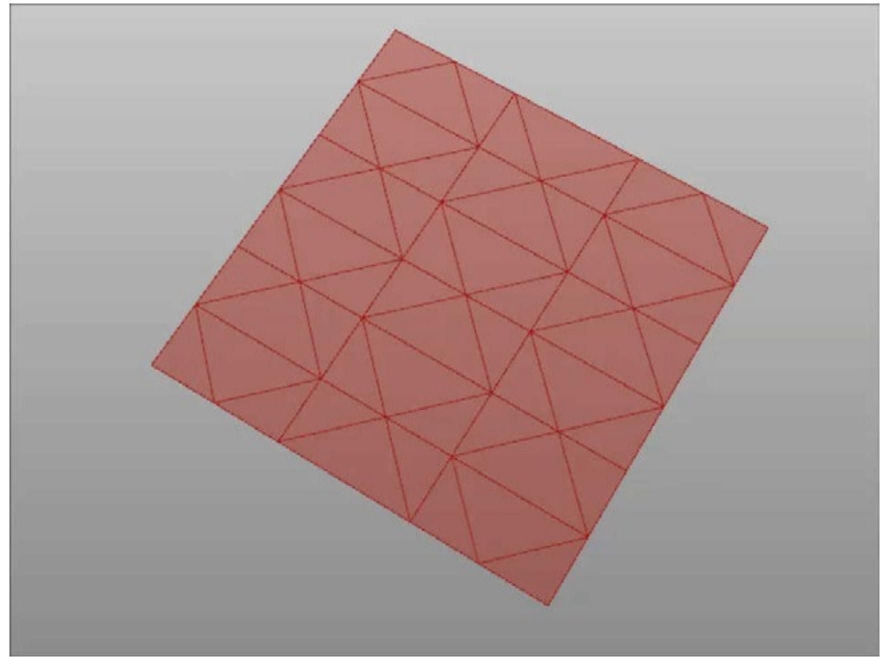

Animation 2.9
Pocket-like square pattern.

The simplex can be also repeated following Resch’s layout: in order to have an unlocked continuous foldable system the surface is assembled by 3 linear array of simplexes, where the middle strip of simplexes is shifted by half edge length. This configuration is needed to obtain a synchronized motion of the whole assembly (Animation 2.9).

Image 2.57. A stress-ribbon rigid deck together with two further ties compose this lightweight bridge. RFR design.

## 2.4 Kinetics of Tension Structures

Tension structures are a particular typology of space structures where a great part of the elements is in tension with further compressive parts that mutually collaborate to obtain a state of equilibrium.

In the recent years, space structures as a whole are becoming lighter, and even lightness has become a fashion in aesthetics. A common phenomenon is that tension structures are becoming more and more popular as these structures extend architects' imagination due to cables lightness, unlimited length and versatility. The combination of tension structures with roof material, such as glass and membrane, expresses the sense of transparency of space and lightness of forms (Wang 2004). Architects continue to be excited by their light weight and their apparent transparency (Kazi Aoual et al 2004).

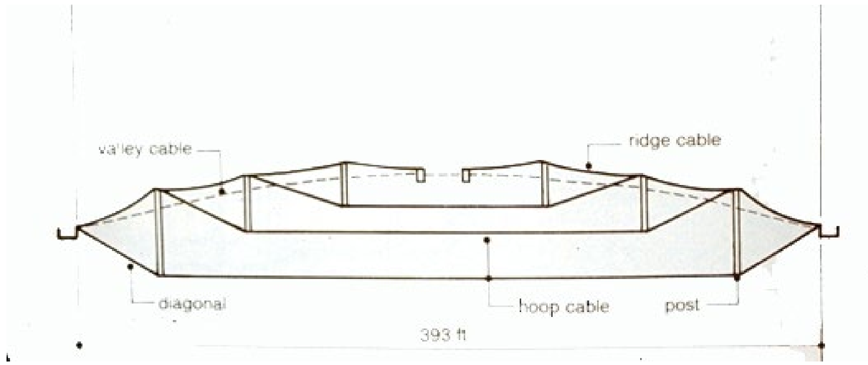


Image 2.58. Geiger's dome, an example of tension structure.

Strut-and-ties assemblies are three-dimensional truss-like structures: normally they are composed by simple one dimensional elements, however the elements that compose these systems can be also two-dimensional or even three-dimensional.
For sake of clarity, in this thesis, tension structures are defined generally as strut-and-ties assemblies, and with this term we refers also to those systems that have one, two or three dimensional 'struts' (here intended as generic compressed, or mainly compressed elements) and one (like cables)or two dimensional (like membranes) 'ties'(here intended as generic tensile elements).
The way how struts are connected among them can be used to distinguish two main families of tension structures: tensegrity and nD-strut-and-nD-tie assemblies.





Following the definition of tensegrity proposed by Wang (2004) clearly defines the differences between the two systems:

*A tensegrity (structure) is a stable (free-standing) volume that is realized by the interaction between isolated struts (island of compression) and interconnected cables (a sea of tension).*

The same definition can be implemented for tensegrity with higher dimensional struts or ties (Table 2.2).
In comparison with the definition of tensegrity systems, strut-and-tie systems remove the restriction of isolation of struts. In strut-and-tie simplexes, struts are allowed in contact, giving the freedom in designing short struts and/or reducing strut number (Wang 2004).

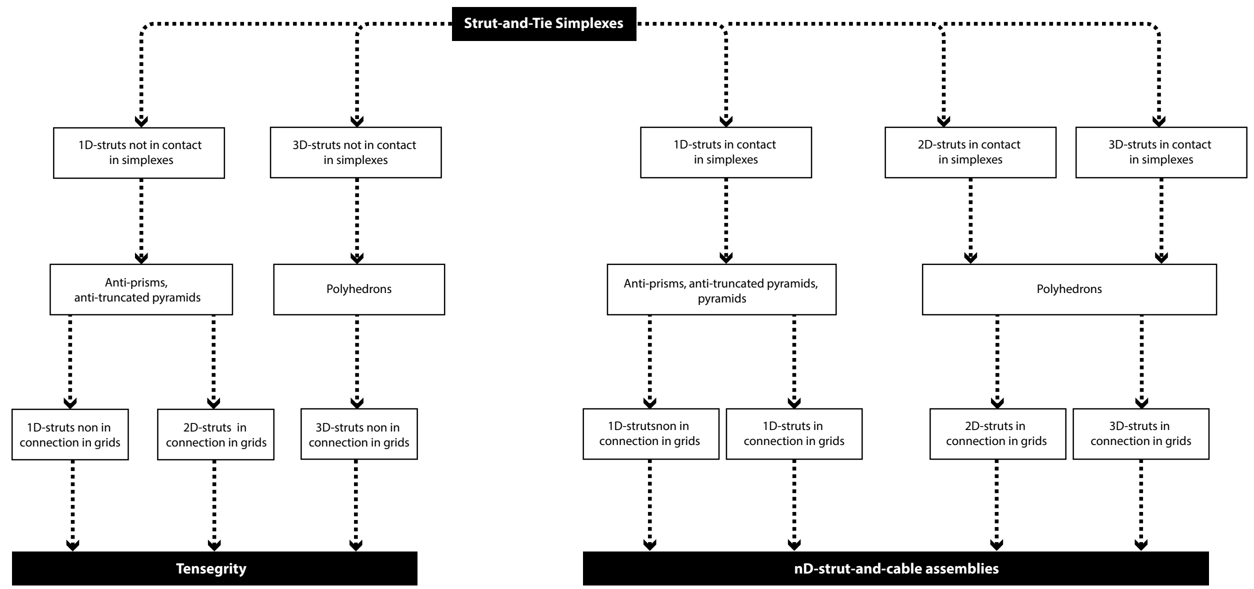


Table 2.2. Cathegorization of tension strctures: in turn adapted from Wang 2004.

What make these systems interesting to be studied are their mechanical characteristics: the strength of these lays in the relation between shape and load path resulting in a combination of lightweight and functionality. Forces are limited to normal actions making optimal use of material and cross section since the stress on the structure is spread evenly, in contrast to bending, where peak stresses at the

outer fibers determines the required strength (De Boeck 2013).
Structural efficiency is maximized by having the majority of elements in tension being the most efficient use of material resulting into relative small cross sections. Finally strut-and-tie assemblies have statically and kinematic non-linear behavior due to the fact that large displacements undergoes in these systems (geometric non-linearity) and ties element can only support tensile forces (physical non-linearity).

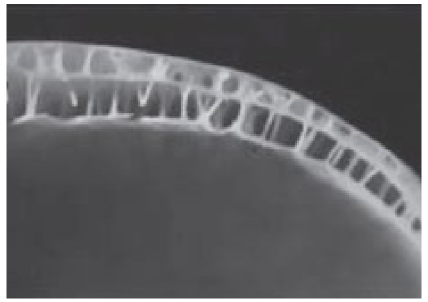
Image 2.59. Magpie skull.

### *Form Finding Procedures*

Form and force are correlated, in that the form of a structure can be determined as the state in which the forces acting in and on it are in equilibrium (Hensel at al 2004). This observation on the nature of structure is particular valid for those assemblies, like tension structures, that organize themselves in an optimal shape in space according to a define set of forces and boundaries conditions.

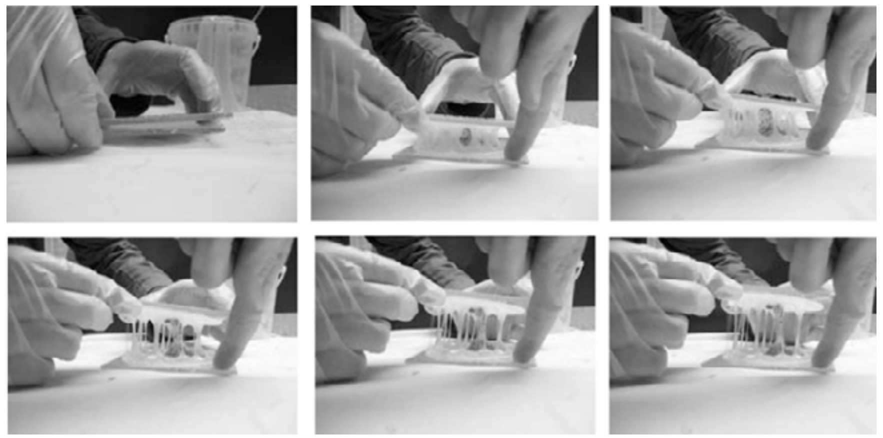
Image 2.60. Form-finding process with a viscous material (image courtesy of Andrés Harris).

This concept is also applied for structure based of strut-and-tie assemblies: these are layout by triggering the structure to adapt in order to find the optimal shape under any load case.

Form finding is a design procedure, based on empirical, mathematical or generative processes that utilize the self-organization of material systems under the influence of extrinsic forces.





The range of possible forms is determined by the choice and definition of the conditions under which the form-finding process takes place (Hensel at al 2004). Complex adaptive systems entail processes of self-organization and emergence.

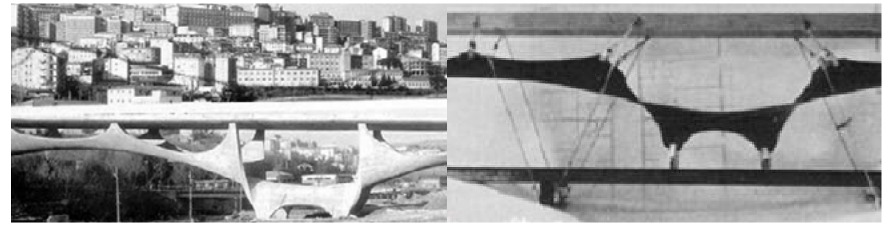
Image 2.61. Left: Basento Bridge, Sergio Musmeci desing. Right: model in neoprene.

Self-organization can be described as dynamic and adaptive process through which systems achieve and maintain structure stability without further external control. Common form-find methods, deploy the self-organization of material systems exposed to forces to achieve optimization of performance capacity (Weinstock 2004).

An interesting definition of form finding has been given recently by the Israeli architect Neri Oxman as result of her research on the work of Buckminster Fuller, another great pioneer on finding forms:

> *They asked not what an object wants to be, but what a material wants to be.*

There are several way to form find a structure: historically the first form-finding procedures have been developed by means of physical models. Well-know are the fully compressed arcs designed by Antoni Gaudì based on catenaries, or the membranes developed by Frei Otto originated by soap-film models (Image 2.62).

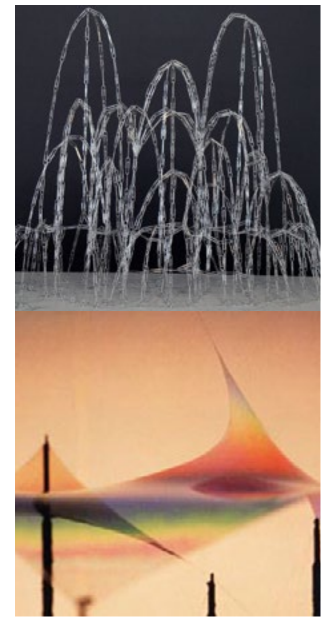
Image 2.62. Top: Church of Colònia Güell model, Antoni Gaudì desing. Bottom: Soap film model for a membrane structure (image courtesy of ILEK).

In the last decades this problem moved mathematics and computer scientists, that developed analytical or heuristically based algorithms to simulate how a material system, or a series of these, emerges with a given set of boundaries conditions. As result of this development, nowadays a wide range of structural design softwares are provided with form-finding engines.

Recently a physical simulation engine has been released with the name of

Kangaroo: Kangaroo is an add-on for Grasshopper™ which embeds physical behavior directly in the 3D modelling environment and allows the designer to interact with it 'live' as the simulation is running. It can be used for various sorts of optimization, structural analysis, animation and more. Even if applications are quite limited for general structural analysis this tool is extremely useful to carry on form-finding tasks and axial deformation analysis: these are the two cases that applies on the kinematics and mechanics of strut-and-ties assemblies. Moreover is possible to simulate material strut-and-tie non-linearity.
For the exploration of form-finding-based kinetic structure this add-on will be used because it allows the user to rapidly investigate instantaneous form-finding structures.

points, lines and facets). Kangaroo is an engine based on particles and springs: a particle can be associate to a point (or structural node), while line and edge facets can be modelled by means of springs.
Let us analyze now the two main Kangaroo components that allows the simulation of some mechanical characteristics associable to general geometric elements (like

The 'spring component' allows to associate for each straight element (linear strut or tie and facet edges) the metrics that describe their elastic behavior (image 2.63).

The component entries are (Image 2.63):

-Connection: the geometric input of a straight element (a line, or a facet edge) described by two points in space.

-Stiffness: the axial stiffness of the element EA.

-Rest Length: the length the spring element tries to reach. Form-finding triggering force is introduced, in my simulations, with this entry by intertwining the rest length factor with the initial imposed strain for the tie element.

-Upper Cutoff: set that the spring works only below a certain distance.





By setting that the upper cutoff is equal to the initial element length, the spring will work only in compression.

-Lower Cutoff: set that the spring works only above a certain distance. By setting that the lower cutoff is equal to the initial cable length, the spring will work only in tension.

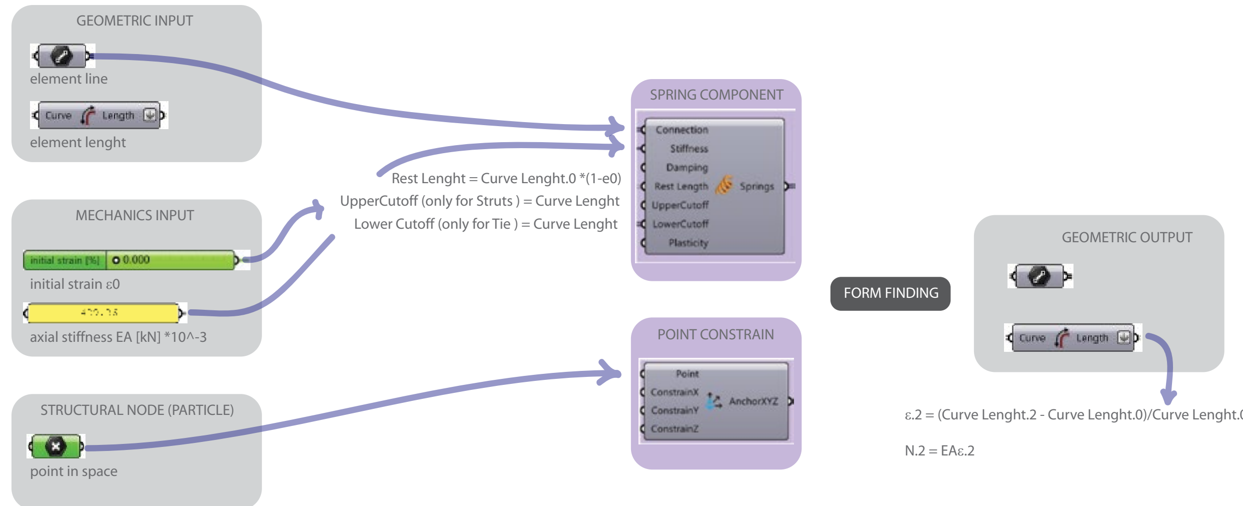


The 'AnchorXYZ component' allows to constrain the translations of a node along the global coordinate system directions, but not its relative rotations.
In spite of this limitation, rigid bodies can be encaster constrained. For instance, it is known from mechanics, that, in order to fully constrain a rigid body in a plane a roll and a pin are enough, while in the space the body can be encaster constrained by means of three not collinear pins.

Image 2.63. Simplified associative network with Kangaroo components.

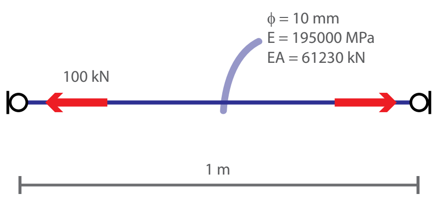


Image 2.64. A prestressed cable pined at its ends

As example, let us make use of the constitutive equations that define the axial deformation phenomenon (Simone 2011) to introduce a prestressing force, with Kangaroo, on a cable pined at its ends (Image 2.64).
A prestressing force of 100 kN has to be introduced on cable whose length $l_0$ is 1m after the force is applied here. The cable has axial stiffness of 61,2 MN. To determine the imposed strain caused by the prestressing force, the following constitutive equation is used:

$$\varepsilon_0 = \frac{N}{EA} 10^3 = 1.63‰$$

This means, that, if the cable is now free at one ends, its rest length $l_1$ is:

$$l_1 = l_0(1 - \varepsilon_0) = 0.998\mathrm{m}$$

That, finally is the entry to input in the ‘spring component’ in order to apply the prestressing force to the cable.

Generally, for more articulated systems, the cable ends are free to move in the space as consequence of the form found equilibrium. By knowing the length of the cable after the form finding process, and by making use of the same constitutive equations for the axial deformation case, axial forces, stresses and strains can be calculated. For instance, the axial stress $\sigma_2$ in a cable, whose equilibrium length $l_2$, is:

$$\sigma_2 = E\varepsilon_2$$

Where the cable strain $\varepsilon_2$ is:

$$\varepsilon_2 = \frac{l_2 - l_0}{l_0}$$

A simple experiment (Image 2.65) of form finding process for a tensegrity prism have been led on the digital environment with the concepts just presented above. The tensegrity prism is formed by three CHS 50-7 steel struts and 20mm circular rubber cables: to this last one, a prestressing force of 10 kN is applied. This prism represents a tensegrity structure because strut ends are only connected to tie ends. Once the form-finding process is triggered by Kangaroo the prism find its equilibrium shape.

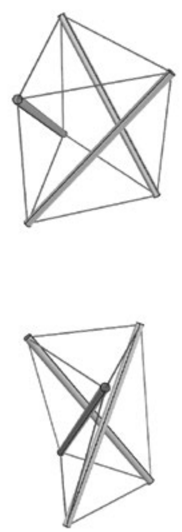

Image 2.65. Form-finding process of a tensegrity prism.





In practice with Kangaroo is also possible to model further elements with their relative mechanical properties. A quadrangular plate element, (so an element that can deform in plane in opposition to a slab element that can deform also out of plane) can be modelled with four nodes, or particles and four edges or springs.

For the sake of simplicity, 2D and 3D element have been modelled as infinitely stiff because the set-up of this element is quite time consuming and not worth to be investigate at this level during researching stage. Furthermore, to have an adequate modelling output, elements must be discretized, having as consequence an increase in the number of springs and particles in the model: this might lead to an increase of the ‘in live’ computational time.

***Preliminary Considerations about the Analysis of Kinetic Tension Structures***

In this section the motion behavior of several strut-and-tie assemblies is analyzed with a particular attention not just to the system kinematics but also to the external forces the trigger motion, and the consequences of theses with regards to stresses and strains.
In fact, contrary to the 1-D and 2-D motion structures previously presented, kinematics and general system behavior (shape at equilibrium as example) of form-finding structures is strictly related to the introduction of external force: moreover, tension structure were defined as structures that deforms with large strains (§2.1). By considering that motion ranges are, for instance, limited by the maximum cable elastic strain, the kinematic study of cable-and-strut systems based only on geometric considerations of cable shortening or strut lengthening is incomplete.

The state-of-the-art of adaptive tension structures concern mainly foldable systems (Motro 2003, Wang 2004, Vu et al 2006). Folding is required to reduce the volume of objects in space. This operation allows for the transportation and storage of folded objects.
The main difference among a foldable structure and the kinetic systems object of this thesis, is that for the first, the designer is mainly interested on the extreme configurations, so fully folded or fully deployed. Generally passive steel cables

give the adequate stiffness to the system when the structure is fully deployed: this can be done by introducing, through the actuators, extra force that overstress the cables. During the foldable state and deploying process passive steel cables are slacken, so that stability in these stages must be given by the actuators.
On the contrary, we are interested in designing a system in which structural stiffness is a result of interaction between all the elements that compose the assembly, such as the struts, the passive ties and the actuators (active struts, like pistons, or active ties like steel cables) in any configuration: so, in any static configuration also the passive cables must work to define shape and equilibrium of the structure.

Image 2.66. A space assembly of simplex connected with passive steel cables, slacken during deployment (image courtesy Vu et al 2006).

In practice cables for static cable-and-strut structures are made out of steel. The implication of the use of steel for the cables in the behavior of kinetic tensile structure is roughly assessed: let us consider a 1 meter long steel rod with an elastic strain of 2%, yielding stress of 520 MPa and radius of 2 cm. This element can only be lengthen up to 1,02 meter, requiring a lengthening force equal to 163,28 kN. As consequence we can see that the motion of a system build with these rods is extremely limited. Furthermore, actuator forces are required to be high: as consequence, during motion, further high compressive forces in the struts are introduced (these might easily lead to buckling of the struts).

A motion structure of this fashion requires more flexible material for cables, or membrane, with much higher yielding strain and lower stiffness. For this reason it has decided to investigate the use of passive rubber cables instead of the steel





commonly used for foldable systems.

The use of rubber cables has some consequence on the characteristic of these structures:

- being yielding and rupture strain around 250/300% for rubber the range of node displacement increases prominently.
- external forces to activate motion are extremely lower compared to those required if steel cable are used.
- system structural stiffness is clearly also strictly related to ties axial stiffness. As consequence the whole structure can experience a drastically drop in stiffness. This is a very important issue if the system is subject to live load, also by considering that even by using steel cable, tensegrity and strut-and-tie structures undertake large displacement due to live loads. Clearly acoustic ceiling are not subjected to live loads, but unpleasant vibration of the structure might arise due to the acceleration caused by actuators.

Rubber has a non-linear elastic behavior (Image 2.67). In practice, with Grasshopper™ it would be possible, by means of other add-ons, to iterate the calculations of form-finding procedures, so that the correct input stiffness can be yielded by considering the actual strain of the cables. This further parameterization is quite time consuming.

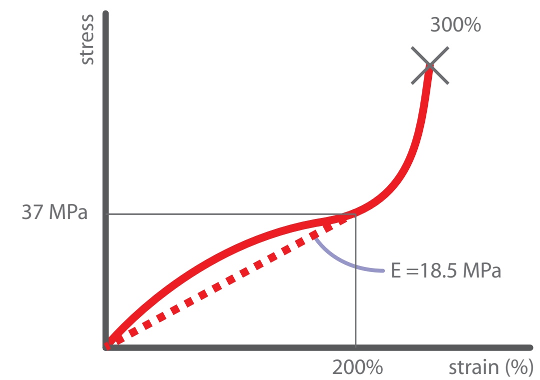


Image 2.67. Stress-strain relationship for rubber.

For sake of simplicity the stress-strain curve has been linearized until the hardening stage. This is a reasonable approximation if the rubber cable strains are limited to 200%.The following table shows the standard material and element parameters used to investigate kinematics of cable-and-tie structures.

| Element | Material | Elastic Modulus [MPa] | Section [mm] | Axial Stiffness [kN] | Bending Stiffness [Nmm^2] |
|---|---|---|---|---|---|
| Strut | Steel | 210000 | CHS 50 - 7 | 429269.4 | 0 |
| Actuator (Hydraulic Piston) | Steel | 210000 | CHS 50 - 7 | 429269.4 | 0 |
| Active Steel Cable | Steel | 195000 | CS 10 | 61230 | 0 |
| Passive Steel Cable | Steel | 195000 | CS 10 | 61230 | 0 |
| Passive Rubber Cable | Rubber | 18.5 | CS 20 | 23.236 | 0 |
| 2D Panel | - | Infinite | - | Infinite | Infinite |
| 3D Element | - | Infinite | - | Infinite | Infinite |

Table 2.3. Geometric and mechanical properties of structural elements used for the study of motion tension structures.





***Generalities about Actuators and Motion Technics for Tension Structures***

Like it has been stated in the introduction to the motion of rigid structures (§2.1 and § 2.1.2) folding a rigid system requires the introduction of an instability, or, more precisely, the introduction of finite mechanisms that will make possible to transform the system's shape (Motro 2003). The creation of mechanisms is usually obtained by suppressing some connections.

In case of tension structure something more can done: one can also introduce mechanisms by changing the length of some connections (cables or struts).
In the case of lengthening cables, in order to have a minimum number of active ties that connect the maximum number of movable struts, the connections should be linked in circuits.
To design this process, Kwan (Kwan et al 1993) introduced the notion of active and passive cables. Active cables are cables that run across the system and, when relaxed, allow the simultaneous lengthening of the cables needed to create mechanisms. The mechanisms are activated by applying actions in the required direction of folding, to lead the system from the unfolded to the folded geometry.
The limitation about the use of steel passive cables was already spotted by Kwan (Kwan et al 1993) by highlighting that passive cables impose a limit on the unfolding of the system.
As well as for rigid systems, motion can be activated extending struts by means of hydraulic and telescopic struts.

In conclusion, activating elements can be classified into two types (Wang 2004):

- Telescopic struts: a telescopic strut is activated by fluid pressure when the magnitude of elongation is relatively large. It requires an external energy supply system and the grid can be deployed simultaneously. Another method is turning screw, which is free of energy supply and is normally used for small magnitude or elongation.

- Releasing cables: cables can be released individually or continuously through joints. Conventionally, releasing cables is realized by a pulley.

Image 2.68. Top: a telescopic strut. Bottom: a mechanical pulley.

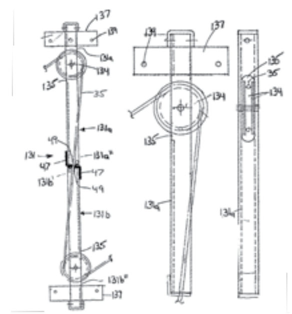

### 2.4.1 Kinetic structures based on 1D tensegrity and 1D-strut-and-cable assemblies

The simplest component constitute this simplexes and grid: a 1D rod, a cable if can withstand only tensile stresses and a strut if is mainly subjected to compressive forces. The way how the struts are connected among them define the typology of the assembly (§2.4).
The elements are here only subjected to axial forces: this make this system easily analyzable (from a mechanical point of view) also with Kangaroo.

From a multi-perspective approach, no sophisticated production is needed to obtain unusual shapes. Elements can be produced and assembled straightforward by standardized nodes leading to a 3 dimensional system (De Boeck 2013).

From literature (Motro 2003 and Wang 2004) several of the possible configurations are graphically presented (Table2.4 and 2.5). This is not an extensive catalogue, in fact, other configurations by means of using higher degree simplexes is possible. Two structural configurations and their relative motion will be studied. The use of both types of actuators will be examined.

It is worth to be mentioned that, with reference to the object of the thesis, the aim of the two research following presented is to obtain an insight of kinematics of simple mechanisms, in order to apply the knowledge here acquired to layout further more complex structures. Moreover, these typologies don't present enough characteristic to be applied in the design of an adaptive structure constructed by paneling: the integration of the systems is possible, but it might require complicated and articulated solutions to the design.





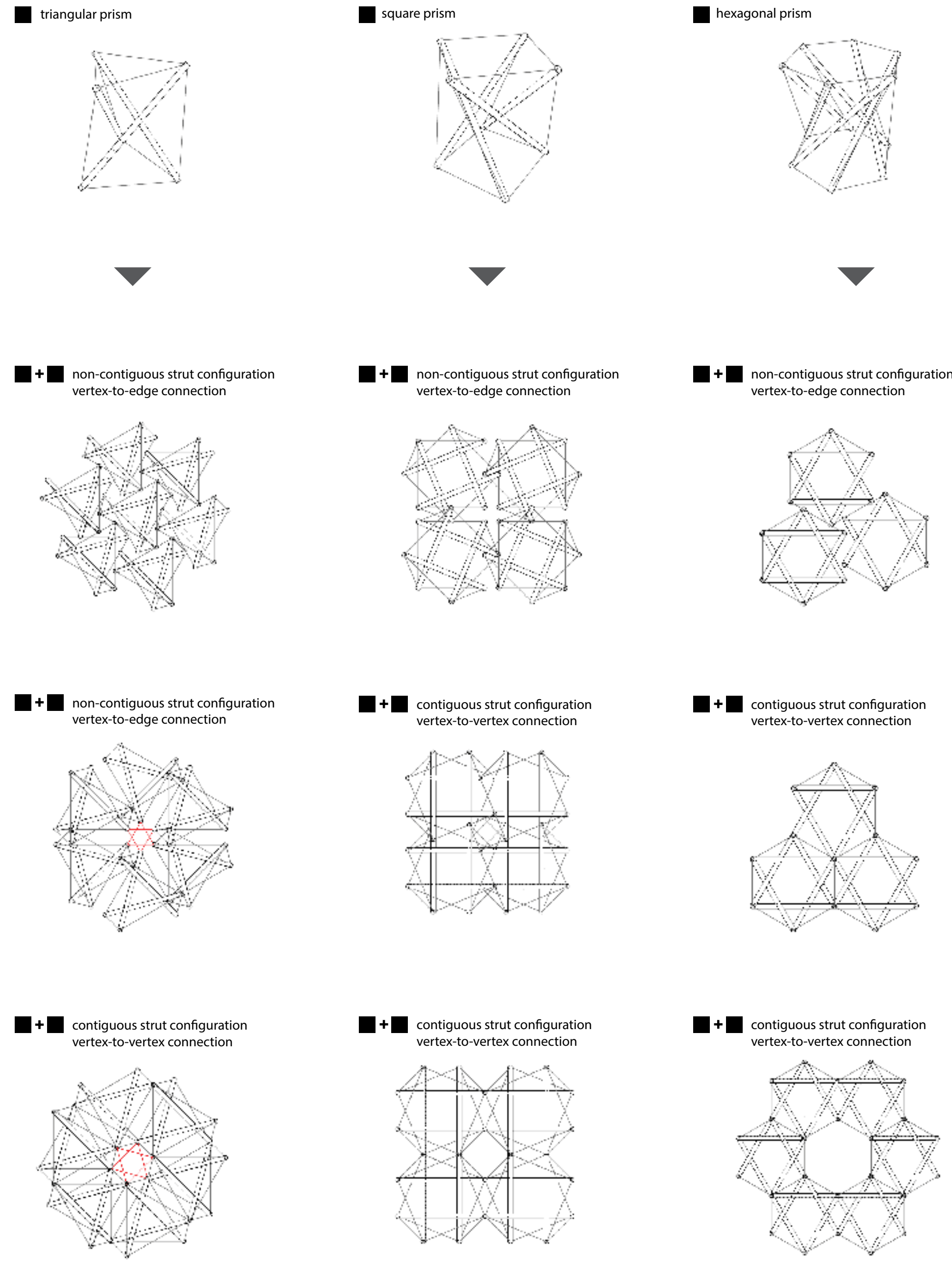


Table 2.4. Cathegorization of 1D-tensegrity simplexes and assemblies: in turn implemented from Wang 2004.

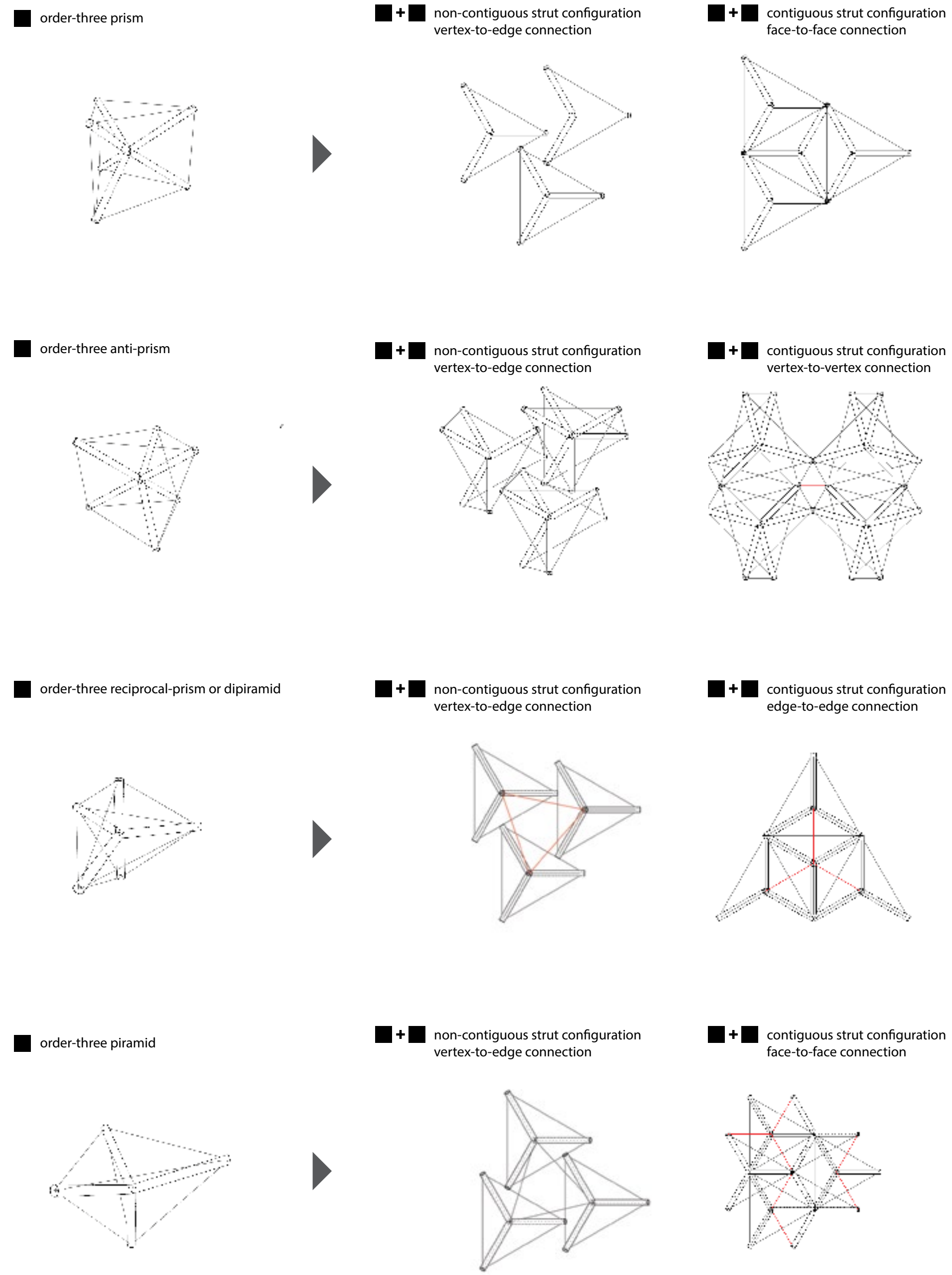


Table 2.5. Cathegorization of 1D-strut-and-cable simplexes and assemblies: in turn implemented from Wang 2004.



Chapter 2 // Motion Structures

***Motion of a 1D-strut-and-cable Pyramid Triangular Grid***

The following structure has been designed having in mind the work of Motro (2003), Wang (2004) d'Estrée Sterk (2003) and Vu et al (2003). Authors' previous design layout was characterized by a surface array of 1D-strut-and-cable modules jointed in two layer simplex by active struts.
The simplex of this structure is a two three-order pyramids (an irregular tetrahedrons), whose vertices are connected through a telescopic strut (Image 2.69).

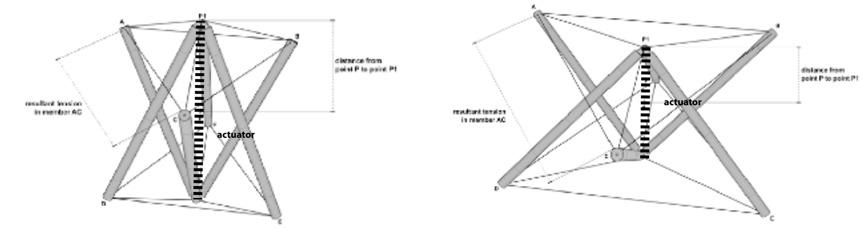


Image 2.69. A by-piramid simplex (image courtesy of d'Estrée Sterk 2003).

Let us first analyze connectivity characteristics and motion only of a single simplex: three families of cables stiffen the module: the diagonals, the star-like and the triangular ones. The first contributes (if prestressed) to deploy the module, while, on the contrary the latest lead the simplex to fold.
The layout of this system has been designed in order to connect the highest number of struts with a telescopic actuator so that a minimum amount of these devices is used (d'Estrée Sterk 2003).
Vu at al (2003) proposed another simplex where the pyramids are hinge connected not now at the apex but at their lower vertices (Image 2.70).

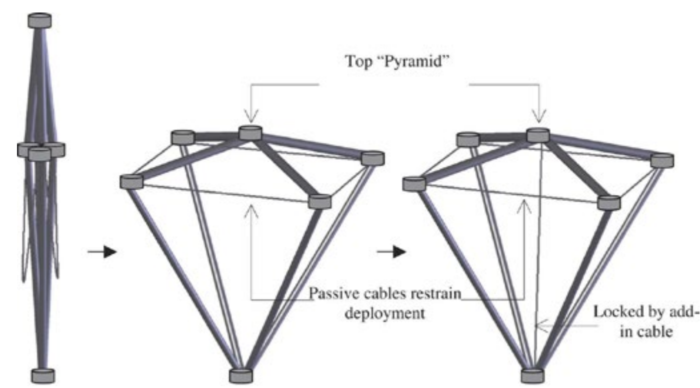


Image 2.70. A by-piramid simplex (image courtesy of Vu at al 2003).

As first step, form-finding process is run by applying to the rubber cables a prestressing force of 10 kN. At a later stage actuator is activate, by means of reducing is length up to a factor of 0,25 (Image 2.71). By retrieving strains at equilibrium, element axial stresses can be estimated. Strains at equilibrium are calculated considering as the initial length the rest length parameter connected to the spring component (Table 2.6).

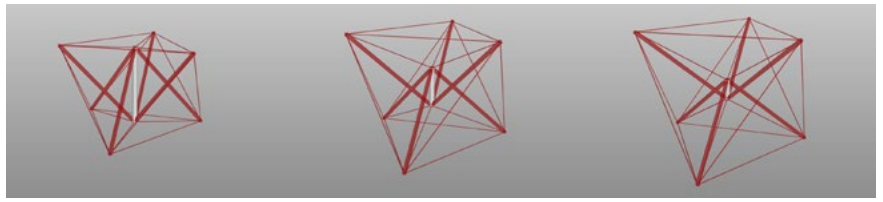

Image 2.71. Motion process of a single simplex.

To note that a wider module opening can be obtained by applying a higher prestressing force to the diagonal cables.

| | Piston Length = 1*L (just after prestressing) | Piston Length = 0,5*L | Piston Length = 0,25*L |
|---|---|---|---|
| Strut strain [%] | -0.0075 | -0.0093 | -0.0136 |
| Strut stress [MPa] | -15.8 | -19.5 | -28.6 |
| Star cable strain [%] | 22.5 | 89.3 | 94.23 |
| Star cable stress [MPa] | 4.2 | 16.5 | 17.4 |
| Triangle cable strain [%] | 22.3 | 102.5 | 123.47 |
| Triangle stress [MPa] | 4.1 | 19.0 | 22.8 |
| Diagonal cable strain [%] | 95.4 | 112.5 | 132.56 |
| Diangonal cable stress [MPa] | 17.6 | 20.8 | 24.5 |

Table 2.6. simplex stresses and strains during motion phases.

The module is now populated on a plane along its three generative directions. Diagonal cables are here eliminated because not necessary to provide structural stability as the connectivity layout of the struts already accomplish with this task. Due to this, when the telescopic struts are activated, the whole structure experiences a deploying of the modules (Animation 2.10).





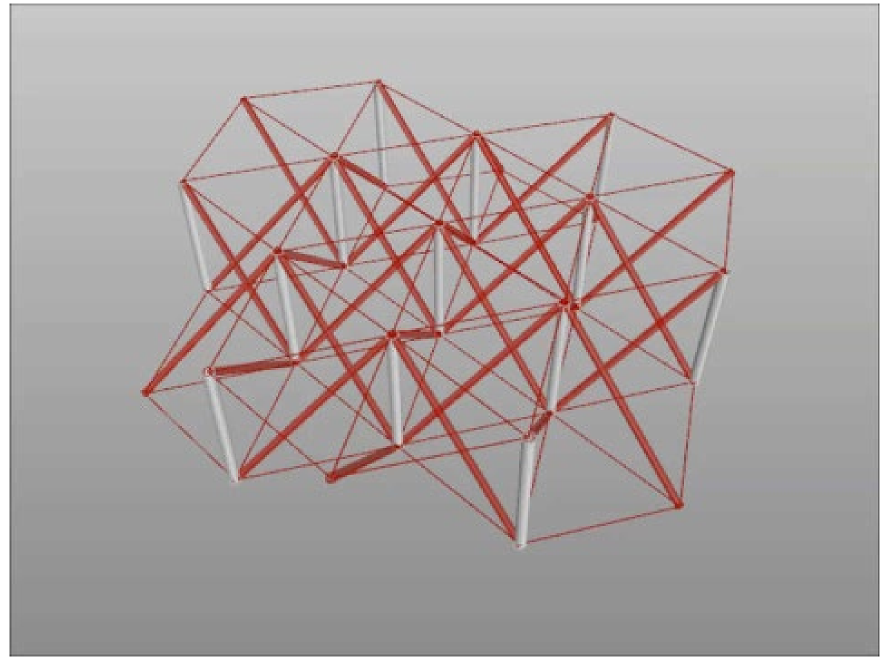

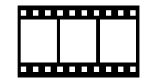

Animation 2.10
Assembly of 1D-strut-and-cable simplexes.

The use of passive cables allows the structure to have in any motion stage a self-stressed equilibrium on the contrary of the example referenced where passive cables made out of steel are lacked during the deployed stage: the main reason of this choice is that design objectives are different. The structural configuration proposed by Vu et al (2003) has been set-up in order to obtain a transportable retractable roof from a very compact to a fully deployed configuration. During motion, stability function is also fulfilled by the actuators.

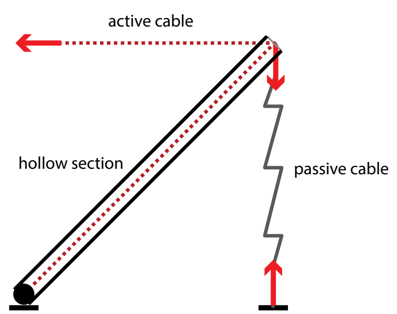


Image 2.72. Basic Mechanism with one strut, one active and one passive cable.

### *Motion of a 1D-tensegrity Triangular Grid*

The motion of a triangular tensegrity prism, and following of a grid, actuated by releasing cables are here investigated. The simplex is composed by three struts, two families of bottom and top rubber cables and a continuous zig-zag steel releasing cable passing inside the hollow struts. In order to avoid unwanted simplex rotation the three bottom nodes have been constrained with pins.
An initial strain is applied to the passive rubber cables: their function is then only to reestablish equilibrium once steel cable are released (Image 2.72).
Initial shape of the simplex (maximum folding configuration allowed) is limited by the strut clashing while the final one (maximum deploying configuration allowed) is limited by clashing between steel cables and struts. As soon as active cables are released, the elastic energy stored in the top passive cables is released causing strut rotation and rising.

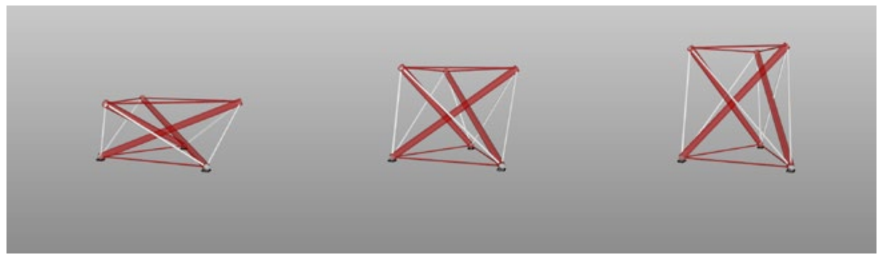

Image 2.73. Motion of an order-three tensegrity prism while releasing the three active cables.

The following concept can also be applied to 1-Dimensional (Motro 2003) or even 2-Dimensional arrays made of any kind of simplexes. The challenge of these kind of assemblies is to layout the family cables in order to minimize the number of active cables that requires expensive mechanical devices (Wang 2004 and d'Estrée Sterk 2003).

Before moving to an assembly of tensegrity prisms let us consider the easier and tested case of a deployable mast composed with SLE's (Gantes 2000). These kind of structures have been used for more than 40 years in the space industry. The difference with tensegrity structures that will be investigated in this section is that passive cables are slacken during all the motion except at the final deployed stage where they are now taut and together with the active ones contribute to stiffen the structure to live load (Image 2.74).
The reason of this layout is that these systems are not required to have a certain





degree of rigidity in the intermediate deploying stages but only at its fully deployed one. To increase structure rigidity the active cable might be prestressed. Layout of a zig-zag cable is then applied to confine pulleys placement in one single spot (Gantes 2000).

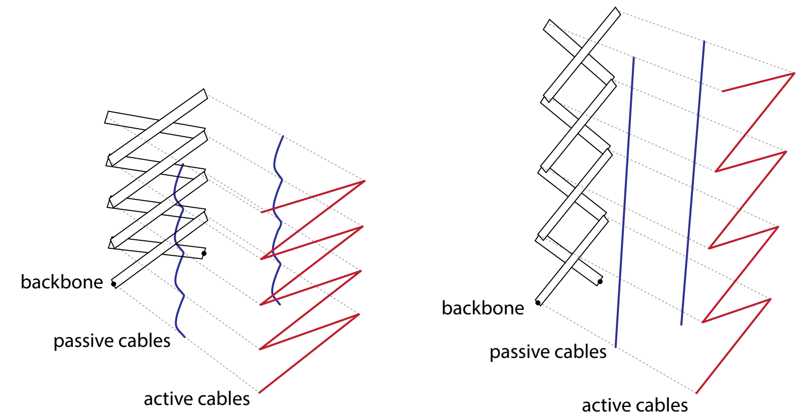


Image 2.74. Structural components for a pantographic mast (in turn adapted from Gantes 2000).

The same 'cable sewing' approach can be used to control the motion of any planar or spatial array of simplexes. An assembly of triangular prisms with non-contiguous strut configuration has been modelled as follows: top and bottom triangles and internal diagonals constitute the passive cables families, while three families of active cables (one for each side of the triangles) run through hollow section and by zig-zaging they form a continuous active cable that connect outer edges of the full assembly. Motion of the full assembly is similar to the simplex one (Animation 2.11).

Table 2.7. Families of sewing cables for the tensegrity assembly.

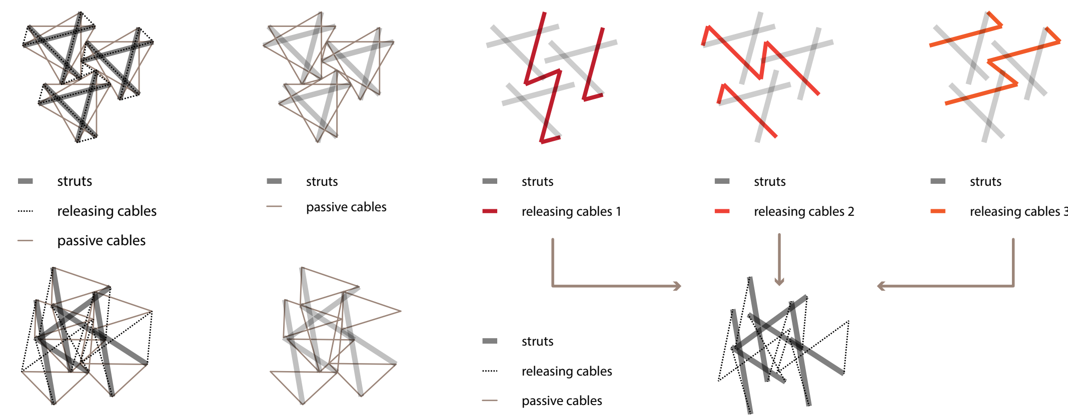

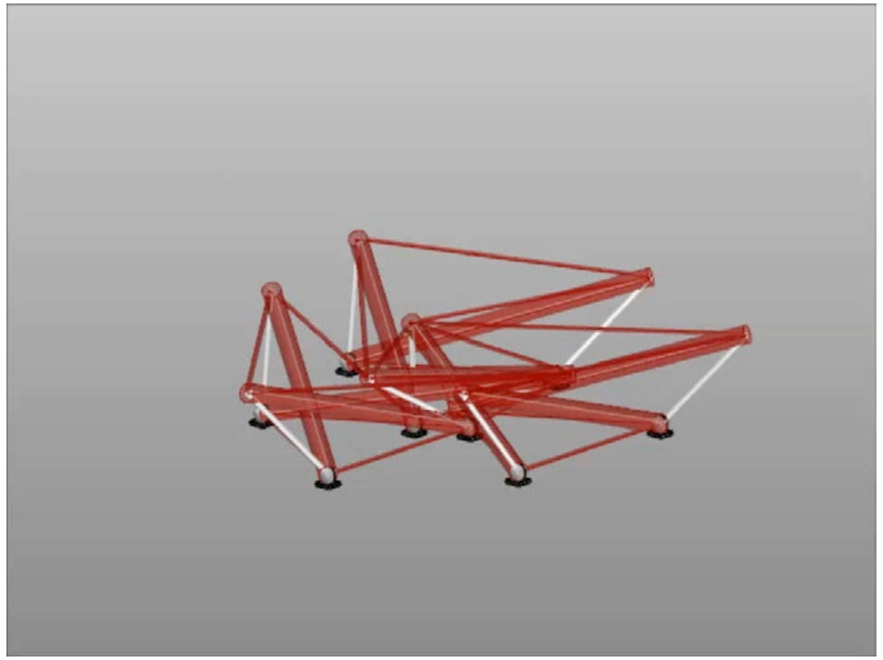

Animation 2.11
Assembly of tensegrity prisms.

From the mechanical point of view another difference is present compared to the model that uses passive slacken cables: because passive rubber cables are storing mechanical energy, every time that active cable change configuration a new form is found. Subsequently, the new shape equilibrium has as consequence the mutation of axial forces in the elements. Contrary to the deployable mast example above introduced this is not a stress-free mechanism.

The model above studied doesn't consider friction forces that might occur between the interfaces of releasing cable and joints: this phenomenon can have the effect to lock the system after releasing active cables if, for instance, the cumulative joint friction force is higher than the energy released by the active and passive cables.





**2.4.2 Kinetic Structures based on Panel-and-cable Assemblies**

In this section the use of 2D rigid panel for struts composing structural assemblies will be investigated. This type of structure haven't been studied yet by others designer, however, the intention of this research is only to investigate the potentiality of this kind of assembly in relation to a possible application where a variable paneling system is needed.
Two motion models will be presented hereafter: these are based on an intuitive space structure design, at its turn depending on the objective to find a 3D-pattern for panel assemblage. This pattern assemblage must follow a ruled repeatable scheme together with the further tie assemblage that must be based on a coherent and sensate force flow consideration.

Image 2.75. Floating Lampshade: rigid panels and cables form a tensegrity structure (image courtesy of intensiondesigns.com).

Image 2.76. Motion sequence of a tensegrity prism with 2D-rigid panel along discreted side facets. Three pistons connect concurrent vertices of the prism bases.

The structure layout starts from the previous work of Wang (2004) regarding space tessellation for the design of 1D-strut-and cable structural grids: the intuition of the author consist on designing 1D-strut-and-cable assemblies by means of space-filling form procedure.This last idea consist on tessellating the space (in one, two or three directions) with 1D-strut-and-cable simplexes having boundary shape of a polyhedron. Repeatable patterns are characterized by having the filling polyhedrons in contact at vertices, edges or even a surface (Table 2.4 and 2.5). Wong substitutes polyhedron edges with 1D-struts or cables. This model is here augmented by substituting a polyhedron surface with a 2D-rigid panel. Here only one pattern will be studied (with two different actuator configurations) but design approach of this system shows characteristics of flexibility in structural design and architectural application. The range of possible configuration is potentially very wide considering the space-tessellation patterns that can be obtained with different types of polyhedrons. Range of possible designs is also related to:

-how 2D-rigid panels are connected among them;

-how the full assembly is constrained is space;

-how force flows through actuators.

An irregular octahedron is the repeatable block: this is formed by two four-side pyramids connected through their base. The octahedron is then arrayed. Different layouts of paneling are possible. Free edges are then substituted with ties.

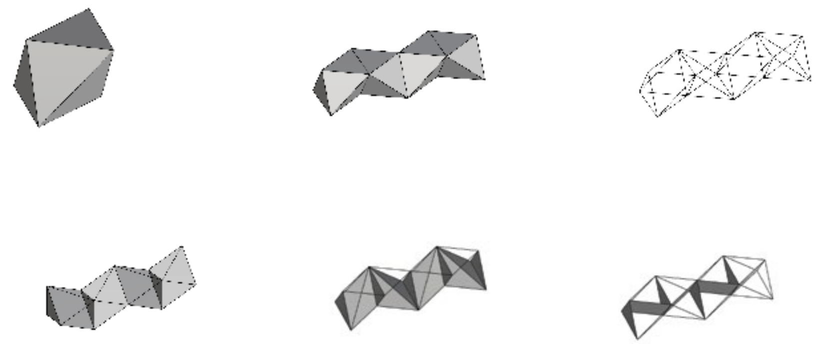

Image 2.77. Generation of structure starting from an octahedron.

For the experiment structures has been space constrained by pin connecting to passive rubber cables.
In the first configuration a line of four zig-zagging pistons interconnect the entire collection of polyhedrons at five hinges (Image 2.78). This was meant to make participate all simplexes to motion with the least number of actuators. When pistons contract the panels drawn from the pyramid base rotate around the y-axis.

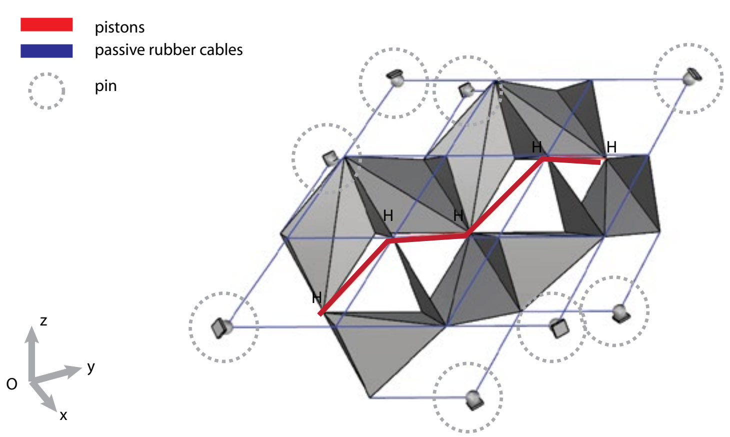


Image 2.78. Assembly actuators and constrains.



Chapter 2 // Motion Structures

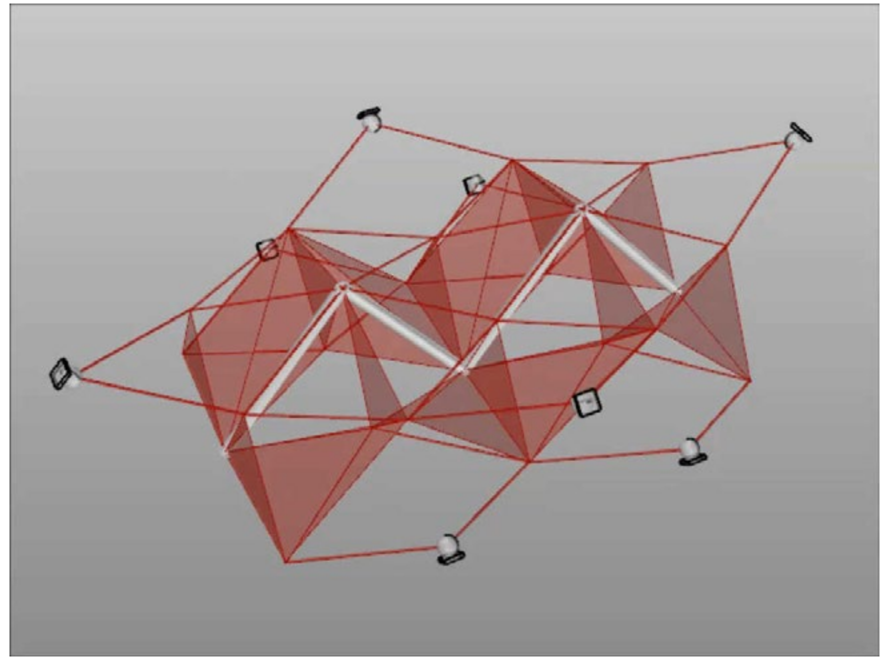

Animation 2.12
Panel-and-cable assembly #1.

In the second configuration a continuous active steel cables also interconnect the entire collection of polyhedrons, here at four roll-constrained nodes (Image 2.79). In this way the motion can be triggered with a single mechanical pulley placed at one of the four nodes.

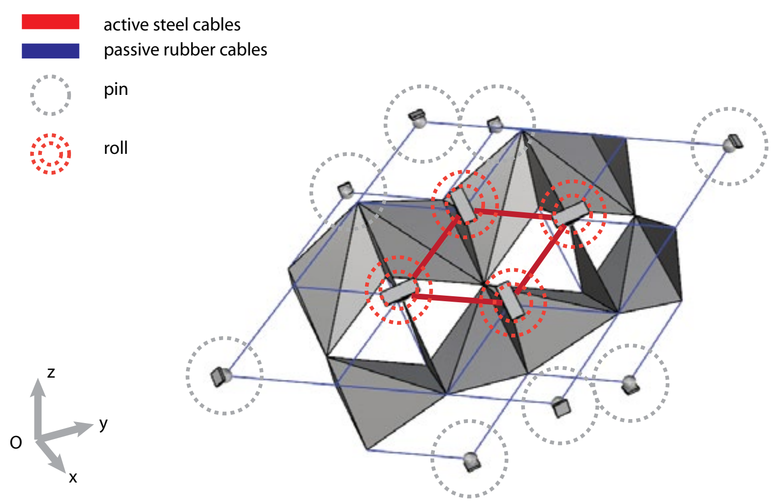


Image 2.79. Assembly actuators and constrains.

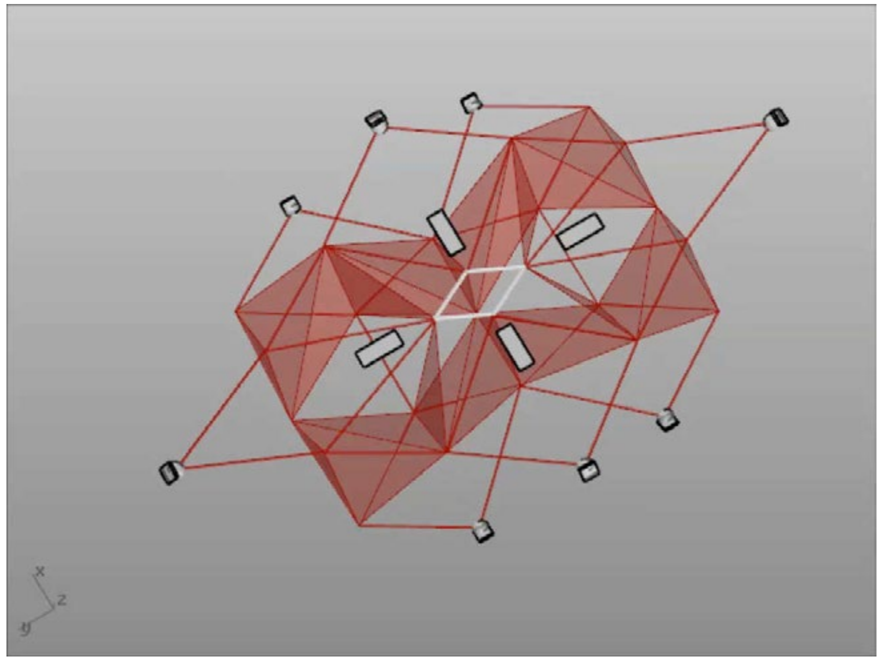

Animation 2.13
Panel-and-cable assembly #2.



Chapter 2 // Motion Structures

Results of this research regarding motion control are quite poor: a more rigorous research must be done by taking in consideration more aspects while layouting this system. These are the position of constrains and their degree of freedoms, relation between actuators and passive cables (by means of a more efficient and well-designed cable network), polyhedron edge connection.
In spite of these results, this typology is worth to be investigated, in order to improve both the aspects of functional integration of the panels (structural and further accessory function) and new possible aesthetic solutions.

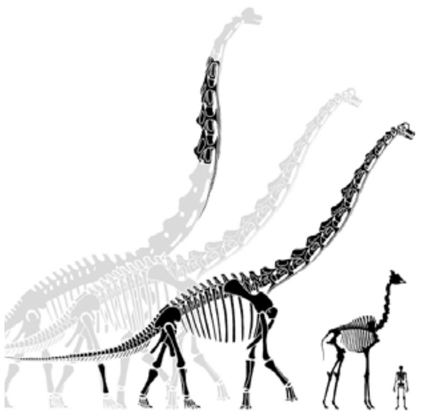

Image 2.80. Backbone systems (image courtesy of Vincenzo Rale).

### 2.4.3 Kinetic Structures based on 3D-tensegrity and 3D-strut-and-cable Assemblies

Tension structure typologies can be further developed by adopting three-dimensional 'compressed' struts. It is important to note here that the majority of research and discourse to date has focused mainly on tension structural typologies constructed from tension cables and unidirectional compression struts. There are few practical examples where compression components consist of subassemblies that form more sophisticated geometries (Frumar 2010). For simplicity, here the 3D bodies are also denoted as 'compressed'.

These systems are worth to be investigate because the use of 3D components in place of linear struts constrains at a higher degree the kinematics of each simplex. When modules are interconnected, this property results in a more rigid and robust framework than conventional strut-and-cable assemblies (Frumar 2009). The outcomes of the examples shown below reveals how easy is to control the motion of these systems.

Other aspects that make these structures interesting to be studied is the fact that they are inspired by those biomechanical systems that, in my opinion, perfectly execute motion: the vertebral systems (Image 2.80). Vertebral systems, in fact, are assemblies of 3D compressed elements (the bones), passive ties (the tendons), and actuators (the muscle fibers). Maybe there is not in nature a better adaptive and kinetic system that through a long evolutionary process, has combined characteristics of flexibility, resilience, strength with minimal energy and material requirements.

Like it has already been done in the previous chapters regarding tension structures with 1D and 2D struts, 3D tension structures can be differentiated in 3D-tensegrity and 3D-struts-and-cables assemblies.
The differentiation between 3D-tensegrity and 3D-struts-and-cables assemblies still follows the definition presented in the precedent introduction at this section. By re-elaborating this definition (Wang 2004) it can be stated that: a 3D-tensegrity system, is here defined as a stable free-standing volume that is realized by the interaction between isolated 3D compressed body, the island of compression, and





interconnected cables, the sea of tension. On the contrary, in 3D-strut-and-cable assemblies the rigid bodies are unified between them through fulcrums.

Generally speaking, these types of structures are composed from an array (linear or on a surface) of interconnected component-based modules where the 3D components can be freeform, symmetrical or eccentric in shape. For the structures object of this research some guidelines suggested by literature (Frumar 2009) will be adopted:

-extreme vertices of a 3D body bound a volume (mainly a polyhedron);

-3D component are discontinuous;

-modules can tessellate in at least one direction.

With this guidelines, a research with the intent to explore potentialities of this system, has been done: this shows that variety of such structures is extremely wide, and is limited to the stereotomic combinations of coherent simplex space tessellations. For sake of simplicity, in this research, the 3D bodies will be represented by triangular spikes interconnected with moment resistant joints (Image 2.81). These triangular panels are mainly generated from the axis of polyhedrons, but is clear that the 3D rigid body can be here formed by any kind of other panel or element, so that the application of these systems for an architectural function based on paneling is possible and potentially successful.

The rules that were followed while composing the assemblies after presented, (in order to have, as consequence, a structural application) are:

-the linear or surface array must have a repeatable and geometric logic pattern.
-the further simplex interconnections must be based on a coherent force flow design approach.

Moreover, a simplex that can connect to other modules in a number of different directions will be of greater use to designers than one that can only extend in a

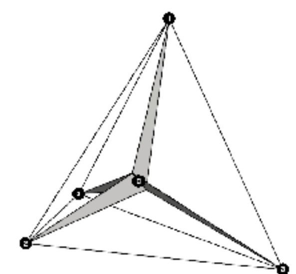

Image 2.81. A 3D-rigid body generated from a tetrahedron.

single direction. A module that can tessellate in three dimensions and at a number of different scales thus enables a more refined level of design control (Frumar et al, 2009).

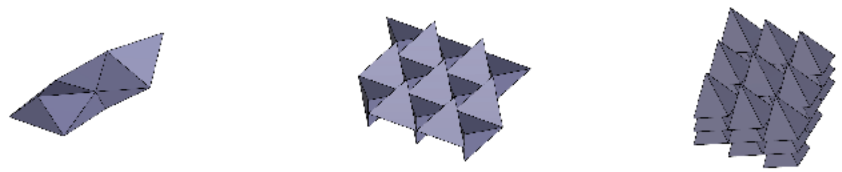

Image 2.82. A linear, surface and space array of tetrahedron simplexes.

Table 2.8 shows, not as extensive catalogue, several of the possible configurations that can be realized. Here, space tessellation is done by using only regular and irregular tetrahedron modules, but the use of higher degree polyhedrons is possible (Frumar et al 2010).
The studies about kinetic behavior of some of these are hereafter presented.

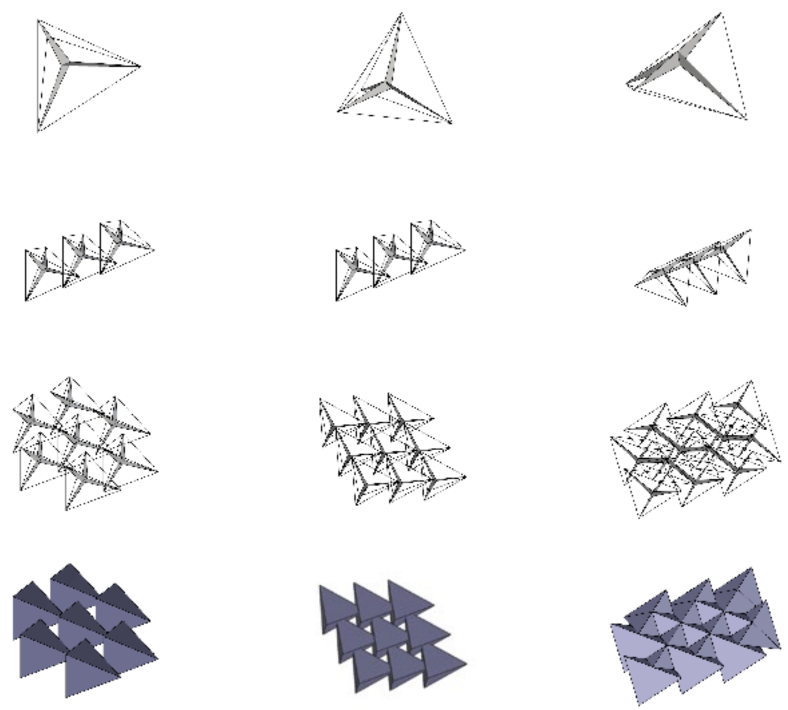

Table 2.8. Tetrahedron space tesselletation.





***Motion of a 3D-tensegrity Mast***

Image 2.83. Tensegrity mast (image courtesy of Frumar et al 2009).

A tensegrity mast is a linear array of regular tetrahedrons. When connecting the simplexes, two families of cables can be now distinguished. Between each element, a closed perimeter of cables connects in sequence the top and bottom vertices of adjacent modules, while four continuous cables connect similar tetrahedron vertices along the linear direction of the array. The first cable family makes the structure continuous, while the second is then used to stiffen the mast: thus a self-stressed system is created.

The kinematic research about the motion of a tensegrity mast starts from the analysis of the precedent static structure designed by Frumar et al (2009).
By intuition, the kinetic mast cable set-up has been augmented by substituting two continuous cables with two lines of actuators, modelled as extendible pistons (Image 2.84): when these are triggered, the full assembly can expand or contract along the direction of the linear array.

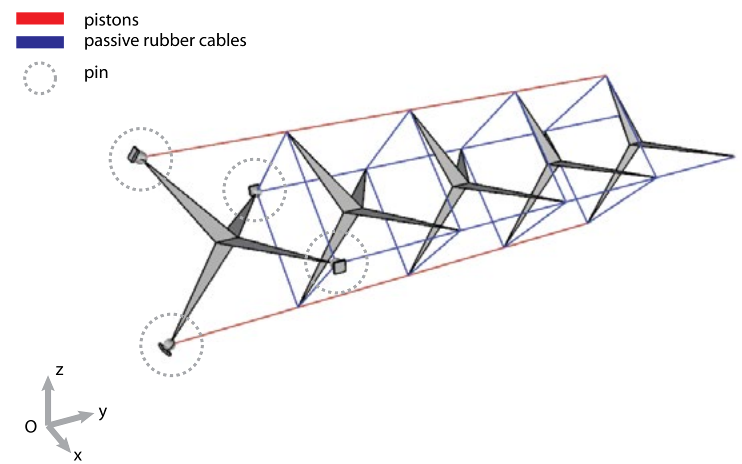


Image 2.84. Assembly actuators and constrains.

The mast can be particularly useful when a very compact configuration is needed for transportation, for instance, and then deployed. For this reason, conceptual design of this have can be envisioned for deployable mast for space application.

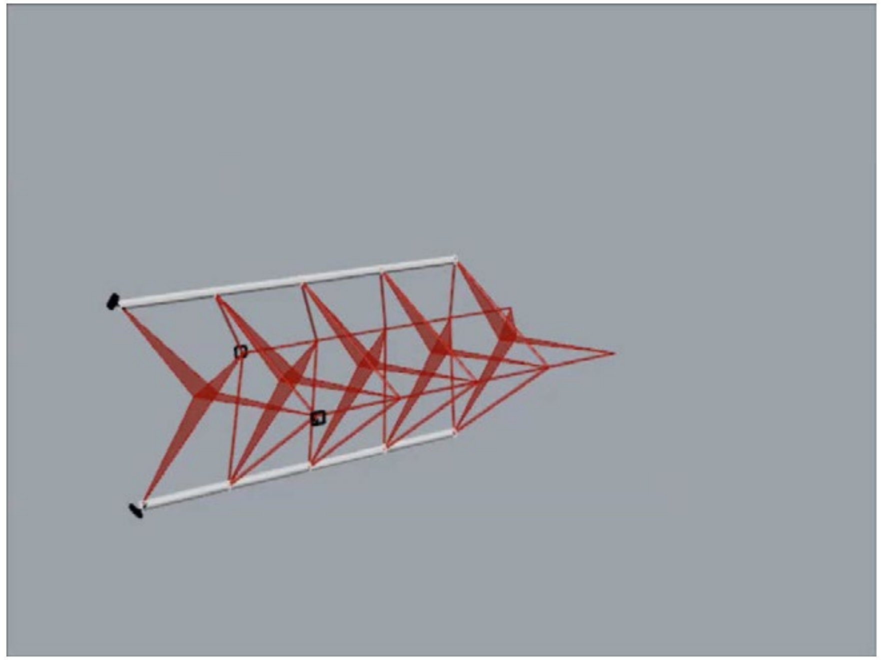

Animation 2.14
Tensegrity mast.





***Motion of a linear arrayed 3D-strut-and-cable structure (or backbone like structure)***

If three-dimensional struts are now connected with a hinge, the structural system is now similar to a backbone (Image 2.85).

In the literature review there weren't found any examples about motion of this type of structures, but already several interesting and inspiring precedents of static backbone-like structures have been designed by Frei Otto and Santiago Calatrava. In these precedents, the array of redundant 3D elements is made static by the adoption of further passive cables or even stiffer circular hollow sections (Image 2.86).

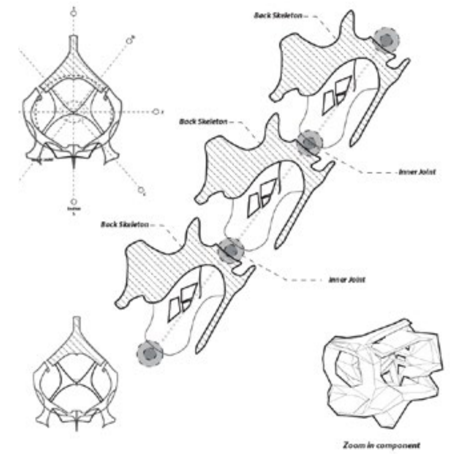

Image 2.85. Mechanical system of a human backbone (image courtesy of Jia Yuan Liu).

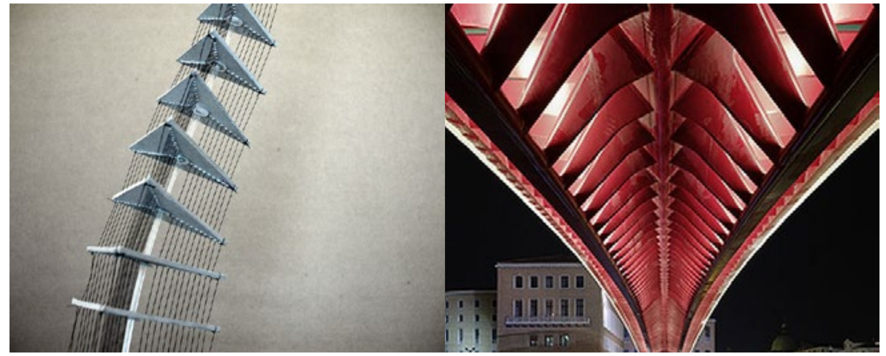

Image 2.86. Left: a backbone mast (image courtesy of ILEK).
Right: Constitution Bridge in Venice, Santiago Calatrava design.

From the kinematic point of view it can be observed that such a system is simply a kinematic chain (§2.1.2) composed by n three-dimensional rigid bodies. From kinematics, is known that a chain composed by n elements, if none of the rigid body is fully constrained in space, has $\infty^n$ possible configurations and $6 \cdot n$ degrees of freedom. The motion of such a system is complex to control unless the rigid bodies are coupled by means of added elements, in this case cables. With this augmentation, and by constraining with 3 pins one simplex of the assembly, the system has now $\infty^1$ possible configurations and the degrees of freedom of the elements is dependent now only to one metric related, for instance, to the kinematic variation of the actuator.

Once the elements are stacked, they are further connected by passive and active cables. The aim of this research is to reproduce elementary motions typical of a backbone system, like bowing and torsion. To do this, continuous or segmented active cables will be used to trigger the full assembly. This design intuition and relative implemented applications for flexible backbone structures, come from the research analysis, also presented before (§2.4.1), of Gantes (2000) on a cable-actuated deployable mast.

In order to start to layout the cables, let us introduce some geometric references: the direction of the arrayed assembly matches with the y-axis so that the cross section lays onto the zx-plane. The rigid bodied are connected between each other's at the fulcrum C, denoted also as the 3D rigid body centroid.

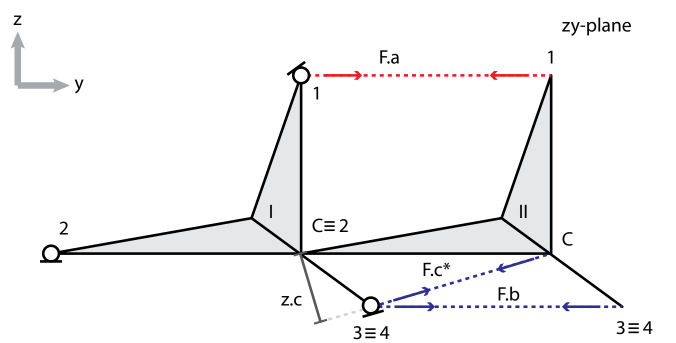


Image 2.87. Static analysis.

The layout of the cable system for activating the bowing motion are planned through a static analysis of rigid bodies I and II in their equilibrium configuration (Images 2.87 and 2.88). It can be observed that, on the zy-plane, in order to obtain a change in curvature, a moment is needed and this can be initiated by forces applied with an eccentricity with respect to the fulcrum C. From this observation, 5 active cables connect the arrayed vertices 1: the axial force $F_a$ introduced along these is characterized by a lever arm of $z_a$. Because rigid body I is fully constrained, a prestressing force $F_a$ introduces a counterclockwise moment equal to $F_a \cdot z_a$. Passive segments of rubber cables, as consequence, must exercise a balancing clockwise moment: to do so they must have a negative lever arm. With this observation, two passive cables are connected to the arrayed vertices 3 and 4, and two further ties connect vertex 3 and 4 with C: for this last two cables only the projected forces onto the zy-plane $F_c$* initiate a moment, because the normal components of force $F_c$ to the plane are elided.
Finally, to have equilibrium, the balancing clockwise moment must be equal to $2F_b \cdot z_b + 2F_c{}^* \cdot z_c$, with $z_b$ and $z_c$ being the lever arms of the respective index referenced axial forces. From this simple mechanical analysis it can be concluded that when the counterclockwise moment is higher in magnitude then the clockwise one, the assembly bows on the zy-plane.
To note that to fully trigger the motion, a minumun number of four mechanical pulleys are needed.

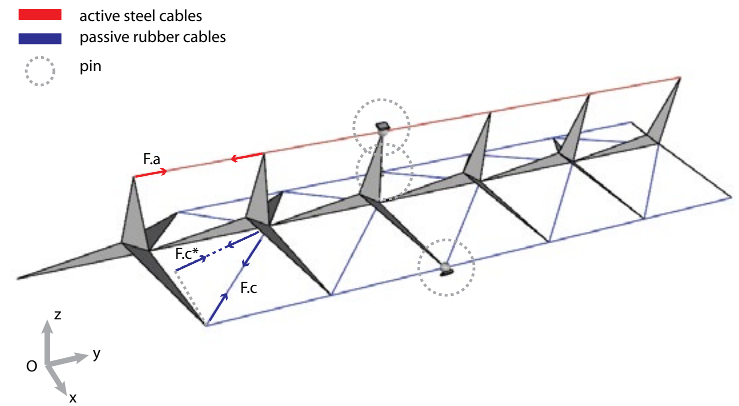


Image 2.88. Assembly actuators and constrains.

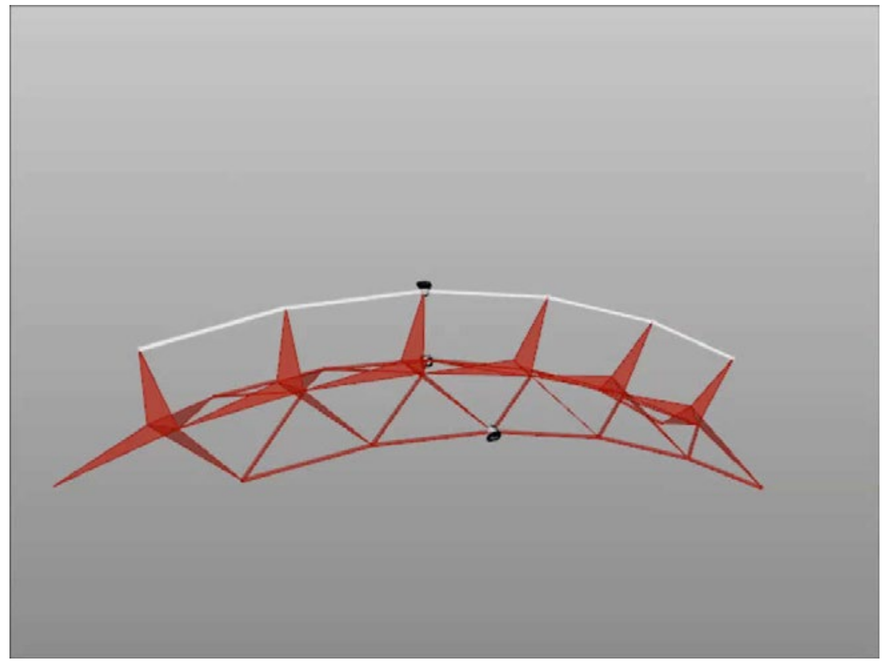

Animation 2.15.
Bowing backbone beam.

By means of the same static analysis approach, the cable system for a twisting backbone beam is layout. In order to make the beam twisting, a moment applied to a rigid body and laying on the zx-plane must be present. By intuition, it can be indicated that one way to introduce this moment is by wrapping the full assembly with continuous helicoidally cables (Image 2.89).

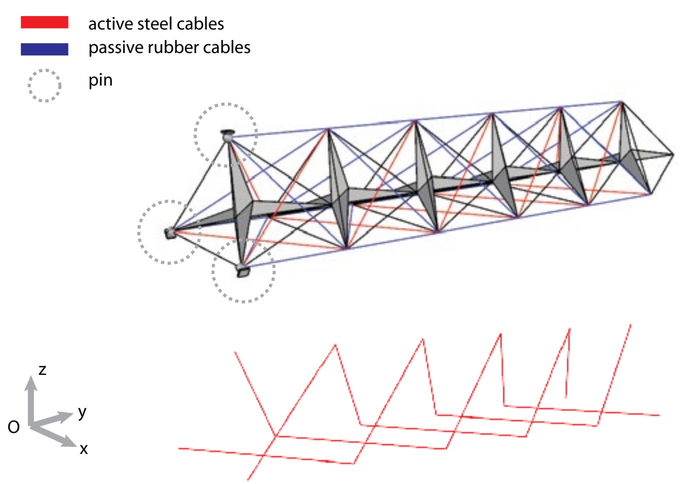


Image 2.89. Assembly actuators and constrains.

Two families of cables augment then the system: three counterclockwise wrapping active cables and other three clockwise wrapping passive cables. Let us project now the three cable axial forces $F_a$ onto the ‘cross section’ zx-plane: The normal components $F_{an}$ and the out of plane moments (moment equal to $F_{an} \cdot z_a$, with $z_a$ the lever arm between the hinge C and the normal force Fan) are elide. On the contrary, the three in plane projected forces introduce the in plane clockwise moments equal

Image 2.90. Static analysis

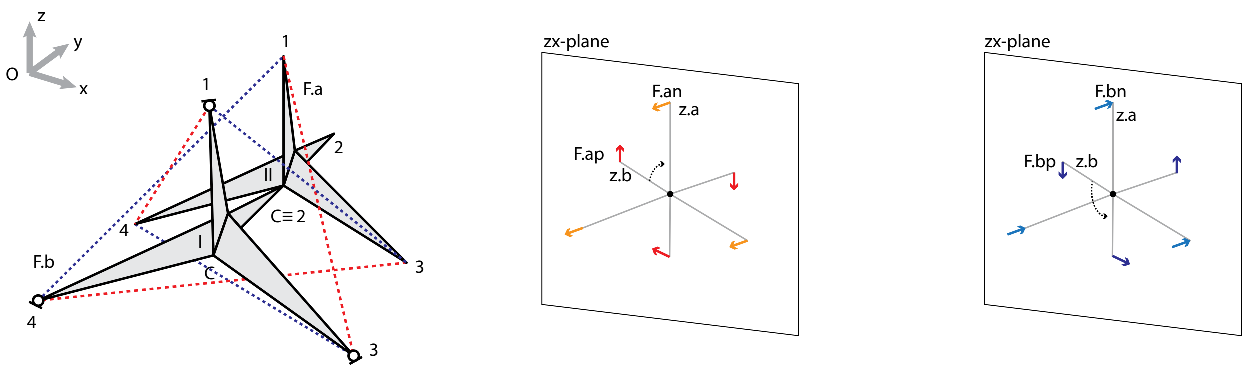






to $F_{ap} \cdot z_b$. With the same method the passive cables axial force are analyzed: out of plane forces $F_{bn}$ and the out of plane moments $F_{bn} \cdot z_a$ are elided, while the in plane projected forces $F_{bp}$ create counterclockwise moments $F_{bp} \cdot z_b$ (Image 2.90).
In the diagram presented the rigid body I is fully constrained in space: if the magnitude of the clockwise moments are higher than the counterclockwise balancing ones, rigid body II rotate around the y-axis.
Further continuous passive cables along the assembly arrayed direction connect adjacent simplexes, but their contribution to the introduction of balancing moment is negligible.

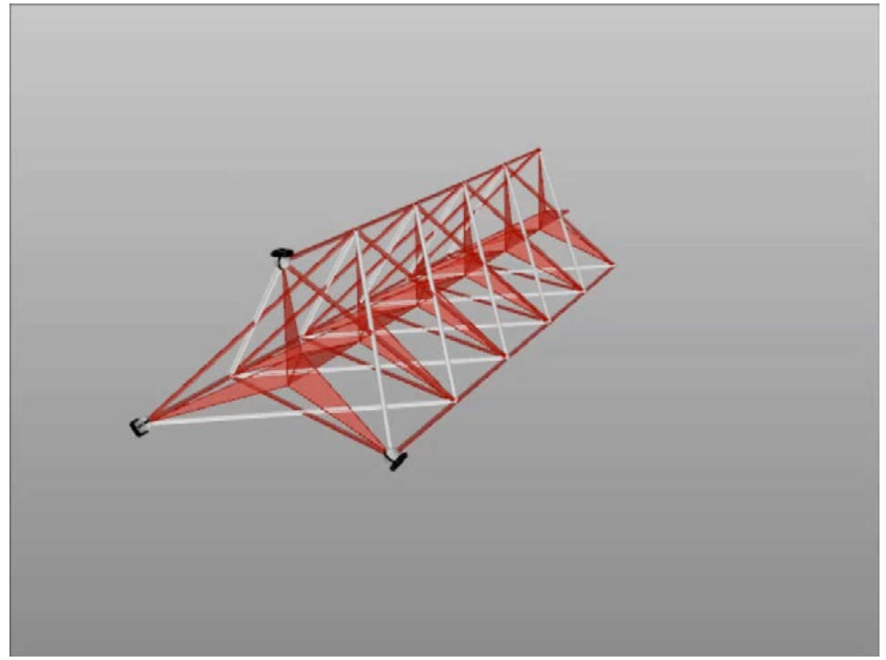

Animation 2.16
Twisting backbone beam.

### *Motion of a Surface Arrayed 3D-strut-and-cable Structure (or surface backbone like structure)*

At a further degree, the systems above studied can be implemented by arraying on a surface the tetrahedron simplexes. Aim of this research is to investigate whether is possible to control the motion of this system and what are the range of possible configuration that can be obtained: particular attention is given to the discrete surface variability from convex to concave. Such application is useful to design, for instance a two-dimensional adaptive system, like the acoustic ceiling object of research of this thesis.

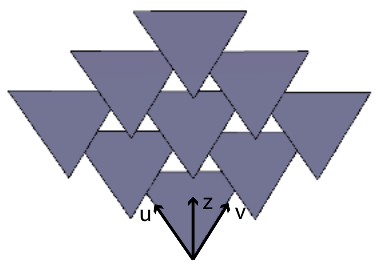


Image 2.91. Surface tesselation directions.

Before starting the kinetic analysis of these systems some geometric references must be introduced: let us denote as u and v the principal arraying directions and as z a further one (Image 2.91).
The assembly object of the following two experiments are composed with 4x4 tetrahedrons system, populated along the u and v directions. The following two experiments don't aim to exhaustively study the motion of surface arrayed backbone structures, but only to give an insight and understanding of the motion phenomena, but clearly, by modifying constrains and actuators layouts others different motion systems can be obtained.

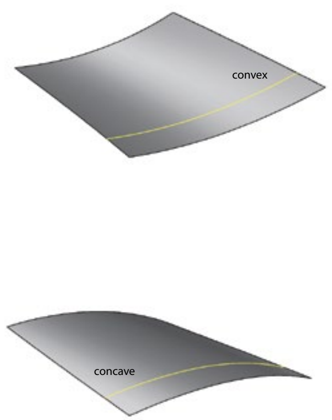


Image 2.92. Curvature changing fot the discrete arrayed surface structure.

As first experiment, four continuous zig-zagging active cables along the u directions connect the simplexes arrayed along this path, while an additional network of passive rubber cables make the full system continuous. These networks are composed by square perimeters of elements that join through two layer, at the lower and higher parts, the system. Struts and active cables are pin constrained in space.
The zig-zagging cables are composed by vertical and diagonal segments. By making use of the knowledge previously presented, it can be observed that in order to activate the system to motion the cables must be shortened. The diagonal segment of these make the assembly wrap on the v directions, while the vertical parts don't play a role in the motion activation of the system as they connect vertices of the same undeformable rigid body (Image 2.93).
If the four cables are activated together, the discrete surface as result is now a single curvature surface with variable curvature along the assembly u direction.





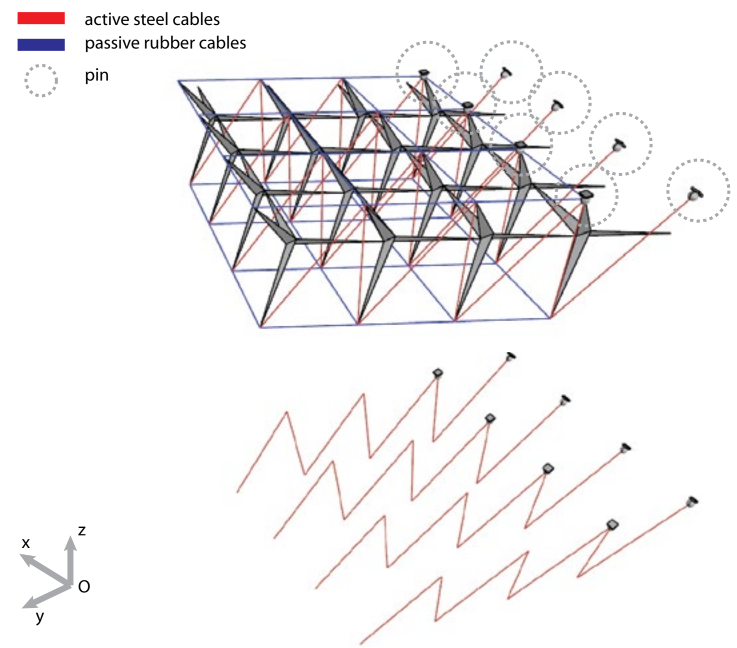


Image 2.93. Assembly actuators and constrains.

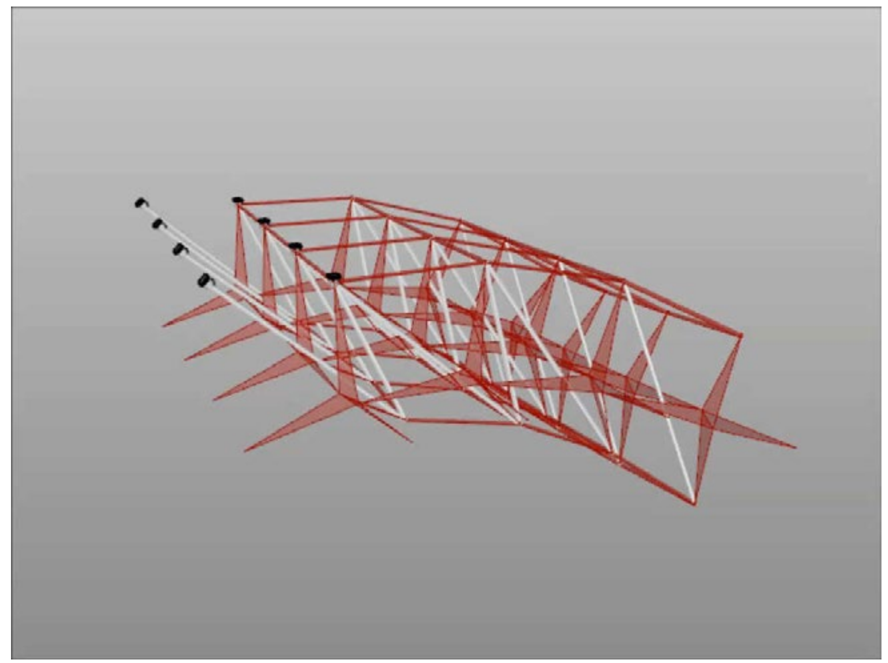

Animation 2.17
Surface arrayed assembly #1.

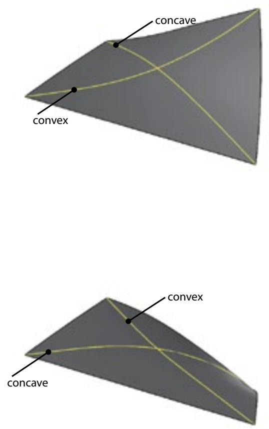


Image 2.94. Curvature changing fot the discrete arrayed surface structure.

As second experiment, a series of pistons connect the simplexes along the z direction. The boundary pistons of the ‘cantilever-like slab’ are then pined at one vertex and constrained with a roll free to slide along the z direction (or along the global coordinate system x-axis) at the other vertex (Image 2.95).
If the pistons are now activated together, the discrete surface changes its curvature both in the u and v direction with alternate curvature signs, like a double curvature hyperboloid surface.

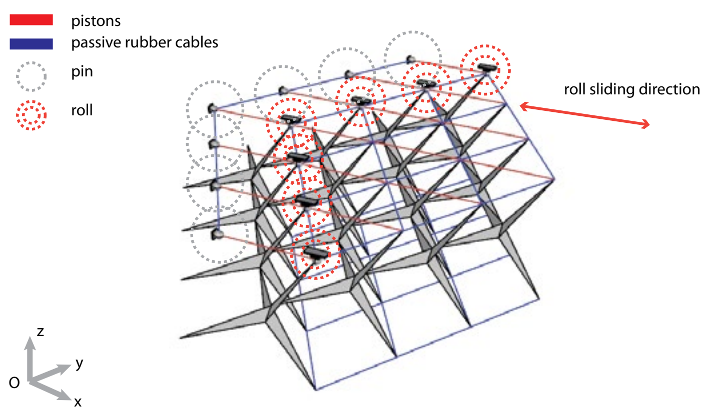


Image 2.95. Assembly actuators and constrains.

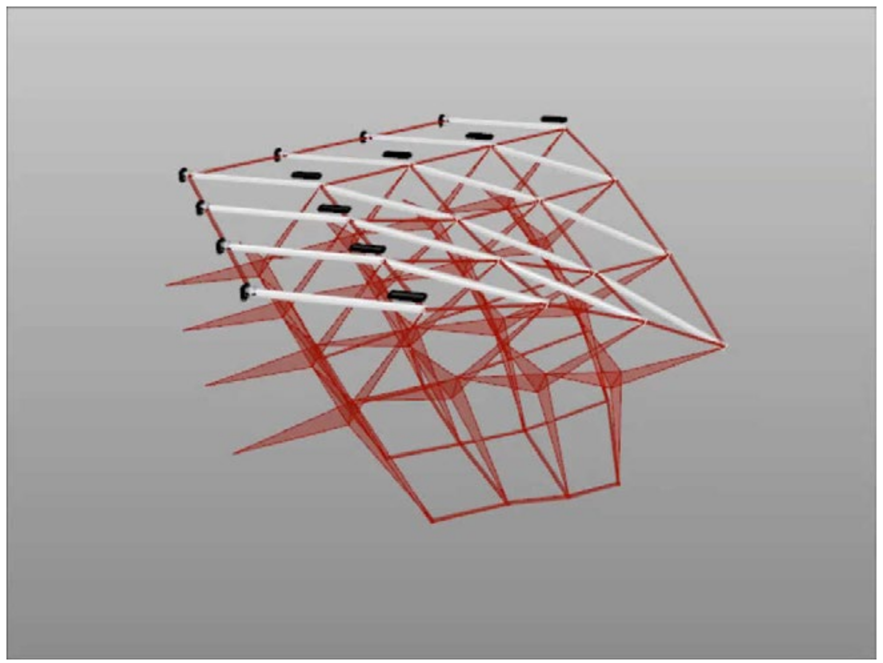

Animation 2.18
Surface arrayed assemby #2.

Chapter 3 //  Considerations on Acoustics

### 3.1 Foundations of Acoustics: Sound and Vibrations

Acoustics is the interdisciplinary science that deals with the study of all mechanical waves in gases, liquids, and solids including vibration, sound, ultrasound and infrasound (Cammarata 2005).

A sound wave is a physical disturbance of molecules within an elastic medium (air, water, or solid) that can be detected by a listener. A sound wave can be seen also as a longitudinal pressure fluctuation that moves through an elastic medium. It is called longitudinal because the particle motion is in the same direction as the wave propagation. If the displacement is at right angles to the direction of propagation, as is the case with a stretched string, the wave is called transverse (Long 2006). The molecular disturbance caused by an acoustic source involves a series of high and low pressure areas termed compression and rarefaction (Salter 1998).

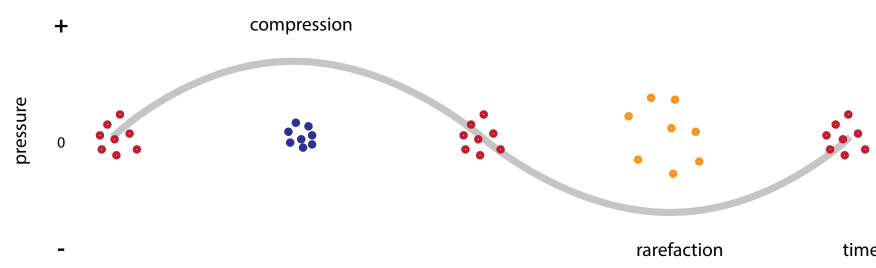


Image 3.1. Full cycle of a continous sine sound wave in  function of tme along the x-axis and pressure on the y-axis

Most sound waves result from a vibrating object: by observing the surrounding environment countless objects in a state of vibration: the windows in your house when a truck drives by, a guitar when its strings are plucked, or tree branches in the wind. Each of these are examples of a sound source. These different waves combine and reach a listener via numerous direct and indirect pathways. The listener's inner ear contains organs that vibrate in response to these molecular disturbances, converting the vibrations in to changing electrical potentials that are sensed by the brain, allowing the phenomenon of hearing to occur (Barron 2001).

Acoustical analysis involves not only the sound source but also who is hearing it (receiver) and everything in between (the path). The path is made up of the environment encompassing both sound source and receiver. The medium of transmission can either be air, or a combination of mediums, involving a conversion to vibration and then back to sound, through solid objects such as walls and floors (Barron 2001).

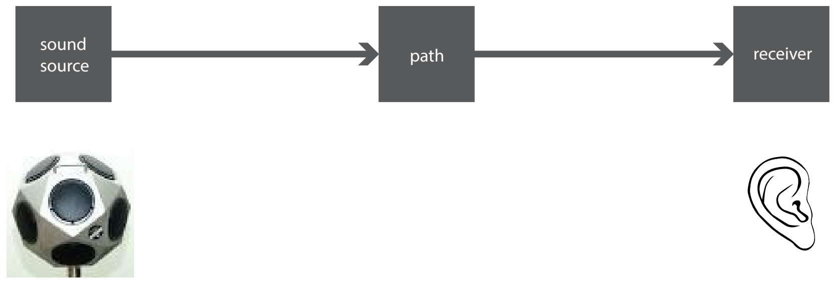


Image 3.2. A generalized source-path-receiver diagram.

The perception of a listener can be influenced by the treatment of either the path or the source. For instance, we can enhance the intelligibility of speech in a conference room by electronically amplifying the spoken voice, or the sound output from a power plant can be reduced to limit the disturbance in a community (Salter 1998).



Chapter 3 // Considerations on Acoustics

### 3.2 Characteristics of Sound Waves

Within this section the most important characteristics of sound wave are introduced: the basic knowledge here reported is fundamental to understand the topic of room acoustics whose principle will be applied later on to tune the soundscape of the theatre object of study by means of the adaptive acoustic ceiling.

Mainly we can distinguish three important characteristics for waves: the amplitude, the frequency and the wavelength (Barron 2001).

#### *Amplitude*

The amplitude of a sound wave is determined by the magnitude of the pressure fluctuation (Salter 1998): for sake of simplicity, acoustician have associated wave amplitude with the sound pressure metric.
Roughly, the concept of sound pressure can be seen as the 'volume' or 'loudness of the sound perceived, so that a variation in sound pressure is perceived as a change in loudness.

The range of pressures to which our ears can respond exceeds a ratio of one to a million (Table 3.1) and the response is not linear, but logarithmic (Barron 2009). The range of sound pressures that humans can detect is enormous. The quietest sound a typical young person can hear is equivalent to 20 micropascals (.00002 Pascal or Pa), while the most intense sound that humans can tolerate is equivalent to a sound pressure of around 200 Pascal). This is a change in magnitude of 10,000,000 to 1. By using a particular logarithmic unit known as the decibel (dB), a wide range of pressure measurements are compressed onto a logarithmic scale (Salter 1998).
The decibel scale is easy and convenient to use when describing sound. The range of decibels most commonly encountered in acoustics extends from 0 to 140 dB (0 dB corresponding to the threshold of hearing, and 140 dB corresponding to the threshold of pain). Within these limits is the dynamic range of the auditory system (Salter 1998 and Barron 2001).

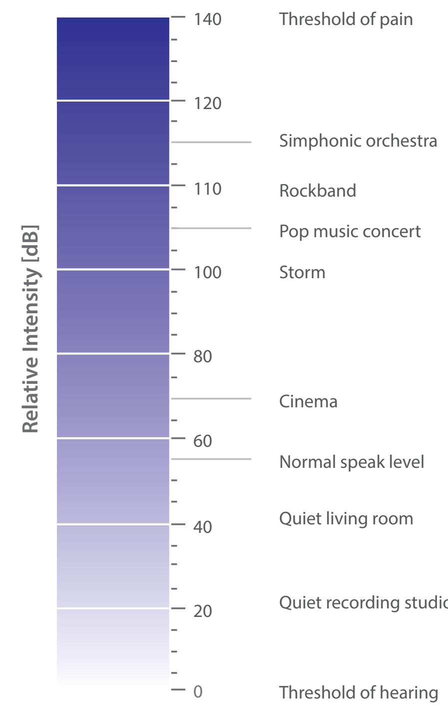


Table 3.1. Comparison of sound pressure and SPL in dB for typical sund sources

A sound pressure expressed using the dB scale is termed the sound pressure level (SPL) and is the most frequently used metric in acoustics. The SPL is defined as:

$$SPL = 10\log\frac{p^2}{p_{ref}^2}$$

where p is the root-mean-square sound pressure in Pa and $p_{ref}$ the reference pressure equal to $2{\cdot}10^{-5}$ Pa (Barron 2001).

### *Frequency*

Frequency intrudes into all aspects of acoustics: The molecular disturbance caused by an acoustic source involves a series of high and low pressure areas (termed compression and rarefaction): the number of compression and rarefaction per time unit determine the frequency of the sound wave (Barron 2009).
A sound's frequency is defined in terms of the number of wave cycles that occur during one second. The unit used for describing frequency is hertz (Hz). For higher frequencies, kilohertz (kHz) is used to indicate the number of oscillations times 1,000 that occur within a second (Barron 2001).

If you drop a rock into the middle of a lake, ripples propagate outward from the point of contact. These circular ripples are comparable to sound waves traveling through air. If you count the number of wave ripples that pass a single point on the lake during one second, you can calculate the wave's frequency. Waves that have a repeated pattern of oscillation are called periodic waves (Salter 1998).

With the knowledge just introduced we can present now the concept of 'tone': a musical tone is a steady periodic sound (Salter 1998).
The simplest type of periodic wave is sine wave. Sine waves (also called pure 'tones') have a single constant frequency. Pure tones are rare, in fact the tone produced by a musical instrument is also built up of a base tone and its derived various harmonics (Van der Linden et al 2006).
A harmonic of a wave is a component frequency of the signal that is an integer multiple of the fundamental frequency: for instance, if the fundamental frequency is f, the harmonics have frequencies 2f, 3f, 4f, and so on (Barron 2009).



Chapter 3 //  Considerations on Acoustics

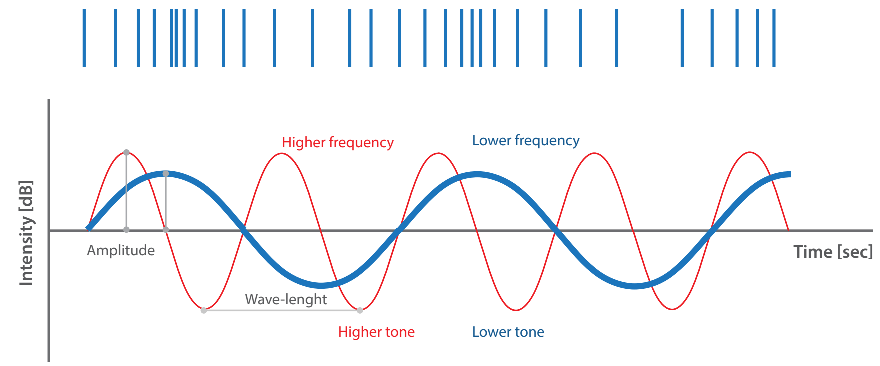


Image 3.3. Comparison of sound wavelenght fr two sine waves with different frequency.

How do these frequencies relate to hearing? When the frequency is in the range of 20 Hz to 20 kHz, the waves are heard as sound waves; these are termed audio frequencies. Human speech contains frequencies that lie between 200 Hz and 5 kHz; the sound of an orchestra can contain frequencies between 25 Hz to 13 kHz or even higher. Frequencies below 20 Hz are sensed as vibration, are not audible to most people, and are termed infrasonic. Frequencies above 20,000 Hz are termed ultrasonic (Salter 1998).

Many situations encountered in buildings involve a combination of both audio and infrasonic frequencies; that is, sound and vibration. For instance, at frequencies up to around 100 Hz, such as those produced by a pipe organ, it is possible to simultaneously hear sound and feel vibrations. Real-world waves are not as periodic as those just described; in fact, most waves usually contain a mixture of many frequencies. While a sine wave is considered technically to be a simple wave, in actuality, almost all waves in nature are complex, in that they contain multiple frequencies (Salter 2000).

The reason a violin and a viola sound different from each other is because each has a different combination of frequencies, which is referred to as the sound source's spectrum .The interaction and behavior of the different frequencies within a spectrum can be quite complex, and are in fact responsible for the rich palette of sound colors that we experience daily. (Salter 1998).
The fundamental musical interval is the octave, which corresponds to a doubling of frequency. Acoustic measurements are also conventionally made over octave intervals, with centre frequencies of 125, 250, 500, 1000 Hz etc (Barron 2001).

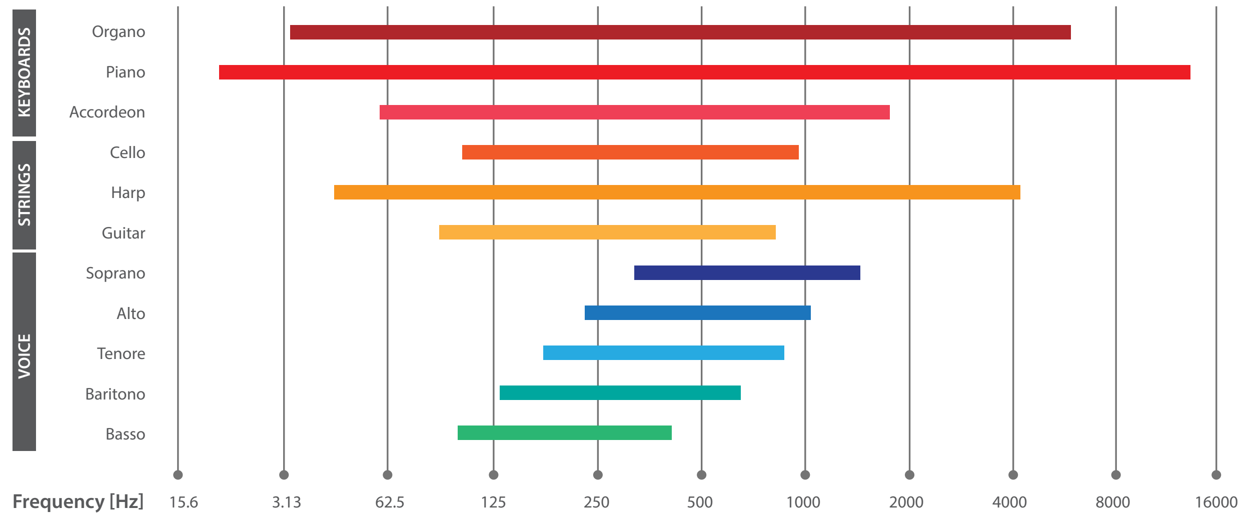


Table 3.2. Frequency ranges of different sound sources.

### *Wavelength*

The wavelength λ is an important parameter in determining the behavior of sound waves. If we take a 'picture' of the wave at a particular instant in time, the wavelength is the distance between successive peaks of the wave (Barron 2009). The wavelength and speed of sound for a simple harmonic wave are related by:

$$\text{speed of sound} = \text{frequency} \times \text{wavelength}$$

So, by knowing the speed of sound within air (equal to 343 m/sec) the wavelength of a specific frequency can therefore be calculated as follows (Barron 2001):

$$\lambda = \frac{c}{f}$$

The wavelength for a sound in the middle of the frequency range of 1000 Hz is thus 0.343 m. The range of wavelength of audible sounds is between 17 m at 20 Hz and 17 mm at 20 kHz. This implies that these wavelengths are comparable to dimensions of room surfaces and common objects (Salter 1998 and Barron 2009).



Chapter 3 // Considerations on Acoustics

## 3.3 Room Acoustics

Room acoustics as a discipline involves the study and analysis of direct and reflected sound in closed space. Appropriate room acoustics are essential in all spaces where sound is to be transmitted to a listener; this includes both speech and music. Room acoustics design criteria are determined according to the room's intended use. Music, for example, is best appreciated in spaces that are 'warm' and reverberant. Speech, by contrast, is more intelligible in rooms that are less reverberant and more absorptive. This means the criteria that create good speech intelligibility are very different from the criteria that create a space suitable for listening to and appreciating music. It is possible to create suitable acoustics for both speech and music in the same space, although this is rarely accomplished without some degree of compromise (Salter 1998).

The term room acoustics typically brings to mind spaces where music is performed and recorded: concert halls, recording studios, and scoring stages, for example. While acoustics are especially important to the success of these spaces, a much wider variety of facilities benefits from well-designed acoustics. Lecture and convention halls, classrooms, board rooms, council chambers, courtrooms, places of worship, theaters, cinemas, and broadcast studios all depend on their acoustical quality. Speech intelligibility is essential in all of these spaces. Different acoustic design criteria are required for rooms where music is to be played, where 'natural' acoustics help support unamplified musical instruments (Salter 1998 and Ballou et al 1987).

Room acoustics is a combination of both art and science (Beranek 1962). Scientific theory plays an important role in defining acoustical measurements and analysis techniques. Still, the best acoustical theory must be combined with creativity, intuition, and experience to be implemented effectively. In other words, while applied acoustics is heavily based in theory, it is also much improved by the empirical judgment of an experienced acoustician (Salter 1998).

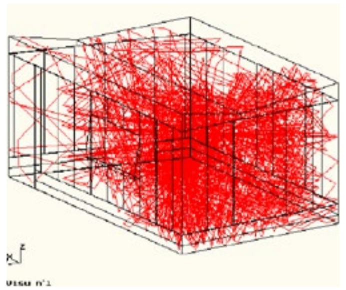

Image 3.4. Digital simulation of a diffuse sound field with 200 rays reflected in a closed room (image courtey of Cammarata 2006).

### 3.3.1 Diffuse Sound Fields

Direct sound is the sound wave that reaches the listener via a direct path, without having bounced off a reflecting surface. A diffuse sound field, on the other hand, refers to the energy from a sound source that reaches the listener indirectly, after reflecting off surrounding surfaces.The buildup of diffuse sound over time is known as reverberation. Reverberation is a collection of time-delayed versions of a sound that have decayed in intensity over time as they arrive at the listener. Reverberation is most often heard in enclosed spaces: in most rooms, the direct and time delayed sounds arrive so quickly in succession that they are perceived as one sound source, arriving from a single location defined by the direct sound. However, if the reflection arrives late enough in time and has a significantly high amplitude, it is heard separately as an echo (Barron 2009).

In this section the interaction phenomena with sound waves and room surfaces will be introduced, together with their relative influence in the room soundscape.



Chapter 3 // Considerations on Acoustics

#### *General Sound Reflections*

The main difference between indoor and outdoor sound propagation is in the level of reflected sound. Indoor environments naturally create more reflected sound than do outdoor environments.
We can divide reflected sound into two main categories (Salter 1998):

- early and middle-reflected sound,
- reverberation (late-reflected sound).

Early reflections contribute more to the subjective perception of reverberance, or 'liveness' of a space. Early and middle reflections occur within the first quarter of a second after arrival of the direct sound. Early sound is considered to be 40 msec after arrival of the direct sound for speech, while for music 80 msec is more appropriate (Salter 1998).

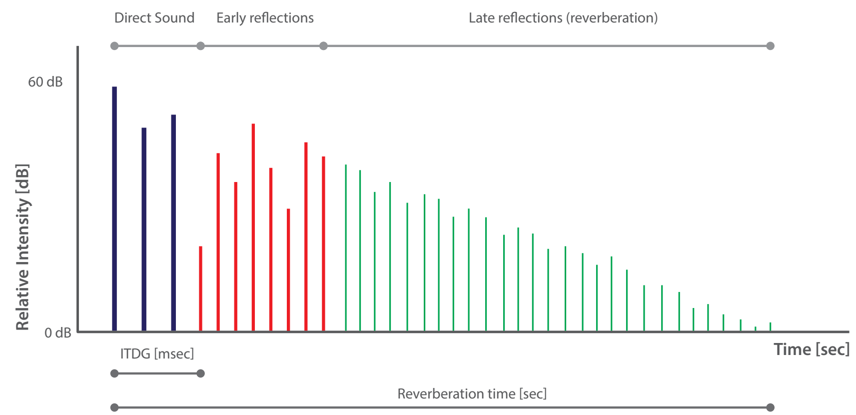


Image 3.5. Reflectogram showing direct sound (in blue), early reflections (in red) and reverberation (green).

The number and quantity of early and middle reflections delivered to any particular listening location depends largely on the room's shape. For this reason, geometric analysis, which involves the study of reflected sound propagation paths modeled as rays radiating from the source of sound, is particularly useful for tracing echo paths and for studying the uniformity of early reflected sound in medium and large-sized spaces (Barron 2009).
The word echo is used for a reflection which is heard as a discrete event, such as can be heard outside when shouting some way from a large wall. An echo is

an intelligible repetition and is not to be confused with reverberation, which is unintelligible. Most reflections in rooms are not heard as echoes (Barron 2009).

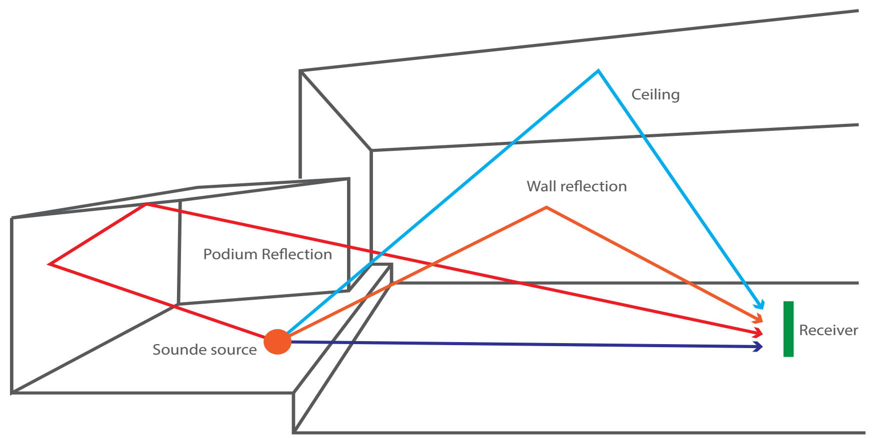


Image 3.6. Sound rays in a theatre: direct and first reflection paths.

Once sound reflections have built up to a point where they are not discernible as discrete events, the late reverberation process takes over. In most well-designed spaces, reverberation is a statistical phenomenon, no longer relying on specific room shape and sound propagation paths. For this reason, the statistical study of room acoustics, which ignores the path of specific reflections but considers reflected sound as an aggregate probability, is employed with respect to reverberation. Statistical analysis methods are applicable to rooms with relatively uniform sound absorbing material distribution and reasonable aspect ratios.
In spaces having a diffuse sound field, where sound is uniformly distributed throughout the space, reverberation decays logarithmically. The reverberation time is defined as the time for reflected sound to decay 60 dB (Salter 2000).

### *Specular Reflections*

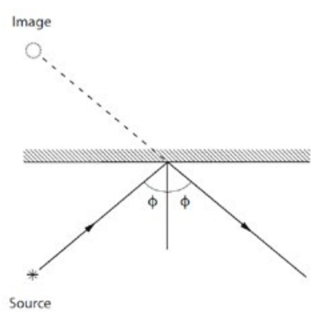


Image 3.7. Lambert's law (imagine courtesy of Barron 2009).

The geometries of reflection for light and sound are identical: specular reflections, those reflections conforming to Lambert's law of reflection, where the angle of incidence equals the angle of reflection, typically occur at smooth, hard, and relatively flat surfaces. Sound reflected by one surface will continue to be reflected between the room surfaces, until its energy is removed by absorption (Barron 2009).



Chapter 3 // Considerations on Acoustics

For a surface to be a good reflector of sound, its dimensions should be at least one wavelength or larger than the lowest frequency being reflected. For instance, the wavelength of the musical note middle C (256 Hz) is approximately 1.35 m long. Two octaves higher, a little above 1 kHz, the wavelength measures just over 0.345 m. In order to adequately reflect low-frequency sounds, which have larger wavelengths, the reflectors must be relatively large (Barron 2001).
Moreover, the reflective panels must have a self-weight not inferior to 150-200 $N \cdot m^2$.

### *Diffusive Reflections*

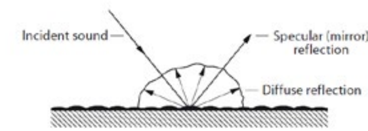


Image 3.8. Partially scattered reflection from a diffusing surface showing specular and scattered components (image courtesy of Barron 2009).

Sound can also reflect in a diffuse manner. The reflection is fragmented into many reflections having less intensity, which are scattered over a wide angle creating a uniform sound field. Diffusion can be created in a variety of ways, most often by introducing surfaces having irregularities in the form of angled planes or convex surfaces sized at least as large as the wavelength being diffused (Salter 1998). Scattering surfaces for sound are an important aspect of auditorium design. Three-dimensional surface ornamentations, columns and statuary serve as diffusing elements and were integral to the acoustics of 17th, 18th, and 19th century performance spaces (Barron 2009).

The depth of the diffusing undulations must be at least one-tenth the wavelength being diffused. However, it is possible, if attempting to create a relatively low-frequency diffuser, for example the octave below middle C, which has a wavelength of 2.7 m, to have specular reflections at higher frequencies. For this reason, in some concert halls, there are macro as well as micro diffusive elements to accommodate diffusion in different frequency (and therefore wavelength) ranges. Fractal mathematics could help create surfaces that diffuse sound over a greater frequency bandwidth. This is accomplished by duplicating the shape of the macro element at micro-scale on the surface of the macro element. Most common diffusers work well between 800 Hz and 4 kHz. Reflections are usually comprised of both diffuse and specular components. In the case of specular reflections, most of the acoustic energy travels in the specific direction dictated by Lambert's law. However, some energy is diffused. Similarly, many diffusers have a strong lobe of

Image 3.9. A pair of suspended acoustic diffusors in the Glasgow Royal Concert Hall, Scotland (image courtesy of Barron 2009).

directional energy directed along the specular reflection path (Barron 2009).

It is common to think of room acoustics geometrically in terms of a reflected ray diagram analysis, but this assumes total specularity, which is an idealization. After three or four consecutive reflections of a ray, the analysis is no longer accurate due to diffusion. Ray diagram analysis has proven to be most useful for time and sound-level distribution of the early reflections and echoes, which are most likely to be specular. Where numerous listening locations are involved it can become a laborious task to calculate the geometric path for each reflection and is seldom done. However, room acoustics software packages are available that can calculate sound paths for a large number of listening locations (Barron 2009).

### *Sound Absorption*

All materials have some sound-absorbing properties. Incident sound energy that is not absorbed must be reflected, transmitted, or dissipated. Absorption of sound in nothing more than the conversion of the mechanical energy coming with waves into heat (Van der Linden et al 2006).
A material sound absorbing properties can be described as a sound absorption coefficient in a particular frequency range. The coefficient a can be viewed as a percentage of sound being absorbed, where 1.00 is complete absorptive material (100%) and 0.01 is minimal (1%) (Barron 2001).

To determine the amount of sound absorption that a room surface has, the surface area is multiplied by the absorption coefficient to yield a result in sabins: one square meter of 100% absorbing material has a value of one metric sabin.
The total sound absorption A within a room can be obtained by adding the amount of absorption in sabins attributed to all surfaces $S_i$ in each frequency range (Salter 1998 and Beranek 2006):

$$A = a_1S_1 + a_2S_2 \ldots + a_nS_n \text{ [m}^2\text{ metric sabin]}$$

Incident sound striking a room surface yields sound energy comprising reflected sound, absorbed sound, and transmitted sound. Most good sound reflectors





prevent sound transmission by forming a solid impervious barrier. Conversely, most good sound absorbers readily transmit sound. Sound reflectors tend to be impervious and massive, while sound absorbers are generally porous, light-weight material (Salter 1998).

There are two three categories of sound absorbers: porous materials commonly formed of matted or spun fibers, membranes and vibrating paneling and resonators created by holes or slots connected to an enclosed volume of trapped air (Salter 1998). According to these three categories, the energy dissipation can be achieved in three relative's way: by friction with air movement in porous materials, by motion of a suspended panel and by means of resonance.
In some cases, the absorptivity of each type of sound absorber can be prominently influenced by the mounting method employed (Van der Linden et al 2006).

Porous absorbers are the most commonly used sound-absorbing materials. When a sound wave penetrates a porous material there is friction between the coming and going air particles in the pores of the material. This friction causes the sound energy (movement) to be converted into heat. The sound is absorbed by the material. In order to ensure that the sound can penetrate the material it must be as porous as possible (Barron 2009).
Common porous absorbers include carpet, draperies, spray-applied cellulose, aerated plaster, fibrous mineral wool and glass fiber, open-cell foam. Porous absorbers are the most commonly used sound-absorbing materials. Porous panel absorbers are usually most efficient at absorbing from mid to high frequencies (Salter 1998).

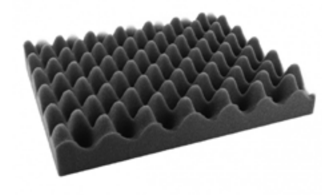

Image 3.10. A porous absorber panel.

When a sound wave hits the surface of a suspended panel, triggers its movement: a pressure is created, and when the panel reaches a partial equilibrium state a depressure is formed. This system can be assimilated to a spring-dashpot-and-mass system, where the mass is represented by the panel, the spring and the dashpot are the air in the interspace which to a certain factor of damping is associate (Cammarata 2005).
Common panel (membrane) absorbers include thin wood paneling over framing, lightweight impermeable ceilings and floors, glazing, and other large surfaces capable of resonating i n response to sound. Panel absorbers are usually most

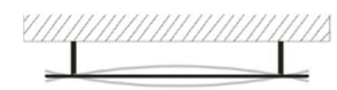

Image 3.11. Diagram of a vibrating suspended panel (image courtesy of Cammarata 2006).

efficient at absorbing low frequencies (Salter 1998).

Resonators typically act to absorb sound in a narrow-frequency range; they include some perforated materials and materials that have openings (holes and slots). The classic example of a resonator is the Helmholtz resonator, which has the shape of a bottle (Barron 2009).
The way in which the Helmholtz resonator work is based on the resonance principle: when an object is struck by a vibration that is equal to this natural frequency, the object will spontaneously start to vibrate. When the resonator is invested by a bundle of sound waves, the air in proximity of its opening are alternatively compressed and decompressed. The air in the holes forms a kind of mass that can vibrate on the air layer that lies behind it, acting as a kind of spring. This type of mass-spring system has its natural frequency (or resonance frequency) (Cammarata 2005).

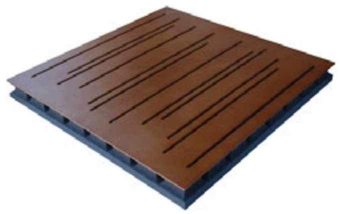

Image 3.12. A wooden absortpive panel provided with longitudinal slots working as the Helmholtz resonator.

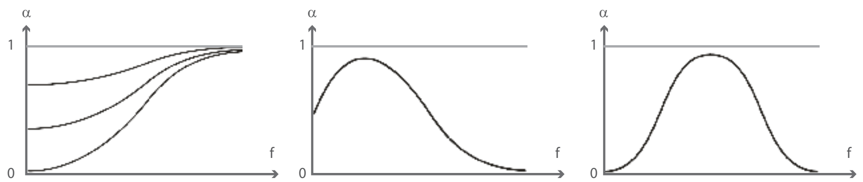


Image 3.13. Typical Absorptive spectrum for (starting from the left) a porous, a vibrating membrane and Helmholtz resonator.



Chapter 3 // Considerations on Acoustics

**3.3.2 Assessment criteria for Room Acoustics**

The acoustical properties that make a room good for speech are often the same as those that make it poor for music, and vise versa (Ballou et al 1987). For good speech intelligibility, room volumes and reverberation times should be low. The first reflections should be primarily from the ceiling, and there is little need for diffusion. Conversely, rooms designed for listening to unamplified music require longer reverberation times, higher volumes and high diffusion. Rooms designed for mixed uses require a judicious compromise between the needs of speech and music (Barron 2009).

Within this section the most important room acoustic metrics are introduced together with requirements needed to be fulfilled in order to design a comfortable room in relation to the type of performance played. This section in widely based of the work of Leo L. Beranek.
Beranek (1962) did a very detailed study of the acoustical factors influencing the appreciation of music, being able to identity a number of objective and subjective attributes of musical-acoustical quality. This review is here implemented considering also acoustic requirements for speech.
One of the results of Beranek's study was the development of a rating scheme for assigning a single number quality judgment for concert halls. These will be here introduced and further used to assess the soundscape of the theatre object of study.

***Reverberation Time***

The listener in a room hears the direct sound followed by a series of early reflections whose paths can normally be precisely defined. Sound that is not absorbed continues to be reflected. The late sound generated by reflections after about 100 ms is called the reverberant sound. Its duration is described by the reverberation time $RT_{60}$, defined as the interval required for sound reflections to decay by 60 dB, one millionth of their original amplitude (Salter 1998).
This objective measurement denotes also the subjective quality of a room for music known as *liveness:* liveness is related primarily to the average reverberation time of the middle octaves centered at 500 and 1000 Hz (Beranek 1962).

The difference in acoustic character between a cathedral and a domestic living room is immediately obvious. The time for sound to decay to inaudibility in a cathedral can be timed with a stop-watch. The room response, which can be heard after a loud, short-duration sound or after a continuous sound is turned off, is known as terminal reverberation.
Reverberation time will vary with frequency. At high frequencies above 1 kHz, the reverberation time inevitably decreases due to air absorption .At low frequencies, the situation can be controlled by the designer (Salter 1998).
For speech there is good reason to keep the reverberation characteristic constant with frequency; a rise in the bass undermines intelligibility. But for music a bass rise in reverberation time is considered by most people as desirable (Barron 2009).

Sabine was the first acoustician to lead a solid study to determine the reverberation time. Its formula applies to rooms that have a relatively diffuse and uniform sound field is presented below:

$$RT_{60} = \frac{0.163 \cdot V}{A + 4mV}$$

where $RT_{60}$ is the reverberation time (sec); 0.163 a constant for metric units, V is the room volume $m^3$; *A* is the total sound absorption in the room in square meters (§3.3.1) and m is the energy attenuation constant for sound traveling through air in units of $m^{-1}$.

The Sabine equation remains valid in most cases (Barron 2009). In order to determine the reverberation time in a diffuse room, it is necessary to sum up all of the room's sound absorption due to each surface material's contribution. This can be accomplished in each frequency range by multiplying the surface area by the sound-absorption coefficient for a particular frequency range, and then summing i n that frequency range for all materials located within the space. Just as reflections are not entirely specular or diffuse, no material is entirely sound-absorbing or sound-reflecting. Rather, a material can have both absorptive and reflective properties, sometimes being reflective in the mid-and-high-frequency ranges and absorptive in the low. This equation is the basis of virtually all reverberation time prediction in auditoria. The calculation is usually performed at each octave





frequency of interest, at least from 125 to 2000 Hz (Salter 1998).
Sabine's equation assumes that the sound energy is equally diffused throughout the room. Actually, this condition is rarely fulfilled due to the large areas existing in a hall characterized by differentiated absorption. Therefore, in practice, there are several formulae describing the reverberation time (Long 2006).
It was discovered by Eyring that the classical formula given by Sabine is not fulfilled when there is considerable room absorption. Eyring pointed out that the reverberation time is shaped dependent: he presented the revised theory thoroughly and derived a form of the reverberation time equation, which is more general than Sabine's formula (Neubauer et al 2001). Eyring's equation reads:

$$RT_{60} = \frac{0.163 \cdot V}{-S \cdot \ln(1-\alpha^*) + 4\mathrm{mV}}$$

where the term $\alpha^*$ is the average absorption coefficient defined as:

$$\alpha^* = \frac{1}{S} \cdot \sum_i S_i \cdot \alpha_i$$

Eyring derived equation for the reverberation time, is theoretically more correct. In practice, however, Sabine's equation is used more often because it very often comes closer to measured values (Salter 1998).

By observing the formulas above presented we can see that the reverberation time is directly proportional to room volume, inversely proportional to the surface area, and inversely proportional to the amount of sound-absorbing material. Excess reverberation results in a blurring of sounds and can reduce speech intelligibility. It is possible to reduce reverberation by the following means: adding sound-absorbing material, by reducing room volume or by increasing surface area (Salter 1998).
Reverberation time remains the single most valuable measurable quantity for the acoustics of an enclosed space. It has the advantage that it is generally constant throughout the room. An immediate preliminary assessment can be made of the suitability of a space for music or speech from knowledge of the reverberation time.
The appropriate reverberation time for an auditorium should be determined principally on the basis of program. Many references are found in the literature to optimum reverberation time also being a function of hall volume (Barron 2009).

A major dilemma exists for reverberation time design for multi-purpose spaces. With orchestral music requiring a 2 second reverberation time and speech only 1 second, use of a single space for both speech and music is usually not possible without an adjustable acoustic system. Selecting a compromise time for such a situation can result in acoustics which are neither able to support intelligible speech nor sufficiently live by musical standards (Barron 2009).

### *Initial Time Delay Gap*

The Initial Time Delay Gap (ITDG) is the interval between the arrival of the direct sound from the stage and the arrival of the first reflection from the walls or ceiling. This measure is generally expressed in millisecond. Its subjective impression is known as *intimacy* (Ballou et al 1987).
The ITDG is usually assessed by taking in considerations the early reflections or the first order reflections (Barron 2009). While designing the hall this measure should be considered in order to avoid echoes (in fact, if the reflection arrives with a time gap higher the 80 msec with respect to the direct sound this is perceived as an echo) and to improve the intimacy, namely the sense of closeness of the listener with players.
The ITDG should be kept as low as possible, but generally for multipurpose theatres and concert hall a value of 40 msec is acceptable (Beranek 1962, Ballou et al 1987 and Barron 2009).

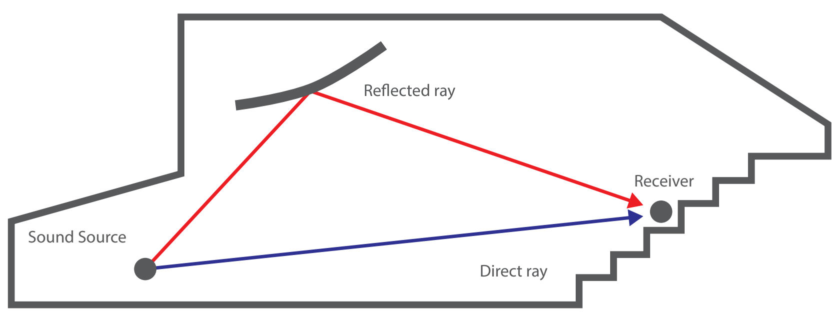


Image 3.14. Geometry for the determination of the ITDG.





### *Brilliance*

A sound is called brilliant if it is bright, clear and rich in harmonics. Brilliance Is a measure of the high-frequency response. The treble frequencies should be prominent and decay slowly (Beranek, 1996). Therefore, it is related to the perceptual attribute timbre. Brilliance can be evaluated by calculating the Treble Ratio (TR) (van Dorp Schuitman 2010):

$$TR = \frac{RT_{2000} + RT_{4000}}{RT_{500} + RT_{1000}}$$

where $RT_f$ is the measured reverberation time in the frequency band with center frequency *f* (Hz).
The treble ratio is not often mentioned in the literature and not much is known about typical values, but assessed good values for concert halls are in the range between 0.75 and 0.95 (van Dorp Schuitman 2010).

### *Warmth*

In a musical context, warmth is defined as liveness of bass or fullness of the bass tones, relative to mid-frequency tones. Like brilliance, it is related to timbre. A common predictor for warmth is the Bass Ratio BR (Beranek, 1962);

$$BR = \frac{RT_{125} + RT_{250}}{RT_{500} + RT_{1000}}$$

In concert halls and opera houses, values for BR are typically in the range 0.9 to 1.5 (Beranek, 1962).
A warm sound room must be provided with a relative long bass reverberation time (Barron 2009).

### 3.3.3 *Preferred Acoustic Ranges*

Like just presented, each performance requires specific acoustic tuning to match with the criteria for room acoustics (Reverberation time, ITDG, brilliance, warmth, etc…). Here the relation between measurement range of acoustic criteria and performance type are presented (Table 3.3). These prescriptions have been taken from the literature review so far referenced in previous sections.

#### *Cinema*

For cinema playback, it is important for embedded audio cues to be reproduced accurately to as many listeners as possible. Speech intelligibility is also very important. Cinema product manufacturers (such as Dolby Laboratories) have published recommended reverberation time ranges for the 500 Hz octave band as a function of room volume (Ellison et al 2010).

#### *Spoken Word*

The goal of an acoustical design for optimum speech performance is to provide for maximum Intelligibility of the speech while also maintaining a natural voice quality (Ellison et al 2010).
Barron (2009) have shown that while early reflections can assist intelligibility by supporting the direct signal from the talker, later reflections can cause one word to blur into the next and thereby degrade intelligibility. He suggests that these unwanted reflections be considered as another form of noise.
The reverberation time must be kept low, around less the 1 second (Ballou et al 1987 and Salter 1998).

#### *Classic Music*

Relative high reverberation time for classical music set a warm and pleasant reverberant soundscape. Different type of classical music also requires different reverberation times with boundaries values for Romantic of 2.2 seconds and Baroque of 1.5 seconds (Beranek 1962).





#### *Opera*

The conflicting acoustic requirements for speech intelligibility and music performance obviously bear on the question of the appropriate reverberation time for opera houses. Short reverberation times are common in opera houses predominantly designed for drama use. But a reverberation time of only 1 second is certainly shorter than ideal for music (Barron 2009).
Conversely, a reverberation time of 1.8 seconds is ideal for orchestral music but is unlikely to leave speech intelligible. Ballou et al(1987) suggest a RT of around 1.6 seconds.

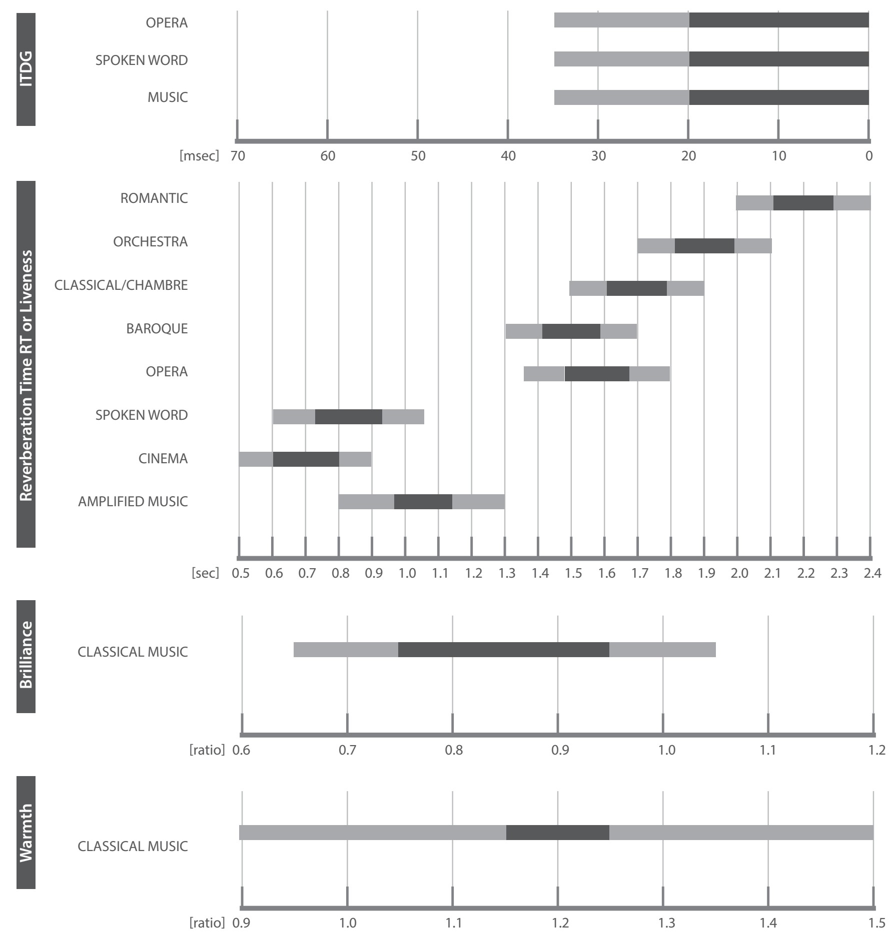


Table 3.3. measurement range of acoustic criteria and performance type: in dark grey the optimal and in light grey the acceptable ones.

### 3.4 Considerations on Acoustics for Multipurpose Spaces

The conscious design of auditoria to accommodate more than one acoustic type of performance is relatively recent. It has become increasingly apparent that for economic reasons auditoria dedicated to just one single use are often unrealistic in all but large cities. A degree of flexibility in use is now becoming the norm (Barron 2009).
Since 1980, there has been an explosion of multipurpose and performing arts theaters. In addition to the major urban centers that have historically devoted halls and theaters to concerts, theatrical performances, dance, films, and lectures, many suburban and rural towns have built or are planning to build such facilities. Often, these projects are part of redevelopment, urban renewal, historic preservation, or adaptive reuse programs. However, unlike the major cities, which can afford to construct separate symphony, opera, and dramatic venues, smaller cities and towns often require facilities that are functionally multipurpose in order to accommodate a variety of artistic pursuits (Salter 1998).
Appropriate acoustics for these new theaters play an important role in their overall success, community acceptance, utility and profitability (Ballou et al 1987).

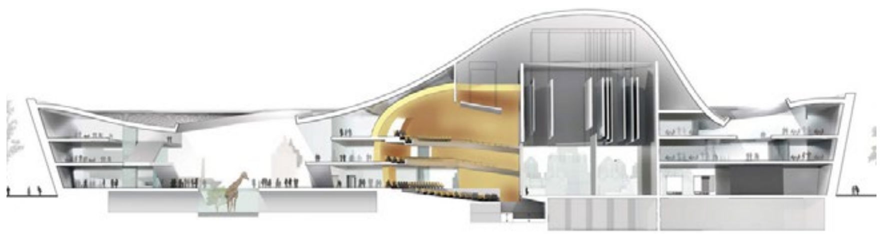

Image 3.15. A new multi-purpose theatre for the Dutch city of Emmen: Henning Larsen Architects desing (image courtesy of henninglarsen.com).

The acoustical properties that make a room good for speech are often the same as those that make it poor for music, and vice versa (§3.3.2). For good speech intelligibility, room volumes and reverberation times should be low. The first reflections should be primarily from the ceiling, and there is little need for diffusion. Conversely, rooms designed for listening to unamplified music require longer reverberation times, higher volumes and high diffusion. Rooms designed for mixed uses require a judicious compromise between the needs of speech and music (Long 2006).





In the general practice, the acoustical design for these multipurpose spaces, particularly in larger rooms, usually demand some degree of compromise (Barron 2009 and Thün et al 2012). This approach is based on the analysis of several scenarios toward the synthesis of an acceptable solution for the several situations. The thesis objective is to overcome this synthesis on the way to optimize the soundscape for various artistic performances: this compromise can be reduced or even eliminated by using active acoustics (Salter 1998 and Barron 2009).
In order to obtain an effective change in the acoustic room, substantial variation must be generated.
Small patches of acoustic absorbent or changes in orientation of small surfaces generally have no significant effects. Acoustic character is more a question of shape than small detail. This means that, for variable acoustics to be meaningful, major changes are required. This is certainly the case with variable reverberation time, which often proves to be the most valuable acoustic change one can achieve (Barron 2009).
Techniques to achieve this proposed result are presented in the next section.

### 3.5 Elements and Techniques for Variable Acoustics

This section is widely based on the research regarding variable acoustics for multi-purpose auditoria made by Barron (2009, Ch.10): author's recommendations about the design of a variable acoustic system synthetizes effectively the relations between acoustics and space or geometric parameters to tune the soundscape according to played performance. The referenced chapter presents also a valuable a collection of some example where variable acoustics has been applied in multi-purpose rooms.
Variable acoustics can be achieved either on electroacoustic systems or motion adjustable elements. Here only the last category is considered.
From the Sabine's equation, it can be seen that the two variables influencing the reverberation time are the internal volume and the amount of acoustic absorbing material. Of these, changes in volume are in principle more attractive but in practice often difficult to incorporate within a functioning auditorium. Although, varying the volume has the advantage compared to varying the acoustic absorption that there is little penalty in terms of sound level (Salter 1998 and Barron 2009).

There are basically two methods to provide variable acoustic volume:
-by a movable panel partition;
-by a movable shutter system.

Movable ceilings are the most common solution for this type of variable-volume hall. Early examples of movable ceilings were tried in the '60s and '70s in North America, mostly using rotating ceiling sections to close higher seating areas (Barron 2009).

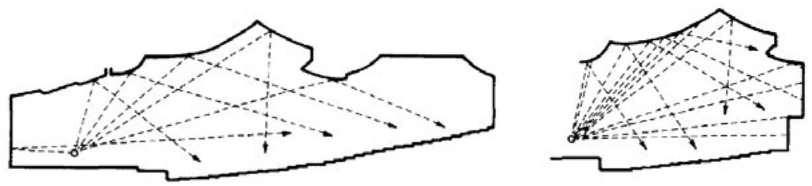

Image 3.16. Veteran's Memorial Auditorium, 2100 or 800 seats, San Rafael, California. On the left ceiling configuration for cocert hall. On the right for drama or opera (image courtesy of Ballou et al 1987).

The alternative shutter system which allows a suspended ceiling to be opened or closed would appear to offer acoustic variability at very little cost. Many auditoria have a void above the ceiling, usually containing structure and ventilation ducting.





Adding this volume to the acoustic volume of the auditorium can provide increase reverberation.
Experience suggests that in order to obtain a successful system, the open area of the ceiling must be 40% or greater of the total ceiling. The void space must behave acoustically as a reverberant volume; if there are significant acoustically absorbent or scattering surfaces in the void, the extra volume may not make a worthwhile contribution to reverberation time (Barron 2009).

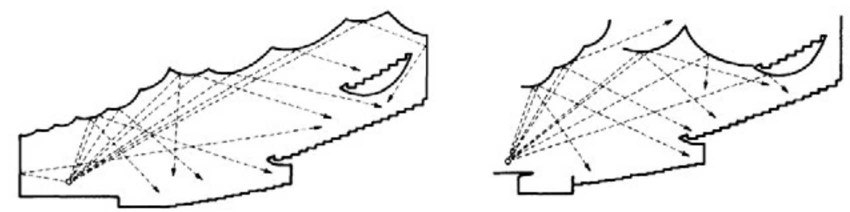

Image 3.17. Edwin Thomas Performing Arts Hall,University of Akron, Ohio. On the left ceiling configuration for concert hall. On the right for opera (image courtesy of Ballou et al 1987).

This solution, in which the void contains roof structure and ventilation ducting (highly absorptive), may not work in practice for these reasons, but this problem can be overcome by coating the void with fully reflective paneling.

Variable absorption is the commonest used approach for variable acoustics.
In order to influence the reverberation time, the area of adjustable absorption must be very large, in fact comparable in size to that of the audience area. This makes variable absorption a progressively more extravagant option the larger is the hall in question.
The most common technique in modern halls for variable absorption is to use acoustic banners.

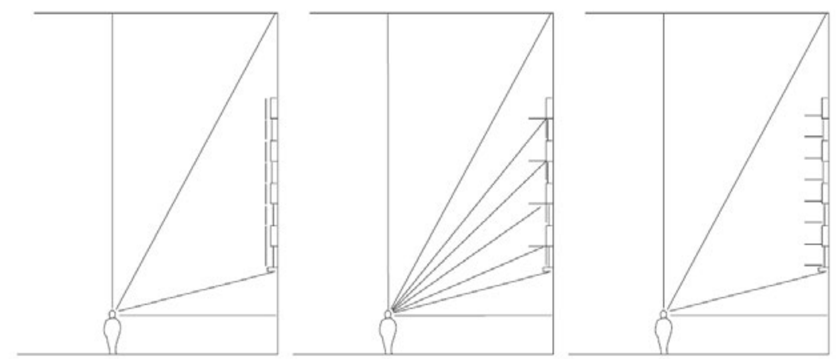

Image 3.18. Variable absorption in the Hong Kong Academy for Performing Arts. The three arrangements of flaps allow three degrees of absorptive panles to be exposed, (Left) Flaps – all closed for long reverberation time; (Center) flaps – half open for medium reverberation time; (Right) flaps – all open for short reverberation time (iamge courtesy of Barron 2009).

### 3.5.1 Precedents

The concert space Sala São Paolo, created in 1999, with a seat capacity of 1509 in the city of São Paolo, Brazil, was designed by Dupre Arquitetura with the acoustics handled by Acustica & Sonica of Sao Paolo and Artec Consultants. This was a renovation project for an old train station hall.
An internal rectangular-plan space open to the sky proved to have proportions similar to those of classical concert halls. This courtyard was covered over but, for present purposes, the interest of this example is the ceiling made of 15 independently movable panels, which can alter the height between 12.2 and 23.7 m. This provides a volume change from 12 000 to 28 000 m3 and occupied reverberation times between 1.9 and 3.0 seconds. The movable panels are loose-fitting so with panels at different heights, the upper space is acoustically linked to the lower. For conferences etc. a reverberation time of 1.5 seconds can be achieved when absorbing banners are placed in the void above the panels. This system of movable panels clearly offers a highly variable acoustic space, though such variability is not cheap (Barron 2009). This is an example of a movable panel partition used in combination with variable absorption.

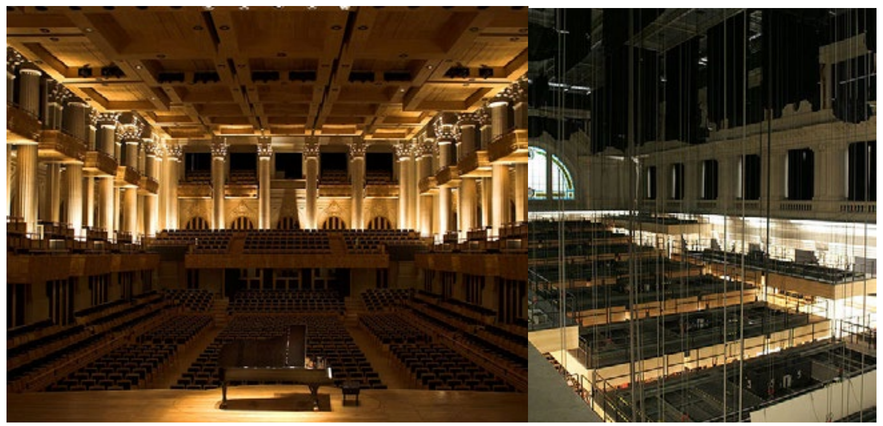

Image 3.19. Sala São Paolo, São Paolo, Brazil: Dupre Arquitetura design with Acustica & Sonica of Sao Paolo and Artec Consultants. On the right: a view of the adjastable ceiling from the under-roof space.

The Milton Keynes Theatre in England designed by Blonski Heard Architects in cooperation with the acoustic consultants Arup Acoustics had to accommodate drama, musicals, opera, ballet, light entertainment and orchestral concerts, with a bias towards drama use. The theatre claims to be Britain's most popular theatre. The fundamental mechanism for changing the acoustics is the movable ceiling. In addition, movable drapes are provided on the sidewalls. The distance between the maximum and minimum heights is 10 m.
For orchestral music, the ceiling is in its highest position and all the drapes are retracted. This configuration provides a volume of 8.5 $m^3$ per seat and gives maximum reverberance. The mid-frequency reverberation time is 1.6 seconds. The intermediate ceiling height provides a lyric theatre suitable for opera and musicals. For opera the drapes remain retracted resulting in a reverberation time of 1.25 seconds. For musicals the drapes are extended to reduce reverberance for amplified sound: with this configuration the measured reverberation time is of1 second. This configuration provides appropriate conditions also for drama.

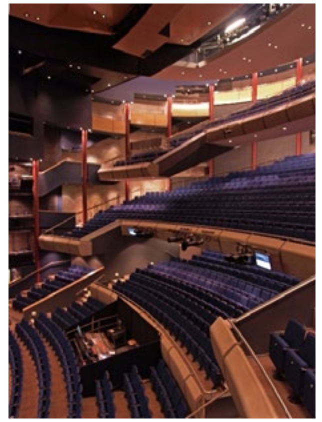

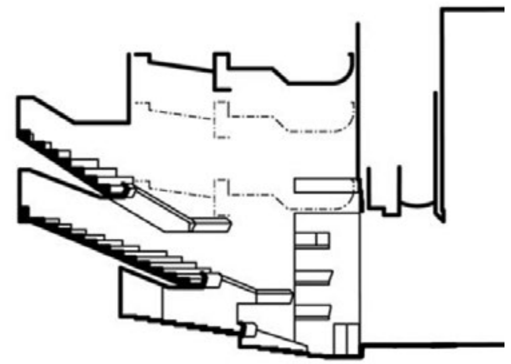

Image 3.20. On the right: long section of the theatre, showing ceiling positions (image courtesy of Barron 2009).

In addition to changing the volume the ceiling provides early reflections over the seating area and its geometry has been carefully shaped to optimize this function. The operation of the variable acoustics is a reasonably quick process: for example, the ceiling can be moved from its maximum to minimum height in a matter of minutes. In terms of acoustic quality, Milton Keynes Theatre is proving excellent for opera and drama and very good for orchestral music. Performances using amplified music are also highly successful (Orlowski 1999).

An example of fully acoustically flexible system in represented by the Paris Espace de Projection at IRCAM (Institut de Recherche et Coordination Acoustique/ Musique). It was completed in 1977, with Piano and Rogers as architects and Peutz et Associes as acoustic consultants. The building is as a research facility for the institute, which is primarily devoted to contemporary music composition and

Chapter 3 // Considerations on Acoustics

performance. The auditorium is rectangular in plan and section with a total volume of 6800 m³. The ceiling is made of three sections which can be lowered or raised independently, offering a volume range of 4:1.

Image 3.21. An the left: auditorium configurationf for chambre mucis. On the right: a configuration for orchestral music (image courtesy of RPBW).

The whole ceiling and all but the lowest section of the four walls consist of panels, each panel containing three rotatable prisms (Image 3.22). The orientation of the prisms within the panels alternates from horizontal to vertical on the walls; a similar direction change is found in the ceiling. Each prism has one face absorbent, one specular reflecting and one diffuse reflecting surface. The state of the prisms in each panel can be altered independently by remote control. This allows either plane reflecting surfaces, highly scattering surfaces or absorbing surfaces, as well as intermediate combinations to be arranged. Regarding its acoustic performance, the reverberation time with 400 audience and 50 performers is a maximum of about 2 seconds. With a combination of a lowered ceiling and absorbing prisms, this can be reduced to 0.5 seconds. This hall provides a fascinating resource for research into the effects of geometry and surface character on acoustics for the listener as well as the performer. It has of course enabled IRCAM to optimize the acoustics for their public concerts. This example offers no model for normal auditoria; the cost of its acoustic variability is high and indeed by music auditorium standards 400 seats is small (Barron 2009).

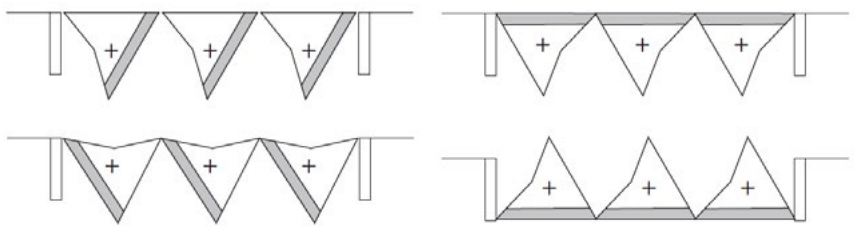

Image 3.22. Possible arrangements in section of the rotatable prisms used on the walls and ceiling (Top left) specularly reflective; (Bottom left) scattering; (Top right) absorbing; and (Bottom right) highly scattering (image courtesy of Barron 2009).





Resonant Chamber (Image 2.11) develops at a further stage the idea of adaptive acoustic ceiling surface by integrating structural sides with acoustic function. The initial prototype of Resonant Chamber was installed in January 2012 at the University of Michigan's Taubman College of Architecture and Urban Planning. The prototype is comprised of a thick, rigid origami surface (§2.3.2) consisting of reflective, absorptive and electro-acoustically enhanced panels equipped with actuators and communication technologies that make it capable of kinetic adjustment, actively transforming the acoustic performance of a host space relative to different types of audience demand.
The research of Resonant Chamber, which is still ongoing, aims to advance this work by exploring the application of multi-functional material treatments within a volumetrically variable acoustic space paired with kinetic operation and digital control via environmental sensing.
A part of folding when the surface is flat, Resonant Chamber is also able to change its curvature: a concave surface focuses reflections at the listening plane when directly under the cell's surface while a convex surface provides evenly diffused reflections at the listening plane at a higher dB range than the flat surface.

Image 3.23. Actuation and suspension details of Resonant Chamber as seen from above (top) and folding surface deformation from below (bottom) (image courtesy of Thün 2012).

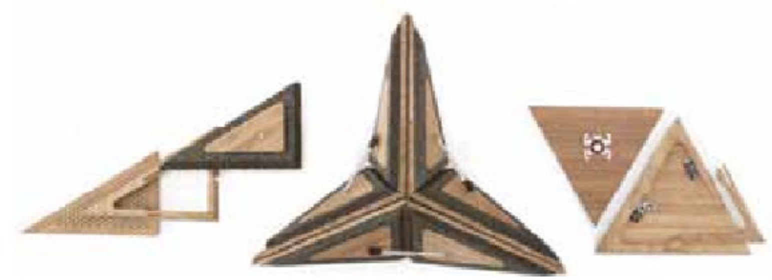

Image 3.24. Composite panel assembly and system components. (image courtesy of Thün 2012).

Throughout acoustic simulations, the research demonstrated that the rigid origami surface with variable absorptive and reflective panels could be configured to achieve a wide range of reverberation times, thereby offering opportunities for multiple program uses within a space (Thün 2012).

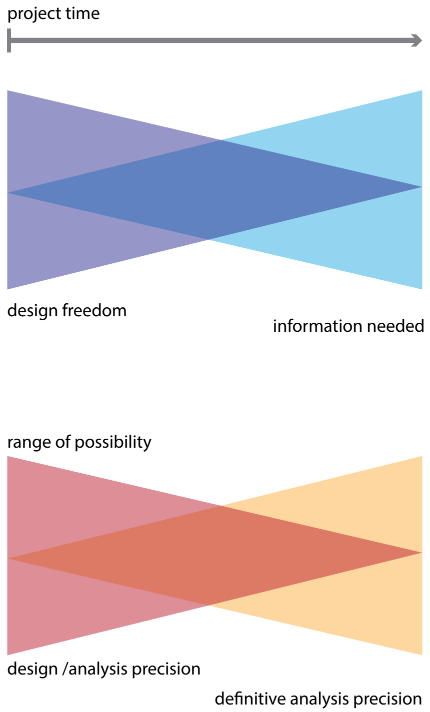


Image 3.25. Top: design freedom vs. amount of information (image courtesy of ir. J.L. Coenders; in turn adapted from MacLeamy curve). Bottom: envisioned use of different precision-defined tools for the assessment along design time.

## 3.6 Associative Geometric Acoustic Tools

In order to assess the acoustics of the room object of study two tools have been developed to consider in live the variations of the acoustic ceiling on the sound scape. The tool are based on a parametric and geometric associative approach and are also developed with Grasshopper™.

The tool developed are rough but particularly useful during the first or conceptual design stage, because allows the user to investigate infinite ceiling configurations, and return immediately to the designer the impression about the characteristic that the ceiling must have in order to fit with the required conditions.

Such design approach is particularly useful in the first design stages: this starts by defining the conceptual outline of the design according to key requirements of the project, followed by the generation of different models and their evaluation. This phase is ideally characterized by a strong collaboration between the designer and consulting experts in different disciplines. The continuous input of new information, resulting from this cooperation, demands a continuous adaption of the initial model, creating a dynamic and cyclic process (Heidegger 2013).



Chapter 3 // Considerations on Acoustics

### *Reverberation Time Assessment Tool*

The Reverberation Time Assessment Tool has been designed in order to evaluate:

-the variation of the effective volume, function of the position of the variable ceiling;

-the variation of the areas exposed to the reverberant sound field, function of the position of the variable ceiling, with particular attention to those surfaces, reflective or absorptive, that compose a possible adaptive ceiling;

-export data to a spreadsheet file format.

To develop this tool the geometry of the theatre object of the case study, the Nieuwe Luxor designed by Bolles + Wilson architects will be used.
As first step a variable ceiling surface is defined. The user can here modify some elementary characteristics of this, such as height, concavity and convexity of ceiling surface in the local u and v directions. This surface will be then populate, in the development stage of the tool, with a system of paneling.
By having defined a variable surface that represents the ceiling variation is possible now to associate the hall Volume V and the Surfaces $S_i$ with the ceiling definition.

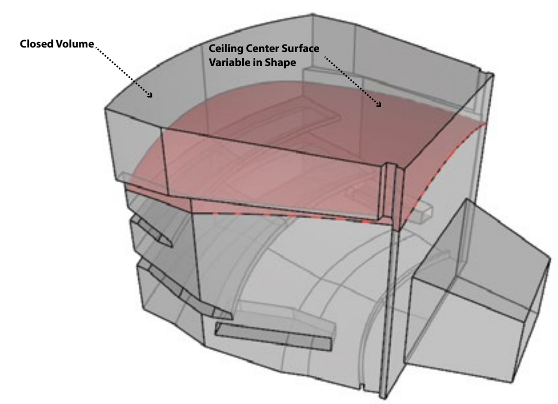


Image 3.26. Geometric 3D model of the case study, Niewe Luxor in Rotterdam, Bolles + Wilson architects design. 3D modelling Matteo Soru, in turn augmented from the model of Kjell Scholts. The hall has been modelled as a water-sealed volume.

Geometrically, the volume V function of the ceiling is found by trimming the closed surface collection that represents the volume with the ceiling surface. The part

of volume above the ceiling surface can be then culled and the effective volume finally can be yield (Image 3.26).
It is worth to mention that, in order to operate a proper trimming procedure, the surface collection that defines the volume must form a closed 'watertight' space region. For this reason, the user is request to first prepare these surfaces with attention and couple them in an edge sealed volume. This procedure is quite standard for the assessment of the acoustics of a room also when acoustics specialized softwares, based on ray-tracing, are used: in fact, normally, softwares require in input a closed volume (or environmental zone) to model accurately the behavior of sounds in a room. Opening, actually, might cause a malfunctioning of the software routine and this can lead to a missed calculation result. For this reason, openings are usually modelled as surfaces that have a full absorption coefficient($\alpha$ equal to 1 for the entire sound wave frequency range), in fact, in reality, all the energy that invests an opening come out from the zone that is equivalent to say that is fully absorbed by the same opening.

Also the surfaces that represent the acoustic areas invested by sound and that contribute to create the soundscape are treated at the same manner: the portion of area above the ceiling are cut out (Image 3.27).

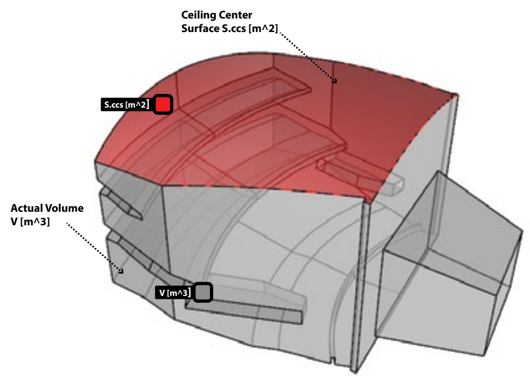


Image 3.27. Effective volume of the hall after being trimmed by the ceiling surface definition.

Particular attention must be paid on the modelling of the areas that represent the paneling of the adaptive ceiling. In order to tune the acoustic qualities of the room, reflective and absorptive paneling compose the ceiling. For the development of the tool an elementary acoustic ceiling composed by a surface array of coupled triangular reflective and absorptive panels joined together at the common edge, has been tested: the reflective panel motion have been set up to follow the ceiling





surface definition while the absorbing ones follow the reflective panel motion and they can further rotate around the common edge.
To note that the use of variable absorption here, instead of a movable panel partition or a movable shuttering system (§3.5) was meant only to develop and test the tool, but the other two systems can easily be integrated within tool functionality.
Starting from the assumption stated by Sabine that the absorptive characteristic of a surface depends to the surface areas (together with their relative acoustic characteristics), the following engineering model is propose: reflective paneling area is easily considered as the effective one, because these panels follow the shape of the ceiling surface in space, while, the area considered for the absorptive ones is the area of the projected panel onto the adaptive ceiling. Finally by knowing the cumulative reflective and projected absorptive areas the ceiling opening area can be found by subtracting to the whole surface area the summations of the paneling ones (Image 3.28).

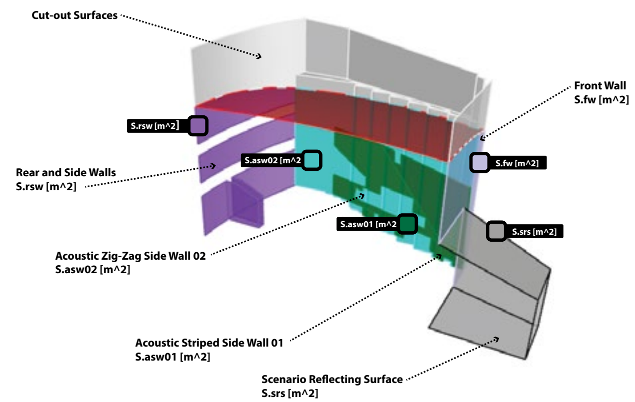


Image 3.28. Families of surface in the hall: in violet the absoprtive rear and side walls, in cyan, the reflective wall, in lavande the relfective front wall and in green a further reflective tilted wall.

The acoustic characteristics of the ceiling openings can be associate to those of acoustic openings (with full absorption coefficient) by considering some theoretical aspects in acoustics: when a sound wave travels in space, its spherical front wave expands, so once it enters into the buffer space between the ceiling and the underside roof, after bouncing on the surfaces here present, its re-emission in the hall room is not guaranteed. Moreover, as the literature states, once the sound waves encounters irregular surfaces like those one that form the underside roof (metallic catwalks, lighting facilities, trussed structural system, in the case of the Niewe Luxor) the energy that they bring in easily dumped. (Barron 2009)
If the above two statements are not enough to consider the energy that enter the

buffer zone being fully dissipated, to keep considering the ceiling opening as fully absorptive some further absorptive area can be added, for instance, in the roof underside, or in the upward ceiling paneling. This last one, being direct in the direction opposite to the reverberant field, doesn't have any direct influence in the sound scape of the theatre room.

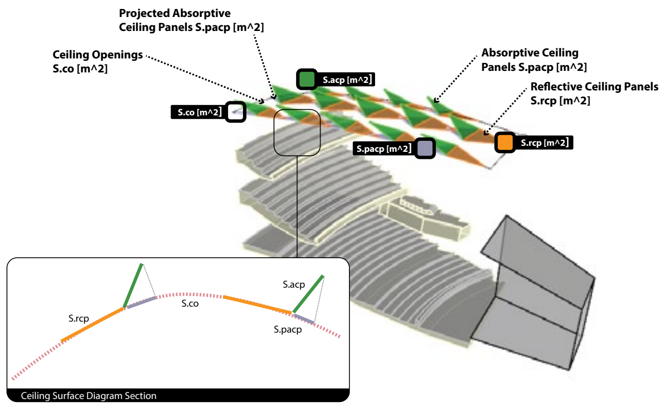


Image 3.29. Modelling of a sampling variable acoustic ceiling: in orange the reflective panels, in green the absortpive ones, and in lavande the effective absorptive panel area as projection on the ceiling surface definition.

The assessment of the area occupied by the audience must be assessed with great precision, in fact this region is very absorptive and can be reached from 30% up to 50% of the total absorption: for this reason a not correct estimation of this can cause large errors. Literature suggests to count the number of seats, and then multiply this by a unit seat area (Beranek 2006 Barron 2009).

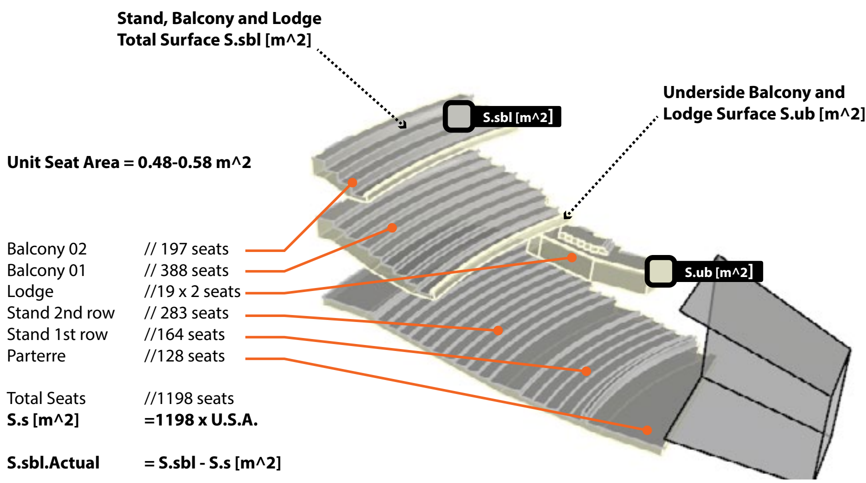


Image 3.30. Calculation of the high absorpive area represented by the audience.





The audience area has such a big influence on the reverberation time that a dedicated formulas has been developed to model the uneven disposition of absorbing area, characteristic this last, of theatres and concert halls (Beranek 2006).

It is worth to mention that at this stage, the position of the panels is simply associated with the shape of variable surface and are not yet integrated with a mechanical variable system. Being the tool geometric associative, this can be then re-used easily when the panel definition will be then intertwined with an adaptive structural system.

Once every area typology is measured, the tool associates to each of this a tag, and then exports the data to a spreadsheet file format. Finally, in Excel, data are post-processed and the Reverberation Time $RT_{60}$ can be estimated, together with other measures important to assess the acoustic of the room (Image 3.30).

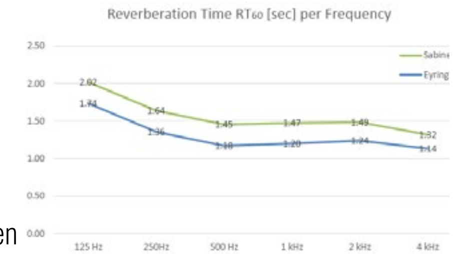


Table 3.4. Output graph of the post-processing excel spreadsheet showing $RT_{60}$ accordind to Sabine's and Eyring formulas.

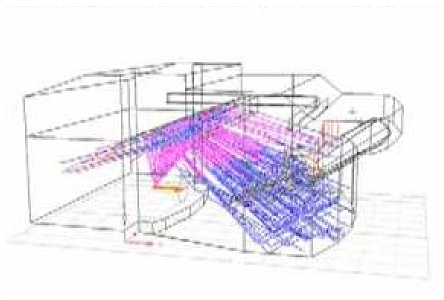

Image 3.31. Interface view of the acoustic ray-tracing software Autodesk™ Ecotect™.

***Ray-tracing Tool***

In this paragraph the development and possible uses of an elementary ray-tracing tool is presented. Generally, in physics, ray-tracing is a technic for calculating the path of waves or particles through a system with regions of defined propagation velocity, absorption characteristics, and reflecting surfaces (Wikipedia). Under these circumstances, wavefronts may bend, change direction, or reflect off surfaces.
The ray-tracing tool has been designed in order to evaluate:

-the variation of the sound source and its influence on the behavior of the propagating sound waves;

-the variation of incident sound waves on a parametric defined variable surface;

-the Initial Time Delay Gap for an even positioned audience in a room. For this intent, as consequence, only direct and first order reflection rays will be assessed with this tool.

At this development stage, the associative geometric based tool is able to assess 'in live' the performance of sound waves when hitting a variable surface in shape. Here the surface represents the adaptive ceiling.
During this phase the tool has been designed to be then used in the applied conceptual design stage to study the effects of the variable ceiling in shape on the acoustic qualities of the theatre hall. The tool is for this reason very usefull to assess the early reflections.

Following the generation of the Ray tracing tool, together with the processing entities that represent the functional core of the Grasshopper file definition are explained.

As first step the sound source energy is modelled. This is a significant modelling stage because any wave source has different characteristics that define the propagation of sound in space. Generally the acoustic energy is radiated uniformly in all direction for a spherical wave, however, other sources of sound may be highly





directional. An orchestra can be modelled as an omnidirectional sound source that irradiates sound energy in all direction with the same intensity; on the contrary, electronic loudspeakers have a limited and designed solid emitting angle. For these reasons, some basic sound source characteristics, like directionality and irradiation amplitude, have been introduced in the tool functionalities.

Image 3.32. On the left on omnidirectional sound source. On the right a directional speaker.

In the digital environment, a sound source is a point in the space that irradiates a bundle of rays with a defined density, within a solid angle range. Geometrically, a ray is a semi-infinite line distinct by a point O and a direction $v_r$. In order to express the ray directionality, the planar angle variable altitude $\alpha$ and azimut $\beta$ (the two variables of spherical coordinate systems) are introduced (Image 3.33).

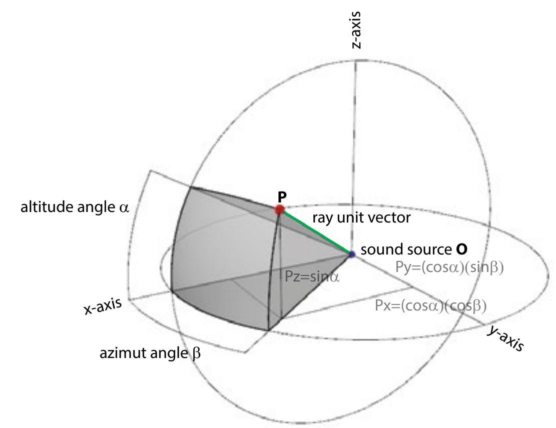


Image 3.33. Geometric parameters for modelling the direction of an acoustic rays by making use of spherical coordinates.

The altitude is the angle between the z-axis and the vector $v_r$ that represents the direction of the ray while the azimut is the angle between the x-axis and the projection of the vector $v_r$ onto the xy-axis having origin point in O.

With these assumptions the direction of the unit vector $v_r$ can be expressed through the position of the end point P function of the angle $\alpha$ and $\beta$, that has coordinates:

$$P = \begin{pmatrix} \cos\alpha\cos\beta \\ \cos\alpha\sin\beta \\ \sin\alpha \end{pmatrix}$$

With the same approach a bundle of rays can modelled by introducing the amplitude angle variables $\alpha_{ampl}$ and $\beta_{ampl}$ that represents together with $\alpha$ and $\beta$ the polar spherical domains of the rays generated by the point sound source. A further variable describe the density of the shot rays.

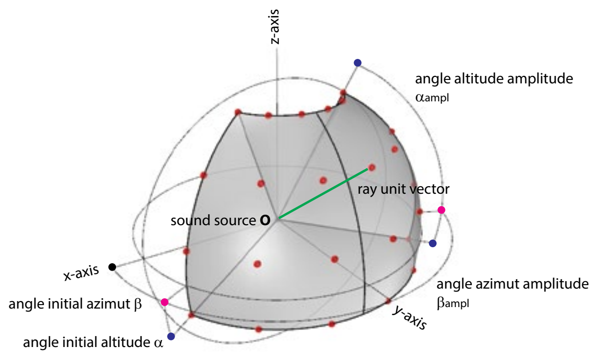


Image 3.34. Sound source implemented with azimut and altitude amplitude.

Having a source of rays is possible now to model the interaction of the rays that symbolizes the acoustic waves with a surface with reflective characteristics. If one of the rays intersect a surface an intersection point I is found (Image 3.35).

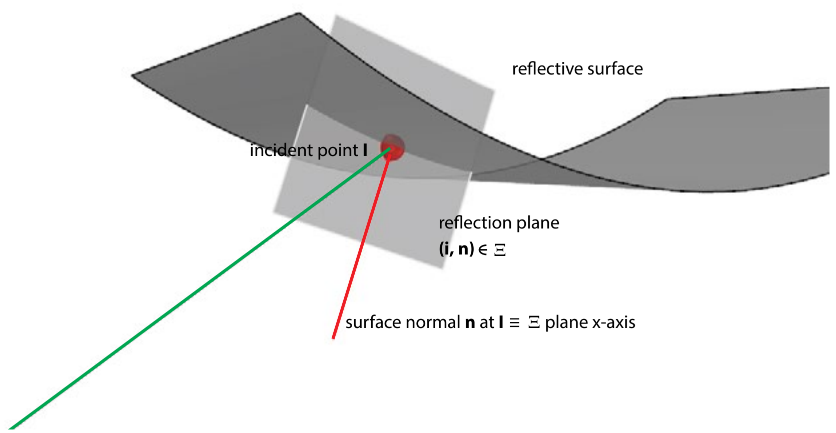


Image 3.35. Geometric definition to describe the reflection of a ray on a surface.





From here is possible to retrieve the surface normal n at I and hereafter build the bisector plane Ξ. This element with origin in I, has as local x-axis the surface normal vector n also denoted with the name of bisector line. Finally, to orientate in the space the plane that describes the reflection phenomena, the origin of the incident ray is assigned to the plane definition.

Now it is possible to calculate the reflection angle $\alpha_{refl}$ between the incident ray I with the help of the surface normal n belonging to the reflective surface. From wave mechanics (Lambert's law) is known that the incident angle is equal to the reflective one for fully reflective surfaces (that is the assumption here adopted to model the tool). With this knowledge the direction of the unit vector of the reflected ray r can be input on this (Image 3.36).

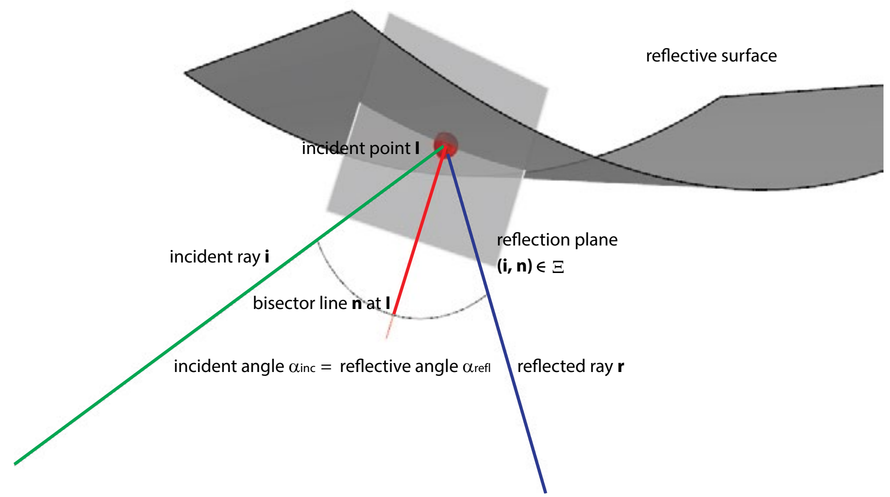


Image 3.36. Calculation by pure geometric consideration of the reflected ray r.

In turn, the reflected ray r can intersect a receiving surface at point R that is modelled in space following audience disposal. By varying the shape of the reflective surface is possible to visualize the effect of the surface configurations on the reflected rays hitting the audience.

With simple geometric considerations, the ITDG can be measured (Image 3.37). By definition, the Initial Time Delay Gap is the interval between the arrival of the direct sound from the stage and the arrival of the first reflection from the walls or ceiling. Because of knowing for each triad the span of the direct, incident and reflected

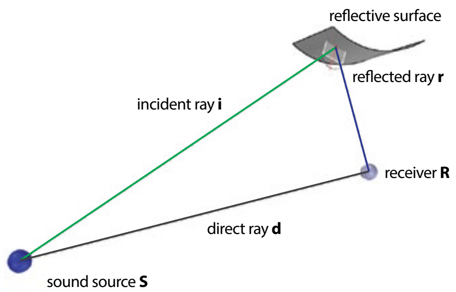


Image 3.37. Geometry to calculate the ITDG.

rays, together with the speed of sound within air, the ITDG is in milliseconds:

$$ITDG[\mathrm{msec}] = \frac{(||S,I|| + ||I,R||) - ||S,R||}{c} \cdot 1000$$

where c, is the speed of sound in air.

$$c\left[\frac{\mathrm{m}}{\mathrm{sec}}\right] = 343$$

The tool has been tested only for the case of the theatre object of study, but is ready to be employed with any other input entries of sound source characteristics, variable reflective surface and audience disposal.

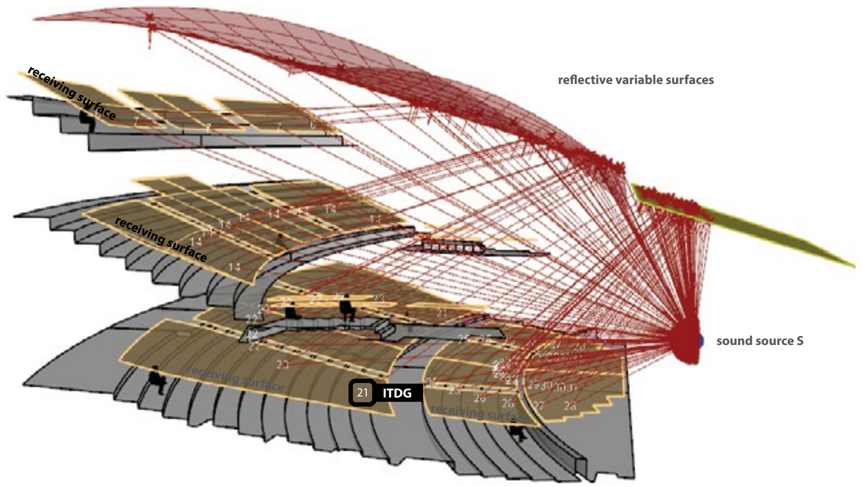


Image 3.38. View of the tool functionality in the Rhinoceros™ digital environment.

To conclude, the first outputs revealed the ray-tracing tool particularly easy to employ and useful to assess the early reflections (image 3.38): these ‘in live’ visual and numerical outputs are particular useful to verify infinite ceiling configurations, especially for those designers that are not widely familiar with room acoustics.

Due to the reasons just mentioned, further implementation of this tool are worth to investigated.

# Part 2

# Case Study

Chapter 4 // Design Concept

**4.1 Introduction to design objective and strategies**

In this chapter the design, at a conceptual level, of a kinetic acoustic ceiling applied as case study to an existing multipurpose theatre will be presented.
Here it is intended to prove that a motion structure can be applied for the case of a variable ceiling: within the design case only the most relevant loading situation, acoustic and structural checks will be performed in order to prove the feasibility of the designed motion structure.

The first step of the design consists on adopting a multi-disciplinary perspective to consider both acoustic and structural aspects: for this reason the knowledge coming from the first part of the thesis, will be synthetically discussed with the perspective to select the most suitable structural typology (Chapter 2) that can in synergy absolve variable acoustic performances (Chapter 3) in conjunction with a paneling system.

An integrated design approach will be used to layout the concept of the acoustic ceiling. Considering several aspect toward the synthesis of an integrate system represents a challenge for the designer: here he must adopted several views in order to consider in contemporary a number of design aspects that might lead to a successful outline: this is a non-linear process, where, continuously, intermediate calculations converge toward an optimal solution.

### *Design Strategy*

Within an integrate design process, the designer is tasked to understand the relations between constraints and their consequences if parameters changes, so adding value through the analysis output achieved with several types of considerations. This process enables reliable decisions to be opted, which take into account the information supplied by the various discipline analysis (Uijtenhaak 2011).
As just explained, integrate design is a very abstract problem that requires a well-structured workflow to follow. The main question that can arise from the above introduction is: how to intertwine acoustic and structural aspects in a coherent deign layout?
One solution to this problem can be found by expressing all the variables (acoustics, kinematics and mechanics metrics) in terms of association of geometries: in this case very abstract geometric entities describe a performance variable or a kinetic variable. As example, for the specific design task, we can increase the reverberation time of the theatre (acoustic variable) by increasing the effective volume of the room (geometric variable) by means of raising the reflective ceiling (kinematic variable).

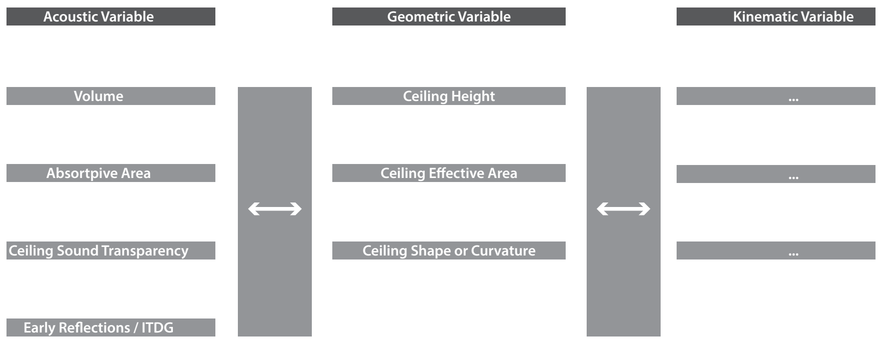


Image 4.01. An abstract framework for the integrate design of the acoustic ceiling.

The entire set of variables can then be expressed, such that the designer must find finally the way to express these lasts as geometric variables: geometry is here intended as a 'bridge' that create an intertwined network of design entities that have an acoustic and structural behavior. This is mainly the reason because in the theoretical part of the thesis a great efforts was done to express room acoustic simulations and kinematics performance of motion systems in terms of



Chapter 4 // Design Concept

pure geometric entities, with the final purpose to then merge in a single digital environment based on the same language.
In this sense a particular framework applied to the case study (Image 4.01) is proposed. This framework can also be further enhanced for more general problems and seems to be very promising in the developing of kinetic systems that require to fulfill accessory functions further then the structural one.

### *Reference Theatre: Nieuwe Luxor*

The case study will developed for the New Luxor Theatre in Rotterdam: this building was designed by the German Architect Bolles+Wilson, commissioned by the City Of Rotterdam and finally inaugurated in 2011.

Image 4.02. Externanl view of the Nieuwe Luxor (image courtesy of bolles+wilson.com)

The Luxor auditorium can contain 1200 people: aim of the design was to develop a multi-purpose auditorium meant to host several performance type. Seats are distributed along a parterre, the stands, two side lodges, a first and a second balcony.

Image 4.03. Internal view of the auditorium (image courtesy of bolles+wilson.com)

Currently, the theatre hosts classic music, cabaret, musical and music theatre, opera and dance performances.
For this reason this building is an ideal case study to test an adaptive ceiling.

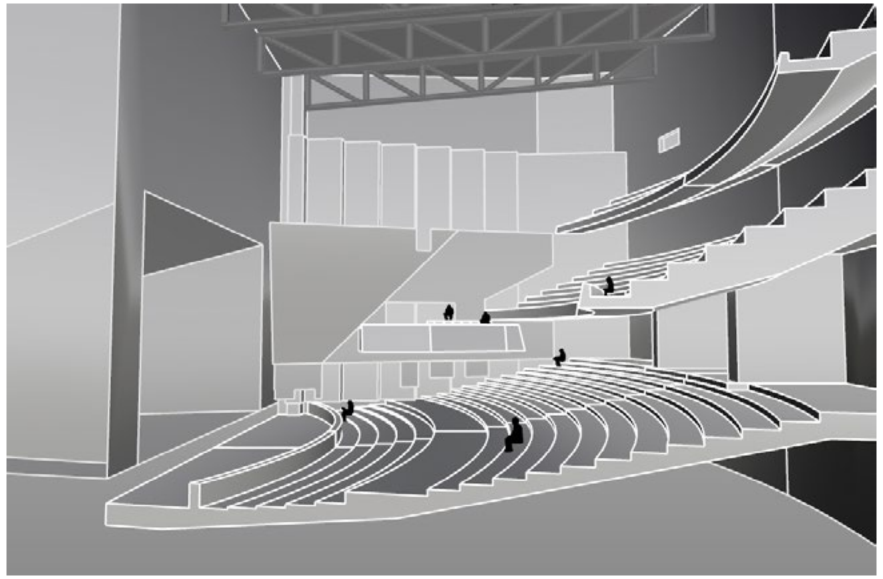

Image 4.04. Geometric 3D model of Niewe Luxor in Rotterdam. 3D modelling Matteo Soru, in turn augmented from the model of Kjell Scholts.





**4.1.1 Considerations of Research Outputs on Kinetic System**

In Chapter 2 a wide range of motion structure typologies have been studied: each of them expresses some performance benefits or problematic, especially in relation to the accessory function that they have to fulfill.
Before selecting a suitable solution let us just list, as results of the research presented in Chapter 3, the requirements that an adaptive acoustic ceiling must have. Here, the desired motions that can lead to tune only the reverberation time and first order reflections will be presented (as RT and first order reflections are the factors that can generally describe the overall sound quality of the theatre).
The system must be designed in order to:

-move vertically. This is meant to reduce or increase the effective reverberant volume of the theatre. To note, that so far, this represents the easiest and most common solution used. Normally, this simple system, is not integrated with further systems.

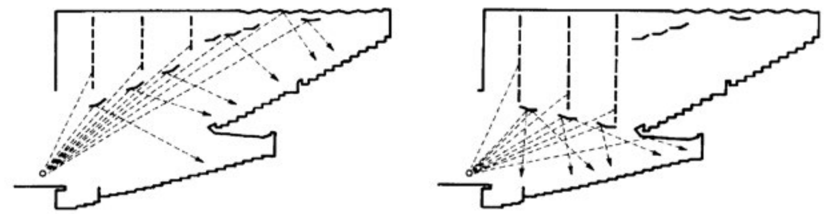

Image 4.05. The Cain Auditorium has a vertically movable ceiling system (Image courtesy of Ballou et al 1987)

-have an adaptive paneling system, that can increase absorption area, or in opposition, can fold in order to make the ceiling partial transparent. In the first case the reverberation time will decrease, while in the second case it will increase, because, being the ceiling partial sound transparent, the volume above the ceiling itself contributes as effective reverberation volume.

Image 4.06. An architectural rendering for an extense solution of the Resonant Chamber prototype. When  the surface deploys, extra absorpting area in provided.

-change is curvature, or better, if the reflective panels are connected to the system, the orientation of the panels in order to orientate first order reflections to the right spots and keep low the ITDG.

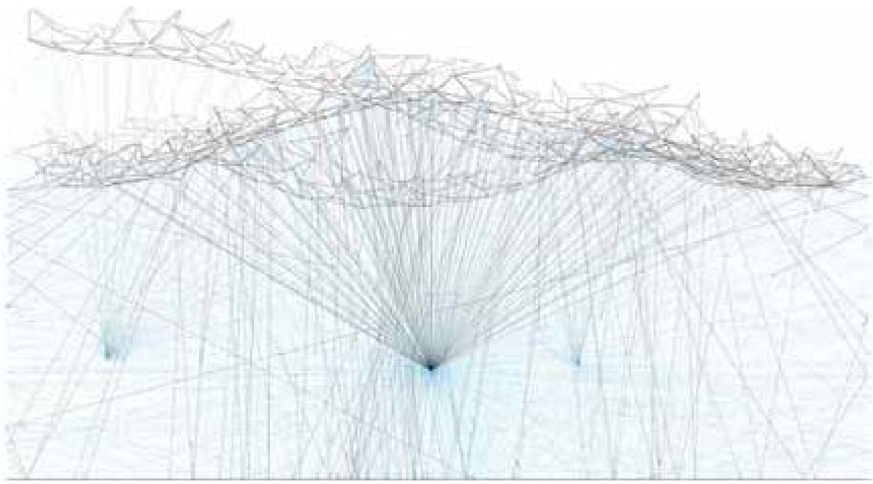

Image 4.07. This extense solution of the Resonant Chamber prototype explores the relation between shape and ray diffusion (image courtesy of Thün et al 2012).

In particular, the last two requirements needs a highly flexible system, easy to control and with a high potential degree of integration between the motion structure and the panels: this means that during motion, the paneling system and structural elements must not clash among them.

Let us now select the structural system and the strategy for variable acoustic that can be synthetized in a working system.

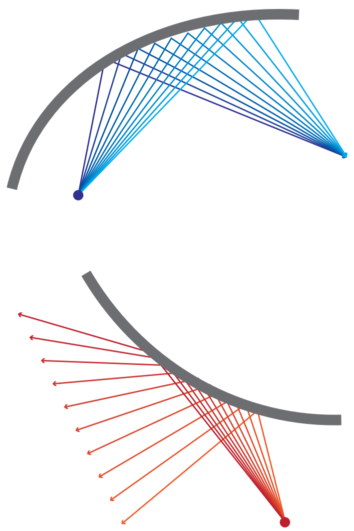

Image 4.08. A convex and a concave surface have a different interactions with acoustic rays

Motion structures based on 1-D bar systems showed to be principally usefully for folding structure: they have all the characteristics that concern effective foldable system, like extremely compactness in the folded stage, high degree of deplorability, easiness to transport and erect. On the opposite, this typology has the problematic of the connection among structural elements and panels that requires extra design efforts regarding the motion coordination of structure and panels.

Kinetic systems based on 2D-rigid paneling are very interesting examples of a structural solution that express a full degree of integration between structural and acoustic function: such origami-like structure would be very useful to be used,





as a well-designed configuration can lead to a good control of the tuning room soundscape. The prototype project presented previously (§2.4.3) proofs that such a system can be very usefully for applications, in general, that require an addition function absolvable by panels. On the contrary, even if possible, is quite difficult to design and control the change of curvature of an origami like-structure: the extensive examples of origami-like pattern, based on plan filling of basic patterns, show that this is possible, but the knowledge required to describe such motion is inaccessible for designer not fluent with advanced mathematics. Although the complexity to control spherical mechanisms for 2D-rigid paneling structure, easy planar mechanism might be used as shuttering system or as variable geometric surface exposed to sound waves.

Among all the tension structures analyzed, the backbone-like system (3D-strut-and-cable assemblies) showed very good characteristic of motion control together with very good potential of integration with panels. In fact the compressive struts that compose these system can be layout in such a matter that structure elements and paneling are generated from the basic polyhedron that describes the ‘bone’ of the system (§2.4.3).

Image 4.09. A backbone system that expresses high degree of flexibility.

From the design point of view, a kinetic system of this manner can be generated by tessellating a plane or surface with directional arrays of polyhedron: the populated surface can, therefore, represents the ceiling. The structural pattern derived from this tessellation must be connected in order to make possible, by kinematics considerations, triggering and controlling motions.
From the kinematics point of view a backbone like structure is a kinematic chain, or a network of chain, whose rigid bodies that compose these, are connected by means of hinges (planar in case of planar motion and spherical in case of space motion).

As reminder, a kinematic chain is a configuration composed by n element, the rigid links: if one of the rigid body is fully constrained in space, the chain has $\infty^{n-1}$ possible configurations and 6·n degrees of freedom: in the planar case the degrees of freedom are 3·n. This means that further n-1 links are needed to make this system statically determinate.

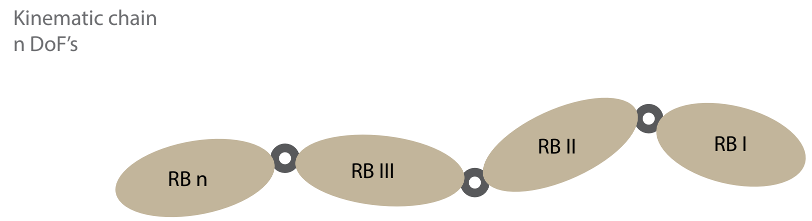


Image 4.10. A kinematic chain.

This systems previously tested turned to be very easy to control: very importantly, the curvature of the surface onto polyhedron (the rigid bodies) and actuators (the links) are arrayed, demonstrated that can be changed in one and two directions. Also this last characteristic make a backbone-like structure the most suitable solution worth to be applied for the design case.
In the next paragraph, the relation between actuator typology and motion control will be further developed.

At this stage a design strategy to change the acoustic must be chosen (§): this must fit also with the structural system adopted.
Variable absorption is the commonest used approach for variable acoustics. In order to influence the reverberation time, the area of adjustable absorption must be very large, in fact comparable in size to that of the audience area. Moreover, for application of ceiling, in room acoustics, it is suggested not to place a consistent amount of absorbing area in this spot, because it has the effect to drop 'loudness' by damping first order reflections .

The reverberation time can also been tuned by means of changing the effective volume of the hall: this option has advantage compared to varying the acoustic absorption that there is little penalty in terms of sound level.
There are basically two methods to provide variable acoustic volume: one consist on moving the panel partition (mainly vertical) and the second on a shuttering





system. In the first case, generally, the change of volume is achieved by shifting up and down the ceiling that is sound-tight; in the second, a shutter paneling system make the ceiling transparent making possible the use of the above space as reverberant volume: in practice the whole volume is now reverberant.

Image 4.11. Two example where a partial transparent ceiling is used. On the right: Tanglewood music center.

Literature prescribes that at least the 40% of the ceiling must be opened in order to make this working as sound partially transparent system. Normally this strategy is used for concert hall, where a partially transparent surface or panels, float in the middle of the room: its position then is adjusted to reflect direct rays to the audience. To note that the roof surface invested by the sound must be in this case reflective and not absorptive. Underroof surface in concert halls are for this reason fully reflective, while this is not often the case for multipurpose theatre which host above the acoustic ceiling installation and further structure for the maintenance, such as catwalks and lighting installations for instance. This is also the case of the theater object of the case study.
The achievement of a fully reverberant volume can be accomplished, in this case, by covering catwalks and trusses with reflective panels, while the main underoof is already covered with scattering diffusing panels. This two last methods seemed to be easy to integrate with the structural typology selected, and they will be then adopted and developed.

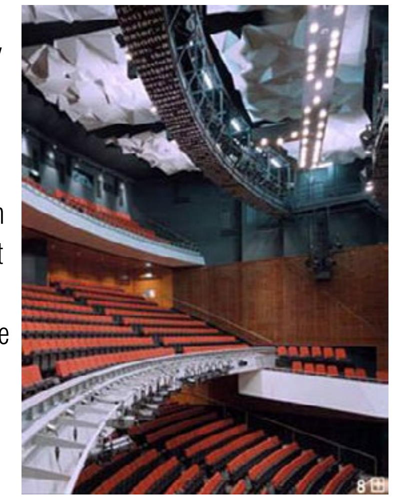

Image 4.12. Internal view of the auditorium (image courtesy of bolles+wilson.com)

## 4.2 Conceptual Design

Conceptual design based on the framework above theorized will be applied considering a design method ‘by layer’: this consist on, firstly design the different layers that must absolve different functions and secondly connect together in a coherent manner that pursue intent of working in synergy. Desing of each layer will be oriented and selected considering the degree of interconnections achievable. Layer design is based on a surface population of a system (structural, motion actuation and acoustics) that must be provided with a functional interfacing solution that consider at the same time geometrical boundaries conditions of related layers.

### *Structural Design*

Two basic separated ceiling systems are designed: a front and a rear ceiling. The first, is an adaptive system that covers most of the ceiling area, and has the main function to tune sound acoustics. Its function is especially to orientate reflected rays to the stands and the first balcony. The second, a static system work as auxiliary of the main system, and its main function, according to the configurations needed, to render the ceiling sound tight, or not to interfere with the kinetic system when a much closed configuration is needed. Its function is also to orientate reflected rays to the second balcony.

Regarding the adaptive system, as first step the roof surface boundary is tessellated with tetrahedrons (§2.4.3), whose relative assembly is then generated by structural elements spanning from the polyhedron barycenter and its relative vertices.

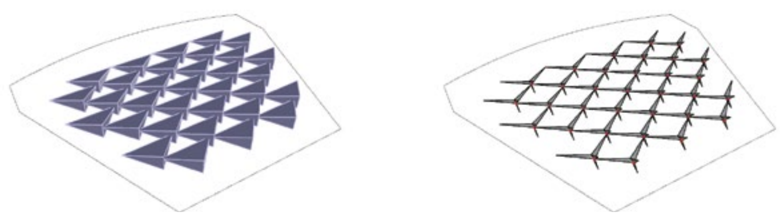

Image 4.13. Surface tesselation and ‘bone’ of the system.

These elements are connected in their barycenter by moment resistant connections. Horizontal elements are meant to interconnect adjacent modulus, through spherical hinges between a fulcrum and the outer horizontal vertices.



Chapter 4 // Design Concept

Upper vertical element vertices are considered to host and connect motion actuators while the lower ones will sustain acoustic paneling: this lasts must then implemented for host in a more effective way the paneling. For this reason the tetrahedron is now augmented with an extra facet so that the lower part of the layer is now an A-shaped frame. This was meant to:

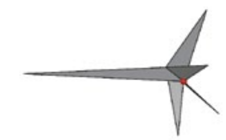

Image 4.03. 3D-compressive strut.

-easily connect static paneling, so that structural and panels form a stable triangular frame;

-create a hosting space to store the folding paneling system that has the function, by shuttering, to ensure the surface to be partially sound transparent when required. The resulting tessellation based on the ceiling geometric boundaries layout consists of 32 rigid bodies coupled in four families or linear group of rigid bodies, and one of this is fully constrained in space. So, a fully constrained middle strip of rigid bodies connects the cantilevering part of two strips in the front and one on the back.

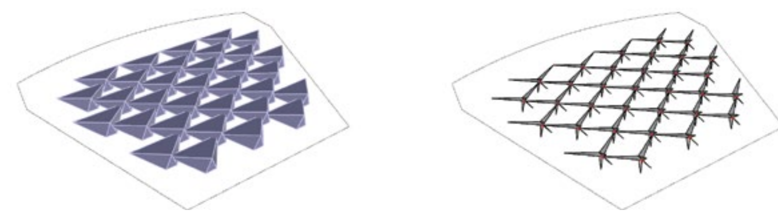

Image 4.15. Surface tesselation and ‘bone’ of the system implemented with A-shapet brackets.

This was meant to control the changing curvature of the ceiling with 3 independent kinematic variables and add more control while finding the optimal shape for the ceiling in relation to needs regarding the orientation of sound rays.

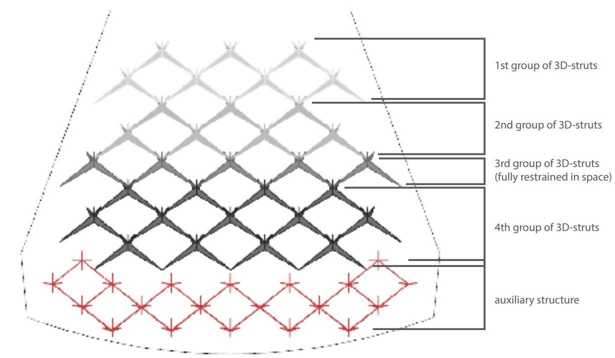


Image 4.16. Groups of structural elements composing the kinetic system and auxiliary substructure.

The auxiliary system is simply a rigid frame whose lower vertices are connected with a pattern of fully reflective panels: this frame can also move up and down, according to needs.

***Kinematic Analysis and Motion Control Design***

Structural elements must be connected now with a network of actuators properly designed to ensure to the full system the necessary degrees of motion that allow changes in geometric configurations. Let us now analyze the spatial kinematics of the conceptual structure above layout: the study regarding degree of mobility for such a system will be divide in plane and out of plane kinematic analysis.

In plane, the structure is a trussed liked system: the front and back cantilevering families of rigid bodies are fully constrained. For the front part the mobility formula reads:

$$m = 3(14-1-16)+32 = 23$$

While for the back part the mobility formula reads:

$$m = 3(13-1-13)+26 = 23$$

This means that on the plane, the frame system is statically indeterminate, so 24 degrees of freedom must be respectively introduced to have a mechanism in the front and back part of the ceiling
From a design perspective this point doesn’t represent a problem to be solved because the ceiling must be designed to change its curvature out of plane (so in the ceiling section plane) by means of out of plane rotation of the rigid bodies.

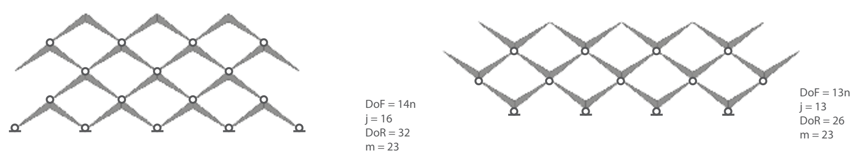


Image 4.17. On plane frame kinematic analysis.

Out of plane, the structure is a sequence in parallel of planar kinematic chains whose adjacent chains are shifted by one module.



Chapter 4 // Design Concept

From the knowledge matured in Chapter 2, there are mainly three methods to make the system statically determinate and to control the motion:

-segments of steel active cables connects adjacent modules. In order to mantain the system stable further passive rubber cables are needed. These lasts must be prestressed in order to be in tension when the steel cables are fully released. With this solution is possible to control locally the change of curvature of the ceiling.

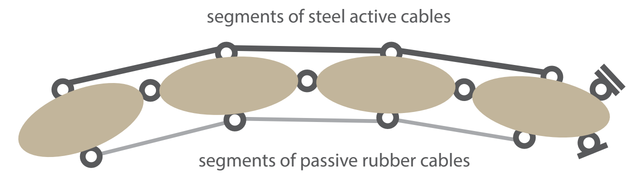


Image 4.19. Segments of steel active cables control the motion.

-a continous zig-zaging active cable connect the whole system, and also in this case passive rubber cables are needed to stabilize the system. With this solution the global change of curvature is controlled by one indipendent variable (steel cable shortening or lenghtening).

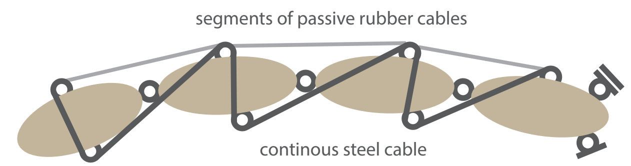


Image 4.20. A continous steel active cable controls the motion.

-series of rigid actuators (hydraulic pistons) connect adjacent modulus.

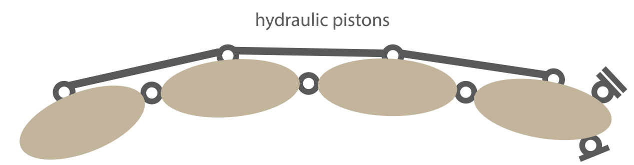


Image 4.21. A serie of hidraulic pistons control the motion.

Hydraulic piston options is choses: the reason is that when not in motion they can withstands both tensile and compressive stresses, so that further balancing passive cables are not needed, resulting in a more simplified structural system.
This last option will be used because it doesn’t require extra passive cables, that, as consequence, simplify detailing of the system.

For the design layout proposes, 42 actuators are needed: these are further classified in three distinct families of actuators. Each is meant to control locally the change of the orientation of the paneling to whose they are associated: so, with three independent kinematic variable is possible to obtain $\infty^3$ possible configurations.

Image 4.22. Groups of hydraulic pistons.

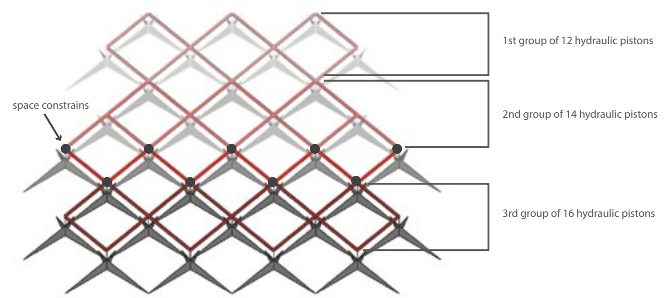


***Panelling Design***

The structural system is based on a tessellation of equilateral triangles on the ceiling plane, along the three triangular directions: this pattern applies to superimpose as additional layer with a wide range of other tiling patterns that has to absolve acoustic functions.

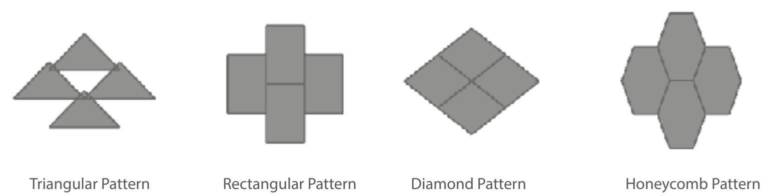


Image 4.23 Possible tesseleting patterns.

A diamond pattern has been selected. The variable acoustic strategy designated requires the ceiling to turn from a fully reflective to a partially sound transparent surface: for this reason, panel are populated in a chess like-pattern: odd modulus are static and restrained to the structural A-shaped brackets, while even modulus can change their configurations in order to create openings in the ceilings. Opening can be created with a paneling folding system, so that this can fold as a butterfly. While folded, the 'butterfly wings' are hosted in the brackets of the structural elements.





Let us now analyze the kinematic relationship that describes the motion of this folding system. The folding panels are joint together with a linear hinge and constrained at the structural elements by means of rolls. The folding mechanism, is a planar mechanism. Mobility analysis for half system yields that the panel has three DoF's of the plane and two degrees of restraint, this means that one independent kinematic variable is enough to describe this motion phenomena.

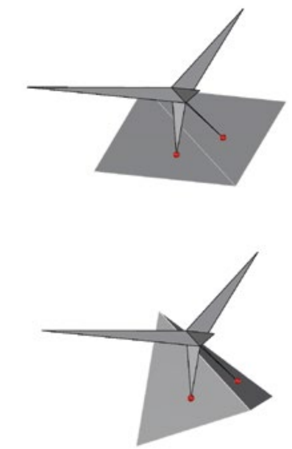

During folding, panels rotate around the common edge, and at the same time the common edge shift vertically. Let us denote as L the distance between the common hinge and the roll in its fully deployed stage, and as H the variable shifting distance of the common edge. Segments H and L respectively the side the rectangular triangle having as an angle the panel rotation $\alpha$, chosen as the independent variable. With this considerations, the folding phenomena can be fully described: when panels rotate by $\alpha$ around the rotation axis, to maintain facets rigidity, the same hinge must move vertically by $L \cdot \alpha$.

Image 4.24. Folding panel concept

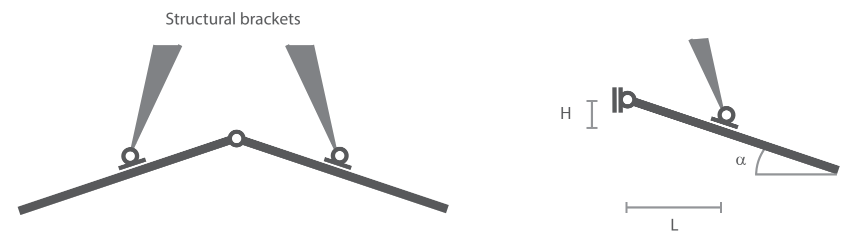


Image 4.25. Kinematic relationships of the foldung panels.

### 4.3 Shape finding (by means of acoustic assessment)

Ceiling section design is very important to direction rays in the theatre room; a part of this, its position is important to determine an ideal ITDG.
By having a system that can change its curvature also locally (Animation 4.1), now is possible to find an optimal configuration to reflect direct rays to target spots.

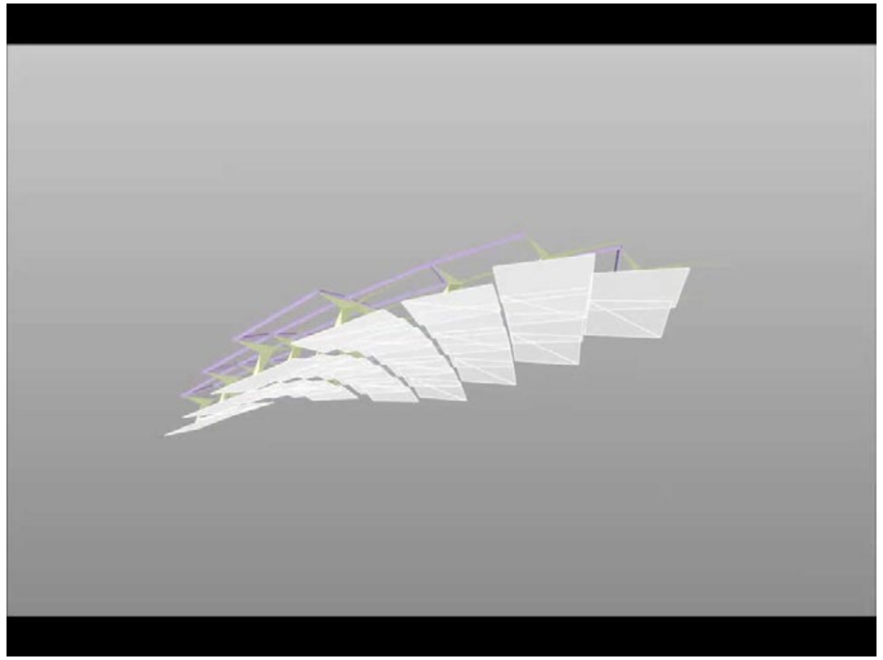

Animation 4.01.
Motion of the structure proposed.

Literature suggests that the optimal ceiling shape is an ellipse whose foci are respectively the sound source point and the receiver point (Image 4.26). The problem turn to be more complicated when different receiver point are placed in the space: in this case, according to the target receiver, the ceiling section can be designed as a discrete surface of segments, that still follow the same rule just introduced (Image 4.27).

Image 4.26. Ideal shape of an acoustic ceiling.



Chapter 4 // Design Concept

Another point must be considered while designing a ceiling configuration: the visual cone of the audience must not interfere with the ceiling geometry.

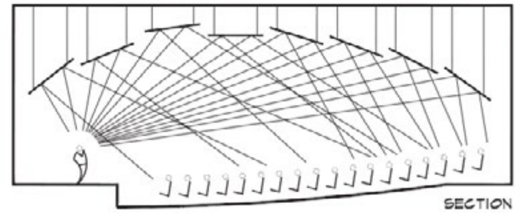


Image 4.27. A ceiling system having different surface curvature according to directional needs. (image courtesy of Long 2006)

Three basic configuration are here proposed: each of these has been basically designed only shifting up and down the ceiling.
The first is meant to provide the highest reverberation time achievable, a configuration ideal for chamber and classical music. A second intermediate outline is set-up to achieve a medium reverberation time, suitable for opera. A third ceiling option provides a low reverberant volume, by lowering the ceiling at the level of the second balcony.

Once the height of the ceiling is chosen, its section can be find by using the ray-tracing tool: from the kinematic point of view, the motion system has been set-up in order to change locally the curvature of the discrete ceiling by means of three independent kinematic variables (actuator extensions or contractions). To yield the potential successful configurations, the relation between actuator lengthening factors and ITDG is chosen: this is done by means of parametric study to find the minimum ITDG value for a set of lenghtening factors.

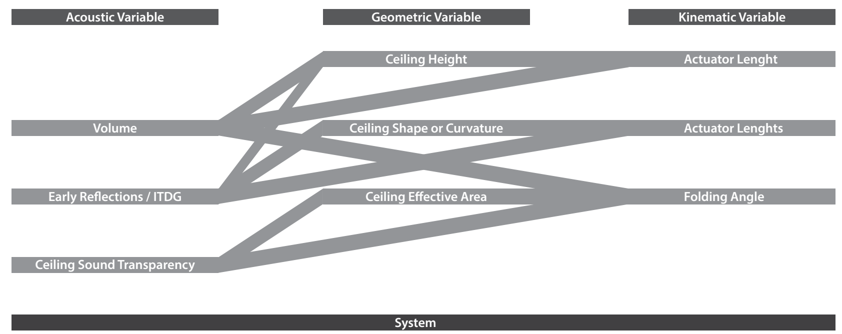


Image 4.28. An applied framework for the integrate design of the acoustic ceiling.

Following, the three configurations will be presented: as summary, the kinematic variable that can tune the whole system are the height of the front and rear ceiling, folding angle of the reflective paneling to make the ceiling partially transparent, and the three actuators variable to tune adaptive surface curvature.
In the appendix C they will be presented more extensively results regarding the above introduced procedure to find the ceiling shape.To note, that a higher volume can be achieved by moving the stage partitions within the flying tower: the effect of this further variable on the reverberation time is not considered for this case study.



Chapter 4 // Design Concept

***Configuration #1***

Design goal for this configuration is to have the highest reverberant volume achievable. To do so, the paneling kinetic system is activated, so that the ceiling is now 73% transparent, and the whole volume of the hall (a part of the volume above the static read ceiling) can be considered here as reverberant volume.
Surface curvature (Image 4.30) changes its sign from concave (in proximity of the rear kinetic ceiling) to convex (on the front of it). This layout is able to orientate reflection as needed in the whole part of the theatre, except to the parterre, whose reflections come from the stage ceiling; more in depth, the first and second families of actuators must be tuned together in order to orientate reflected rays towards the stands, while the lengthening factor of the third family can be found easier as the orientation of the reflected rays toward the 1st balcony is not intertwined with other kinematic variable. The minimum of the graph (Graph 4.1) shows the optimal set of lengthening factors.

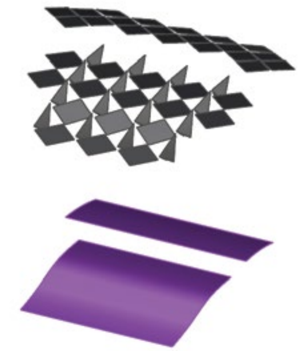

Image 4.29. Discrete versus continous surface.

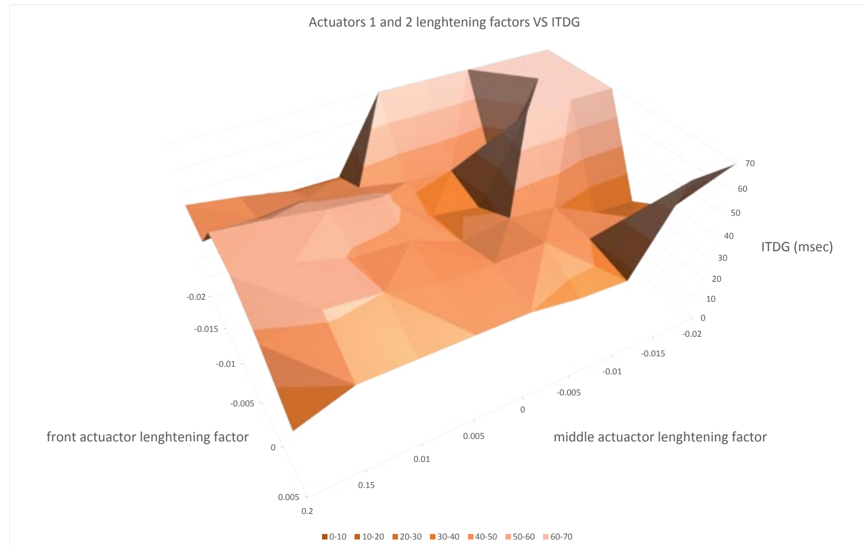


Graph 4.1. ITDG for the stands function of actuator lenghetning factors for the groups 1 and 2.

The ceiling has here an average height of 15 meters from the 1st row stands. This has to keep as low as possible to achieve an acceptable ITDG, but at the same time it must be considered here that a very low ceiling can interfere with the visual cone of the audience on the second balcony. The configuration of the auxiliary system has the function to direct reflected rays to the 2nd balcony.

Animation 4.02.
Configuration #1.

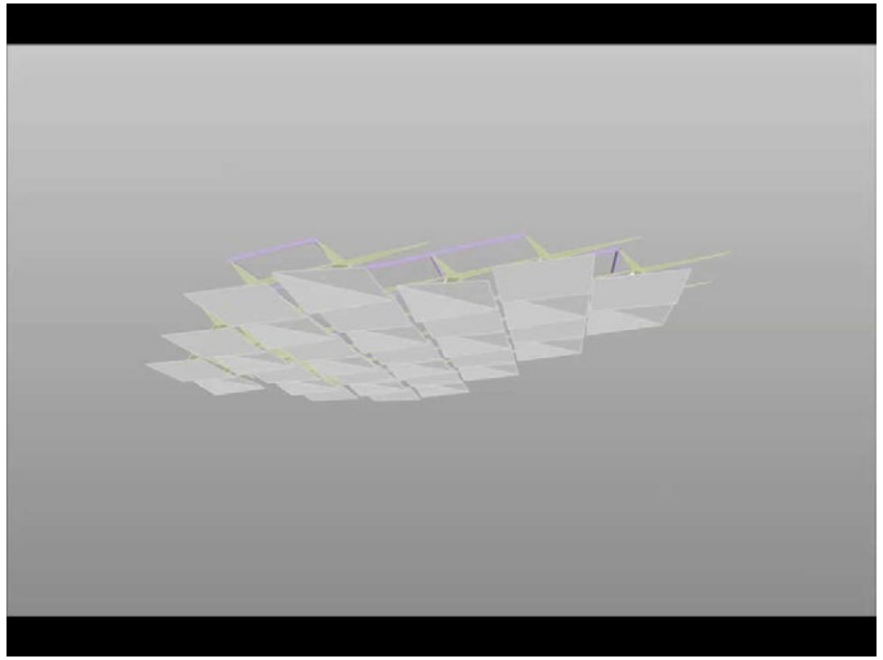

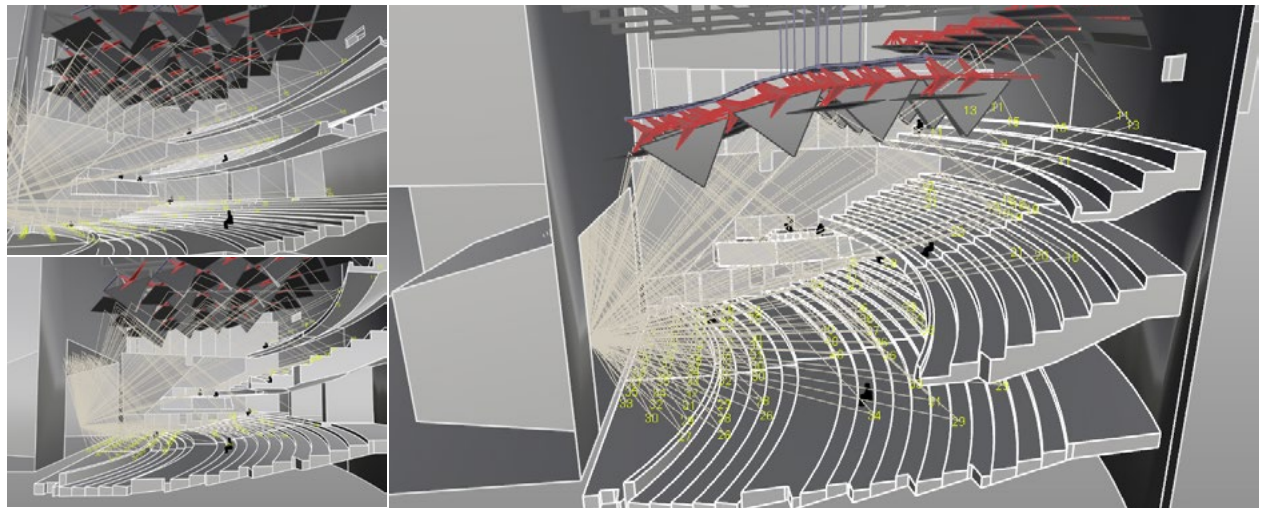

Image 4.30. Raytracing tool output in Rhinoceros.



Chapter 4 // Design Concept

***Configuration #2***

Design goal for this configuration is to obtain an intermediate reverberation time, around 1,4/1,6 sec, acceptable for performance like opera.
The front and middle part of the ceiling change its curvature to orientate reflected rays to the stands and 1st balcony, while the rear part of it bends in order not to interact with the direct rays so that these are now reflected properly by the auxiliary system to the 2nd balcony. In order to yield an optimal ITDG, the correct relation between the front and middle actuators are studied parametrically (Graph 4.2).

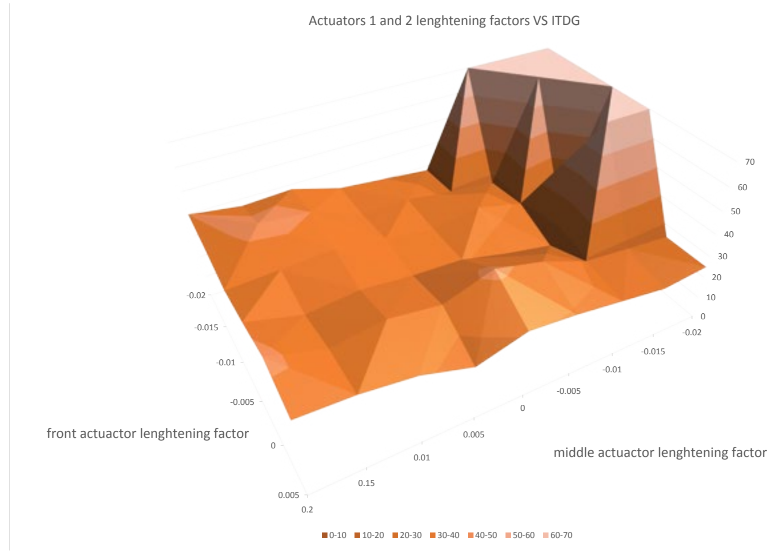


Graph 4.2. ITDG for the stands function of actuator lenghetning factors for the groups 1 and 2.

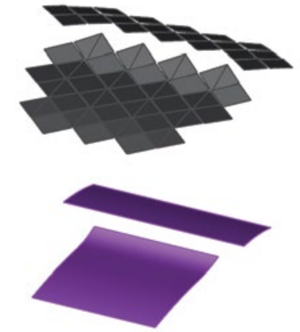

Image 4.31. Discrete versus continous surface.

Also here the ceiling has an average height of 15 meters from the 1st row stands: this was meant to keep as low as possible the ITDG but at the same time it must be considered here that a very low ceiling can interfere with the visual cone of the audience on the second balcony.
Results of the analysis with the acoustic tools shows that this configuration is suitable as space to host opera and its related performance.

Animation 4.03.
Configuration #2.

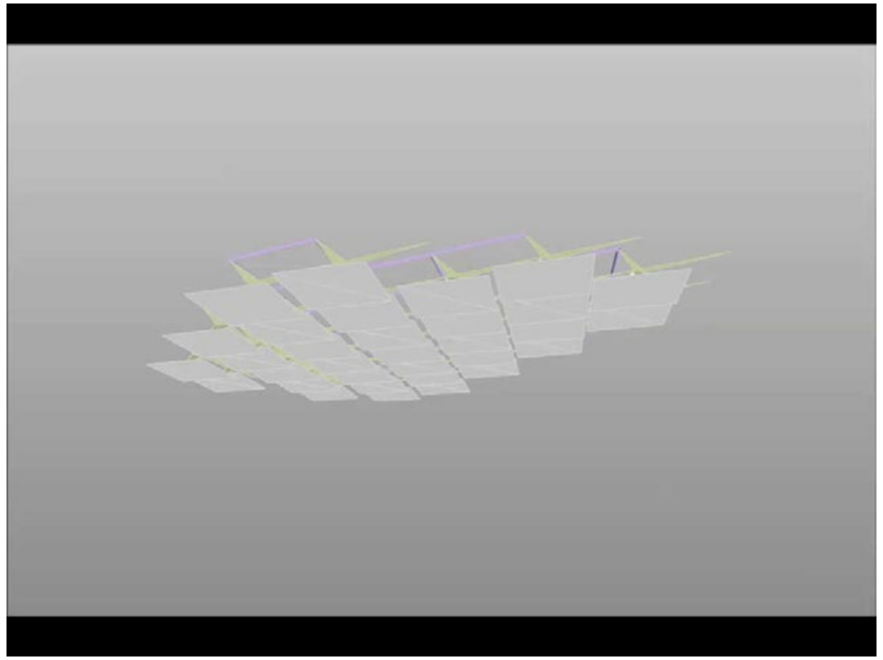

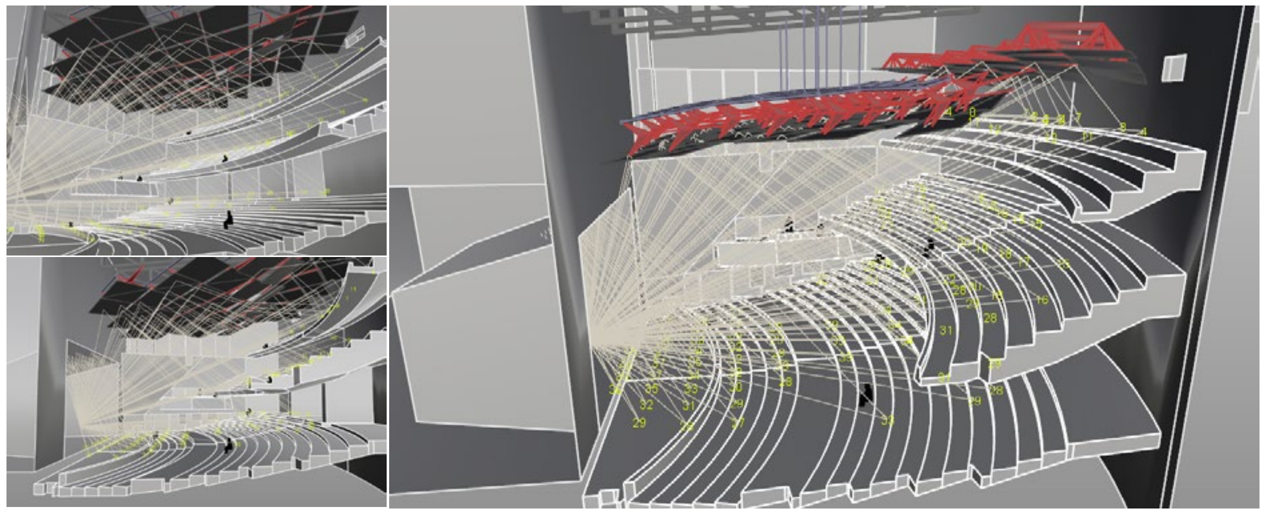

Image 4.30. Raytracing tool output in Rhinoceros.



Chapter 4 // Design Concept

***Configuration #3***

Also for this configuration a parametric study has been done to yield the optimal set of lengthening actuator to obtain an ideal ITDG for the stands (Graph 4.3) and 1st balcony (Graph 4.4).
This extreme configuration has the goal to provide a very low reverberation time. To do so, the ceiling is lowered significantly, having an average height of 11.5 meters from the 1st row stands. This has the effect to provide a very low ITDG, so a very intimate soundscape. On the rear part of the ceiling the curvature is concave so that reflected rays can be concentrated on the 1st balcony.

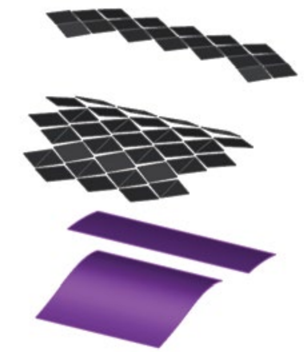

Image 4.32. Discrete versus continous surface.

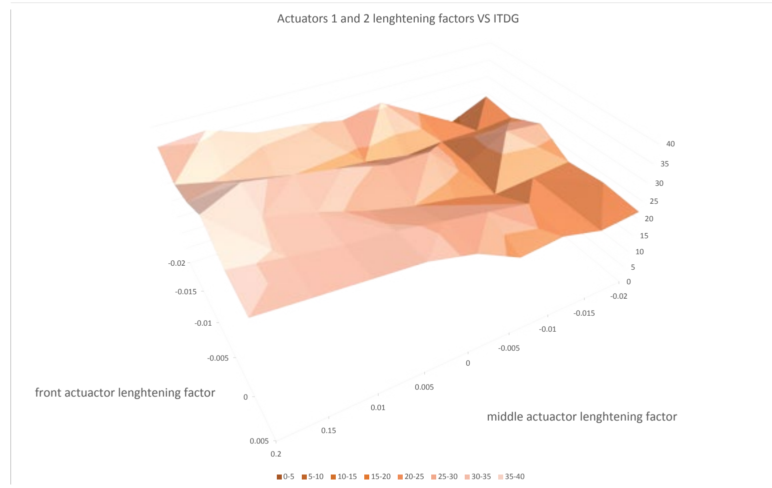


Graph 4.3. ITDG for the stands function of actuator lenghetning factors for the groups 1 and 2.

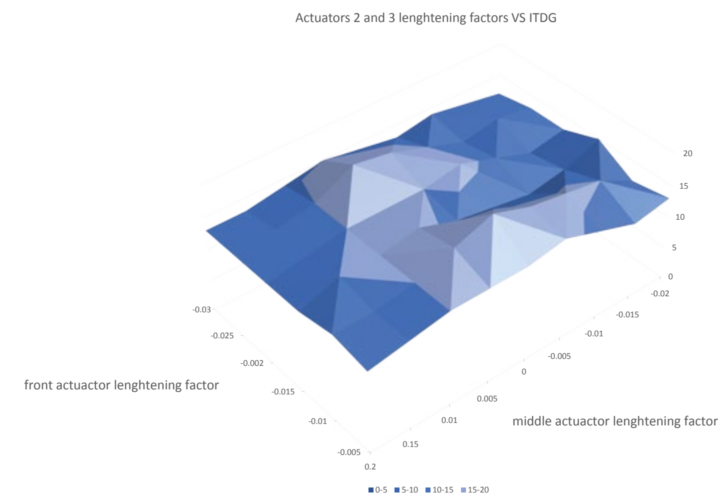


Graph 4.4. ITDG for the 1st function of actuator lenghetning factors for the groups 3 and 2.

Animation 4.04.
Configuration #3.

Results of the analysis with the acoustic tools demonstrates that this configuration is suitable as space for speech and amplified music.

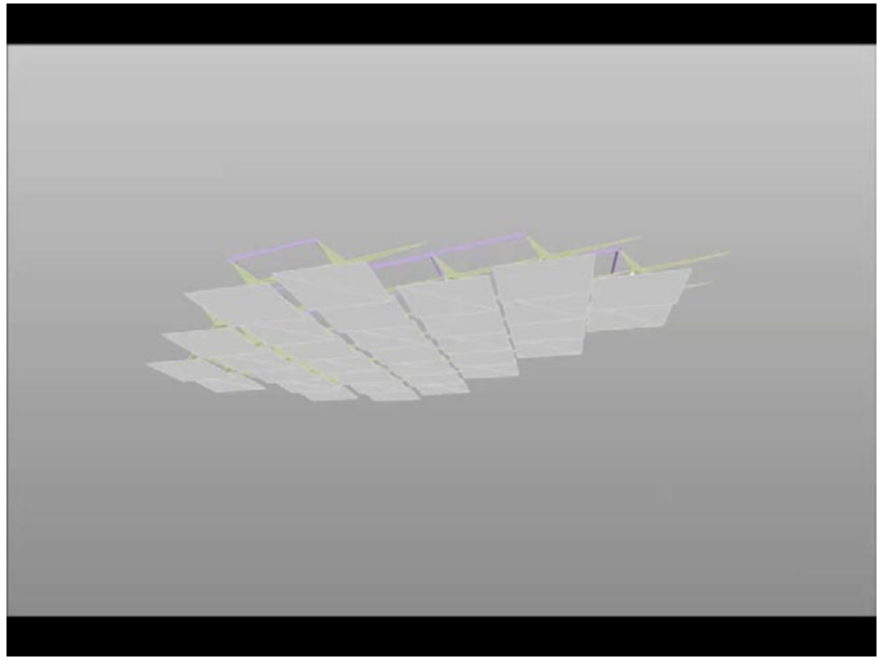

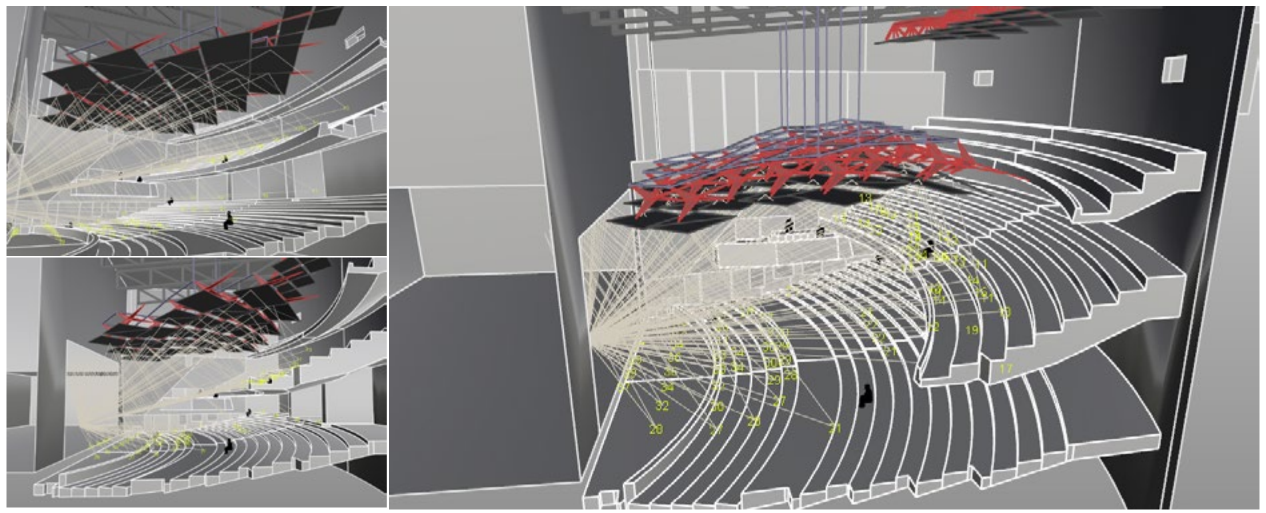

Image 4.33. Raytracing tool output in Rhinoceros.

### *Conclusions*

To summarize, the three ceiling configurations represent the result of the integrated design approach above theorized.
As recap, a table showing the kinematic variable versus configurations is hereafter presented:

| | Adaptive Ceiling Lowering [m] | Auxiliary Ceiling Lowering [m] | Shuttering Panel Angle | 1st Group Piston Length Factor | 2nd Group Piston Length Factor | 3rd Group Piston Length Factor |
|---|---|---|---|---|---|---|
| Configuration #1 | -2.5 | -1.3 | 75° | +0.012 | -0.02 | -0.01 |
| Configuration #2 | -3.6 | -2.8 | 0° | -0.005 | -0.002 | +0.02 |
| Configuration #3 | -6.0 | - | 0° | +0.01 | -0.015 | -0.03 |

Table 5.1. Kinematic variables.

The table below shows the average values of the ITDG in several spots of the theatre: results display that for the three configuration is possible to achieve from acceptable to optimal values.

| ITDG | Parterre | Stands 1st row | Stands 2nd and 3rd rows | 1st Balcony | 2nd Balcony |
|---|---|---|---|---|---|
| Configuration #1 | 30 | 30 | 32 | 25 | 10 |
| Configuration #2 | 30 | 25 | 35 | 20 | 10 |
| Configuration #3 | 30 | 20 | 25 | 15 | - |

Table 5.2. Initial Time Delay Gap.

Chapter 5 // Further Design Considerations

### 5.1 Structural Assessment

In this section a synthesis of the results regarding the structural analysis of the three ceiling configuration are presented. As first step the baked geometry is imported within the GSA environment and then material properties, constrains, section and load cases are applied to the elements: this can be done by exporting the Rhinoceros geometry as .DXF extension.

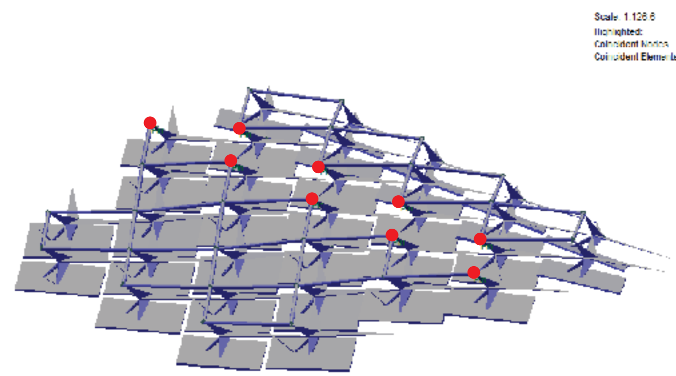


Image 5.01. The structure within the GSA environment. In red bullets the pins.

For the calculation the following elements (Table 5.1) and their relative material properties (Table 5.2) are then used.

| Element | Type | Section or Thickness [mm] |
|---|---|---|
| Piston | beam | CHS-150/7 |
| Bone Plate | 2D-shell element | 20 |
| Reflective Panel | 2D-shell element | 80 |

Table 5.01. Structural elements.

| Material | Class | Young Modulus [GPa] | Shear Modulus [GPa] | Poisson's ratio [-] | Density [t/ m ^ 3] |
|---|---|---|---|---|---|
| Steel | S235 | 205 | 68.3 | 0.3 | 7.85 |
| Timber | C30 | 8 | 0.750 | 0.5 | 0.38 |

Table 5.02. Material Properties.

Regarding the panels, it is worth to mention that these elements are modelled as 80 mm thick wooden slabs, the same element used to assess the reverberation time in the theatre: for sake of simplicity, here timber is considered as elastic isotropic. Regarding the actuators, it has been chosen a steel section that can be assumed to be easily integrated with the products that the market offers. About the 3D-compressed-struts, these are modelled as rigid flat triangular unstiffened plates connected by means of a moment resistant connection. Further, implication of the use of such elements will be discussed in general regarding possible detailing enhancements.
Panels and bones are modelled by using shell elements, which consider both in plane and out of plain effects.

To note that the structure is modelled like constrained in the space by means of pins. This is a rudimentary modelling of the conditions of a possible system that connects the ceiling to unmovable points (in the roof theatre or even existing trusses). For this case study the vertically movable system is not designed in detail, because, for academic purposes, it was more interesting focusing on potentially new typology of kinetic system rather than reviewing the state-of-the-art of acoustic variable solutions. In reality, for further considerations, constrained nodes must be here designed as linear springs as representative of the stiffness of the vertically movable structure.





### 5.1.1 Load cases and combinations

Only limited case loads are taken here in consideration. Namely, the dead load of the structure, the imposed load of the installations (that can be hydraulic pistons accessory components acoustic electronic amplifiers or lighting systems) and a live load considering maintenance situations (Image 5.02).

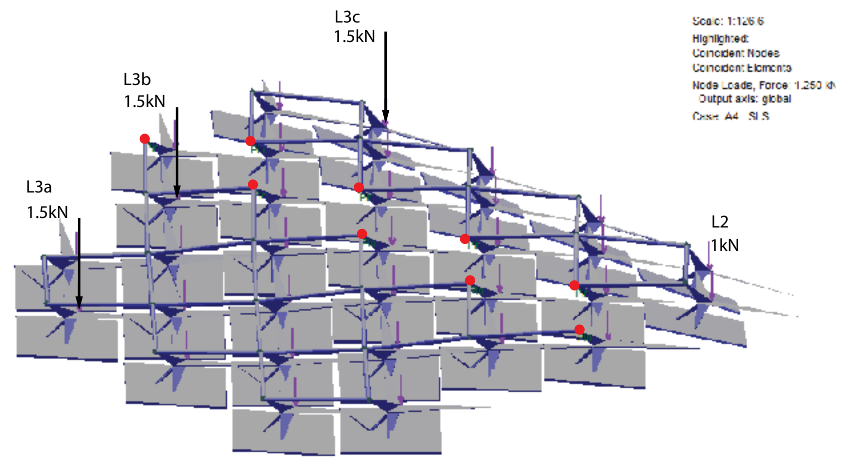


Image 5.02. Loads for the structure: in black the maintenance node loads, in three different locations, while in violet the installation loads.

The imposed load is consider 1kN of magnitude, and applied in each 3D-compressed strut, while the live load consider a nodal force of 1.5 kN applied with different asymmetrical position to the structure: in this last case, 3 different live loads have been considered. A table of load cases and combination is further presented.

| ID | Name | Type | Total Magnitude [kN] |
|---|---|---|---|
| L1 | Self-Weight | Dead | 180 |
| L2 | Installation | Imposed | 32 |
| L3 a-b-c | Manteinance | Live | 1.5 |

Table 5.03. Load Cases.

| ID | Type | Combination |
|---|---|---|
| A1 | ULS1 | 1.35(L1 + L2) + 1.5(L3a) |
| A2 | ULS1 | 1.35(L1 + L2) + 1.5(L3b) |
| A3 | ULS1 | 1.35(L1 + L2) + 1.5(L3c) |
| A4 | SLS | L1 + L2 |

Table 5.04. Load combinations.





### 5.1.2 Results

Here, a brief overview of the result of FEM analysis is presented.
A compendium of stress plots for the whole structures can be found in the Appendix A, while in this section only the highest values related to the related element are summarized. Is very important to mention that results are presented qualitatively, and only with the aim to show how forces and stresses distributes in the structure, in fact, the aim of this section and chapter is not to unity check of verify the stability of the elements. For this reason, and more importantly for further detail design purposes, is worth of attention the free body diagram of the 'bone' (Image 5.3).

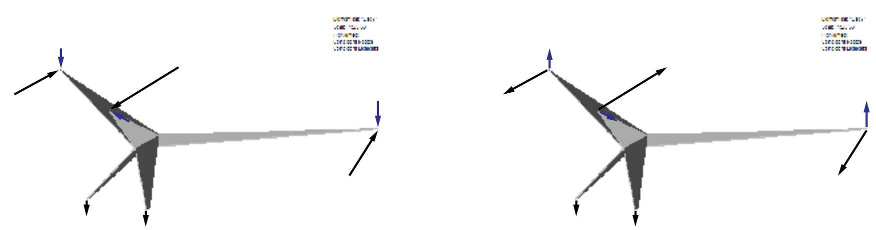

Image 5.03. Free body diagram and relative forces on the bones.

Stresses are following presented considering the most unfavorable conditions at ULS, while displacement are assessed at SLS.

| Bone Plate | Stress [MPa] | Configuration | Load Case |
|---|---|---|---|
| Max absolute Stress (element outer surface) | 52.6 | 1 | A1 |
| Max Tensile Stress (at the middle of element ) | 43.5 | 3 | A1 |
| Max Compressive Stress ( at the middle of element) | 50.7 | 2 | A1 |
| Max Shear Stress ( at the middle of element) | 26.9 | 2 | A1 |
| Von Mises Stress (element outer surface ) | 52.4 | 2 | A1 |

Table 5.05. Stresses on the 3D-struts.

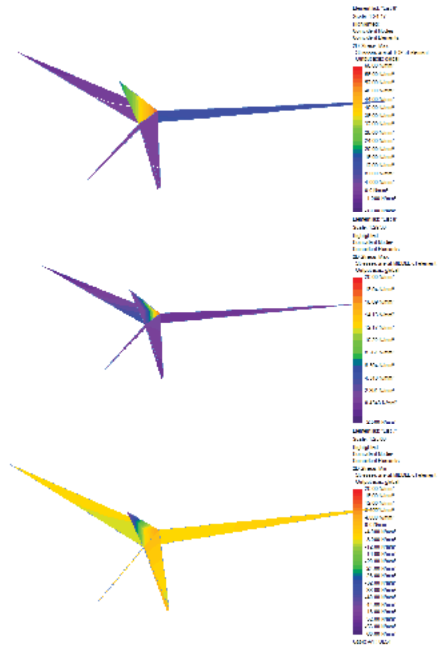

Image 5.04. Top: absolute maximum stress (on the outer surface of the elements). Middle: first principal stress (on the middle of the elements). Bottom: second principla stress (on the midle of the elements)

Table 5.06. Actuactors axial stresses.

| Actuators | Stress [MPa] | Configuration | Load Case |
|---|---|---|---|
| Max Tensile Stress | 48.2 | 2 | A1 |
| Max Compressive Stress | 13.1 | 2 | A1 |

Table 5.07. Reflective panel bending stress.

| Panels | Stress [MPa] | Configuration | Load Case |
|---|---|---|---|
| Max Bending Stress | 1.09 | 2 | A1 |

Table 5.08. Displacement at SLS.

| CG Bone Displacement | Displacement [mm] | Configuration | Load Case |
|---|---|---|---|
| Max Displacement | 359 | 3 | A4 |
| Average Displacement | 31 | 3 | A4 |



Chapter 5 // Further Design Considerations

### 5.2 Proposes for Detailing

There are several issues that must be further designed at a more advanced level regarding the structure. Concerning the bone plates, these have been designed following the diagrammatic layout coming from the theoretical study of 3D-compressed struts systems.
In spite of, from the kinematic point of view this design approach is valuable, from the mechanical perspective several more aspect might be investigated, with particular attention to the design of the bone spike, in order to avoid instability issues. In particular this last point was not taken in consideration within the structural analysis part: here it was not verified that instability might occur, but the high slenderness ratio of the bone spikes suggests that the design of the bone might follow stability considerations.
Following some concepts for designing such system are briefly presented.

A first solution could be to adopt stiffeners in the outer edges of the spikes. From the production point of view stiffening plates can be welded with the bone plates (Image 5.06).

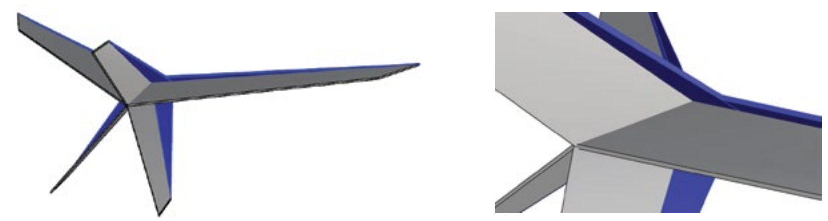

Image 5.06. In blue the stiffening plates.

Out of plane stiffness can be also improved by using composite sections, made out of plates, separated and connected by further backing plates (Image 5.07). From the production perspective these sections can be laser cut and then joint by means of bolts.
In order to improve the stability of the elements also hollow sections can be adopted. As sketch (Image 5.08) are proposed a solution with a custom made profile or by means of circular hollow sections. Spikes connections reveals that further efforts for designing this element are required.

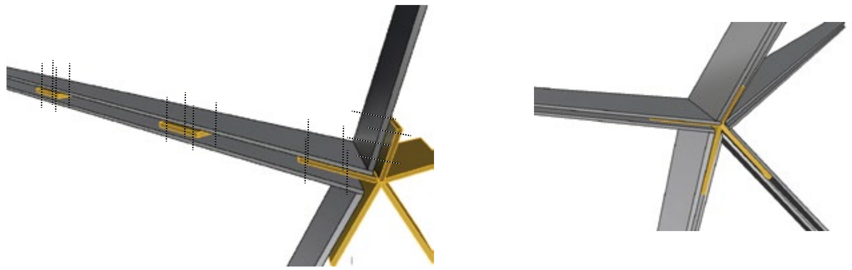

Image 5.07. In gold the baking plates.

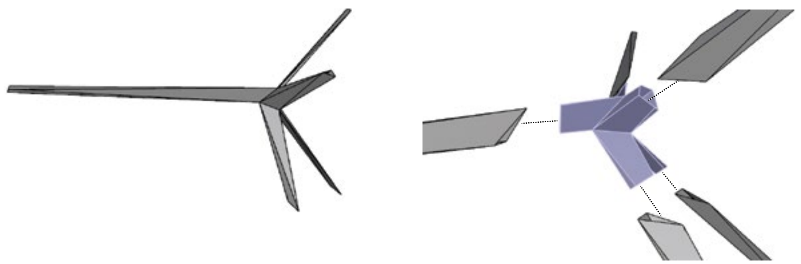

Image 5.08. Bone solutions with custom hollow sections.

Another aspect that must be studied is the connection between the bones, and the bones and the actuators by means of spherical hinges. An easy solution would be to adopt the spider system typical from glass structure that are already produced in the building industry and that can be used to accommodate spherical hinges.

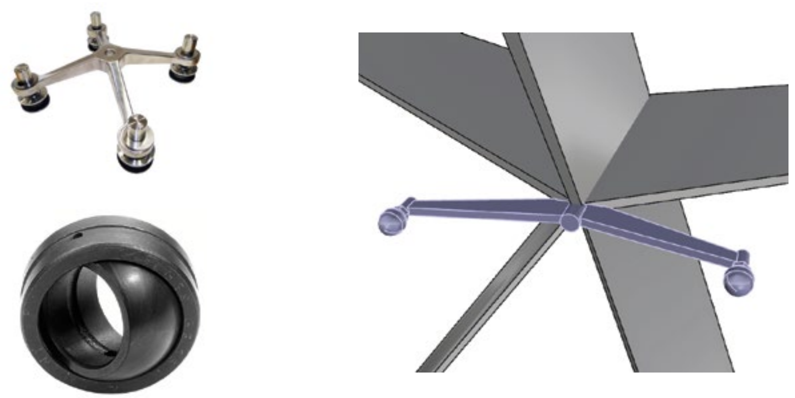

Image 5.09. On the left: a spider system and a spherical hinge. On the right: a sketch of possible integration of spider system with the 'bone'.





## 5.3 Acoustic Evaluation

In section 4.3 a set of ceiling sections derived from first order reflection analysis were baked: here, the reverberation times related to the three configuration are exposed and briefly discussed.

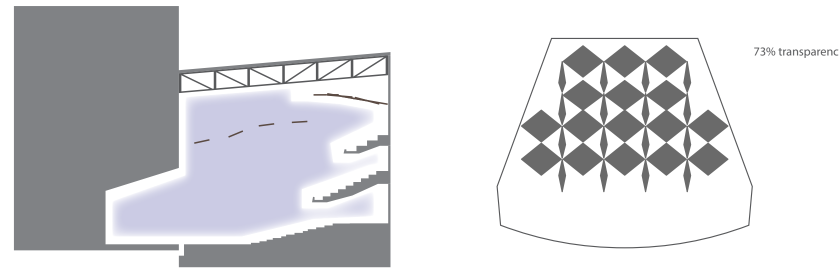


Image 5.10. On the left: reverberant volume. On the right: ceiling silhouette.

The first configuration is designed to have the highest reverberant volume achievable. To do so, the paneling kinetic system is activated, so that the ceiling is now 73% transparent, and the whole volume of the hall (a part of the volume above the static roof ceiling) can be considered here as reverberant volume.
Results of the analysis with the acoustic tools developed shows that this configuration offers a reverberation time of 1.6 seconds, suitable as space to host chambre and classical music. To note, that the assumption that consider the reverberant volume as effective is valid if the underroof surface of the theatre are mainly reflective or diffusive, so that the elements present in the underroof (the five trusses and two catwalks) must be covered with reflective or diffusive surfaces.

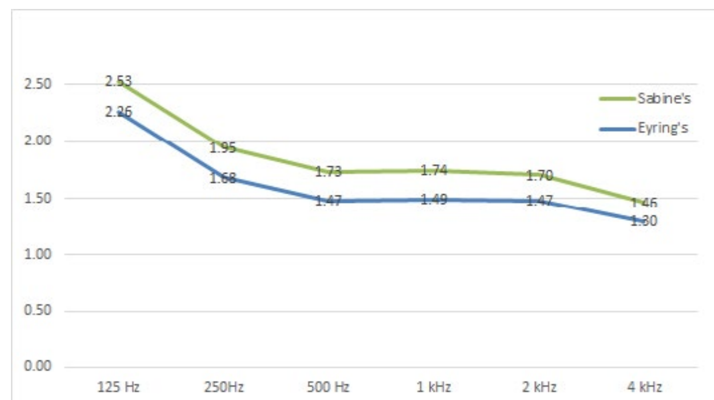


Graph 5.01. Revereberation Time (sec) versus sound frequency (kHz) for the first configuration.

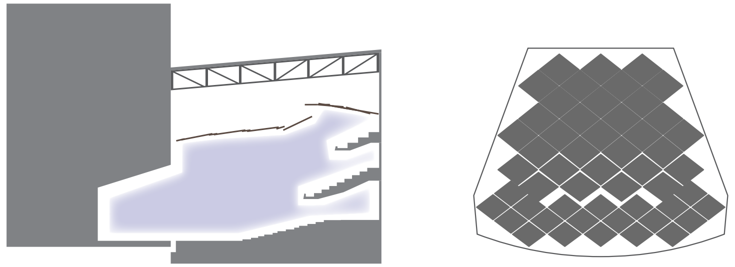


Image 5.11. On the left: reverberant volume. On the right: ceiling silhouette.

The second configuration is designed to achieve an intermediate reverberation time, around 1.4 seconds. The kinetic and the auxiliary ceiling system cooperate now together to achieve a sound tight surface: this is now 35% so less than the 40% prescribed by literature.
Results shows that, with a reverberation time of 1.4 seconds, this configuration is suitable as hosting space for opera.

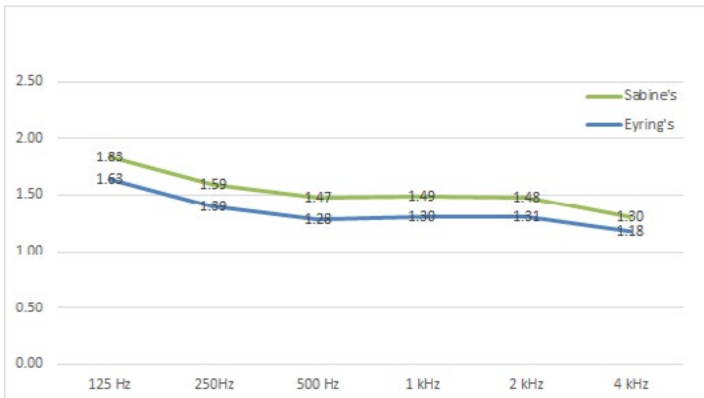


Graph 5.2. Revereberation Time (sec) versus sound frequency (kHz) for the second configuration.

The third configuration is designed to provide a very low reverberation time. To do so, the ceiling is lowered significantly, having an average height of 11.5 meters from the 1st row stands. This has the effect to provide a very low ITDG, so a very intimate soundscape.
To obtain this layout the 2nd balcony has been culled from the effective volume, so that that the underside surface of this works in together with the kinetic system to provide a global ceiling surface transparency of 28%, so less than the 40% prescribed by literature. With this layout, the theatre can host now 1000 seats. On the rear part of the ceiling the curvature is concave so that reflected rays can be concentrated on the 1st balcony.

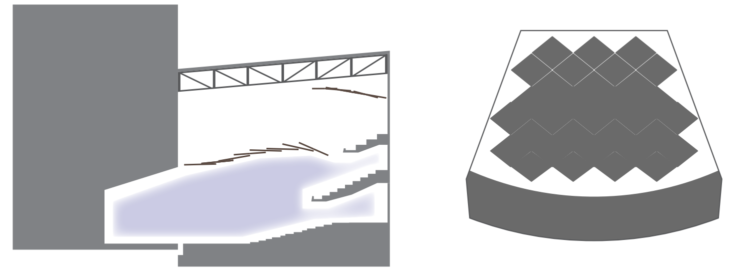


Image 5.12. On the left: reverberant volume. On the right: ceiling silhouette.

Results demonstrates that, with a reverberation time of 1.1 seconds this configuration is suitable as space for speech and amplified music.

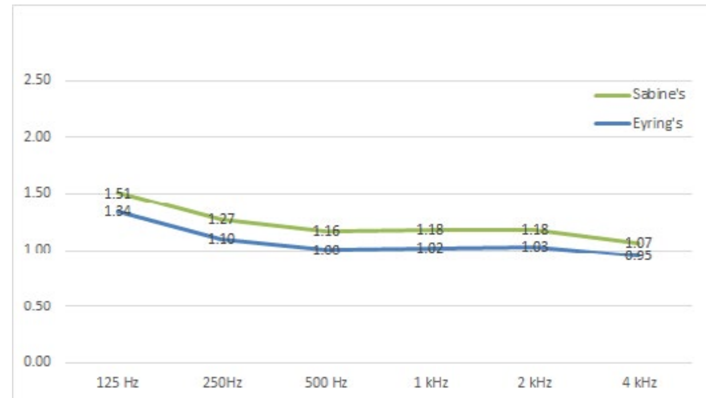


Graph 5.3. Revereberation Time (sec) versus sound frequency (kHz) for the third configuration.

To conclude, graphs show that with the designed kinetic structure, is possible to increase the reverberation time from a minimum value of 1.1 seconds to a maximum achievable value (in relation to the theatre case of study) of 1.61, so, by a range of 48%.

Chapter 6 // Conclusions

This chapter describes the conclusions related to the conducted research. Section 6.1 discusses the conclusions to research methodology adopted for studying kinetic structures, utility of parametric room acoustic assessment tools and the design strategy adopted for the case study. In section 6.2 recommendations for further research and development in the field of kinetic structures applied for adaptive functions in civil engineering are presented.

**6.1 Conclusions**

This MSc thesis was developed to research possible applications of motion structures to create an adaptive sound environment for a multipurpose-theatre. In support of the research, an ecologic design approach, as beforehand theorized by Thun et al (2011) and with other terminology and extensions by Hensel et al (2004), Lelieveld (2013) Teuffel (2011), has been developed.
Conclusions related to the research methodology described in this MSc Thesis are:

-Parametric and associative design tools have proven to be a suitable solution to build a working multidisciplinary design framework at the early stage. Within this framework is possible to simulate and assess early performance situations.

-The used strategy demonstrated to be an effective way of simulating in the same digital environment multiple engineering aspects. Being the tool based on the use of pure parameters and association of geometries, the variables of the different design features had to be express in terms of geometric entities.

Key aspects of kinetic structures has been studied with an eye oriented to possible application in civil engineering where an accessory function based on panels is required. Particular attention was given to propose a strategy for synthetize kinematics aiming to study motion behavior in a more accessible and intuitive way, also easy to visualize.
The following conclusions regarding the study of kinetic structures can be done

-In general, regarding the study of motion structures, the geometric associative approach is more accessible and intuitive method to study kinetic systems.

-Structure based on backbone systems is a very suitable typology to adopt when designing a kinetic structure with high flexibility demands. Moreover it was discovered that this typology is easy both to design and to motion control, being this based on an elementary model of kinematics (kinematic chains).

-Motion flexibility and space tessellation characteristics of backbone structures demonstrated that is possible to overcome the state of the art of existing adaptive acoustic ceiling by introducing as a governing variable the curvature of the overall ceiling.

-In a theoretical perspective, the research on motion structures demonstrated that is possible to innovate and expand the use of kinetic systems to achieve an instant adaptation to context and needs, also with the use of biomechanical inspired systems.





## 6.2 Recommendations

Further research on this topic is required. This section proposes some recommendation for possible future research in the field of motion structures. The thesis was meant prevalently to enquire if a possible use of a motion structure for room acoustics was possible, but research outputs shown potentiality to be employed in other functions for civil engineering.
The points addressed here are based on interesting topics and design possibilities that have been met during the research and that are worth to be further developed.

-With particular attention to kinetic tension structures: although the research and development have led to some promising results, it needs to be highlighted that the current knowledge regarding these systems, is immature due to both the fact that the research topic is recent and the difficultness to study it.
Kinematics of these systems, and in particular of backbone systems needs to be further researched, with particular attention of investigating new space constrain and internal restrain conditions, to design more flexible and effective structural systems.

-The structural model proposed has been validate in its equilibrium configuration for a design case free from dynamics loads. In order to extend the application of motion structures for other civil engineering cases where these loads are present, dynamic and, more in depth, static behavior of these system must be investigated.

-By making use of a very soft material for different tension structures, it was demonstrated that is possible overcome the limit of a foldable tension structure (where mainly the only boundary conditions of fully folded or developed are interesting) to in-a-continuous equilibrated tension structure. The use of such soft material allows system to undergo very large displacement, but on the contrary it might comports a drastically drop in stiffness of the whole system. For this reason the use of soft material must be studied and validate.

-The Design solution proposed makes use of a high number of expensive mechanical devices together with a high number of complicated structural joints. It is recommended for further researches to pay attention to design a system that requires a minimum number of actuators as possible, by developing or propping smarter layout that are meant to concentrate these in few spots . With this purpose, the use of continuous active cables connecting several elements of the assembly has to be investigated more in depth (maybe integrating with the extensive knowledge and previous experience of cable actuated systems coming from deployable structures for space application). Moreover, it is recommended to include in the early design stage also joint and actuator strategies.

-Acoustic assessment tools demonstrated to be effective at the early design, but their definition is still very limited to rough estimations. It is worth to mention that these tools have been developed mainly as necessity, but at the end it turn out that possible implementations of the tools can be easily expanded also by means of developing appropriate user friendly add-ons or toolboxes for the parametric environment.

// Bibliography

Aish R., Woodbury R., Multi-Level Interaction in Parametric Design. *Springer*, 2005.

Ballou G. & al., Handbook for Sound Engineers. *Glen Ballou Editor*, 1987.

Barron F., Industrial Noise Control and Acoustics. *Marcel Dekker, Inc.*, 2001.

Barron M., Auditorium Acoustics and Architectural Design. *Spon*, 2009.

Beatini V., Kinematic shaping. Mechanisms that determine architecture of space. *Doctoral Thesis in Shapes and Structures for Architecture at the University of Parma*, 2006.

Beranek L. L., Music, acoustics and architecture. *Wiley*, 1962.

Beranek L. L., Analysis of Sabine and Eyring equations and their application to concert hall audience and chair absorption. *Journal of the Acoustical Society of Americas*, Vol. 120, n 3, 2006.

Cammarata G., Acustica e Illuminotecnica. *Reader for the Course of Building Physics at the University of Catania*, 2005.

Chen Y., You Z., Mobile assemblies based on the Bennett linkage. Proceedings A, n461. *Proceedings of the Royal Society of Mathematical, Physical and Engineering Sciences*, 2005.

Chen Y., You Z., An Extended Myard Linkage and its Derived 6R Linkage. *Journal of Mechanical Design*, n130, 2008.

Chen Y., You Z., 6R Linkage and its Deployable Structure. Report n OUEL 2254/02 from the *Department of Engineering Science of the University of Oxford*, 2000.

Chen Y., You Z., Tarnai T., Threefold-symmetric Bricard linkages for deployable structures. *International Journal of Solids and Structures*, n42, 2005.

De Boeck J., Tensegrity bridges: Concept design of pedestrian bridges using tensegrity as load carrying system. MSc Thesis at the Delft University of Technology, *TU Delft Academic Repository*, 2013.

De Temmerman N., Design and Analysis of Deployable Bar Structures for Mobile Architectural Applications. *PhD Thesis at the Free University of Brussel*, 2007.

Demaine E., Geometric Folding Algorithms. *Cambridge University Press*, 2007.

Deng Z., Huang H., Li B., Liu R., Synthesis of Deployable/Foldable Single Loop Mechanisms With Revolute Joints. *Journal of Mechanisms and Robotics*, n3, 2011.

d'Estrée Sterk T., Using Actuated Tensegrity Structures to Produce a Responsive Architecture. *ACADIA22 Conference 2003 Proceedings*, 2003.

Ellison S., Schwenke R., The Case for Widely Variable Acoustics. Proceedings of the International Symposium on Room Acoustics, *ISRA*, 2010.

Ferro G., Chiaia B., Cornetti P., Studio grafico della cinematica dei sistemi labile. *Video lecture for the course of Scienza delle Costruzioni at the Turin Polytechical University*, 2013.

Fox M., Kemp M., Interactive architecture. New York. *Princeton Architectural Press*, 2009.

Friedman N., Investigation of highly flexible, deployable structures: review, modeling, control, experiments and application. *These de Doctorat de l'Ecole Normale Superieure de Cachan*, 2012.

Frumar J.A., ZhouY.Y. , Xie Y.M., Burry M.C., Tensegrity Structures with 3D Compressed Components: Development, Assembly and Design. *Journal of the International Association for Shell and Spatial Structures* Vol. 50 n2 August, 2009.

Frumar J.A., Zhou Y.Y., Kinetic Tensegrity Grids with 3D Compressed Elements. *ACADIA22 Conference 2009 Proceedings*, 2010.

Gantes C.J., Deployable Structures. *WIT Press*, 2000.

Heiddegger V., EnergyFacade: operational energy optimizing tool for conceptual facade design. MSc Thesis at the Delft University of Technology, *TU Delft Academic Repository,* 2013.

Hensel M., Menges A., Weinstock M., Frei Otto: in conversation with the design and emergency group, in Emergence: Morphogenetic Design Strategies *AD*, Volume 73, n3, 2004.

Hernandez Merchan C.H., Deployable Structures. Thesis for the Degree MSc in Architecture Studies at the Massachusetts Institute of Technology, *MITLibraries*, 1987.

Issa R., Essential Mathematics for Computational Design - SecondEdition. *Robert McNeel and Associates*, 2009.

Kazi Aoual M.N., Quirant J., Motro R., Towards Tensegrity Systems Design. Novel Approaches in Civil Engineering. Lecture Notes in *Applied and Computational Mechanics*, Volume 14, 2004.

Khabazi M., Algorithmic Modelling with Grasshopper. *www.khabazi.com/flux*, 2009.

Kolarevic B., Architecture in the Digital Age Designing and Manufacturing. *Spon*, 2003.

Kooiman L., Muzikale Beleving, Binnen & Buiten. MSc Thesis at the Delft University of Technology, *TU Delft Academic Repository*, 2012.

Kroner W. M., An Intelligent and Responsive Architecture. *Automation in Construction*, n6, 1997.

Kwan A.S.K, You Z., Pellegrino S., Active and passive cable elements in deployable/retractable masts. *International Journal of Space Structures*, Vol. 8 n1/2, 1993.

Le Corbousier, Vers une architecture. *Arthaud*, 1977.

Lelieveld C., Smart Materials for the Realization of an Adaptive Building Component. PhD Thesis at the Delft University of Technology, *TU Delft Academic Repository,* 2013.

Liu S.Y., Chen Y., Myard linkage and its mobile assemblies. *Journal of Mechanism and Machine Theory*, n44, Elsevier, 2009.

Long M., Architectural Acoustics. *Elsevier Inc.*, 2006.

Meriam J.L., Engineering mechanics: SI version. Vol. 2, Dynamics. *Wiley*, 2003.

Motro R., Tensegrity: structural systems for the future. *Hermes Science Publishing Limited*, 2003.

Negroponte N., Soft architecture machines. Soft architecture machines. Cambridge, USA, *MIT Press*, 1975.

Neubauer R., Kostek B., Prediction of the Reverberation Time in Rectangular Rooms with Non-Uniformly Distributed Sound Absorption. *Archives of Acoustics - ibn.de*, 2001.

Orlowski R.J., The Design of variable acoustics at the new Milton Keynes Theatre. *Proceedings of the Institute of Acoustics* Vol. 21 Part 6, 1999.

Payne A., Issa R., Grasshopper Primer - Second Edition. *Robert McNeel and Associates*, 2009.

Pezzi A., Considerazioni sull'Acustica delle Sale. *Report for the course of Applied Acoustic at the Bologne University*, 2003.

Raichel D., The Science and Applications of Acoustics. *Springer*, 2006.

Resch, R., The Topological Design of Structural and Architectural Systems. *AFIPS* Conference Proceedings 42, National Computer Conference, 1972.

Salter C.M., Acoustics: architecture, engineering, the environment. *William Stout Publishers*, 1998.

Simone A., An introduction to the Analysis of Slender Structures. TU Delft Reader for the course CIE4190 Analysis of Slender Structures, 2011, *TU Delft CiTG Blackboard Document*.

Tachi T., Geometric Considerations for the Design of Rigid Origami Structures. Proceedings of the *International Association for Shell and Spatial Structures Symposium*, 2010.

Teuffel P., From adaptive to high-performance structures. *Proceedings of the International Conference on Adaptive Architecture*, London, 2011.

Thün G., Velikov K., Sauvé L., McGee W., Design Ecologies for Responsive Environments: Resonant Chamber, an Acoustically Performative System. ACADIA 12 Synthetic Digital Ecologies, *Proceedings of the 32nd Annual Conference of the Association for Computer Aided Design in Architecture*, 2012.

Uijtenhaak T., Communicating 'structural' design options sing dashboard portals for exploring alternatives. MSc Thesis at the Delft University of Technology, *TU Delft Institutional Repository,* 2011.

Van der Linden A.C., Zeegers A., Bouwfysica. *ThiemeMeulenhoff*, 2006.

van Dorp Schuitman J., Auditory modelling for assessing room acoustics. PhD Thesis at the Delft University of Technology, *TU Delft Institutional Repository,* 2010.

Vu K.K., Richard Liew J.Y., Krishnapillai Anandasivam, Deployable tension-strut structures: from concept to implementation. *Journal of Constructional Steel Research*, n62, 2006.

Wang B.B., Free-standing tension structures: from tensegrity systems to cable-strut systems. *Spon*, 2004.

Weinstock M., Morphogenesis and the Mathematics of Emergence in Emergence: Morphogenetic Design Strategies. *AD*, Volume 73, n3, 2004.

You Z., Chen Y., Motion structures: deployable structural assemblies of mechanisms. *Spon*, 2012.

Zevi B., Storia dell'Architettura Moderna. *Mondadori*, 2004.

Zhang Y., Finger S., Behrens S., Introduction to Mechanisms. *http://www.cs.cmu.edu/~rapidproto/mechanisms/chpt4.html*, 2014.



// Bibliography

**Appendix A // Results of Structural FEM Analysis**

In this section the result of the structural analysis by means of adopting Oasys GSA as FEA software are presented. The analysis results are considered for the three static configuration of the case study.

The plates that composes the 3D-compressed-struts are very slender (thickness [0.2]/length ratio [3.1] = 0.064) so that the stresses can be analyzed by means of Bernoulli's hypothesis for thin shells.
For thin plate analysis Oasys GSA output the component ($\sigma_{xx}$, $\sigma_{yy}$, $\sigma_{zz}$, $\sigma_{xy}$, $\sigma_{yz}$, $\sigma_{zx}$) of the stress tensor. The software also calculate the other derived stress values ($\sigma_{max}$, $\sigma_{min}$, $\sigma_{max\ shear}$, $\sigma_{von\ Mises}$). In this appendix only the absolute maximum stress value $\sigma_{max}$ (corresponding to the first principal or second principal stress in a plate element, being the material isotropic) are presented.

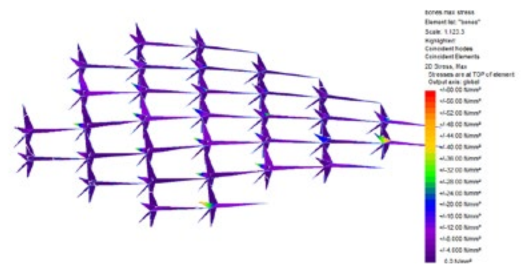

Configuration #1. Max stress 52.6 MPa.
Load Case A1.

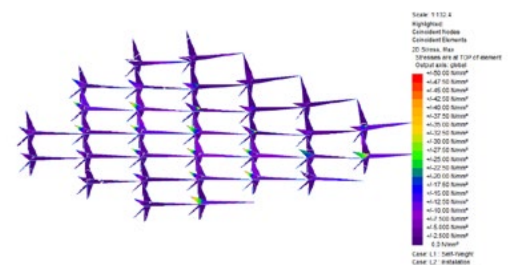

Configuration #2. Max stress 48.2 MPa.
Load Case A2.

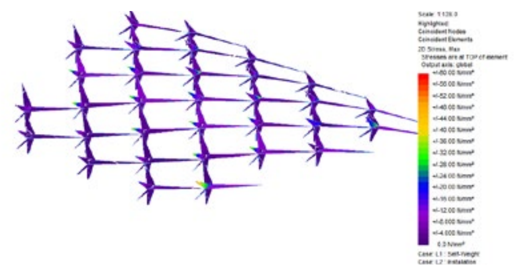

Configuration #3. Max stress 50.3 MPa.
Load Case A1.

Being the pistons restrained with spherical pins, where not local moments are here applied, they can be subjected only to compressive or tensile forces. Maximum axial stresses for the axially loaded elements are hereafter presented.

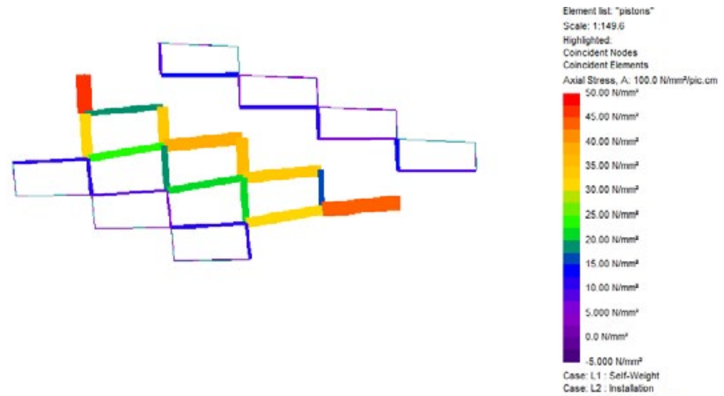

Configuration #1. Max tensile stress 45.3 MPa. Max compressive stress 4.7 MPa Load Case A1.

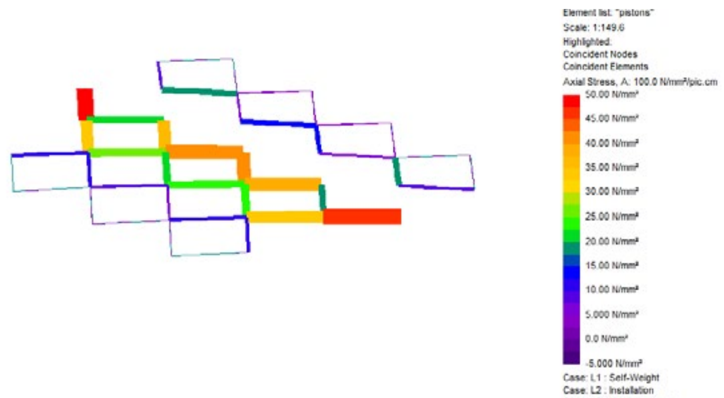

Configuration #2. Max tensile stress 48.2 MPa. Max compressive stress 13.1 MPa Load Case A1.

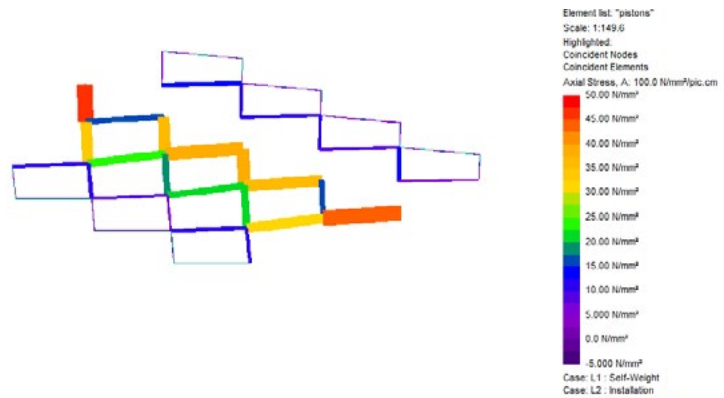

Configuration #3. Max tensile stress 46.7 MPa. Max compressive stress 9.3 MPa Load Case A1.





Bending stress is checked in the timber panels used to model the reflective acoustic ceiling. To be mentioned, timber, for purposes of simplifications, is modelled as orthotropic material.

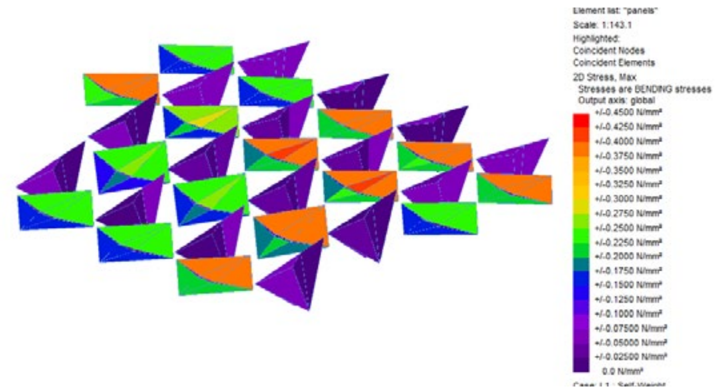

Configuration #1. Max stress 0.41 MPa. Load Case A1.

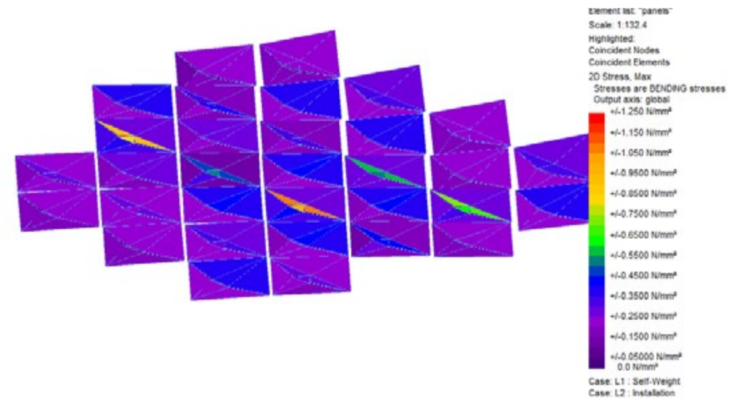

Configuration #1. Max stress 1.09 MPa. Load Case A1.

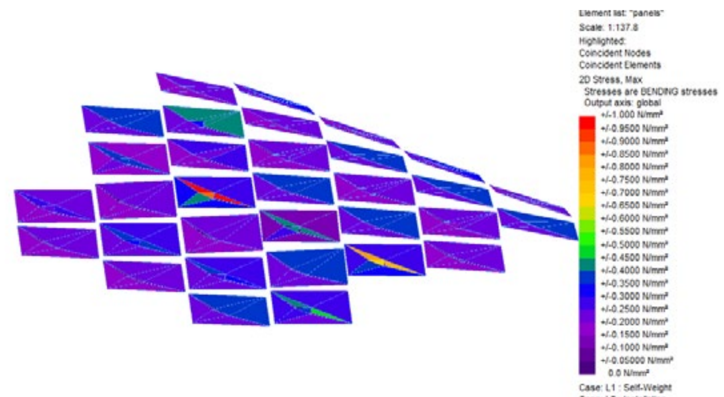

Configuration #3. Max stress 0.98 MPa. Load Case A1.

Node displacement are assessed at SLS. A part of the boundary elements that undergo large displacements, averagely this value is around 20 mm for other nodes.

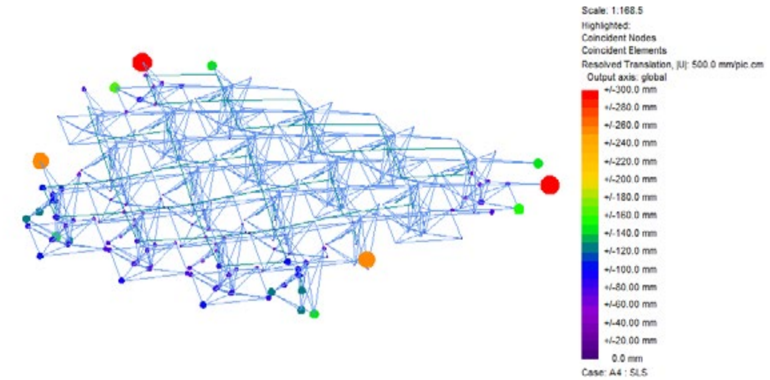

Configuration #1. Max displacement 394 mm. Load Case A4.

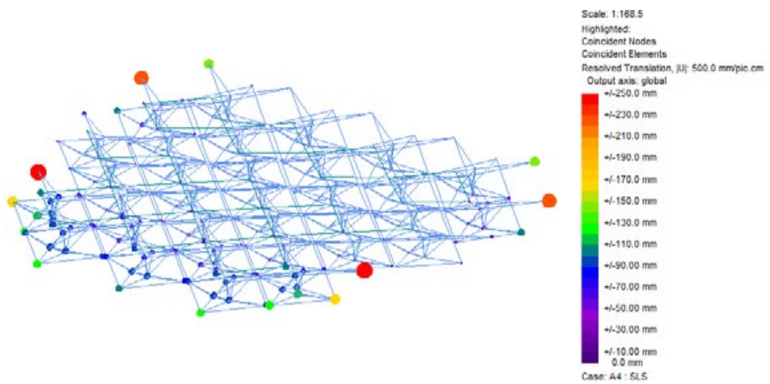

Configuration #2. Max displacement 246 mm. Load Case A4.

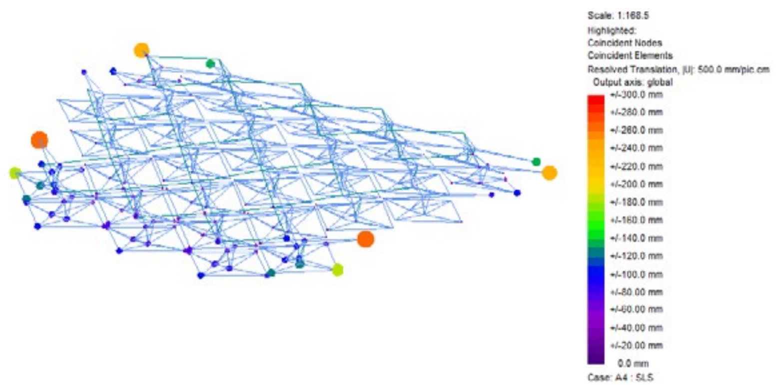





## Appendix B // Input and results of Reverberation Time

Data regarding the calculation of the reverberation time for the three configurations are here presented. A procedure regarding the process is explained at §3.6.

**Theatre Geometric Details**

| | |
|---|---|
| Volume V [m^3] | 18419.31 |

**Acoustic Calculation Sheet Processing Data from GH Output**

Air Absorption Coefficient per m^3 and Total Volume Air Absorbtion per Frequency

| | | | | | | |
|---|---|---|---|---|---|---|
| Absorption Coefficient 4m[m^–1] | 0 | 0.001 | 0.003 | 0.004 | 0.009 | 0.027 |
| Total Area Absorbtion [m^2 Sa] | 0.00 | 18.42 | 55.26 | 73.68 | 165.77 | 497.32 |

Absorption Coefficient per m^2 and Total Area Absorbtion per Frequency

| Surface Type | Area S [m^2] | Material ID | | 125 Hz | 250Hz | 500 Hz | 1 kHz | 2 kHz | 4 kHz |
|---|---|---|---|---|---|---|---|---|---|
| Reflective Ceiling | 491.67 | #50 Plywood Panel | Absorption Coefficient [α] | 0.14 | 0.10 | 0.06 | 0.05 | 0.04 | 0.04 |
| | | | Total Area Absorbtion [m^2 Sa] | 68.83 | 49.17 | 29.50 | 24.58 | 19.67 | 19.67 |
| Audience | 593.01 | #60 Upholsterd Seats | Absorption Coefficient [α] | 0.60 | 0.74 | 0.88 | 0.96 | 0.93 | 0.85 |
| | | | Total Area Absorbtion [m^2 Sa] | 355.81 | 438.83 | 521.85 | 569.29 | 551.50 | 504.06 |
| Stands Accessory | 813.59 | #38 Wood Parquet | Absorption Coefficient [α] | 0.04 | 0.04 | 0.07 | 0.06 | 0.06 | 0.07 |
| | | | Total Area Absorbtion [m^2 Sa] | 32.54 | 32.54 | 56.95 | 48.82 | 48.82 | 56.95 |
| Balcony Undersides | 690.17 | #46 Plaster | Absorption Coefficient [α] | 0.18 | 0.06 | 0.04 | 0.03 | 0.02 | 0.02 |
| | | | Total Area Absorbtion [m^2 Sa] | 124.23 | 41.41 | 27.61 | 20.71 | 13.80 | 13.80 |
| Absortpive Rear and Side Walls | 826.20 | #9 Fiberglass Board | Absorption Coefficient [α] | 0.18 | 0.76 | 0.99 | 0.99 | 0.99 | 0.99 |
| | | | Total Area Absorbtion [m^2 Sa] | 148.72 | 627.91 | 817.93 | 817.93 | 817.93 | 817.93 |
| Reflective Zig-Zag Side Walls | 972.09 | #50 Plywood Panel | Absorption Coefficient [α] | 0.14 | 0.10 | 0.06 | 0.05 | 0.04 | 0.04 |
| | | | Total Area Absorbtion [m^2 Sa] | 136.09 | 97.21 | 58.33 | 48.60 | 38.88 | 38.88 |
| Reflective Tilted Side Walls | 486.05 | #30 Wood Panels | Absorption Coefficient [α] | 0.30 | 0.25 | 0.15 | 0.10 | 0.10 | 0.10 |
| | | | Total Area Absorbtion [m^2 Sa] | 145.81 | 121.51 | 72.91 | 48.60 | 48.60 | 48.60 |
| Scenario Front Wall | 393.29 | #38 Fiberglass Board | Absorption Coefficient [α] | 0.18 | 0.06 | 0.04 | 0.03 | 0.02 | 0.02 |
| | | | Total Area Absorbtion [m^2 Sa] | 70.79 | 23.60 | 15.73 | 11.80 | 7.87 | 7.87 |
| Inner Stage Walls | 513.97 | #32 Gypsum | Absorption Coefficient [α] | 0.20 | 0.18 | 0.15 | 0.12 | 0.10 | 0.10 |
| | | | Total Area Absorbtion [m^2 Sa] | 102.79 | 92.51 | 77.10 | 61.68 | 51.40 | 51.40 |
| Total Area S [m^2] | 5780.03 | | Area Absorbtion S.i*α.i [Sa] | 1185.62 | 1524.69 | 1677.90 | 1652.01 | 1598.47 | 1559.16 |
| | | | Average Absoprtion Coefficient [α^] | 0.21 | 0.26 | 0.29 | 0.29 | 0.28 | 0.27 |
| | | | Eyring Mean Absoprtion Coefficient [α.EY] | 0.23 | 0.31 | 0.34 | 0.34 | 0.32 | 0.31 |

Reverberation Time RT60 [sec] per Frequency

| Method | | | | | | |
|---|---|---|---|---|---|---|
| Sabine's | 2.53 | 1.95 | **1.73** | **1.74** | 1.70 | 1.46 |
| Eyring's | 2.26 | 1.68 | **1.47** | **1.49** | 1.47 | 1.30 |

| Method | Warmth | Brilliance |
|---|---|---|
| Sabine's | 1.29 | 0.91 |
| Eyring's | 1.33 | 0.94 |

**Theatre Geometric Details**

| | |
|---|---|
| Volume V [m^3] | 12083.27 |

**Acoustic Calculation Sheet Processing Data from GH Output**

Air Absorption Coefficient per m^3 and Total Volume Air Absorbtion per Frequency

| | | | | | | |
|---|---|---|---|---|---|---|
| Absorption Coefficient 4m[m^–1] | 0 | 0.001 | 0.003 | 0.004 | 0.009 | 0.027 |
| Total Area Absorbtion [m^2 Sa] | 0.00 | 12.08 | 36.25 | 48.33 | 108.75 | 326.25 |

Absorption Coefficient per m^2 and Total Area Absorbtion per Frequency

| Surface Type | Area S [m^2] | Material ID | | 125 Hz | 250Hz | 500 Hz | 1 kHz | 2 kHz | 4 kHz |
|---|---|---|---|---|---|---|---|---|---|
| Reflective Ceiling | 633.89 | #50 Plywood Panel | Absorption Coefficient [α] | 0.14 | 0.10 | 0.06 | 0.05 | 0.04 | 0.04 |
| | | | Total Area Absorbtion [m^2 Sa] | 88.75 | 63.39 | 38.03 | 31.69 | 25.36 | 25.36 |
| Audience | 593.01 | #60 Upholsterd Seats | Absorption Coefficient [α] | 0.60 | 0.74 | 0.88 | 0.96 | 0.93 | 0.85 |
| | | | Total Area Absorbtion [m^2 Sa] | 355.81 | 438.83 | 521.85 | 569.29 | 551.50 | 504.06 |
| Stands Accessory | 813.59 | #38 Wood Parquet | Absorption Coefficient [α] | 0.04 | 0.04 | 0.07 | 0.06 | 0.06 | 0.07 |
| | | | Total Area Absorbtion [m^2 Sa] | 32.54 | 32.54 | 56.95 | 48.82 | 48.82 | 56.95 |
| Balcony Undersides | 690.17 | #46 Plaster | Absorption Coefficient [α] | 0.18 | 0.06 | 0.04 | 0.03 | 0.02 | 0.02 |
| | | | Total Area Absorbtion [m^2 Sa] | 124.23 | 41.41 | 27.61 | 20.71 | 13.80 | 13.80 |
| Absortpive Rear and Side Walls | 454.25 | #9 Fiberglass Board | Absorption Coefficient [α] | 0.18 | 0.76 | 0.99 | 0.99 | 0.99 | 0.99 |
| | | | Total Area Absorbtion [m^2 Sa] | 81.77 | 345.23 | 449.71 | 449.71 | 449.71 | 449.71 |
| Reflective Zig-Zag Side Walls | 816.71 | #50 Plywood Panel | Absorption Coefficient [α] | 0.14 | 0.10 | 0.06 | 0.05 | 0.04 | 0.04 |
| | | | Total Area Absorbtion [m^2 Sa] | 114.34 | 81.67 | 49.00 | 40.84 | 32.67 | 32.67 |
| Reflective Tilted Side Walls | 486.05 | #30 Wood Panels | Absorption Coefficient [α] | 0.30 | 0.25 | 0.15 | 0.10 | 0.10 | 0.10 |
| | | | Total Area Absorbtion [m^2 Sa] | 145.81 | 121.51 | 72.91 | 48.60 | 48.60 | 48.60 |
| Scenario Front Wall | 157.81 | #38 Fiberglass Board | Absorption Coefficient [α] | 0.18 | 0.06 | 0.04 | 0.03 | 0.02 | 0.02 |
| | | | Total Area Absorbtion [m^2 Sa] | 28.41 | 9.47 | 6.31 | 4.73 | 3.16 | 3.16 |
| Inner Stage Walls | 513.97 | #32 Gypsum | Absorption Coefficient [α] | 0.20 | 0.18 | 0.15 | 0.12 | 0.10 | 0.10 |
| | | | Total Area Absorbtion [m^2 Sa] | 102.79 | 92.51 | 77.10 | 61.68 | 51.40 | 51.40 |
| Total Area S [m^2] | 5159.45 | | Area Absorbtion S.i*α.i [Sa] | 1074.44 | 1226.57 | 1299.47 | 1276.06 | 1225.01 | 1185.70 |
| | | | Average Absoprtion Coefficient [α^] | 0.21 | 0.24 | 0.25 | 0.25 | 0.24 | 0.23 |
| | | | Eyring Mean Absoprtion Coefficient [α.EY] | 0.23 | 0.27 | 0.29 | 0.28 | 0.27 | 0.26 |

| | Reverberation Time RT60 [sec] per Frequency | | | | | |
|---|---|---|---|---|---|---|
| **Method** | | | | | | |
| Sabine's | 1.83 | 1.59 | **1.47** | **1.49** | 1.48 | 1.30 |
| Eyring's | 1.63 | 1.39 | **1.28** | **1.30** | 1.31 | 1.18 |

| **Method** | **Warmth** | **Brilliance** |
|---|---|---|
| Sabine's | 1.16 | 0.94 |
| Eyring's | 1.17 | 0.96 |



Appendix B // Reverberation Time

**Theatre Geometric Details**

| | |
|---|---|
| Volume V [m^3] | 8930.16 |

**Acoustic Calculation Sheet Processing Data from GH Output**

Air Absorption Coefficient per m^3 and Total Volume Air Absorbtion per Frequency

| | | | | | | |
|---|---|---|---|---|---|---|
| Absorption Coefficient 4m[m^–1] | 0 | 0.001 | 0.003 | 0.004 | 0.009 | 0.027 |
| Total Area Absorbtion [m^2 Sa] | 0.00 | 8.93 | 26.79 | 35.72 | 80.37 | 241.11 |

Absorption Coefficient per m^2 and Total Area Absorbtion per Frequency

| Surface Type | Area S [m^2] | Material ID | | 125 Hz | 250Hz | 500 Hz | 1 kHz | 2 kHz | 4 kHz |
|---|---|---|---|---|---|---|---|---|---|
| Reflective Ceiling | 491.67 | #50 Plywood Panel | Absorption Coefficient [α] | 0.14 | 0.10 | 0.06 | 0.05 | 0.04 | 0.04 |
| | | | Total Area Absorbtion [m^2 Sa] | 68.83 | 49.17 | 29.50 | 24.58 | 19.67 | 19.67 |
| Audience | 550.55 | #60 Upholsterd Seats | Absorption Coefficient [α] | 0.60 | 0.74 | 0.88 | 0.96 | 0.93 | 0.85 |
| | | | Total Area Absorbtion [m^2 Sa] | 330.33 | 407.41 | 484.48 | 528.53 | 512.01 | 467.97 |
| Stands Accessory | 756.25 | #38 Wood Parquet | Absorption Coefficient [α] | 0.04 | 0.04 | 0.07 | 0.06 | 0.06 | 0.07 |
| | | | Total Area Absorbtion [m^2 Sa] | 30.25 | 30.25 | 52.94 | 45.38 | 45.38 | 52.94 |
| Balcony Undersides | 690.17 | #46 Plaster | Absorption Coefficient [α] | 0.18 | 0.06 | 0.04 | 0.03 | 0.02 | 0.02 |
| | | | Total Area Absorbtion [m^2 Sa] | 124.23 | 41.41 | 27.61 | 20.71 | 13.80 | 13.80 |
| Absortpive Rear and Side Walls | 450.44 | #9 Fiberglass Board | Absorption Coefficient [α] | 0.18 | 0.76 | 0.99 | 0.99 | 0.99 | 0.99 |
| | | | Total Area Absorbtion [m^2 Sa] | 81.08 | 342.33 | 445.94 | 445.94 | 445.94 | 445.94 |
| Reflective Zig-Zag Side Walls | 485.00 | #50 Plywood Panel | Absorption Coefficient [α] | 0.14 | 0.10 | 0.06 | 0.05 | 0.04 | 0.04 |
| | | | Total Area Absorbtion [m^2 Sa] | 67.90 | 48.50 | 29.10 | 24.25 | 19.40 | 19.40 |
| Reflective Tilted Side Walls | 486.05 | #30 Wood Panels | Absorption Coefficient [α] | 0.30 | 0.25 | 0.15 | 0.10 | 0.10 | 0.10 |
| | | | Total Area Absorbtion [m^2 Sa] | 145.81 | 121.51 | 72.91 | 48.60 | 48.60 | 48.60 |
| Scenario Front Wall | 88.18 | #38 Fiberglass Board | Absorption Coefficient [α] | 0.18 | 0.06 | 0.04 | 0.03 | 0.02 | 0.02 |
| | | | Total Area Absorbtion [m^2 Sa] | 15.87 | 5.29 | 3.53 | 2.65 | 1.76 | 1.76 |
| Inner Stage Walls | 513.97 | #32 Gypsum | Absorption Coefficient [α] | 0.20 | 0.18 | 0.15 | 0.12 | 0.10 | 0.10 |
| | | | Total Area Absorbtion [m^2 Sa] | 102.79 | 92.51 | 77.10 | 61.68 | 51.40 | 51.40 |
| Total Area S [m^2] | 4512.27 | | Area Absorbtion S.i*α.i [Sa] | 967.10 | 1138.38 | 1223.09 | 1202.30 | 1157.96 | 1121.48 |
| | | | Average Absoprtion Coefficient [α^] | 0.21 | 0.25 | 0.27 | 0.27 | 0.26 | 0.25 |
| | | | Eyring Mean Absoprtion Coefficient [α.EY] | 0.24 | 0.29 | 0.32 | 0.31 | 0.30 | 0.29 |

| | Reverberation Time RT60 [sec] per Frequency | | | | | |
|---|---|---|---|---|---|---|
| **Method** | | | | | | |
| Sabine's | 1.51 | 1.27 | **1.16** | **1.18** | 1.18 | 1.07 |
| Eyring's | 1.34 | 1.10 | **1.00** | **1.02** | 1.03 | 0.95 |

| **Method** | **Warmth** | **Brilliance** |
|---|---|---|
| Sabine's | 1.19 | 0.96 |
| Eyring's | 1.21 | 0.98 |

Appendix C // Raytracing Parametric Analysis

## Appendix C // Raytracing Parametric Analysis

In this final appendix are presented the parametric study of the actuators lenghtening factors versus the ITDG together the relative plots: in order for the stands for the three configuration and for the 1st balcony for the 3rd configuration.

| front actuactor lenghtening factor | middle actuactor lenghtening factor | | | | | | | | |
|---|---|---|---|---|---|---|---|---|---|
| | -0.02 | -0.015 | -0.01 | -0.005 | 0 | 0.005 | 0.01 | 0.15 | 0.2 |
| -0.02 | 70 | 70 | 70 | 70 | 70 | 38 | 38 | 42 | 45 |
| -0.015 | 70 | 70 | 35 | 40 | 41 | 45 | 47 | 45 | 42 |
| -0.01 | 70 | 70 | 70 | 35 | 38 | 53 | 55 | 58 | 60 |
| -0.005 | 30 | 31 | 41 | 43 | 40 | 48 | 49 | 55 | 58 |
| 0 | 40 | 42 | 40 | 46 | 45 | 45 | 50 | 52 | 48 |
| 0.005 | 70 | 70 | 36 | 37 | 40 | 40 | 40 | 40 | 32 |

Actuators 1 and 2 lenghtening factors VS ITDG

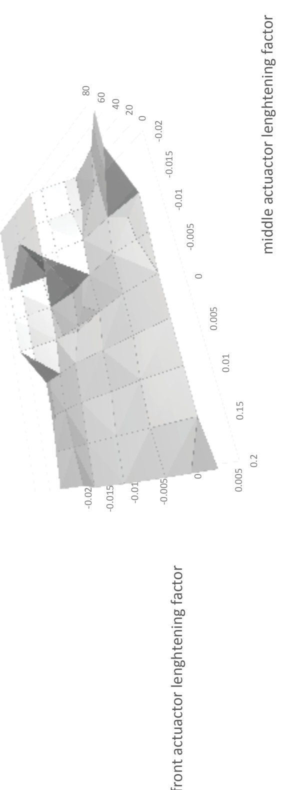


| front actuactor lenghtening factor | middle actuactor lenghtening factor | | | | | | | | |
|---|---|---|---|---|---|---|---|---|---|
| | -0.02 | -0.015 | -0.01 | -0.005 | 0 | 0.005 | 0.01 | 0.15 | 0.2 |
| -0.02 | 70 | 70 | 70 | 28 | 30 | 32 | 38 | 37 | 40 |
| -0.015 | 70 | 70 | 27 | 29 | 32 | 32 | 40 | 42 | 38 |
| -0.01 | 70 | 21 | 29 | 34 | 31 | 34 | 37 | 36 | 35 |
| -0.005 | 70 | 70 | 22 | 26 | 31 | 32 | 34 | 32 | 38 |
| 0 | 25 | 27 | 29 | 37 | 42 | 35 | 38 | 35 | 42 |
| 0.005 | 25 | 23 | 26 | 29 | 31 | 25 | 32 | 35 | 36 |

Actuators 1 and 2 lenghtening factors VS ITDG

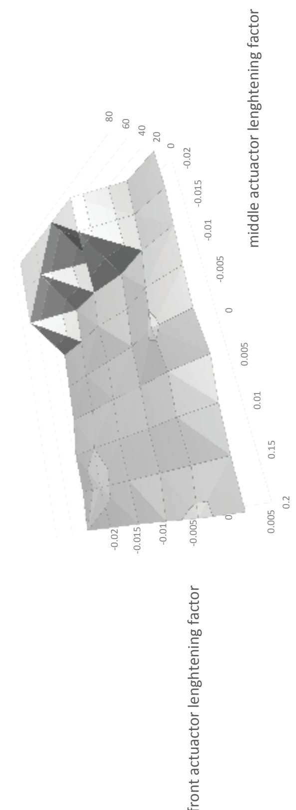


| front actuactor lenghtening factor | middle actuactor lenghtening factor | | | | | | | | |
|---|---|---|---|---|---|---|---|---|---|
| | -0.02 | -0.015 | -0.01 | -0.005 | 0 | 0.005 | 0.01 | 0.15 | 0.2 |
| -0.02 | 24 | 19 | 25 | 31 | 29 | 31 | 32 | 36 | 35 |
| -0.015 | 23 | 22 | 22 | 21 | 23 | 24 | 25 | 29 | 32 |
| -0.01 | 27 | 28 | 22 | 29 | 29 | 32 | 34 | 36 | 35 |
| -0.005 | 22 | 21 | 20 | 23 | 25 | 28 | 32 | 35 | 40 |
| 0 | 23 | 21 | 25 | 27 | 29 | 31 | 32 | 34 | 36 |
| 0.005 | 22 | 21 | 24 | 23 | 29 | 32 | 33 | 34 | 35 |

Actuators 1 and 2 lenghtening factors VS ITDG

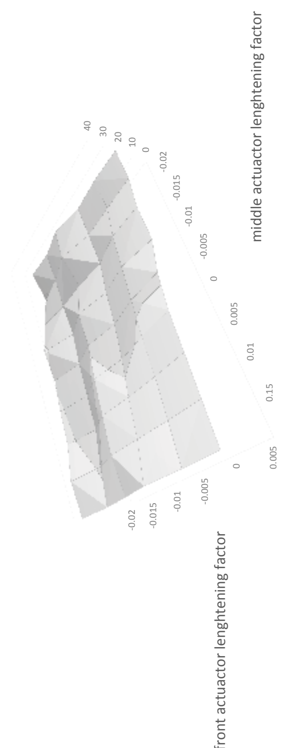


| rear actuactor lenghtening factor | middle actuactor lenghtening factor | | | | | | | | |
|---|---|---|---|---|---|---|---|---|---|
| | -0.02 | -0.015 | -0.01 | -0.005 | 0 | 0.005 | 0.01 | 0.15 | 0.2 |
| -0.03 | 12 | 13 | 14 | 13 | 14 | 15 | 14 | 13 | 13 |
| -0.025 | 13 | 14 | 13 | 15 | 17 | 18 | 15 | 14 | 13 |
| -0.002 | 13 | 12 | 14 | 16 | 15 | 15 | 15 | 14 | 13 |
| -0.015 | 15 | 13 | 12 | 13 | 14 | 16 | 15 | 15 | 13 |
| -0.01 | 12 | 15 | 16 | 17 | 19 | 17 | 15 | 14 | 14 |
| -0.005 | 13 | 12 | 14 | 16 | 15 | 15 | 15 | 14 | 13 |

Actuators 2 and 3 lenghtening factors VS ITDG